Self-inactivating gammaretroviral vectors for the gene therapy of Chronic Granulomatous Disease

Dissertation
zur Erlangung des Doktorgrades
der Naturwissenschaften

vorgelegt beim Fachbereich Biowissenschaften
der Johann Wolfgang Goethe-Universität
in Frankfurt am Main

von
Bibiana Moreno Carranza
aus Barcelona, Spain

Frankfurt 2008

Vom Fachbereich Biowissenschaften der Johann Wolfgang Goethe-Universität als Dissertation angenommen.

Dekan: Prof. Dr. Volker Müller

Gutachter: Prof. Dr. Anna Starzinski-Powitz
Prof. Dr. Bernd Groner

Datum der Disputation: …….

a mis padres, hermana y abuela

"Caminante, son tus huellas
el camino y nada más;
caminante, no hay camino,
se hace camino al andar.

Al andar se hace camino
y al volver la vista atrás
se ve la senda que nunca
se ha de volver a pisar.

Caminante no hay camino
sino estelas en la mar..."

Antonio Machado

TABLE OF CONTENTS

TABLE OF FIGURES

ABBREVIATIONS

Ab	antibody(ies)
ADA-SCID	Adenosine Deaminase-deficient Severe Combined Immunodeficiency
AIDS	Acquired Immunodeficiency Syndrome
Amp	Ampicillin
ATP	Adenosintriphosphat
AAV	Adeno-associated Virus
BM	Bone Marrow
Bp	base pair(s)
CFU	Colony Forming Unit(s)
cDNA	Complementary DNA
CGD	Chronic Granulomatous Disease
Cpm	Counts per minute
CTE	Constitutive RNA Transport Element
CRM-1	Chromosome Region Maintenance 1
DEPC	Diethylpyrocarbonat
DMEM	Dulbecco`s Modification of Eagle's Minimum Essential Medium
DMSO	Dimethylsulfoxid
DNA	Desoxyribonucleotid acid
DNase	Desoxyribonuclease
dNTP	Desoxynucleosidtriphosphat(s)
EBV	Epstein-Barr Virus
E. Coli	*Escherichia Coli*
eGFP	Enhanced Green Fluorescent Protein
EDTA	Ethylene diamin tetraacetate
env	Envelope (glycoprotein)
FACS	Fluorescence Activated Cell Sorting
FAD	Flavin Adenine Dinucleotide
FBS	Fetal Bovine Serum
FCS	Fetal Calf Serum
FITC	Fluorescein-Isothiocyanat
flt-3	FMS-Like Tyrosine Kinase 3
gag	group specific antigen (internal structural protein)
GaLV	Gibbon-ape Leukemia Virus
G-CSF	Granulocyte-Colony Stimulating Factor
GDP	Guanosine diphosphate
GDI	Guanine-nucleoside Dissociation Inhibitor
GFP	Green Fluorescent Protein
G-CSF	Granulocyte Colony Stimulating Factor
GM-CSF	Granulocyte-Macrophage Colony Stimulating Factor
GP	Glycoprotein
GTP	Guanosine triphosphate
GVHD	Graft Versus Host Disease
HFV	Human Foamy Virus
HIV	Human Immunodeficiency Virus
HLA	Human Leukocyte Antigen
HSC	Hematopoietic Stem Cell
IFN	Interferon
kDa	Kilo Dalton(s)
Kb	kilo Base(s)
LB Medium	Luria Bertani Medium
LMO2	LIM domain only 2
LM-PCR	Ligation Mediated PCR

LTR	Long Terminal Repeat
mA	miliAmper(s)
min	minute(s)
ml	milli litre(s)
mM	milli Molar
moAb(s)	monoclonal Antibody(ies)
Mo-MLV	Moloney Murine Leukemia Virus
MRP8/14	Myeloid-Related Protein 8/14
mRNA	Messenger RNA
NADPH	Nicotinamide Adenosine Dinucleotide Phosphate
NK cell	Natural Killer cell
nM	nanoMolar
nm	nanometer(s)
ORF	Open Reading Frame
PBLs	Peripheral Blood Lymphocytes
PBSC	Peripheral Blood Stem Cells
PCR	Polymerase Chain Reaction
PEG-ADA	Polyethylene Glycol-ADA
PIC	Pre-Initiation Complex
rpm	revolutions per minute(s)
RTC	Reverse Transcription Complex
PB1	Protein-binding module 1
PBS	Phosphate Buffered Saline
	Primer Binding Site
PMNs	Polymorphonuclears
pol	Polymerase
PX	PhoX homology domain
RNA	Ribonucleic acid
ROS	Reactive Oxygen Specie(s)
RPMI	Roswell Park Memorial Institute Nr.1640 Medium
RSL	R region stem loop
SCID	Severe Combined ImmunoDeficiency
SDS	Sodium Dodecyl Sulfate
sec	second(s)
SFFV	Spleen Focus Forming Virus
SIN	Self-inactivating
SOC	Super Optimal Catabolite repression broth
SU glycoprotein	Surface glycoprotein
SSC	Saline Sodium Citrate
TAP	Tip-Associated Protein
TBE	Tris-Borate-EDTA
TM glycoprotein	Transmembrane glycoprotein
TPR motif	Tetratrico-peptide Repeat motif
UTR	Untranslated Region
V	Volt(s)
VSV	Vesicular Stomatitis Virus
WPRE	Woodchuck Post-transcriptional Regulatory Element

A. INTRODUCTION

A.1 Chronic Granulomatous Disease

A.1.1 Clinical manifestations

In 1954, Janeway and colleagues first reported five cases of children suffering from recurrent severe infections and hypergammaglobulinemia (Janeway *et al.*, 1954). Later on, more cases of children with the same symptomatology were described. These patients additionally showed granulomatous lesions and infiltration of visceral organs (Landing and Shirkey, 1957; Bridges *et al.*, 1959).

The disease was first named "fatal granulomatous disease" of childhood, since it was considered as a syndrome whose sufferers invariably died in the first decade of life. In 1966 it was shown that the disease is related to a failure in phagocytic function of granulocytes (Holmes *et al.*, 1966).

It is currently accepted that the failure of phagocytes to generate reactive oxygen species (ROS), which are important for the microbicidal activity, is responsible for the development of the disease. As a consequence of this defect, patients are unable to ward off infections caused by catalase-positive bacteria and fungi (Winkelstein *et al.*, 2000).

Nowadays, infections of the soft tissues and upper and lower respiratory tracts, lung abscesses, bronchitis, liver abscesses, gastroenteritis and development of sterile granulomas in hollow organs without clinical evidence of infection are, *inter alia*, the most common clinical manifestations described as symptoms of this disease which is now termed "Chronic Granulomatous Disease" (CGD) (Rosh *et al.*, 1995; Barese and Goebel, 2006).

A.1.2 The NADPH oxidase enzyme complex

Phagocytosis of invading pathogens is normally accompanied by an increase of O_2 consumption of the cell (up to 100-fold), known as respiratory burst (Light *et al.*, 1981). The O_2 accepts electrons from the reduced nicotinamide adenine dinucleotide phosphate generating superoxide anion. The superoxide anion is the precursor of a number of reactive oxygen species (ROS) that plays an essential role in killing many types of microorganisms. This conversion is catalyzed by the NADPH oxidase, which is a phagocytic, multi-protein enzyme complex present in the plasma and specific granule membranes of phagocytes. It is comprised of $gp91^{phox}$ and $p22^{phox}$, which form a membrane-bound heterodimer referred to as flavocytochrome b_{558}, and several cytosolic components ($p47^{phox}$, $p67^{phox}$, $p40^{phox}$, the small G-protein Rac2 and MRP8/MRP14).

A.1.2.1 The flavocytochrome b_{558} complex of NADPH oxidase

Flavocytochrome b_{558} is a stable membrane-associated heterodimeric complex, which comprises not only the $gp91^{phox}$ and $p22^{phox}$ subunits (Parkos *et al.*, 1987), but also a flavin adenine dinucleotide (FAD) and two heme prosthetic groups (Fig. 1).

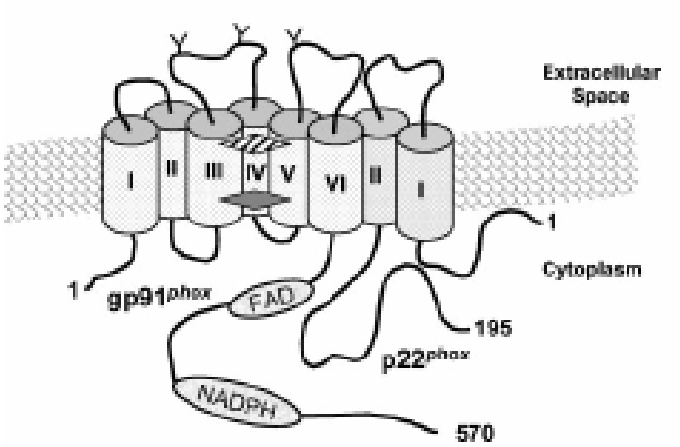

Fig. 1: Model of flavocytochrome b_{558}. Both $gp91^{phox}$ and $p22^{phox}$ are shown, with the aligned hemes (solid and hatched diamonds) and the sites for FAD and NADPH binding on $gp91^{phox}$ indicated (Quinn and Gauss, 2004).

$Gp91^{phox}$ (β-subunit) is a post-translationally glycosylated protein essential for oxidase function. This subunit is synthesized as a glycosylated 65-kDa precursor in the endoplasmatic reticulum microsomes and contains high mannose-type carbohydrates. Mature $gp91^{phox}$ has N-linked complex carbohydrate chains which are acquired for further processing in the Golgi complex and are resistant to digestion with endonuclease H (Porter *et al.*, 1994). The cytosolic N-terminal and C-terminal domains of $gp91^{phox}$ are linked through six transmembrane α-helices with conserved histidine residues that coordinate two heme prosthetic groups (Cross *et al.*, 1995; Yu *et al.*, 1998; Biberstine-Kinkade *et al.*, 2001; Biberstine-Kinkade *et al.*, 2002). FAD and NADPH cofactors bind to the C-terminal domain, which serves as a redox center and may also be involved in the recruitment of the cytosolic factors required for activation and functionality of the oxidase (Rotrosen *et al.*, 1990; Rotrosen *et al.*, 1992; Sumimoto *et al.*, 1992; Doussiere *et al.*, 1993). The presence of all redox components in $gp91^{phox}$ supports the theory that this subunit mediates the sequential electron transfer from cytosolic NADPH via FAD to molecular oxygen to form superoxide anion.

Compared to $gp91^{phox}$, the topology of $p22^{phox}$ (α-subunit) is less well characterized. However, antibody and proteolysis experiments in combination with computational predictions suggest that, in addition to two membrane-spanning domanins, a large part of the N-terminal region of $p22^{phox}$ is intracytoplasmic. The carboxy terminus of $p22^{phox}$ is hydrophilic and contains a prolin-rich sequence providing a high affinity binding site for $p47^{phox}$, which is essential for recruitment of cytosolic components. The N-terminus

plays an important role in gp91^{phox}-p22^{phox} heterodimer assembly as inferred from deletion mutagenesis analysis of this region (Taylor *et al.*, 2004; Zhu *et al.*, 2006).

P22^{phox} forms a mutually stabilizing complex with gp91^{phox} in a stoichiometric 1:1 noncovalent association. The heterodimerization process of gp91^{phox} and p22^{phox} is coupled to the maturation of gp91^{phox} and to the transport of the heterodimer into the membrane. Full maturation of gp91^{phox} includes the sequential incorporation of two heme prosthetic groups into the 65-kDa precursor, the heterodimerization with p22^{phox} in the endoplasmatic reticulum and the addition of N-linked oligosaccharides in the golgi complex. All these events are required for the following transport of the heterodimer to the plasma membrane (Yu *et al.*, 1997; Yu *et al.*, 1998). Therefore, a defect in one of the two subunits completely prevents insertion of the heterodimer into the plasma and specific granule membranes of phagocytes (Parkos *et al.*, 1989).

A.1.2.2 The cytosolic components of NADPH oxidase

The flavocytochrome b_{558} complex recruits two essential cytoplasmatic subunits (p47^{phox} and p67^{phox}) and several cofactors (Rac2, p40^{phox}, MRP8/MRP14, etc.).

The p47^{phox} subunit contains four domains: i) an N-terminal phox homology (PX) domain, which has a membrane-targeting role *via* its specific phosphoinositide-binding module (Kanai *et al.*, 2001), ii) two tandemly organized Src homolgoy (SH3) domains (Leto *et al.*, 1994), iii) an auto-inhibitory domain and iv) a C-terminal proline-rich (PRR) domain with six potential serine phosphorylation sites (Fig. 2a).

In resting phagocytes, p47^{phox} can be found as a monomer as well as in a multimeric complex (1:1:1) with p67^{phox} and p40^{phox}. P47^{phox} remains in an auto-inhibitory conformation by an intermolecular interaction of the SH3 domains with the auto-inhibitory region. Phosphorylation of serines at the C-terminus induces unfolding of p47^{phox} which is a prerequisite for its translocation to the plasma membrane and for direct binding to p22^{phox} (Fontayne *et al.*, 2002). P47^{phox} seems to act as an adaptor protein by generating the optimal sterical conformation enabeling p67^{phox} to bind to gp91^{phox}.

The p67^{phox} is known as activator of the NADPH oxidase and is able to bind to NADPH and gp91^{phox}. Therefore it is likely that p67^{phox} is directly involved in electron transfer. However, translocation to the plasma membrane and cytochrome association of p67^{phox} is dependent on co-translocation of p47^{phox} and its prior interaction with the flavocytochrome b_{558} (Fig. 2b).

The central middle part of p67^{phox} possesses a PRR domain followed by two SH3 domains that mediate interaction with p47^{phox}. There is also a protein-binding module, PB1, which is located between two SH3 domains.The PB1 domain interacts with the PC motif of p40^{phox} (Nakamura *et al.*, 1998; Ito *et al.*, 2001) in the cytosol of resting

polymorphonuclear cells. The N-terminus of $p67^{phox}$ contains the $gp91^{phox}$ binding-domain or activation domain enrolled in oxidase activation. A tetratrico-peptide repeat (TPR) motif, which is the last motif at the N-terminus end, is the NADPH binding site of the protein (Dang *et al.*, 2000) and includes a unique type of binding domain for monomeric GTPases like Rac2 (Fig. 2b).

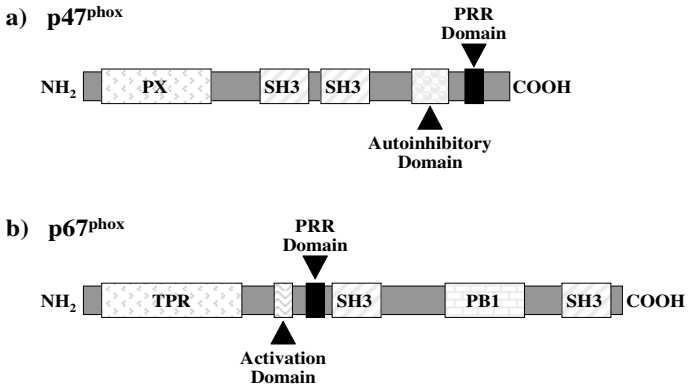

Fig. 2: Structure and major functional domains of $p47^{phox}$ and $p67^{phox}$. (a) Functionally important domains of the $p47^{phox}$ protein include the amino terminus PX domain, tandem SH3 domains, the autoinhibitory domain and the proline-rich (PRR) domain. (b) The N-terminal domain of $p67^{phox}$ contains a tetratrico-peptide repeat (TPR) motif and an activation domain that is essential for activity of the assembled oxidase. Additionally, $p67^{phox}$ contains a PRR motif followed by tandem SH3 domains with an intervening PB1 motif. (Quinn and Gauss, 2004).

It has been demonstrated that $p67^{phox}$ clearly undergoes phosphorylation at some residues situated at both C- and N-terminal ends (Dang *et al.*, 2003), although the physiological role of this event is still unclear.

The small G-protein Rac2 (21 kDa) is a member of the Ras superfamily and is required to activate the NADPH oxidase. Rac2 is the predominant Rac isoform in human neutrophils. It plays essential and unique roles in neutrophils including rolling *via* L-selectin, cytoskeletal reorganization by the induction of F-actin assembly, chemotaxis in response to several chemoattractants, and superoxide generation in response to several agonists (e.g. phorbol 12-myristate 13-acetate (PMA) or formyl-Met-Leu-Phe (fMLP)) (Roberts *et al.*, 1999; Martyn *et al.*, 2005).

Upon cell stimulation, Rac2 is released from its cytosolic binding protein Rho guanine-nucleoside dissociation inhibitor (GDI), translocates to the membrane and alternates from an inactive GDP-bound form to an active GTP-bound state. Thus, Rac2 acquires a conformation able to interact with the TPR motif of $p67^{phox}$ by its effector domain (also called Switch I domain). It also to binds directly to the flavocytochrome b_{558} by its insert domain in a GTP-dependent manner (Diebold and Bokoch, 2001). This last binding event, however, is still uncertain and an alternative model has been proposed where the Switch I domain of Rac2 plays a dual role in the GTP-dependent assembly of the oxidase. This model proposes that the N-terminal half

of the Switch I domain binds to $p67^{phox}$, while the C-terminus mediates binding to flavocytochrome b_{558} (Hoffman and Cerione, 2001).

Some other roles of Rac2 in NADPH oxidase assembly and activation have been proposed. It has been postulated that Rac2 acts as activator of signaling pathways leading to $p47^{phox}$/$p67^{phox}$ translocation in a Rac-GTP/$p67^{phox}$ interaction-independent manner (Price *et al.*, 2002). Additionally, other studies showed PAKs as target of Rac2 proteins, which may phosphorylate $p47^{phox}$, therefore inducing translocation to the membrane (Knaus *et al.*, 1995).

The particular contribution of the $p40^{phox}$ cytosolic subunit of the NADPH oxidase to the assembling process and to the underlying electron-transfer mechanism is still unclear. $P40^{phox}$ contains a single SH3 domain, an N-terminal PX domain, as found in $p47^{phox}$, and a C-terminal PC motif which binds to the PB1 domain in $p67^{phox}$ (as mentioned above). So far, it has been found in the cytosol of fractionated, resting neutrophils and it has been shown not to be required for superoxide formation (Someya *et al.*, 1993). A widely accepted theory implies that $p40^{phox}$ might play a role in stabilizing the assembly of multimeric complexes of $p67^{phox}$ and $p47^{phox}$. However, some additional roles have been postulated for $p40^{phox}$ such as enhancing translocation to the plasma membrane by its interaction with PI-3 phosphates via the PX motif (Kanai *et al.*, 2001), and/or regulating activation responses dependent on specific stimulus (Malech and Hickstein, 2007).

S100A8 (calgranulin A) and S100A9 (calgranulin B), also designated as MRP8 and MRP14, respectively, belong to the S100 multigenic family of calcium-modulated proteins of the EF-hand type, which exhibit functions during various cellular processes such as cell cycle progression and modulation of cytoskeletal-membrane interactions. MRP8 and MRP14 are highly expressed in neutrophils and macrophages and are involved in inflammation and myeloid cell maturation. Additionally, these proteins form MRP8/MRP14 heterocomplexes which have been shown to be secreted by activated monocytes. MRP8/MRP14 complexes are involved in several functions. They directly interact with tubulin to induce polymerization of microtubules (Vogl *et al.*, 2004) and act as transport proteins carring arachidonic acid in its secreted form thereby modulating inflammatory processes (Kerkhoff *et al.*, 1999).

It is generally thought that neutrophil activation is also dependent on increase in the cytoplasmatic free calcium concentration. This augment induces MRP proteins translocation from the cytosol to the cytoskeleton and to the plasma membrane (Pozzan *et al.*, 1983; Roth *et al.*, 1993).

More recently, a direct role for the two calcium-binding proteins in oxidase activation has been demonstrated in a heparin-bound purified cytochrome b_{558} complex. Even in absence of all cytosolic factors and stimulating agonists, the MRP8/MRP14 heterodimer

is able to partially activate the oxidase. However, addition of $p67^{phox}$ to the same system has shown to be required to obtain a fully active oxidase, suggesting a cumulative effect of both proteins (Paclet et al., 2007).

A.1.3 Regulation of the oxidase assembly

To prevent damage to surrounding healthy tissue by an excessive or inappropriate superoxide release, the assembly of the NADPH oxidase complex must be under tight control. This is achieved by partitioning components of the system in different cellular compartments.

In resting phagocytes only 15% of the flavocytochrome b_{558} is located in the plasma membrane whereas the remaining 85% is stored within the membrane of specific granules and secretory vesicles (Borregaard *et al.*, 1983; Ginsel *et al.*, 1990). The activating and assembling components are present in the cytosol either alone, like Rac2, or in complexes linked via reciprocal SH3-domain interactions, like $p67^{phox}$, $p47^{phox}$ and $p40^{phox}$.

NADPH oxidase assembly is triggered upon cell activation by binding of opsonized bacteria or inflammatory mediators to cell surface receptors. Activation of the cells initiates several molecular events that result in membrane translocation of the cytosolic components and their assembly with the flavocytochrome b_{558} (Fig. 3).

Briefly, the stimulated receptors initiate signaling pathways leading to the activation of several protein kinases. These kinases, including protein kinase C (PKC) mediate phosphorylation of $p47^{phox}$. Unfolding of the intramolecular, autoinhibitory conformation of $p47^{phox}$ is most likely the initial step in oxidase activation. The exposed SH3 domains are then able to mediate an interaction with $p22^{phox}$, which creates an optimal conformational context for $p67^{phox}$ to bind to $gp91^{phox}$ through its N-terminus. In Rac2 GDP is exchanged for GTP, then Rac2 translocates to the membrane and binds to $p67^{phox}$ to complete the assembly. The role of $p40^{phox}$ in this process is still under debate. A well accepted theory suggests that $p40^{phox}$ is an inhibitory element of the oxidase, which only functions as a membrane recruitment mediator in resting cells (Kuribayashi *et al.*, 2002). Upon activation Rac2 might replace $p40^{phox}$ (Rinckel *et al.*, 1999) and thereby release the enzymatic complex from its major inhibitor (Vergnaud *et al.*, 2000).

Each step in the assembly process seems to induce several conformational modifications in the different subunits in order to mediate more intimate interactions and to obtain a properly assembled and fully active structure (Nauseef, 2004; Sheppard *et al.*, 2005).

There are some other events related to NADPH oxidase activation including the generation of arachidonic acid by phospholipase A2 and binding of the NADPH to the assembled complex to finally initiate electron transfer.

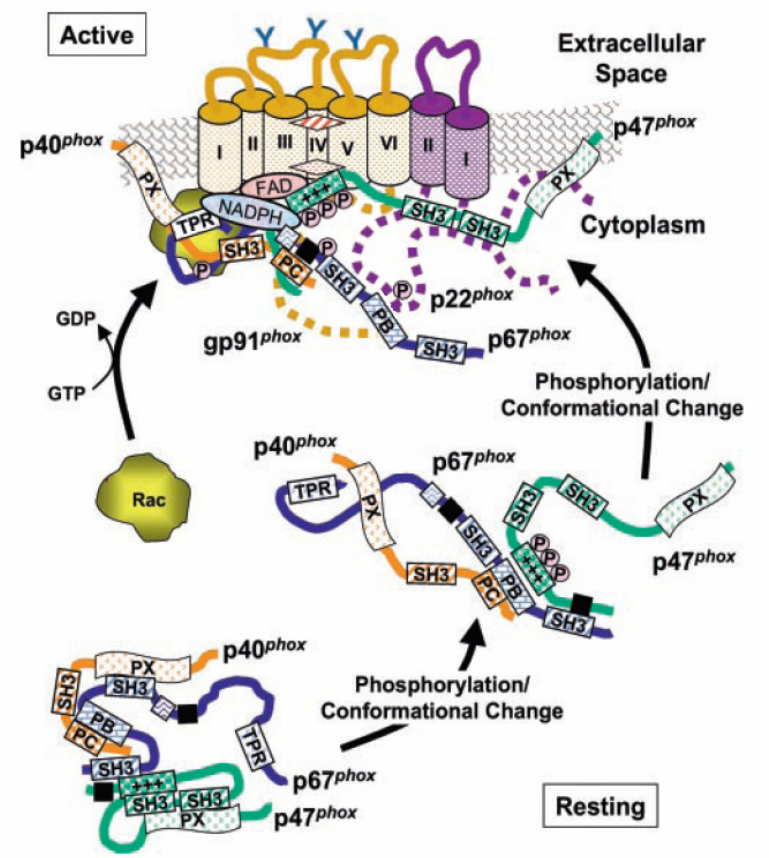

Fig. 3: Model for the activation and assembly of the NADPH oxidase. Changes in the phosphorylation state of $p47^{phox}$ induce unfolding from an autoinhibitory conformation. This leads to activation and to unmask essential binding domains. The exposure of PX domains of $p47^{phox}$ facilitates translocation to the cell membrane. Final interaction of the $p67^{phox}$ and Rac2 with flavocytochrome b_{558} induces conformational change, resulting in electron flow (Quinn and Gauss, 2004).

Thus, the oxidase becomes activated in the phagosomal membrane of neutrophils producing high concentrations of superoxide into this compartment with subsequent generation of additional ROS. Superoxide anion radical (O_2^-) can react to generate hydrogen superoxide (H_2O_2) in a reaction known as dismutation. In the presence of iron, superoxide and H_2O_2 react to generate hydroxyl radicals. In inflamed areas the phagocyte enzyme myeloperoxidase (MPO) form hypochlorous acid from H_2O_2 and chloride; as well as singlet oxygen, by catalyzing the oxidation of halide ions. Recently, it has been shown that also ozone can be generated by exposure of singlet oxygen to antibodies normally bound to microorganisms (Cross and Segal, 2004).

Although the high production of ROS is generally assumed to be the anti-microbial mechanism of polymorphonuclear (PMN) cells, some other theories have been described. It is possible that the depolarizing effect of ROS in the plasma membrane and its further compensating flux of H^+ and K^+ into the phagosome mediates killing of microorganisms through ionic activation of proteases (Reeves *et al.*, 2002).

Ultimately, the inactivation of the oxidase is the result of a shift in the balance between the activating and deactivating signals. The phosphorylation and hyperphosphorylation

of $p47^{phox}$, an increase in the rate of GTP hydrolysis on Rac2 and the disassembly of the complex are the major factors contributing to the termination of NAPDH oxidase activity (Decoursey and Ligeti, 2005).

A.1.4 Molecular defects

Mutations in one of the four genes coding for the essential subunits of the NADPH oxidase ($gp91^{phox}$, $p47^{phox}$, $p67^{phox}$ and $p22^{phox}$) lead to CGD (1:200.000 births).

Approximately 75% of the 410 known defects are due to mutations in the $gp91^{phox}$ gene (CYBB, GenBank accession number X04011). This gene maps to the X chromosome (Xp21.1 locus) resulting in an X-linked mode of inheritance. Therefore, males bearing a $gp91^{phox}$ mutation will be affected and females who inherited the mutation will be carriers. The carrier state for a $gp91^{phox}$ defect is also detrimental, depending on the percentage of normal neutrophils. During embryogenesis one of the two X chromosomes present in female cells undergoes lyonization, a random process of inactivation by packaging of one of the X chromosomes in repressive heterochromatin. This is required for the so-called dosage compensation, so that the female does not have double the amount of X chromosome gene products as compared to male individuals (Mills *et al.*, 1980). There appears to be no selective advantage for functional cells over non functional cells. Some female carriers presenting 5-10% functional cells are healthy whereas others have experienced symptomatology resembling CGD (Johnston *et al.*, 1985; Woodman *et al.*, 1995). These observations suggest that not only the presence of healthy cells is important, but also the levels of superoxide production within individual cells.

The remaining cases (about 25%) of CGD are autosomal recessively (AR-CGD) inherited and therefore equally distributed between males and females. About 25% of all AR-CGD cases are caused by mutations in the NCF1 gene (7q1.23 locus) which encodes the $p47^{phox}$ protein. Deficiencies in the NCF2 gene (1q25 locus) which encodes $p67^{phox}$ represent only about 5% of cases, and aberrant $p22^{phox}$ encoded by the CYBA gene (16q24 locus), are even less common.

Rac2 deficiency causes severe neutrophil dysfunction, actin dysfunction, predisposition to bacterial infections similar to CGD, and leukocyte adhesion deficiency type 1 (LAD-1), as observed in an infant with dominant-negative mutation in Rac2. Although Rac2 is not essential for superoxide formation, clearly there is an agonist-specific deficiency in oxidase function (Williams *et al.*, 2000). Moreover, genetic defects neither in $p40^{phox}$ nor in MRP8/14 have been reported for CGD so far.

About 95% of all mutations identified in these genes result in a complete absence or greatly reduced level of the corresponding protein. The mutations include partially or completely deleted genes, aberrant protein expression or mutations that affect mRNA

stability (Kaneda *et al.*, 1999). In the remaining 5% of cases the presence of a normal oxidase does not imply the absence of phenotype (Barese and Goebel, 2006). In these cases immunological crossreaction against the oxidase also leads to the absence of superoxide production. Alternatively, loss-of-function mutations possibly result in normal protein levels but they are inactive or only weakly active (Heyworth *et al.*, 2003). Therefore, a classification of several phenotypic subtypes depending on the expression level of the oxidase, assessed by immunoblot analysis, was established. The subtypes are referred to as X91, A47, A67, and A22, with superscripts ^{0}, $^{-}$, or $^{+}$ indicating absent, low or normal protein levels, respectively (Heyworth *et al.*, 2003).

A.1.5 Current therapy for CGD

The survival of CGD patients has vastly improved due to early diagnosis of the disease, advancements in identification of acute infections and their prompt and aggressive treatment with intravenous broad-spectrum antibiotics or antifungal drugs (for example, Amphotericin B and/or Intraconazol). Although lifelong prophylactic antibacterial handling has also been crucial for the observed reduction in the incidence of infections; the overall mortality is still about 5% per year for X-CGD patients and 2% per year for patients with AR-CGD (Assari, 2006; Barese and Goebel, 2006).

Recombinant human interferon gamma (IFN-γ) is used to treat CGD patients because it partially corrects the CGD phenotype in selected patients with low $gp91^{phox}$ activity (Ezekowitz *et al.*, 1988). Normally, IFN-γ is secreted from $CD4^{+}$ Th1 cells, $CD8^{+}$ cells, γ/δ T cells and activated NK cells. It plays a role in activating lymphocytes to enhance anti-microbial and anti-tumor effects. In addition it regulates the proliferation, differentiation, and the response of lymphocyte subsets. A follow up study of 76 patients demonstrated that the prolonged use of recombinant IFN- γ in CGD patients is safe and its administration correlates with a persistent reduction in the frequency of serious infection and mortality (Weening *et al.*, 1995). However, the mechanism by which IFN-γ may enhance oxidase activity is not well understood (Ahlin *et al.*, 1999; Ishibashi *et al.*, 2001).

As a disease that affects the myeloid cell compartment of the hematopoietic system, CGD has been cured by matched sibling or unrelated allogeneic bone marrow (BM) transplantation several times (Hobbs *et al.*, 1992; Ho *et al.*, 1996). In a retrospective study with 27 patients underwent human leukocyte antigen (HLA)-identical hematopoietic stem cell (HSC) transplantation after myeloablative conditioning. About 80% of the cases (22 of 27) reached a cure of the disease, even if pre-existing infections resistant to conventional therapies, inflammation or inflammatory sequelae were present. The overall survival rate was 89%; the 4 patients that died after transplantation belonged to a group of patients with one or more contra-indications. In one case the reinfused HSC cells did not engraft after immunosuppressive conditioning and had

autologous reconstitution. This implies that transplantation of unmodified HSC in combination with myeloablative regimen is a valid therapeutic option for CGD patients having an HLA-identical donor (Seger *et al.*, 2002).

If there is a lack of a suitable donor for the patients, allogeneic BM transplantation is not commonly recommended to treat CGD for several reasons. First, the limited availability of highly compatible donors. Second, the risk of infections during myeloablative conditioning and post-transplant immunosuppression. Third, the occurrence of graft-versus-host disease (GVHD). Therefore, the genetic modification of autologous hematopoietic stem cells represents a real alternative. Moreover, even correction of a minority of leukocytes could likely lead to a clinical improvement, since partial chimerism in X-CGD females carriers has been observed (Mills *et al.*, 1980; Johnston *et al.*, 1985) and after allogeneic bone marrow transplantation often lead to reduced or absent symptomatology (Kamani *et al.*, 1988; Hobbs *et al.*, 1992).

A.2 Gene therapy

Gene therapy is a promising biomedical technology that uses nucleic acid transfer, either RNA or DNA, to treat or prevent a disease (Mulligan, 1993). Gene therapy attempts to reach a direct, long-term curative effect by restoring the gene defect rather than to treat the symptomatology as almost all conventional therapies do. Although it was considered as a curative therapy *per se*, it may also be regarded as a complementing or an improving strategy for conventional therapies (Robbins and Ghivizzani, 1998).

Several diseases are proposed as good candidates for gene therapy. Cancer diseases represent almost 70% of all gene therapy trials up to date and the remaining 30% is shared between cardiovascular and neurological diseases, monogenic hereditary diseases and infectious diseases (preferentially HIV/AIDS) (Chuah, 2005).

There are many requirements for a successful gene therapy, including a clear understanding of the pathogenesis of the disease with extensive knowledge of the molecular defect(s), the availability of an effective therapeutic gene(s), an appropriate target tissue or cell for gene delivery, and an animal model that closely simulates the disease for preclinical studies (Robbins and Ghivizzani, 1998).

A gene therapy vector is a vehicle that delivers the therapeutic sequence into the patient's target cells. There are several vectors available and the choice of the most appropriate one for each particular disease is crucial for the outcome of the therapy. Many factors must be taken into consideration. One important factor determining the choice of vector type is the delivery method; e.g. if the gene transfer has to be done in the body of the patient by injection, inhalation or cutaneous application (*in vivo*) or if into subrrogate viable cells that have been temporarily removed from the patient and are subsequently transferred back into the target tissue (*ex vivo*) (Wood and Fry, 1999;

Selkirk, 2004). The *ex vivo* delivery is clearly more time consuming, expensive, and cumbersome, but permits selection of the genetically altered cells before re-implantation (Evans et al., 1998). Other factors that play a role in the selection of the best gene transfer system are i) the timing of expression needed (length or special time points), ii) the type and dividing state of the target cell, iii) the size of the transgene, iv) the efficient and easy production of the vector, v) the risk of an immune response against proteins encoded by the vector, vi) the requirement to administer the vector more than once and vii) the safety and regulatory issues (Wood and Fry, 1999; Pfeifer and Verma, 2001).

A.2.1 Gene transfer vector systems and their application

Several systems have been or are being developed ranging from non-viral vectors to viral-based vectors. Unfortunately, there is no such thing as a 'perfect universal vector'; the vectors that are currently available all have both advantages and disadvantages. Some of the actual vectors and their characteristics are represented in Table 1.

Table 1: Classification and characteristics of gene transfer vectors

Vector classification	Advantages	Disadvantages
Gammaretroviruses (ssRNA)	• Permanent integration • Well characterized • No immune response against vector • Long term expression • About 8 kb packaging capacity • Ease of production	• Infects only dividing cells • Insertional mutagenesis • Low titers
Lentiviruses (dsRNA)	• Permanent integration • Infects non-dividing cells • High titers • About 8 kb packaging capacity • Stable expression	• Insertional mutagenesis
Adenoviruses (dsDNA)	• High titers • Infects non-dividing cells • Up to 36 kb packaging capacity • Broad infectivity	• Life threatening immunogenicity • Short term expression • Does not integrate
Adeno-associated viruses (ssDNA)	• Broad infectivity • Infects non-dividing cells • Non-cytophatic • Stable expression • Low immunogenicity	• <5 kb packaging capacity • Limited integration (10% integrated and 90% episomal) • Lower transduction efficiency than adenovirus
Liposomes	• Avoids use of cytopathic virus • Cell-specific targeting	• Low efficiency of transfection
Ballistic delivery	• Simple method	• Requires "exposed" tissues or cells • Transient expression
Direct DNA injection	• Simple method	• Short-term expression

(Wood and Fry, 1999; Selkirk, 2004; O'Connor and Crystal, 2006)

The major advantages of non-viral vectors lie in the large size capacity for therapeutic DNA and in the fact that they are generally safer as they don't elicit major immune responses. Thus, at least theoretically, they represent the best choice. However, the drawbacks are three fold. These systems are far less efficient in nucleic acid transfer to the nucleus in comparison to viral vectors, the expression of transgene is transient and DNA vectors are rapidly inactivated in the presence of serum (Lechardeur and Lukacs, 2002; Witlox et al., 2007).

Up to date about 70% of the gene therapy trials have used viral vectors derived from naturally infecting viruses. The adenovirus-based vectors are the most commonly used vectors (25% of all the gene therapy trials). They are efficient vehicles with high transduction efficiency and high level of gene expression. However, their genetic material does not integrate into cell genome and is not replicated at cell division. Therefore, usage of these viruses is not appropriate for therapies which require transmission of the transgene also into the derivative cells (Evans *et al.*, 2001). Additionally, the adenoviral vectors are known to elicit strong immunogenic reactions, an undesired side effect which has promoted further improvement of the system. The most common strategy is based on deletion of all coding non-essential viral regions apart from the packaging signal and the inverted terminal repeats which are needed for genome packaging and replication. To generate viral particles of these so-called helper-dependent or gutless adenoviruses, all viral genes and the proteins needed for its genome replication, packaging and capside formation are supplied *in trans* by coinfecting the virus producing cells with helper virus. Although this system has reduced the immunogenicity and toxicity of these vectors and has increased the packaging capacity of transgenic DNA up to 36 kb, technical limitations make it extremely difficult to obtain vector stocks devoid of replication-competent particles. The replication-competent particles account for 0.1–1% of all of the viral particles present. This drawback may hinder their general use in clinical applications especially when high doses need to be administrated. These stocks may therefore be strongly immunogenic (Dai *et al.*, 1995; Schiedner *et al.*, 1998; Raper *et al.*, 2003). Nowadays, new systems are being developed to reduce or even avoid the packaging of the helper vector by flanking the packaging region of the helper virus with loxP sites or attP/attB sites, which are then induced to recombine in coinfected recombinase-expressing cells. Thus, the packaging region of the helper virus is eliminated avoiding packaging of the helper adenovirus (Ng *et al.*, 1999; Alba *et al.*, 2007).

In those cases where a steady protein expression in the target cell and its progeny is required only retroviral and adeno-associated viral (AAV) vectors are able to promote stable integration into the genome and therefore remain life-long within the cellular genome. It was previously observed that in the absence of a helper virus, wild-type AAV integrates by site-specific recombination into chromosome 19 of the host cell genome. Therefore AAV vectors were believed to mediate stable protein expression in

the target cell and its progeny by a site-specific integrative gene transfer mechanism (Coffin, 1992). However; recent data suggest that although AAV vectors drive long-term expression of the transgenes, they integrate randomly into the host genome at sites of dsDNA breaks in a very inefficient manner (Miller *et al.*, 2004). The majority of AAV vectors seems to persist in tissues as tandemly organized episomes formed by head-to-tail recombination (McCarty *et al.*, 2004) which are the responsibles for the long-term expression found in preclinical and clinical trials (Schnepp *et al.*, 2005; Choi *et al.*, 2006). Furthermore, AAV vectors display two more disadvantages limiting their possibility of application. Their restricted packaging capacity is less than 5 kb, and large-scale production of the virus is very inefficient (Seth, 2005).

In contrast to AAV, the proviral DNA of retroviruses efficiently integrates in the target cell genome, which is an essential step in their replication cycle. In this way, retrovirus-based vectors ensure chromosomal integration and life-long persistence of viral genomes into the infected cell and their daughters. However, it has been shown that retroviral vectors may also bring about untoward side effects related to their inherently mutagenic capacity after genome integration. This phenomenon is also known as insertional mutagenesis (for more details see *A.2.2.3 Self-inactivating retroviral vectors* and *A.2.3 Success and risks of gene therapy*).

Nevertheless, 23% of all gene therapy trials have used retrovirus-based vectors while AAV were used in only 3.7% of studies. These numbers underline the usefulness and success of the retroviral vectors in preclinical studies which is mainly due to the achieved therapeutic effect and its observed biological safety (Fig. 4).

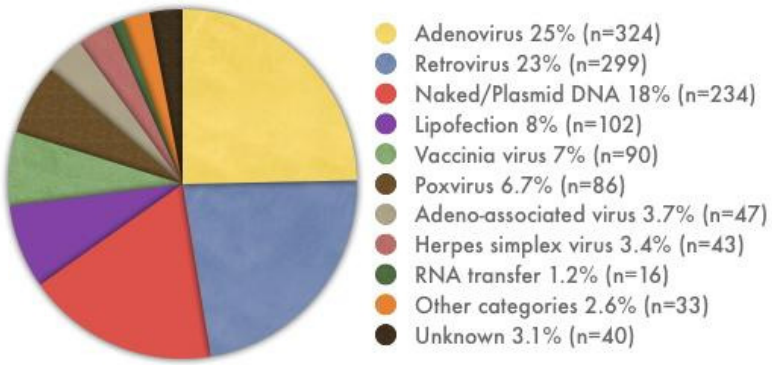

Fig. 4: Vectors used in Gene Therapy Clinical Trials.

http://www.wiley.co.uk/genetherapy/

A.2.2 Retroviral vectors

Retroviruses are RNA viruses belonging to the viral family of *Retroviridiae*. Some of them are pathogenic in humans leading to diseases such as immunodeficiencies and neurological disorders or malignancies. Retroviruses are classified into three genera: the gammaretroviruses including the Murine Leukemia Virus (MLV), the lentiviruses to

which classifies the Human Immunodeficiency Virus 1 (HIV), and the spumaviruses with the Human Foamy Virus (HFV) as prototype of the genus (Coffin *et al.*, 1997; Heneine *et al.*, 1998).

A.2.2.1 Retroviruses and their replication

Retroviruses are enveloped viruses that carry a 7–12 kb RNA genome which is linear, single-stranded, nonsegmented, and of positive polarity. Through the attachment of their surface glycoproteins (SU) to specific plasma membrane receptors, retroviruses enter the host cell. The association between SU and the receptor is a highly specific event, and is required to trigger a conformational change of the viral transmembrane (TM) protein (Fig. 5b).

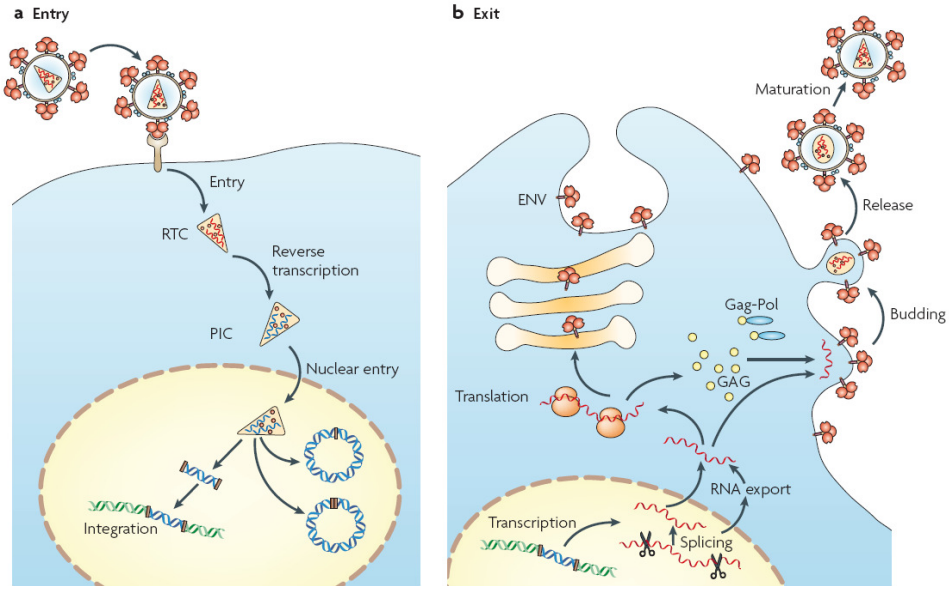

Fig. 5: The retroviral life cycle (Goff, 2007). See text for detailed information.

The fusion of the lipid bilayers of the cell with the viral membrane is initiated by this interaction (Coffin *et al.*, 1997), either directly at the cell surface or after internalization by an endocytic route (Mothes *et al.*, 2000; Katen *et al.*, 2001). This allows delivery of the virion core (RNA) into the cytoplasm. Reverse transcription of the viral RNA into double-stranded linear DNA is initiated in the cytoplasm in the context of a large complex; the reverse transcription complex (RTC). Viral DNA synthesis may be completed before (e.g. MLV) or after delivery into the nucleus (Fig. 5a). Delivery is supported by the formation of preintegration complexes (PIC) containing a double stranded DNA copy of the viral genome together with a number of viral and cellular proteins required for subsequent incorporation of viral DNA into the host's genome (Fassati and Goff, 2001). Upon integration, the provirus achieves the status of a cellular gene and can be transcribed by the cellular RNA polymerase II (Fig. 5b). The viral DNA is transcribed and the viral RNAs are processed and exported out of the nucleous into the cytoplasm by a highly, redundant, regulated mechanism. Three viral structural

protein precursors are translated in the cytoplasm and transported to the plasma membrane. Nascent virions are assembled from these proteins on host membranes, and immature particles are released from the cells. Finally maturation of the virions, results in a reorganization of the core and the acquisition of virus infectivity (Goff, 2007).

Retrovirus genomes commonly contain three essential genes, among other accessory genes. They encode three proteins with multiple functions in the mature virus.The *gag* protein directs the synthesis of internal virion proteins that form the matrix, the capsid, and the nucleoprotein structures. The *pol* protein codes for a reverse transcriptase, integrase and protease.The *env* protein is initially synthesized as a larger poly-protein from which the envelope proteins SU and TM are derived after translation. An additional, smaller, coding domain, *pro*, which encodes the virion protease is commonly found between *gag* and *pol* genes. *Gag*, *pro* and *pol* genes are transcribed in a single unique transcript, which undergoes posttranscriptional processing to generate the required proteins. The messenger RNA (mRNA) of *env* is a subgenomic RNA, created by alternative splicing of the polycistronic *gag*-, *pro*- and *pol*-coding mRNA (Fig. 6 and Fig. 7).

Two identical repeats, the long terminal repeats (LTR), are placed at both ends of the integrated proviral DNA. These noncoding sequences contain the major regulatory elements for viral gene expression (promoter, enhancer and polyadenylation signals) and can be divided into three elements: U3, R and U5. The promoter region, with the regulatory sequences such as the TATA box and the transcription start site are situated at the 5'LTR, and the polyadenylation signal is found at the boundary between R and U5 of the 3'LTR (Fig. 7).

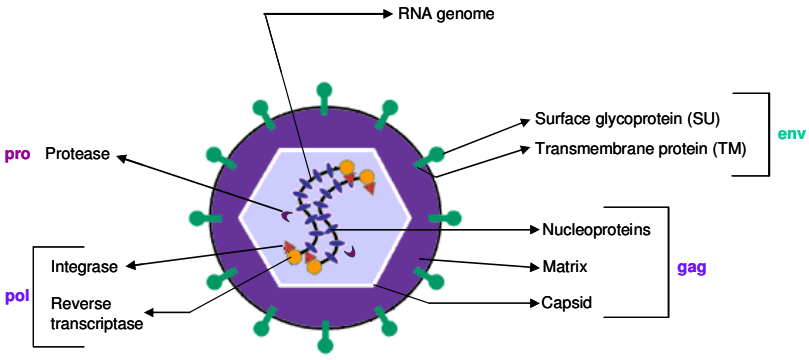

Fig. 6: Schematic representation of a retroviral particle. Two copies of the single stranded genomic RNA are packaged in a viral particle. The capsid contains the viral RNA in interaction with the nucleoproteins. Three enzymatic proteins (reverse transcriptase, protease and integrase) are also packaged into the capsid. The matrix interconnects the capsid with the outer envelope that is formed by a lipid bilayer of cellular origin in which complexes of viral proteins (SU and TM) are inserted.

The origin of the LTR duplications lies in the process of reverse transcription, where the enzyme jumps from one end of the template to the other. The new viral genomic RNA,

transcribed from the integrated DNA, spans the entire coding region and contains a sequence named *psi* (Ψ) which is important in the viral replication process. The Ψ sequence is located at the 5' untranslated region (5' UTR), or leader, and represents a packaging signal. Thus all Ψ-containing RNA molecules, and no other, are efficiently packaged into the new emerging virions (Coffin *et al.*, 1997). Furthermore, the leader region contains the primer binding site (PBS) and the splice donor site (SD) required as regulatory sequences for the splicing event that drives translation of the *env* gene. The PBS is the binding site for a transfer RNA that functions as the primer for reverse transcriptase which initiates synthesis of the minus (-) strand complementary to the viral RNA.

Gammaretroviruses depend on an actively dividing host cell for replication (Miller *et al.*, 1990). Viral entry and DNA synthesis can be completed at normal rate in all stages of the cell cycle. However, complete DNA integration is dependent on nuclear membrane disassemble during mitosis (Roe *et al.*, 1993). Besides gammaretroviruses, lentiviral PICs are able to penetrate the nucleus and mediate integration, also in non-dividing cells (von Schwedler *et al.*, 1994). Although nuclear localization signals and removal of capsid protein from the PICs have been proposed as mediators of this event, this process is still unclear (Dismuke and Aiken, 2006; Fassati, 2006; Hearps and Jans, 2006).

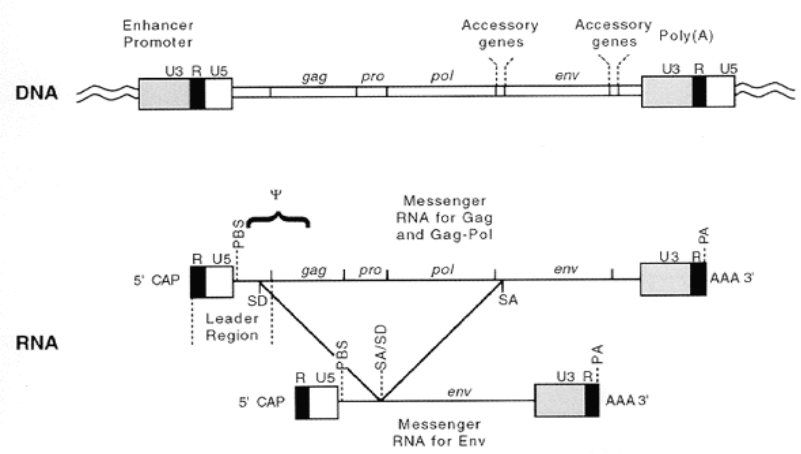

Fig. 7: Schematic representation of the generalized retrovirus genome. The proviral DNA integrated into the genomic DNA of the host cell is shown at the top. The genomic transcript is shown on the second line and the spliced messenger RNA for the Env protein is shown on the third line.

A.2.2.2 Gene therapy vectors derived from retroviruses

The extensive investigations and the obtained deep knowledge of the retroviral replication system have been crucial for the development of retroviral-based vectors. Safety issues and enhanced properties for both the transgene expression as well as the increase in titer of viral particles were achieved. The establishment of a three-component system, the pseudotyping of viral particles (transductional targeting),

the use of cis-actin modules for improvement of virus production and transgene expression and the transcriptional targeting of transgenes all contributed to the development of safe and efficient retroviral gene therapy vectors.

The three-component system was introduced as a result of the need for larger transfere inserts and safety reasons. This system consists in a three vector packaging design (Markowitz *et al.*, 1988). The vector construct carrying the transgene contains merely the LTR sequences needed for integration of the virus into the target cell and the Ψ signal for packaging the genomic viral RNA into the viral capsid. The *gag*, *pol*, and *env* genes, which are essential for the normal replication cycle, are separated onto two different plasmids (helper plasmids) in which the Ψ signal and LTRs are removed (Fig. 8).

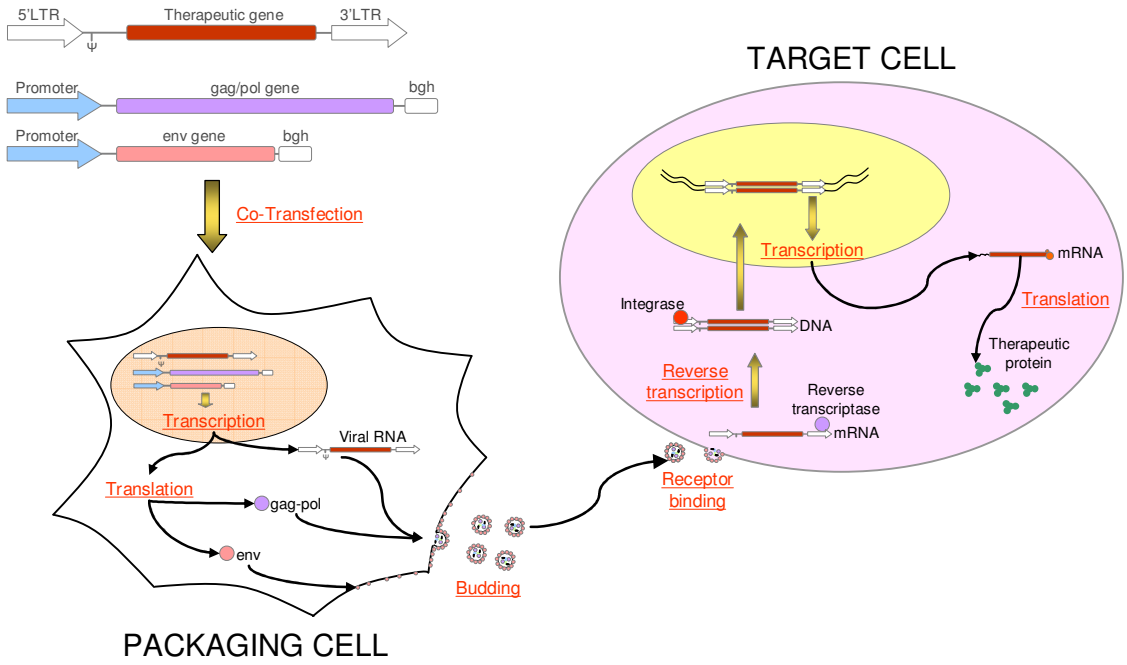

Fig. 8: Representation of gammaretroviral particle production and transduction of a target cell. See text for detailed information.

In the case of lentiviral vectors, viral accesory sequences are commonly included in the transfer and helper plasmid such as the Rev Response Element (RRE) and the *rev* gene sequence since they have shown to be involved in the cytoplasmatic accumulation of viral RNA (Coffin *et al.*, 1997). These three plasmids are then co-transfected into producer cells. The helper plasmids give rise to all the components required for formation of the new viruses. The retroviral vector is transcribed and encapsidated in the emerging virions. These new virions are able to infect cells and promote integration of the transgenes into the cellular genome, but no viral particles can be further generated (Fig. 8). This system not only offers more space for transgene sequences into the transfer vector, but also avoids the possibility of homologous recombination between the three plasmids which could give rise to replication-competent retroviruses (Miller and Buttimore, 1986; Miller et al., 1986b). Nowadays, there are some packaging cell

lines available which are stably transfected with the *gag*, *pol* and *env* genes. None of them contains the Ψ sequence avoiding the formation of replication competent particles after transient transfection of the transfer vector.

The host range of retroviral vectors is defined by the specificity of the SU/receptor interaction and can be expanded or altered by a process known as pseudotyping. Pseudotyped vectors consist of vector particles bearing glycoproteins (GPs) derived from other enveloped viruses. Such particles possess the tropism of the virus from which the GP was derived. However, not every combination of envelope GP and retroviral core give rise to highly infectious pseudotyped particles. The viral assembly and budding seems to be governed by the intracellular trafficking and the direct or indirect interaction between these two elements (GP and core) (Sandrin and Cosset, 2006; Bouard *et al.*, 2007).

Murine leukemia virus (MLV) core particles are efficiently pseudotyped with many surface proteins from most heterologous retroviruses and from many families of enveloped viruses (Kolokoltsov *et al.*, 2005). Among others, two envelopes are extensively used for pre-clinical and clinical studies due to their attractive cell tropism, the envelopes of Gibbon-ape Leukemia Virus (GaLV) and Feline Endogenous Virus (RD114). GaLV pseudotyped gammaretroviral vectors have shown great viral particle stability and excellent gene transfer efficiencies for primary T lymphocytes and human hematopoietic cell ($CD34^+$) (Bauer *et al.*, 1995; Bunnell *et al.*, 1995; Uckert *et al.*, 2000). RD114 pseudotyping has shown to promote efficient, single exposure transduction of human repopulating cells capable of establishing multilineage hematopoiesis in immunodeficient mice (Kelly *et al.*, 2001).

Vesicular stomatitis virus glycoprotein (VSV-G) is one of the most efficiently used envelopes for lentiviral vectors derived from Human immunodeficiency virus (HIV) and Simian Immunodeficiency Virus (SIV) (Sandrin *et al.*, 2004). VSV-G pseudotyping implies not only an efficient assembly and budding of viral particles but also expands the host range of cell and tissue types, and allows efficient concentration of virions to produce high-titer vector stocks (Akkina et al., 1996). However, it has two main drawbacks; the cellular toxicity if expressed continouslly at high levels and its inactivation in the presence of human serum (Cronin *et al.*, 2005).

The tropism of the RD114 and GaLV viruses is of great interest also for lentiviral vectors; however, these combinations of GP and transfer vector showed reduced infectivity. Therefore, an alternative to VSV-G pseudotyping was developed by replacing the cytoplasmatic tail of the RD114 and GaLV envelope with that of MLV GP or by replacing the *env* cleavage site sequence with a HIV protease site. Both strategies have been tested resulting in increased titers and preserving the host range of the former

GPs (Christodoulopoulos and Cannon, 2001; Sandrin *et al.*, 2002; Di Nunzio *et al.*, 2007).

Moreover, engineered peptide ligands are currently being developed for cell surface receptors into retroviral recombinant Env glycoproteins currently. This enhances the efficient targeting of specific cell types. However, these attempts are still hampered by low transduction efficiencies and further investigations are required (Maurice *et al.*, 2002; Verhoeyen *et al.*, 2005).

Known sequences that improve post-transcriptional processing and RNA transport from the nucleus into the cytoplasm are splice sites (SS), post-transcriptional regulatory elements (PRE) and the retroviral constitutive RNA transport elements (CTE).

Cellular pre-mRNAs that retain functional splice sites, are actively retained in the nucleus by splicing commitment factors (Chang and Sharp, 1989; Legrain and Rosbash, 1989). Efficient splicing may promote mRNA export and translation. Thus, introduction of SS creating artificial introns may increase the transgene expression level when placed in the 5' untranslated region (UTR) of the transgene (Huang and Carmichael, 1996; Luo and Reed, 1999).

On the other hand, unspliced-RNA is required to complete retroviral replication. Therefore many retroviruses have evolved several systems to evade the requirement for splicing in nuclear export of RNA. Complex retroviruses (including lentiviruses) use virally encoded proteins (e.g. the Rev protein of lentiviruses) to couple the export of intron-containing viral RNAs to the Crm1 pathway of the host cell. In contrast, simple retroviruses such as the gammaretroviruses act through cis-acting RNA export elements termed constitutive transport elements (CTE) which bind to the cellular tip-associated protein (TAP) (Bray *et al.*, 1994; Gruter *et al.*, 1998).

Besides the above mentioned systems, the PRE of woodchuck hepatitis virus (WPRE) has shown to act independently of transcription and splicing. With this element, the nuclear export of the viral RNA is directly coupled to the Crm1 pathway (Popa *et al.*, 2002). If the WPRE sequence is introduced into the 3' untranslated region of both gammaretroviral and lentiviral vectors it is possible to enhance both virus titer and transgene expression by 2-10 fold in many cell types (Ailles and Naldini, 2002; Kraunus *et al.*, 2004). The ability of the WPRE to act directly and independent of the presence or absence of the Rev system when positioned in the 3' UTR, indicates additional effects on the termination and/or polyadenylation process (Popa *et al.*, 2002). However; the use of the WPRE sequence also containing fragments of the promoter and protein coding sequences of the WHV X protein raised concerns about the safety in clinical applications (Kingsman *et al.*, 2005). Several studies have shown that expression of the X-gene is linked to liver oncogenesis under some circumstances (Terradillos *et al.*, 1997; Kim *et al.*, 1998). Therefore, a modified version devoid of promoter and residual

open reading frames (ORFs) was developed thereby reducing the potential harmful effects, but retaining the beneficial effects on titer and transgene expression (Schambach *et al.*, 2006a).

Cell- or tissue-specific transgene expression, also known as transcriptional targeting, may be achieved by utilization of tissue-specific regulatory sequences to induce the expression of the therapeutic genes only in a determined cell type. Conventional transcription from retroviral vectors is dependent on promoter and enhancer elements located in the U3 region of the LTR, which impel in almost all the cases, a constitutive expression. Although an independently controlled transcriptional unit can be introduced in the backbone, the expression obtained is usually influenced by the activity of the LTR. Some strategies have been proposed to solve this problem. One approach is the replacement of the constitutive transcriptional control elements (promoter and enhancers) within the U3 region of the retroviral LTR with cell-specific promoter sequences (Moore *et al.*, 1991; Ferrari *et al.*, 1995; Diaz *et al.*, 1998; Jager *et al.*, 1999). Another alternative is the use of a self-inactivating vector configuration (see below). In this case an internal promoter is required to drive transgene expression since SIN-vectors originate integrated proviruses lacking the LTR promoter/enhancer sequences (Yu *et al.*, 1986; Dai *et al.*, 2004; Almarza *et al.*, 2007).

A.2.2.3 Self-inactivating retroviral vectors

As already mentioned, the integration of retroviral vectors in the host genome could lead to the transactivation of hit genes due to the presence of enhancer/promoter elements in the LTRs. If the retroviral insertion occurs near to, or into proto-oncogenes this might lead to clonal dominance or even malignant transformation. Recent preclinical and clinical studies have demonstrated that the potential of the insertional mutagenesis event to generate clonal imbalance or leukemic outgrowth is even higher than predicted (Otsu *et al.*, 2000; Soudais *et al.*, 2000). This difference is due to the semi-random integration pattern of the used vectors. MLV derived vectors strongly tend to integrate in transcriptional units preferentially near transcriptional start sites and CpG islands whereas HIV-1 and related lentiviral vectors favor insertions within the transcribed regions (Laufs *et al.*, 2003). Recently these differences have been mainly attributed to the integrase gene and associated cellular factors (Lewinski *et al.*, 2006). Both insertional strategies may be deleterious and most likely deregulate expression of the affected gene or disrupt active transcription units in the case of lentiviral vectors.

To prevent undesired transcriptional effects on the internal transgene and hit genes caused by the enhancer and promoter in the LTRs, self-inactivating vectors were constructed by deleting the transcriptional enhancers and promoter in the U3 region of the 3' LTR. After one round of vector replication, these changes are also copied into both the 5' LTR producing an inactive provirus. The transcription of the therapeutic

gene should then be driven by an internal promoter placed downstream of the RNA packaging signal and immediately upstream of the transgene (Yu *et al.*, 1986; Dougherty and Temin, 1987; Hawley *et al.*, 1987).

The first drawback of this strategy is the suboptimal RNA processing that leads to a lower virus titer obtained with the self-inactivating vectors in comparison with their LTR-driven counterparts (at least ten-fold lower). Lower titers implies higher manipulation of target cells which could lead to a decrease in the repopulation capacity (Guenechea *et al.*, 2000; Puig *et al.*, 2002). Moreover, the concentration of infectious virions was found to be critical since higher virus titers promote more efficient transduction than promoted by a longer exposure to a large volume of virus suspension with a low titer (Miller *et al.*, 1986a; Hogge and Humphries, 1987). This problem was solved by the incorporation of cis-acting modules to enhance both RNA processing in packaging cells and transgene expression (see above). With this strategy new vectors were designed with an increased safety and enhanced viral particle production (Schambach *et al.*, 2000; Schambach *et al.*, 2006c). *In vitro* studies with primary hematopoietic cells infected with SIN viral vectors containing a strong internal promoter still have transforming abilities caused by insertional mutagenesis, but this occurred with significantly lower frequency than their LTR-driven counterparts (Modlich *et al.*, 2006). Additionally, recent studies have shown that the characteristics of the internal promoter used are also an important issue. For example, the incorporation of more physiological promoter sequences (such as the human elongation factor 1α promoter (Schambach *et al.*, 2006b)) or promoters which are less dependent on enhancer elements may further decrease the potential of insertional activation (Baum *et al.*, 2004).

The onset and harmfulness of clonal imbalances, both non-malignant and malignant, might be associated with the up-regulation of a cellular proto-oncogene near the integration site as well as due to several characteristics of the virus used. They include vector dose (copy number f the vector in the cellular genome), the effects caused by the expression of the transgene (Li *et al.*, 2002) and/or other elements within the vector backbone, which are likely to be context dependent (Baum *et al.*, 2004). Moreover, it is clear that not only the vector sequence and the insertion site prompt a clonal imbalance, but that other factors, such as genetic and epigenetic lesions, pre-existing self-renewal potential, age of the treated patients, etc., may also play and important role. The conjunction of all these factors ultimately influence the fate of the gene-corrected cell clones *in vivo,* whereby those cells with a selective advantage are clearly favoured (Baum, 2007b).

A.2.3 Success and risks of gene therapy

In 1989 Rosenberg and colleagues launched the first well-documented gene therapy study with melanoma patients treated with retrovirally transduced tumor-infiltrating

lymphocytes encoding the antibiotic resistant gene neomycin (Rosenberg *et al.*, 1990). One year later, in 1990, the first therapeutic human gene trial was approved. Two children suffering from a severe combined immunodeficiency (SCID) caused by a genetic defect in the purine catabolic enzyme adenosine desaminase (ADA) were enrolled in the study. In the patients, large amounts of deoxyadenosine, an ADA substrate, accumulate intra- and extra-cellularly. In T-cells, this product is preferentially converted into the toxic compound deoxyadenosine triphosphate in T-cells, leading to defective T- and B-cell functions. Unfortunately, gene therapy failed in these two patients. They received polyethylene glycol-ADA (PEG-ADA) as enzymatic substitution as well as infusion of autologous, genetically modified T-cells transduced with a retroviral vector encoding ADA, a setting likely to abrogate the selective advantage conferred to the transduced cells (Blaese *et al.*, 1995).

These first clinical gene therapy trials served as a proof of principle for the safety and feasibility of gamma-retroviral gene transfer in peripheral blood leucocytes (PBLs) or hematopoietic stem cells (HSCs). Since then, over 1200 trials have been completed, are ongoing or have been approved world wide (Edelstein *et al.*, 2004).

The first successful clinical trial has been performed in patients with X-linked severe combined immunodeficiency (X-SCID) by the groups of Drs. M. Cavazzana-Calvo and A. Fisher in Paris in 1999 (Cavazzana-Calvo *et al.*, 2000). X-SCID patients generally present an early block in T and natural killer (NK) lymphocyte differentiation associated with mutations of the gene encoding the gamma chain (γ_c) cytokine receptor subunit. γ_c is an essential part of the interleukin-2, -4, -7, -9, -15 and -21 receptors, which participate in the delivery of growth, survival, and differentiation signals to early lymphoid progenitors. Although, patients with X-linked SCID generally have normal B-cells numbers they function poorly, because of the lack of T-cell. X-SCID is invariably fatal if therapeutic bone marrow transplantation is not performed. Ten X-SCID children, who met the eligibility criteria, where chosen for the clinical trial. Autologous $CD34^+$ cells were transduced *ex vivo* with a Moloney MLV (Mo-MLV)-based vector carrying the γ_c chain gene. The cells were then transplanted into the patients by infusion. 9 out of 10 patients, who received more than $1x10^6$ gene corrected cells/kg, developed a functional adaptive immune system. The strong selective advantage observed for the transduced lymphocyte precursors was the crucial factor for the positive outcome of the therapy (Cavazzana-Calvo *et al.*, 2000; Fischer *et al.*, 2000). However, between 2002 and 2005 three of the 9 successfully treated children developed a clinical disease related to the uncontrolled proliferation of mature or immature T cells with leukemia-like characteristics. One of the patients did not respond to the treatment and died from a relapse of this complication. Subsequent studies revealed, in two of the three cases, malignant T-cell leukemia clones carrying proviral integrations within or near to the LMO2 oncogene (Hacein-Bey-Abina *et al.*, 2003b). LMO2 encodes a cysteine-rich protein with two LIM-domains that has a central and crucial role in

hematopoietic development and is highly conserved. There is a tissue-specific negative regulator in the promoter region (Hammond *et al.*, 2005) and its specific role in T-cell tumorigenesis results from a reprogramming of gene expression after enforced expression in T-cell precursors (McCormack *et al.*, 2003).

The strong enhancer activity of the LTR leading to ectopic expression of the endogenous hit genes, but not the conjunction with the effect of the therapeutic transgene, was responsible for the development of the leukemia-like lymphoproliferative disease (Thrasher *et al.*, 2006; Pike-Overzet *et al.*, 2007). Nevertheless, the overall success rate of the gene therapy and the frequency of accompanying side effects should be considered in relation to the mortality rate of X-SCID patients who undergo unrelated allogeneic transplantation, which is about one third of the treated patients (Haddad *et al.*, 1998).

Several clinical trials were later performed evaluating the efficacy and feasibility of the gene therapy (Aiuti *et al.*, 2002). The adverse events have led to a more accurate analysis of the risks raised by these vectors (genotoxicity) and to the development of chromosomally integrating vectors with reduced risks of oncogenesis (SIN vectors).

A.3 Gene therapy for CGD

As mentioned in the begining CGD is a primary immunodeficiency disease resulting from a monogenetic defect of the hematopoietic system. Although significant improvement in the life expectancy of patients occurred with the use of antimycotics, broad-range antibiotics and/or recombinant IFN-γ in combination with a early diagnosis of the disease (Cale *et al.*, 2000), CGD is still associated with high morbidity and mortality (Winkelstein *et al.*, 2000).

HSC transplantation is a highly recommended treatment in those cases where a HLA-identical donor exists even with active infections that are refractory to conventional therapy. However, the availability of such a suitable donor is limited and the HSC transplantation with a non-matched donor is inadvisable due to the high mortality rates. Therefore, the genetic modification of autologous HSC by gene therapy, is proposed as a curative and reasonable alternative treatment of the disease in patients lacking a compatible donor (Barese *et al.*, 2004).

The firsts gene therapy trials for CGD were initiated in 1995 based on the observation that reconstitution of NADPH oxidase activity can be achieved *in vitro* and *in vivo* by means of transduction with retroviral vectors carrying the defective gene of the enzymatic complex (Pollock *et al.*, 1995; Mardiney *et al.*, 1997). Preclinical *in vitro* experiments have shown the restoration of oxidase activity in Epstein-Barr virus (EBV)-transformed B cell lines obtained from the 4 subgroups of CGD patients as well as in human myeloid leukemia X-CGD cell line generated by gene knock out of $gp91^{phox}$

in PLB-985 cells (Zhen *et al.*, 1993; Chanock *et al.*, 1996). CGD human bone marrow progenitor ($CD34^+$) cells have also been used to assess the restoration of NADPH oxidase activity with retroviral vectors. These cells were first transduced with vectors carrying the corresponding therapeutic gene and then *in vitro* differentiated to granulocyte-like cells. These experiments showed that high and stable reconstitution of the respiratory burst *in vitro* can be obtained in gene corrected X-CGD $CD34^+$ patient derived cells (Becker *et al.*, 1998; Ott *et al.*, 2002). Moreover, transplantation of transduced X-CGD $CD34^+$ peripheral blood stem cells (PBSC) into non-obese diabetic/severe combined immunodeficient mice (NOD/SCID) achieved up to 22% corrected human neutrophils *in vivo* (Brenner *et al.*, 2003). Knockout mouse models have also served to ensure the ability of the gene corrected cells to ward off occurring infections by challenging experiments. The mice were also used to define the required percentage of corrected neutrophils to achieved clear protection against frequently infecting agents (Mardiney *et al.*, 1997; Dinauer *et al.*, 2001).

Dr. H. L. Malech and colleagues conducted the first two human clinical gene therapy trials for CGD. The first trial included 5 adult patients suffering from $p47^{phox}$ deficiency and 5 X-CGD patients were treated in the second study. In these trials no conditioning was used prior to reinfusion of the gene modified, mobilized autologous $CD34^+$ HSCs (Malech *et al.*, 1997; Malech, 2000). Although gene transfer efficiencies were estimated to be high *in vitro*, the percentage of corrected granulocytes *in vivo* did not reach 1% and rapid decrease over time was observed. Various modifications were introduced in the second trial. The use of flt-3 ligand and GM-CSF for the mobilization procedure instead of G-CSF, the use of RetroNectin to co-localize target cells and virions (Hanenberg *et al.*, 1996; Moritz *et al.*, 1996) and to avoid the negative effect of supernatant components (Kuhlcke *et al.*, 2002). Transduction was performed for 4 days instead of 3 and the multiple cycles of mobilization-infusion. Although all these modifications slightly increased the gene transfer efficiency, it was not possible to reach effective levels *in vivo* (Malech *et al.*, 2004).

These results emphasized the need for improved transduction efficiencies by optimization of the cytokines that need to be used, improving RetroNectin-based transduction, optimization of pseudotyping and by the use of “activated” cells (Kiem *et al.*, 1998; Uchida *et al.*, 1998). Moreover, in contrast to the SCID diseases, the functional NADPH oxidase does not confer any survival or proliferative advantage. Therefore a bone marrow conditioning of the recipient prior to reinfusion might help increasing the engraftment capacity of the modified repopulating cells (Malech and Hickstein, 2007).

In 2004 the groups of Dr. M. Grez and Prof. R. A. Seger conducted a successful clinical CGD gene therapy trial. Long-term high-level oxidase activity was restored in two X-linked CGD patients by *ex vivo* retroviral-mediated gene transfer (Ott *et al.*, 2006). A

major difference between this study and former studies was the myelosuppressive conditioning regime using busulfan applied to the patients prior to reinfusion of the gene corrected cells. Transduction efficiency, measured as $gp91^{phox}$ expressing $CD34^+$ cells, achieved 45.2% and 39.5% respectively. Thereafter, 15% gene corrected granulocytes were detected at day +65 and +84, respectively. These levels of gene marked cells where sufficient to eradicate previous existent bacterial and fungal infections, which were refractory to conventional therapy in both patients. Furthermore, between the 2nd and 8th month after gene therapy, corrected granulocytes expanded to over 55% and 48% respectively and stabilized at that level for more than a year. Analysis of the clonality of the marked cells at this plateau phase by linear-amplification mediated PCR (LAM-PCR) (Schmidt *et al.*, 2002) revealed that only a minority of clones contributed to hematopoiesis. This clonal dominance is not likely due to the transgene and neither to the busulfan conditioning because in former clinical trials, nor $gp91^{phox}$ as transgene alone and neither busulfan conditioning treatment alone conferred any selective advantage to gene marked clones (Aiuti *et al.*, 2002; Barese *et al.*, 2004). Indeed, the most predominant clones were associated with and appeared to be activated by vector insertion in one of three genes, MDS1-Evi1, PRDM16 or SETBP12. These genes are involved in myeloid cell growth and differentiation, and their activation by vector integration provided them a selective advantage (Ott *et al.*, 2006). MDS/Evi1 has previously been related to severe clonal imbalance and even malignant processes in murine models due to retroviral insertion (Kustikova *et al.*, 2005; Modlich *et al.*, 2005). In contrast, rhesus macaques engrafted with retroviral vector transduced $CD34^+$ cells showed 14 MDS/Evi1 insertions in 9 different animals, without evidence of clonal expansion of these MDS/Evi1 hit population.

The high frequency of integrations in a particular locus, regardless of the dysregulation of the expression, suggests that there might be a cluster of retroviral insertion which cannot be due to chance (Calmels *et al.*, 2005). It indicates that the retroviral insertion alters the self-renewal or hematopoietic fitness potential of HSCs following integration (Stein *et al.*, 2006). Nevertheless the expansion of gene marked cells provided a substantial therapeutic benefit since this phenomenon strengthened the immune response against new bacterial and fugal infecting pathogens of both patients.

However, despite of the positive results one of the patients died almost two years after transplantation due to a colon perforation which led to a severe bacterial sepsis. The cause of death is still under investigation but the observation that the percentage of expressing cells decreased over the time although maintaining constant numbers of proviral integrations points out the silencing of the transgene as responsible mechanisms for a loss in oxidase function (Dr. M. Grez, pers. commun.).

In 2005 Prof. R. A. Seger and colleagues treated a 5 year old boy using again the same protocol (conditioning, dose and gene transfer vector). Although the levels of

superoxide producing cells did not reach 6% after transplantation and decreased until almost undetectable levels, the therapeutic benefit was even clearer. The treatment helped to cure a cord compression due to a fungal infection leading to an excellent improvement in the clinical situation of the patient.

These data indicated that gene therapy can be considered as a curative therapy *per se* with great therapeutic potential and also as a temporary treatment until a subsequent BMT is feasible in late stage disease patients. However, there is still the requirement for new safer gene transfer vector with improved performance for later clinical applications.

A.4 Aims of the present study

Insertion of self-inactivating retroviral vectors in the host genome offers a major advantage for gene therapy due to their estimated reduced genotoxicity. Therefore, the aim of the present study was the generation of $gp91^{phox}$ driving, self-inactivating retroviral vector for the efficient transduction and functional reconstitution of the NADPH oxidase activity in X-CGD cell lines and in an X-CGD mouse model. The following objectives were tackled:

- Increase the biological safety of gene transfer as a therapy for CGD by constructing a self-inactivating retroviral vector encoding the $gp91^{phox}$ gene.
- Efficient transduction of X-CGD PLB-985 human derived cells which can be used as a model to study gene therapy of CGD using the retroviral vector.
- Analysis of the NADPH oxidase activity in the transduced X-CGD PLB-985 cells.
- Assess the tissue specificity of myeloid-specific promoters in the context of SIN vectors both *in vitro* and *in vivo* using the X-CGD cell line and mouse model.
- Evaluate the *ex vivo* and *in vivo* reconstitution of the oxidase activity after transduction of primary murine X-CGD $Sca\text{-}1^{+}$ and Lin^{Neg} cells.

B. MATERIALS AND METHODS

B.1 Equipment and Necessary Materials

Ajustable Pippetors - Pipetman		Gilson, BadCamber, Germany
Autoclave		Integra Biosciences, Baar, Switzerland
Autoradiography-film	HyperfilmTM MP	Amersham Pharmacia, Little Chalfont, UK
	Kodak BioMac MS	Sigma-Aldrich, Steinheim, Germany
Balance – EMB600-2		Kern and Sohn GmbH, Germany
Biodyne B positively-charged nylon 6.6		Pall Corporation, Darmastadt, Germany
Blooting Paper		Carl Roth GmbH and Co., Karlsruhe, Germany
Bright Star-Plus® Membrane #AM10104		Ambion Inc., Cambridgeshire, UK
Electrophoresis Combs		Bio-Rad Laboratories Inc, Munich, Germany
Electrophoresis Trays		Bio-Rad Laboratories Inc, Munich, Germany
Hypercassette™		Amersham Pharmacia, Little Chalfont, UK
Horizontal gel electrophoresis chamber – DNA SubCell™		Bio-Rad Laboratories Inc, Munich, Germany
Electrophoresis chamber for SDS-PAGE - Mini Protean 3		Bio-Rad Laboratories Inc, Munich, Germany
Intensifying screens		Amersham Pharmacia, Little Chalfont, UK
Hybridization tubes		Appligene Oncor, Illkirch, France
Hyb-oven		Gesellschaft für Labortechnik GmbH, Burgwedel, Germany
Thermomixer comfort		Eppendorf GmbH, Wesseling-Berzdorf, Germany
Immobilon-FL PVDF #FL00010		Milipore, Billerica, MA
Liquid scintillator analyzer #TRI-CARB® 1500		Packard, Frankfurt am Main, Germany
1.5 and 2 ml Microcentrifuge tubes		Eppendorf, Hamburg; Sarstedt, Nümbrecht, Germany
Microspin S-300HR Columns #27-5130-01		Amersham Biosciences, Freiburg, Germany
NucAway™ spin Columns #AM10070		Ambion Inc., Cambridgeshire, UK
PCR-block		(GeneAmp 2400) Perkin-Elmer, Weiterstadt, Germany
Ph-meter		Knick, Berlin, Germany
Pipete helper – Pipetus®-akku		Hirschmann Laborgeräte, Eberstadt, Germany
Power Source – Power Pac300		Bio-Rad Laboratories Inc, Munich, Germany
Spectra MAX 340 reader		Molecular Devices
Stratalinker™ 1800		Stratagene Company, Zuidoost, Netherlands
Thermomixer comfort		Eppendorf GmbH, Wesseling-Berzdorf, Germany
Vortexer		Janke and Kunkel, Staufen, Germany
Water bath		Gesellschaft für Labortechnik, Burgwedel, Germany

B.2 Materials for Molecular Biological Experiments

B.2.1 Chemicals, Enzymes and Reagents for Molecular Biological Experiments

Acetic acid	Carl Roth GmbH and Co., Karlsruhe, Germany
AEBSF #A8456	Sigma Aldrich, Taufkirchen, Germany
Agarose Electrophoresis Grade #15510.027	Invitrogen Corporation, Scotland, UK
Ammonium acetate – NH_4OAc	Carl Roth GmbH and Co., Karlsruhe, Germany
Ampicillin	Roche, Mannheim, Germany
Ampli-Taq-DNA-polymerase	Biosystems, Weiterstadt, Germany
Antarctic Phosphatase #M0289L	New England Biolabs, Inc., Inc. GmbH, Frankfurt a

APS (ammonium peroxydisulfate)	Merck, Darmstadt, Germany
Boric acid – H_3BO_3	Carl Roth GmbH & Co., Karlsruhe, Germany
Bromphenolblue #B8026	Sigma Aldrich, Taufkirchen, Germany
Bradford-reagent	Bio-Rad Laboratories, Inc., CA, USA
B-mercaptoethanol #M3148	Sigma Aldrich, Taufkirchen, Germany
Chloridric acid - HCl #4625.1	Carl Roth GmbH & Co., Karlsruhe, Germany
Chloroform	Carl Roth GmbH & Co., Karlsruhe, Germany
Chymostatin #C-726878	Sigma Aldrich, Taufkirchen, Germany
DEPC (Diethyl Pyrocarbonate) #D5758	Sigma Aldrich, Taufkirchen, Germany
DNA Polymerase I, Large (Klenow) Fragment #M0210S	New Engl& Biolabs, Inc., Frankfurt a M , Germany
DNeasy™ Tissue Kit	Carl Roth GmbH & Co., Karlsruhe, Germany
Dried milk powder	Carl Roth GmbH & Co., Karlsruhe, Germany
EDTA #4706.1000	AppliChem, Darmstadt, Germany
Ethanol, 100% #T1713	Carl Roth GmbH & Co., Karlsruhe, Germany
Ethidium Bromide #2218.2	Carl Roth GmbH & Co., Karlsruhe, Germany
Formaldehyde loading dye #8552	Ambion Inc., Cambridgeshire, UK
Glycerine #3783.1	Carl Roth GmbH & Co., Karlsruhe, Germany
Glycine	Carl Roth GmbH & Co., Karlsruhe, Germany
Glycogen #901393	Roche, Mannheim, Germany
Hyb Hybridization Buffer	Ambion Inc., Cambridgeshire, UK
IPTG (Isopropyl-β-D-1-thiogalactopyranoside)	Sigma Aldrich, Taufkirchen Germany,
Isopropanol	Carl Roth GmbH & Co., Karlsruhe, Germany
JumpStart™ REDTaq® ReadyMIX™ PCR Reaction Mix #P0982	Sigma Aldrich, Taufkirchen, Germany
Leupeptin #1017101	Roche Diagnostics, Indianapolis, USA
LB Agar #22700-025	Life Technologies, Karlsruhe, Germany
LB Broth Base #12780-029	Life Technologies, Karlsruhe
Magnesium chloride	Perkin Elmer, Weiterstadt, Germany
MAXIscript® Kit #AM1316	Ambion Inc., Cambridgeshire, UK
Methanol	Carl Roth GmbH & Co., Karlsruhe, Germany
MicroSpin S-300 HR Columns	Amersham Biosciences, Freiburg, Germany
NEBlot® Kit #N1500S	New England Biolabs, Inc., Frankfurt a M, Germany
NorthernMax® Kit #AM1940	Ambion Inc., Cambridgeshire, UK
NucAway™ columns	Ambion Inc., Cambridgeshire, UK
NucleoSpin®RNA II Kit #740955.50	Macherey-Nagel Inc., Düren, Germany
Phenol/Chloroform/Isoamylalcohol (25:24:1)	Carl Roth GmbH & Co., Karlsruhe, Germany
Pfu Turbo DNA-polymerase	Stratagene Company, Amsterdam, The Netherlands
PMSF (phenylmethylsulfonyl fluoride) #P7626	Sigma Aldrich, Taufkirchen, Germany
Potassium acetate – KAc	Sigma Aldrich, Taufkirchen, Germany
Potassium chloride – KCl	Carl Roth GmbH & Co., Karlsruhe, Germany
Potassium phosphate – KH_2PO_4	Carl Roth GmbH & Co., Karlsruhe, Germany
pTRI RNA 18S #AM7339	Ambion Inc., Cambridgeshire, UK
QIAquick- gel extraktion kits	Qiagen GmbH, Hilden, Germany
QuikChange®Site-Directed Mutagenesis Kit #200519	Strategene, La Jolla,
Restriction endonucleases	New England Biolabs, Inc., Frankfurt, Germany
RNase A	Sigma Aldrich, Taufkirchen, Germany

RotiLoad loading buffer		Carl Roth GmbH & Co., Karlsruhe, Germany
Rotiphorese® Gel 30		Carl Roth GmbH & Co., Karlsruhe, Germany
Roti®szint ecoplus #0016.2		Carl Roth GmbH & Co., Karlsruhe, Germany
Size Marker	Protein	BenchMarkTM Prestained Protein Ladder Invitrogen Corporation, Karlsruhe, Germany
		Bio-Rad Laboratories, Inc., CA, USA
	DNA	Smart Ladder; Eurogentec, Seraing, Belgium
		2-Log Ladder, NEB Inc., Frankfurt a.M., Germany
	RNA #15623-200	Invitrogen Corporation, Karlsruhe, Germany
Sodium chloride – NaCl #9265.2		Carl Roth GmbH & Co., Karlsruhe, Germany
Sodium hydroxide – NaOH #6771.1		Carl Roth GmbH & Co., Karlsruhe, Germany
Sodium phosphate – Na_2HPO_4		Carl Roth GmbH & Co., Karlsruhe, Germany
SuperScript™Reverse transcriptase		Invitrogen Corporation, Scotland, UK
SuperSignal ® West Pico Chemiluminescent Substrate #34080		Pierce, Rockford, USA
TEMED (N,N,N',N'-Tetramethylethylendiamin)		Carl Roth GmbH & Co., Karlsruhe, Germany
Tris #AE15.2		Carl Roth GmbH & Co., Karlsruhe, Germany
Tris HCl		Carl Roth GmbH & Co., Karlsruhe, Germany
Triton X-100		Sigma, Taufkirchen, Germany
T4 DNA-ligase		New England Biolabs, Inc., Frankfurt, Germany
10x SDS #24730.020		Gibco, Scotland, UK
10x SSC #15557.044		Invitrogen Corporation, Scotland, UK
10x TBE #15581.026		Invitrogen Corporation, Scotland, UK

B.2.2 Antibodies (Ab) for Molecular Biological Methods (Western Blot)

Actin (I-19): sc-1616	Santa Cruz Technologies
MoAb48 (Verhoeven *et al.*, 1989)	Kindly provided by Dick Roos
IRDye 800 Conjugated Goat (polyclonal) Anti-Rabbit IgG # 926-32211	LI-COR Bioscience GmbH Bad Homburg, Germany
IRDye 680 Conjugated Goat (polyclonal) Anti-Rabbit IgG # 926-32220	LI-COR Bioscience GmbH Bad Homburg, Germany

B.2.3 Oligonucleotides

B.2.3.1 Primer for PCR

$Gp91^{phox}$ wild-type cDNA (human)	
5'-Primer (gp-for-01)	TTGTACGTGGGCAGACCGCAGAGA
3'-Primer (gp-rev-02)	CCAAAGGGCCCATCAACCGCTATC
β-actin cDNA	
5'-Primer (ACT5')	ATGATATCGCCGCGCTCGTCGTC
3'-Primer (ACT3')	TTCTCGCGGTTGGCCTTGGGGTTCAG
Synthetic $gp91^{phox}$ cDNA (human)	
5'-Primer (gp91S-2for)	AAAGAGTGCCCCATCCCCCAGTTC
3'-Primer (gp91S-2rev)	CGCCCACGATTCTGATGT
GAPDH	
5'-Primer (GAPDH/5)	ACCACAGTCCATGCCATCAC
3'-Primer (GAPDH/3)	TCCACCACCCTGTTGCTGTA

B.2.3.2 Oligonucleotides for Cloning

Gp91^{phox} wild-type cDNA – Modified primers to mutate the cryptic splice acceptor	
5'-Primer (BM-P9)	GCTGTCCTTCCTC**C**GGGGTTCCAGTGCG
3'-Primer (BM-P10)	CGCACTGGAACCCC**G**GAGGAAGGACAGC
Leader 11 – Modified primers to introduce a NotI cleavage site at the 3' end	
P1 – standard primer also used for sequencing	GGAGGTTCCACCGAGATTTGG
BM-P7 – modified primer	GCAGCTAGCTGCGGCCGCTATTTTC
MRP8 intron – Modified primers to introduce a NdeI cleavage site at both ends of the first	
5'-Primer (BM-P1)	GCATATGGATCCTTGGGGAGGGTCAGGGAAGTG
3'-Primer (BM-P2)	GCATATGGATCCCCAGGGCAGTACGCAGAGGA
c-fes promoter – Modified primers to introduce a 5'NotI and a 3'SalI sites	
5'-Primer (NotI TOPO fes 7)	GAATGCGGCCGCGAATTCCGTG
3'-Primer (SalI TOPO fes7)	AGTGTGCTGGAAGTCGACCTTCGG
c-fes promoter and gp91^{phox} - Modified primers to introduce a 5'HindIII and a 3'NdeI sites	
5'-Primer (cfes for HindIII)	AAGCTTCGAATTCCGTGAGGTG
3'-Primer (gp91rev NdeI)	CATATGGTTAGAAGTTTTCCTTGTTG
EFs promoter - Modified primers to introduce a 5'NotI and a 3'SalI sites	
5'-Primer (EF1 for)	CCGGTACCGAGCGGCCGCTTCGTGAGGC
3'-Primer (EF1 rev)	GGTGTGTGCCGTCAGCTGACACAAGACC
SP146 promoter – Modified primers to introduce a 5'NotI and a 3'SalI sites	
5'-Primer (Li NotI for)	AAGCGGCCGCCGGTACCGAGCTCTTAC
3'-Primer (Li SalI rev)	GGATCCGTCGACAACCGGTACTGGG

B.2.3.3 Oligonucleotides for Sequencing

BM-P7	GCAGCTAGCTGCGGCCGCTATTTTCAG
BM-P8	GTGAATTCGATATCGCTAGCGG
BM-P11	CCATTCCTACCCTGCTGCC
BM-P12	CCCACTCCCATGCCCTCTCCAC
fes 4 for	GGCGGCCGCTCGAATTCCG
gp91S-1for	CGTGTGCCGGAACCTGCTGTC
gp91S-1rev	CGCTGTAGGGGTCGCTGTTGTTCA
gp91S-2for	AAAGAGTGCCCCATCCCCCAGTTC
gp91S-2rev	CGCCCACGATTCTGATGT
gp91S-3for	AAGTACTGCAACAACGCCACCAAC
gp91S-3rev	GGTGCTGGCTGGCGATGGTCTTA
gp91S-4for	GCAGAGCATCAGCAACAGCGAGAG
gp91S-4rev	CCCCGCAGGAAGGACAGCAGGTT
Int-prom-for	TCCCGCCCCCGTCTGAAT
MHforLEAD	GCCCCCGTCTGAATTTTTGCTTTCGG
M13for	ACGACGTTGTAAAACGACGGCCAG
M13rev	TTCACACAGGAAACAGCTATGACC
MRP8ex1for1	CCTGCATGTCTCTTGTCAGCTGTC
MRP8for1	GGAGGAATGTTCTCACTGAGTGC
MRP8int1for	CCGTGTGTGTGCACATGT
MRP82rev	AGGAAAGCTTGGCCAGCTGC
P1	GGAGGTTCCACCGAGATTTGG
P5	GAACGTCTTCCTCTTTGTCTGG
P6	GGCATGGATGATTGCACTTCACTC

P9	CCGCATCGTTGGGGACTGGACAG
P10	CTACTTCTACTGGCTGTGCCGGG
P11	GCAAGTCAACACCCTAATACCAG
P11N1	TCTGGCCCTCGGGGAGTGCATTTC
P12	CCCCCTGCTTAAAAATGGAC
P16	CCGCGAGTGCACACGCTGGGCC
R8	GAGCATTTGGCAGCACAACCCAC
R11	CCGCTATCTTAGGTAGTTTCCACG
R13	CTGTTATATTATGCACAGCC
R15	GAAAGGTGAGATTCCTGTCCAG
R16	GCCAGTGCCAGTGCTGACCCAAG
R20	CCTCAGGTCGGGCCACAAAAACG
R21	GAAACGACCGCTGGCCAGCTTAC
RSVfor1	TCTGACATGGATTGGACGAAC
RSVfor2	TTATTAGGAAGGCAACAGAC
WPREdown	ACGAGTCGGATCTCCCTTTGGGC
WPRE1for	CCCAAGCTTCAATCAACCTCTGGATTAC
WPRE M661 for1	AATCCTGGTTGCTGTCTCTTTTAG
WPRErev2	TACCAGTCAATCTTTCAC

B.2.4 Bacterial *E.Coli* strains

One Shot® (TOP 10F')	Invitrogen Corporation, Karlsruhe, Germany
Genotype: F [*lacI*^{q} Tn*10* (tet^R)] mcrA Δ(mrr-hsdRMS-mcrBC) Φ80lacZΔM15 ΔlacX74 recA1 deoR araD139 Δ(ara-leu)7697 galU galK galK rpsL (str^R) endA1 nupG	
MAX Efficiency® Stbl2™ #10268	Invitrogen Corporation, Karlsruhe, Germany
Genotype: F$^-$ mcrA Δ(mcrBC-hsdRMS-mrr) recA1 endA1 lon gyrA96 thi supE44 relA1 λ$^-$ Δ(lac-proAB)	
DH5α	Stratagene Company, Zuidoost, Netherlands
Genotype. F ¢80dlacZΔM15 Δ(lacZYA-argF) U169 deoR recA1 endA1 hsdR17(rk- , mk+) PhoA supE44 λ- thi-1 gyrA96 relA1	
XL1-Blue Supercompetent cells #200236	Stratagene Company, Zuidoost, Netherlands
Genotype: *sup*E44 *hsd*R17 *rec*A1 *end*A1 *gyr*A96 thi *rel*A1 *lac*$^-$ F' [proAB$^+$lacIq lacZ ΔM15 Tn*10* (tet^R)]	

B.3 Molecular biological methods

B.3.1 Phenol/Chloroform/Isoamyl alcohol extraction of nucleic acids

To remove undesired protein contaminants from nucleic acids an equal volume of Tris-buffered phenol/chloroform/isoamyl alcohol at a ratio of 25:24:1 (v/v/v) was added to the sample in a microcentrifuge tube and the mixture was vortexed for 30-60 sec. The two phases were separated by centrifugation at 13.000 rpm for 10 min. The aqueous nucleic acid-containing phase, which is normally the upper phase except for the case of high concentration of salt-containing sample, was transferred to a fresh reaction tube and subjected to a further round of extraction with chloroform.

B.3.2 Ethanol (or 2-propanol) precipitation of nucleic acids

In order to recover nucleic acids from solution, the salt concentration was brought to 200 mM with 3 M NaOAc (pH 4.8-5.0) and 2.5 volumes of -20ºC ethanol or 1 volume 2-propanol were added. After 30 min to overnight incubation at -20ºC or 15 min at -80ºC (only ethanol precipitation), the precipitate was centrifuged at 13.000 rpm for 20 min. The pellet was washed with 70% ethanol, centrifuged for another 3 min to remove the salt and air dried. DNA was re-suspended in dH_2O.

B.3.3 Determination of nucleic acid concentration

The concentration of nucleic acid was determined by measuring their optical density (OD) at 260 and 280 nm. An OD_{260}=1 is equivalent to 50 µg/ml double stranded DNA or 40 µg/ml RNA. The OD_{280} is used as an indication of the purity of the nucleic acid; for pure nucleic acid it should be 1.8 for DNA and 2 for RNA.

B.3.4 Restriction endonuclease digestion of DNA

Usually 3-5 units of restriction enzyme (New England Biolabs, Inc. GmbH, Frankfurt am Main, or Fermentas GmbH, St.Leon-Rot) were used for each µg DNA. For analytical digestions 0.5 µg DNA was cleaved in 1x endonuclease buffer for 1 hour at 37ºC (unless otherwise recommended by the supplier) and analyzed in a 0.5-1% agarose electrophoresis gel. For preparative digestions, with further processing such as cloning, southern blot, etc., DNA was digested at a concentration of 1 µg/10 µl in recommended buffer. This reaction was carried out for 4 hours to overnight at adequate temperature. The quality of the digestion was controlled by gel electrophoresis.

B.3.5 Removal of 5' phosphate groups of DNA (Antarctic Phosphatase)

Since phosphatase-treated fragments lack the 5' phosphoryl termini required by ligases, they can not self-ligate. This property can be used to decrease the vector background in cloning strategies. Typically, 10 U of enzyme were added either to the digestion mixture or to the eluted fragment and incubated under recommended conditions for 1 hour. Thereafter the reaction was heated at 65ºC to inactivate the enzyme prior to subsequent cloning steps.

B.3.6 Blunting ends reaction (DNA Polymerase I, Large (Klenow) Fragment)

This methodology is usually applied to fill-in 5' overhangs and/or to remove 3' overhangs to form blunt ends. DNA polymerase I, Large (Klenow) Fragment is a proteolytic product of *E.Coli* DNA Polymerase I which retains polymerization and 3'→5' exonuclease activity, but has lost the 5'→3' exonuclease activity. It is useful for cloning strategies that require a blunt end fragments for ligation. Usually, 10 U of enzyme were added to the digestion mixture or to the eluted fragment in combination

with 33µl dNTPs. This new mixture was incubated 30 min at 25ºC and heat inactivated by heating for 20 min at 75ºC.

B.3.7 Size separation of nucleic acids by agarose gel electrophoresis

The required amount of agarose was dissolved in 100 ml electrophoresis buffer TBE (90 mM Tris-base, 90 mM H_3BO_3, 2.5 mM EDTA, pH 8.3) (Miura *et al.*, 1999). Ethidium Bromide was added at a concentration of 0.3 µg/µl. The molten gel was poured into a horizontal chamber. Combs with the appropriate number and size of the teeth were used to make the loading slots. Once the gel was set, electrophoresis buffer was added and samples were loaded onto the gel in 6x loading buffer (0.25% Bromophenol blue, 0.25% Xylencyanol and 30% Glycerin in water). The gel was run at 35-45 mA (50-100 V) at RT for the required time. DNA was finally visualized by transillumination with 302 nm UV radiation.

B.3.8 Isolation/ purification of DNA fragments from agarose gels

To isolate an appropriate DNA fragment from an agarose gel, Gel Extraction Kit (Qiagen GmbH) was used as recommended by the manufacturer. Briefly, the DNA band of choice was cut out from the gel under long wave UV light with the aid of a scalpel. The gel piece was melted at 50ºC in the high-salt supplied buffer. 1 volume of Ethanol was added prior to bind the DNA to a silica membrane. After washing away the agarose and unbound impurities, the DNA was eluted in TE buffer (10 mM Tris·HCl, 1 mM EDTA, pH 8.0).

B.3.9 DNA fragment ligation

This method was used to combine two DNA fragments which were obtained by endonuclease restriction of plasmid DNA, size separation by agarose gel electrophoresis and finally purification of the fragments from agarose gel.

50-100 ng vector DNA were incubated with a 1:1 up to a 3:1 molar ratio of insert DNA in a total volume of 15 µl with 4 U of T4 DNA ligase (New England Biolabs, Inc.) and incubated for 6 hours to overnight at 16ºC. As a control sample a reaction which only contains vector DNA was set up and processed as the experimental samples.

B.3.10 Topo cloning kit

For some cloning steps, an intermediate PCR (see. Polymerase chain reaction) process was used to introduce specific cleavage sites for further endonuclease restriction and ligation with the required vector. In these cases, the digestion of the obtained PCR products is often ineffective leading no ligation products. Therefore, by means of a topoisomerase, these fragments were first ligated to a plasmid, the pCR®2.1-TOPO® (Invitrogen Corporation). After the PCR process, usually accomplished with PfuI Turbo

polymerase which has an error rate lower than Taq polymerase, 10 min incubation with 1 U of Taq polymerase was required to hang TAs at the ends of the fragments. These TA ends were needed to efficient ligate the PCR- fragments to the Topo vector by the topoisomerase. The TA-containing PCR product was incubated with the pCR®2.1-TOPO® vector for 5 min at RT. The recombinant plasmid, which harbors the required fragment with the new cleavage sites, was finally amplified by transformation into *E. Coli* bacteria (see. Chemical transformation of *E. Coli*).

B.3.11 Chemical transformation of *E.Coli*

This technique is used both for propagation of different plasmids and for screening of ligation reactions as follows. A DNA sample (typically 0.01-1 µg) in 0.5-2 µl volume was added to ice thawed $CaCl_2$-competent *E. Coli* (50 µl). After mixing by pipetting up and down, the mixture was incubated on ice for 30 minutes. Cells were heat-shocked in a water 42° C bath for generally 30 seconds, then immediately cooled on ice for 2 min. The transformed *E. Coli* cells were finally mixed with 250 µl SOC medium (supplied from Invitrogen Corporation), incubated for 1 hour at 37ºC in the shaker, plated onto LB-agar plates supplemented with ampicillin (100 µg/ml) and grown overnight at 37ºC. The antibiotic resistance is used for subsequent selective outgrowth of bacteria containing plasmid which encodes for the antibiotic resistance gene β-lactamase.

B.3.12 Plasmid DNA preparation

Small scale method

This method is suitable for preparation of small amounts of DNA (5-10 µg). Briefly, a 2 ml overnight culture of *E. Coli* harboring an appropriate plasmid or a ligation product was transferred to a microcentrifuge tube and centrifuged at 13.000 rpm for 5 min. The bacterial pellet was re-suspended in 300 µl buffer 1 (10 mM HCl, 10 mM EDTA, pH 8) containing 100 mg/ml RNAase. After incubation for 5 minutes at RT, the cells were lysed by addition of 300 µl buffer 2 (200 mM NaOH; 1% [w/v] SDS) and several inversions of the suspension. Thereafter 300 µl buffer 3 (3 M KAc, pH 4.8) were added in order to neutralize the lysis. The samples were then incubated for 5 minutes on ice and further centrifuged at 13.000 rpm for 15 min at 4°C. The supernatant containing the low molecular plasmid DNA was transferred into a new Eppendorf tube and precipitated by addition of two volumes of ethanol. After centrifugation at 13.000 rpm for 20 min at 4°C, the obtained plasmid DNA pellets were washed two times with 70% ethanol and air dried at RT. At last the DNA was re-suspended in 30 µl dH_2O.

Large scale method

To prepare a high amount of plasmid DNA for further cell culture applications, NucleoBond®PC 500 EF (Macherey-Nagel) was used essentially as recommended by the manufacturer. Briefly, a 200 ml overnight culture of *E. Coli* harboring an appropriate

plasmid was centrifuged at 4.000 rpm for 20 min at 4ºC. The bacterial cell pellet was prepared for plasmid purification by lysis procedure employing an alkaline/SDS solution. KAc was then added to the lysate, which causes the formation of a precipitate containing chromosomal DNA and other cellular compounds and which neutralizes the lysate. Plasmid DNA, which remains in solution was bound to the anion-exchange resin and eluted after washing of the column. The eluted DNA was finally precipitated with one volume of 2-isopropanol and centrifugation at 4.000 rpm for 30 min at 4ºC.

B.3.13 Nucleic Acid isolation from cultured cells

Total DNA isolation from cultured cells

DNeasy Blood & Tissue Kit was used for rapid purification of total DNA from fresh or frozen animal cultured cells as recommended by the manufacturer (Qiagen GmbH). Briefly, up to $5x10^6$ cells were centrifuged 5 min at 1.200 rpm and re-suspended in phosphate buffered saline (PBS, 137 mM NaCl, 2.7 mM KCl, 4.3 mM $Na_2HPO_4*7H_20$, 1.4 mM KH_2PO_4). Samples were lysed using proteinase K and guanidine hydrochloride buffer. This chaotropic salt removes water from hydrated molecules in solution and thereby provides also the optimal DNA-binding conditions for the silica-based membrane. After binding to the membrane and wash away the contaminants, the DNA was eluted in elution buffer (10 mM Tris·Cl, 0.5 mM EDTA, pH 9.0).

Total RNA isolation from cultured cells

Total RNA was purified using a Nucleospin® RNA II kit (Macherey Nagel) according to the instructions of the manufacturer. Briefly, up to $5x10^6$ cells were centrifuged 5 min at 1.200 rpm and re-suspended in a solution containing large amounts of chaotropic salts and β-mercaptoethanol which immediately lysate cells, inactivated RNases and creates appropriate binding conditions for the silica membrane. The sample was homogenized by passing through a 0.9 mm syringe needle and loaded to the column. After desalting the membrane, digestion of the DNA and wash away the contaminants, the total RNA was eluted in DEPC water. Integrity of prepared RNA was assessed by denaturing agarose gel electrophoresis. As the RNA is degraded, the 28S and 18S rRNA bands become less distinct, the intensity of the ribosomal bands relative to the background staining in the lane is reduced, and there is a significant shift in their apparent size as compared to the size standards.

B.3.14 Polymerase Chain Reaction (PCR)

The polymerase chain reaction (PCR) is a method for oligonucleotide primer directed enzymatic amplification of a specific DNA sequence of interest. A prerequisite for amplifying a sequence using PCR is to know, unique sequences flanking the segment of DNA to be amplified so that specific oligonucleotides can be obtained. Generally the PCR product is amplified from the DNA template using a heat-stable DNA polymerase

from Thermus aquaticus (Taq DNA polymerase) and using an automated thermal cycler (Perkin-Elmer/Cetus) to put the reaction through 25 or more cycles of denaturing, annealing of primers, and polymerization. After amplification by PCR, the products are separated by polyacrylamide gel electrophoresis and are directly visualized after staining with Ethidium Bromide.

This method was used routinely to quantify the mean copy number of proviral integrants in the transduced populations. A multiplex semi-quantitative system was standardized using a sample with known copy number. In this case the sample and the PCR program was set up as follows:

1 x Semi-quantitative PCR-Mix:	Semi-quantitative PCR-Program:
12.5 µl JumpStart™ REDTaq® ReadyMIX™ 1 µl gp91^{phox} Primer for (10 µM) 1 µl gp91^{phox} Primer rev (10 µM) 1 µl GAPDH Primer for 1 µl GAPDH Primer rev 8.5 µl Template (25, 50 and 100 ng)	1. 95°C → 5 min 2. 95°C → 30 sec 3. 59°C → 30 sec 4. 72°C → 35 sec 5. 72°C → 7 min 6. 4°C → ∞ 25 x Steps 2 – 4

In the case of X-CGD PLB-985 cells, a stock of 10 µM GAPDH primers was used, and a 1.5 µM stock was used for the primary mouse cells. The different loaded genomic DNA quantities were used to verify the efficiency of the primers. Following the PCR cycling the samples were loaded and run onto a 1% agarose gel containing Ethidium Bromide, and visualized under UV light. The intensity of bands was quantified with the Quantity One software (Bio-Rad Laboratories Inc).

Furthermore, this method was also used to amplify fragment from genomic DNA or plasmid DNA for further cloning steps. Usually modified primer sequences were used in order to introduce specific cleavage sites for future designed cloning strategies. In that case, the PCR was preformed with PfuI turbo polymerase which has an exonuclase 5' → 3' and proof reading activity to avoid possible mistakes during the amplification process. For a high fidelity synthesis maximal allowable template DNA quantities in conjunction with limiting number of PCR cycles were performed.

B.3.15 Reverse transcription polymerase chain reaction (RT-PCR)

This technique is used to amplify DNA fragments from a cDNA template that has been obtained from RNA. For this purpose the SUPERSCRIPT™II reverse transcriptase Kit was used following manufacturer instructions (Invitrogen Corporation). Briefly, total RNA from transfected cells was mixed with dNTPs, random primers and

SUPERSCRIPT^{TM}II reverse transcriptase. After heat the mixture to 65ºC for 5 min and quick chill it on ice, enzyme buffer, DTT and RNase OUT were also added to the microcentrifuge tube. The mixture was incubated 2 min at 25ºC prior to addition of 200 U of Reverse Transcriptase. An incubation step for 50 min at 42ºC was performed to let the transcriptase work. And finally, after heat inactivation of the polymerase for 15 min at 70ºC the DNA was ready to be amplified by the DNA polymerase as commented above.

B.3.16 Site-Directed Mutagenesis

In vitro site-directed mutagenesis, also known as site-specific mutagenesis or oligonucleotide-directed mutagenesis is a molecular biology technique in which a mutation is created at a defined site in a DNA molecule, usually a circular molecule known as a plasmid. In general, site-directed mutagenesis requires that the wild-type gene sequence be known.

The QuickChange® Site Directed Mutagenesis Kit (Stratagene Company) was used following the instructions of the manufacturer. The primer reaction was prepared by mixing 25ng of template dsDNA with 125ng of each primer containing the desired mutation, dNTPs, 1x reaction buffer and 2.5 U of PfuI Turbo DNA polymerase. The reaction was set in a PCR-cycler with the following parameters:

Segment	Cycles	Temperature	Time
1	1	95ºC	30 sec
2	12	95ºC	30 sec
		55ºC	1 min
		68ºC	1 min / kb of plasmid

After temperature cycling, the reaction was placed on ice for 2 min to cool the reaction, and then 10 U of DpnI restriction enzyme were added to the mixture to digest the methylated, nonmutated, parental dsDNA. The digestion was incubated at 37ºC for 1 hour prior to chemically transformation into XL1-Blue supercompetent cells.

In the present study this technique was applied to mutate one cryptic splice acceptor site, however maintaining the same codified aminoacid (Fig. 17).

B.3.17 Preparation of high specific activity DNA probe

Radiolabeling of a specific DNA probe was performed with the NEBlot® Kit as indicated by the provider (New England Biolabs, Inc.). Summarizing, in an RNase-free tube, 25 ng of template DNA was dissolved in nuclease free H_2O. After denaturing by boiling in a water-bath for 5 min the tube was placed in ice for 5 min. Thereafter the DNA was mixed with the following reagents in the order listed: i) 5 µl 10x Labeling buffer, ii) 2 µl of dATP, 2 µl of dTTP and 2 µl dGTP, iii) 5 µl α^{32}P dCTP and iv) 1 µl DNA Polymerase I – Klenow Fragment. The reaction was incubated at 37ºC for 1 hour.

Purification from unincorporated nucleotides was performed by gel filtration on spin-column (MicroSpin S-300 HR Columns, GE Healthcare) following manufacturer instructions. Briefly, the resin in the column was re-suspended by vortexing and the cap was loosened one-fourth turn and the bottom closure was snap off. After placing the column in microcentrifuge tube for support a centrifugation step at 3000 rpm for 1 min was preformed. Then the column was placed new microcentrifuge tube, and the sample was applied to the top-center of the resin being careful not to disturb the bed. After a new centrifugation set at 3000 rpm for 3 min the purified sample was collected in the bottom of the support tube. To determine the radioactive nucleotide incorporation 2 µl of the purified sample were mixed with 1 ml of Roti®szint Ecoplus and analyzed in a Liquid scintillation analyzer.

B.3.18 Southern Blot

A Southern blot is a method routinely used in molecular biology to check for the presence of a DNA sequence in a DNA sample. Southern blot combines agarose gel electrophoresis for size separation of DNA with methods to transfer the size-separated DNA to a filter membrane for probe hybridization.

A 0.7% TBE agarose gel was prepared as previously described. The gel was poured to about 0.6 cm in thickness and allowed to solidify at RT. Restriction digested DNA (up to 15 µg) was mixed with the appropriated volume of 6x loading buffer (0.25% Bromophenol blue, 0.25% Xylencyanol and 30% Glycerin in water) and loaded the wells of the gel. The gel was run at ~ 5 V/cm (distance measured between the electrodes of the electrophoresis chamber) until the bromophenol blue dye front had migrated almost to the bottom of the gel. A picture of the gel was taken under UV light exposure with a transparent ruler placed alongside the gel so that the distance that any band of DNA had migrated could be read directly from the photographic range.

A partial depurination of DNA was performed by soaking the gel in 1/50 HCl for 10 min at RT with constant gentle agitation. Then the gel was rinsed with dH_2O and denatured in 1.5 M NaCl; 0.4 M NaOH for at least 30 min. In the meanwhile the preparations for the downward transfer was done: i) the unused gel above the wells was removed using a scalpel, ii) the membrane (Biodyne B positively-charged nylon 6.6, Pall Corporation, Darmastadt, Germany) was cut slightly larger than the gel, iii) 6 filter paper sheets were cut to the same size than the membrane, iv) enough paper towels were cut to the same size than the membrane and v) a filter paper bridge large enough to cover the area of the gel and reach across into the transfer buffer (1.5 M NaCl; 0.4 M NaOH) reservoirs was cut.

Thereafter the downward transfer was assembled as follow depicted:

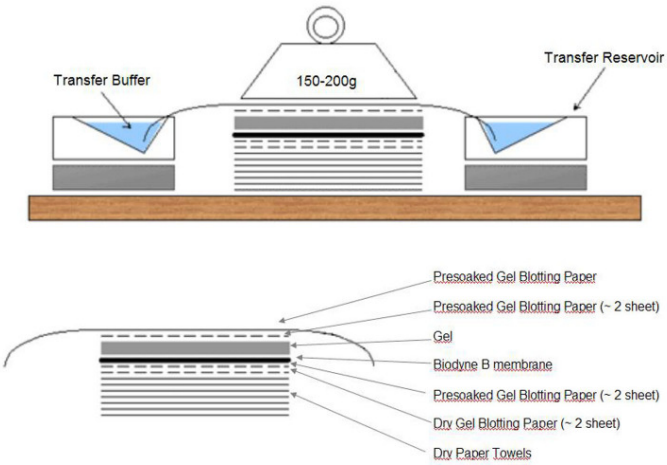

Adapted from www.piercenet.com

The transfer was let for 3 - 4 hours, thereafter was disassembled and verified by examining the gel under UV light. The position of the bands of size marker was marked and then the lane was cut to avoid crosslink with the probe. The membrane was neutralized by incubation in 0.5 M Tris pH 7.5, 1 M NaCl for at least 30 min before incubation with 8-12 ml ULTRAhyb hybridization buffer (Ambion Inc.) for 1 hour to O/N at 65ºC. The PRE fragment, present in all retroviral vectors, was used as a probe for hybridization. The volume of radiolabeled specific probe, prepared as above described, needed for a final concentration of ~10^6 cpm/ml of hybridization solution was denatured by 5 min incubation in boiling water and immediately added direct to the ULTRAhyb hybridization buffer (Ambion Inc.) used to prehybridize the blot. The hybridization was preformed at 65ºC and O/N incubation. Membranes were washed with 2x SSC 0.5% SDS and 0.1x SSC 0.1% SDS at 42°C until elimination of the background radioactivity. The membrane is then sealed and exposed to X-ray film (Kodak BioMax MS Film) for at least 16 hours at -80°C with intensifying screens.

B.3.19 Northern Blot

Analysis of 3 to 7.5 µg total RNA by Northern Blot was accomplished using the NorthernMax® Kit according to the instructions of the manufacturer (Ambion Inc.). The samples were mixed with loading buffer in a proportion of 1:2 and Ethidium Bromide was added to a final concentration of 10 µg/ml. After denaturation of RNA by incubation 15 min at 65ºC the samples were loaded into a MOPS formaldehyde denaturing gel. The gel was run at ~ 5 V/cm until the bromophenol blue dye front had migrated almost to the bottom of the gel. Examination of the gel by exposure to UV light, was preformed to asses the integrity of the RNA. A downward transfer from gel to a positively charged nylon membrane was set up and let it proceed for approximately 3 hours with the provided transfer buffer. After transfer the RNA was immediately crosslinked to the membrane by ultraviolet light exposure. Prehybridization and hybridization were performed with 8-12 ml of supplied hybridization buffer at 42ºC for

1 hour and overnight respectively in a hybridization tube. The PRE fragment, present in all retroviral vectors, was used as a probe for hybridization. The volume of radiolabeled specific probe, prepared as described above, needed for a final concentration of ~10^6 cpm/ml of hybridization solution was denatured by 5 min incubation in boiling water and immediately added directly to the hybridization buffer used to prehybridize the blot. The hybridization was preformed at 65ºC and O/N incubation. Membranes were washed, sealed and exposed to X-ray film (Kodak BioMax MS Film) for 4 hours at -80ºC. In order to assess the loaded quantity of RNA, ^{32}P-αCTP 18S rRNA probe was prepared by *in vitro* transcription with the MAXIscript® kit (Ambion Inc.) following manufacturer recommendations. Summarizing, the pTRI-18S plasmid (Ambion Inc.), T3 polymerase and the rest of the components needed for the transcription reaction were mixed and incubated at 37ºC for 1 hour. Turbo DNA was then added to the mixture to remove the template DNA, and finally the reaction was purified from free nucleotides by gel filtration using Ambion's NucAway™ spin columns. The membrane was incubated for 1 hour with new ULTRAhyb hybridization buffer (Ambion Inc) (without stripping step) and then hybridized with the loading control probe overnight at 68ºC. After extensive washing of the membrane, it was again sealed and exposed to X-ray film (Kodak BioMax MS Film) for about 4 hours at -80ºC.

B.3.20 Western Blot

Western blotting is based on the one-dimensional gel electrophoresis of proteins and can provide information about the molecular size of a certain protein. The whole procedure of western blotting comprises gel electrophoresis, transfer of the proteins to a polyvinylidene difluoride (PVDF) membrane, incubation of the membrane with specific antibodies and the detection of specific signals.

B.3.20.1 Preparation of protein from cultured cells

Cultured selected cell lines were harvested by ultracentrifugation at 500 x g for 5 min at 4ºC and washed once with cold-phosphate-buffered saline. The cells were re-suspended to a concentration of 5x10^7 cells/ml in fresh prepared immunoprecipitation buffer (20 mM Tris·HCl, pH 8.0, 150 mM NaCl, 1 mM EDTA and 1% Triton X-100) containing protease inhibitors (20 µg/ml chymostatin, 2 mM PMSF, 10 µM leupeptin and 1 mM AEBSF). After incubation on ice for 30 min with occasionally vortex, the mixture was centrifuged at 14.000 rpm for 2 min at 4ºC. The supernatant was transferred to a new microcentrifuge tube and freezed at -80ºC until required. To measure protein concentration, 1 µl sample or protein standard was mixed with 250 µl of Bradford Reagent in a 96 well plate. The mixture was incubated for 5 min at RT and the absorbance was measured at 595 nm wave length on a plate reader (SoftMaxpro). The obtained values were then compared with the linear regression obtained from the protein standard values.

B.3.20.2 SDS polyacrylamide gel electrophoresis

30 µg of cell extracts were separated by SDS-PAGE. To this end a 5% polyacrylamide stacking gel and a 10% resolving gel were prepared in between the Spacer and Short glass plates. After complete polymerization, the gel was placed into the electrophoresis tank and mounted with running buffer (25 mM Tris-Base; 192 mM Glycine; 0.1% [w/v] SDS; pH 8.3). The protein samples were mixed with an equal volume 4x sample buffer (350 mM Tris pH 6.8; 30% Glycerin; 10% SDS; 9.3% DTT; 0.01% Bromphenolblue), and then loaded onto the lanes. Gels were run about 30 min at 80 V throughout the stacking gel and further 3-4 hours at 120 V.

B.3.20.3 Immuno-blot / Western Blot

After separation by SDS-PAGE, proteins were blotted via electrophoresis onto a PVDF membrane using a semi-dry technique (Towbin *et al.*, 1979). The membrane was cut to gel size, soaked in methanol and placed on top of 3 filter papers which where placed on a fiber pad. Both the filter papers and the fiber pad were pre-soaked in blotting buffer (2.01 mM Tris-Base; 15 mM Glycin; 20 [v/v] Methanol) and placed on the anode. The SDS-PAGE gel was removed from the glass plates and placed on top of the membrane. Another 3 sheets of filter paper and one fiber pad pre-soaked with blotting buffer were placed on top of the gel and followed by the cathode. Protein transfer was conducted for 2 hours at 120 V.

B.3.20.4 Immunostaining of blotted proteins

Blotted membranes were blocked at RT for 45 min with 3% non-fat dried milk in PBST (0.1% Tween20 PBS) with moderate shaking. Blots were then incubated with 5 ml of moAb48 primary Ab 1:400 diluted in 3% non-fat dried milk in PBST for O/N at 4°C with shaking. The next day an incubation of 1 hour at RT was performed. Blots were then washed three times in PBST for 10 min. Incubate with IRDye 680 Conjugated Goat (polyclonal) Anti-Rabbit IgG Ab 1:10.000 diluted in 3% non-fat dried milk in PBST for 45 min at room temperature. At last the blots were washed again three times for 10 min with PBST and one last time with PBS. Then the blots were scanned with the Odyssey Scanner. To control for equal protein loading, the blots were incubated with Actin (I-19)-R SC-1616-R rabbit polyclonal IgG 1:500 diluted in 3% non-fat dried milk in PBST for 2.5 hours, then wash 3 times in PBST for 10 min each wash. An incubation of 30 min with IRDye800 secondary Ab 1:10.000 diluted in 3% non-fat dried milk in PBST was performed and followed by 3 washed for 10 min with PBST and one last time with PBS. Finally the blots were scanned with the Odyssey Scanner.

B.4 Specific equipment for cell culture

Cell culture dishes	Greiner, Frickenhausen, Germany
	Becton Dickinson, Heidelberg, Germany
Cell culture flasks	Greiner, Frickenhausen, Germany
	Becton Dickinson, Heidelberg, Germany
Cell scraper	Corning, Wiesbaden, Germany
Cell strainer (100 µm, 40 µm)	Becton Dickinson, Heidelberg, Germany
Cryocontainer	Nalgene, Rochester, NY, USA
Cryotube	Nalgene, Rochester, NY, USA
FACS-scan	Becton Dickinson, Heidelberg, Germany
FACS-calibur	Becton Dickinson, Heidelberg, Germany
14ml Polypropylene Round-Bottom Tube #35.2059	Becton Dickinson, NJ, USA
Incubator	Heraeus, Hanau, Germany
KOVA Glasstic® Slide	Hycor #87144, Kassel, Germany
Light microscope	Zeiss, Göttingen; Leica, Wetzlar, Germany
Microcentrifuge	Eppendorf, Hamburg, Germany
MiniMACS™ separator #130-042-102	Miltenyi Biotec, Bergisch Gladbach, Germany
MS Columns #130-041-301	Miltenyi Biotec, Bergisch Gladbach, Germany
Non-Tissue Culture Treated Plate, 24Well	Becton Dickinson, NJ, USA
Stericup-filter	Millipore, Eschborn, Germany
Sterilbank	Heraeus, Hanau, Germany
Sterilfilter (0,22 µm; 0,45 µm)	Millipore, Eschborn, Germany
Tissue culture flask	Greiner, Frickenhausen, Germany

B.5 Materials for cell culture

B.5.1 Chemicals and Reagents for Cell Culture

Anti FITC MicroBeads	Miltenyi Biotec, Bergish Gladbach, Germany
Calcium chloride	Sigma, Taufkirchen, Germany
Chloroquine	Sigma, Taufkirchen, Germany
DMEM (high glucose)	Life Technologies (#21969-035), Karlsruhe, Germany,
DMSO dimethylsulfoxid	Sigma, Taufkirchen, Germany
DNase I (RNase-free)	Roche (#776785), Mannheim, Germany
EasySep® Magnet #18000	Stemcell Technologies, Vancouver, Canada
EasySep® Mouse Sca-1 Selection Kit #18756	Stemcell Technologies, Vancouver,
EDTA	Sigma, Taufkirchen, Germany
Enfluran (2-Chloro-1.1.2-trifluoro-Ethyldifluoromethylether (Ethrane))	Abbott, Wiesbaden, Germany
FACS™ Lysing Solution 10x Concentrate	BD Biosciences Pharmigen (#349202),
FBS (fetal bovine serum)	Seromed (#S0115), Berlin, Germany
	StemCell Technologies (#06400), Vancouver, Canada
Formaldehyde	Roth, Karlsruhe, Germany
Glutamine (L-glutamine)	BioWhittaker, Verviers, Belgium
HBSS (hanks' balanced salt solution)	Sigma (#H6648), Taufkirchen, Germany
HEPES	Sigma, Taufkirchen, Germany
HSA (human serum albumin)	DRK-Blutspendedienst, Springe, Germany
Methocult GF M3434	StemCell Technologies, Vancouver, Canada
PBS (ohne Ca^{2+} und Mg^{2+})	BioWhittaker, Verviers, Belgium

Dulbecco's Phosphate Buffered Saline	PAA Laboratories GmbH
Penicillin-Streptomycin #P11-010	PAA Laboratories GmbH
Polybrene	Sigma, Taufkirchen, Germany
Poly-L-lysine solution	Sigma, Diagnaostics INC., St. Lous, USA
Protaminsulfate	Sigma (#2162), Taufkirchen, Germany
RetroNectin	Takara, Shiga, Japan
rmIL-3 (recombinant murine interleukin 3)	PeproTech, Frankfurt, Germany
rmIL-6 (recombinant murine interleukin 6)	PeproTech, Frankfurt, Germany
rmSCF (recombinant murine stem cell factor)	PeproTech, Frankfurt, Germany
RPMI 1640 (without Glutamine)	Life Technologies (#31870-025), Karlsruhe, Germany
StemSep-Systeme	StemCell Technologies, Vancouver, Canada
Tris	Roth, Karlsruhe, Germany
Tuerk Solution	Sigma, Taufkirchen, Germany
Trypan blue (0,4% solution)	Sigma(#T8154), Taufkirchen, Germany
Trypsin –EDTA	Life Technologies (#25300-054), Karlsruhe, Germany

B.5.2 Antibodies for FACS analysis

Purified anti-mouse CD16/CD32 (Fcγ III/II Receptor)	BD Biosciences Pharmigen
Mouse γ1 – APC (x40)	BD Biosciences Pharmigen
CD45R (B220)-PE Ord.no.130-091-828	Milteny Biotech GmbH
APC anti-mouse CD117 (c-kit) (2B8) Cat.553356	BD Biosciences Pharmigen
PE anti-mouse CD3 Molecular Complex (17A2)	BD Biosciences Pharmigen
Anti-mouse Ly-6A/E (Sca-1) R-Phycoerythrin Conj. Cat.No.:MSCA04	Caltag Lab
Simultest ^{TM} Control γ1/ γ1 Cat.No.349526	BD Biosciences Pharmigen
PE anti-mouse Ly-6G (Gr-1) and Ly-6C (RB6-8C5) Mat.	BD Biosciences Pharmigen
PE anti-mouse CD11b (Integrin α_M chain, Mac-1 α	BD Biosciences Pharmigen
PE rat IgG2a,k Cat.No.:553930 (was:11025A)	BD Bioscience Pharmigen
7-AAD Cat.No.:51-68981E (559925)	BD Biosciences Pharmigen
Anti-Flavocytochrome b558 moAb (#D162-3)	MoBiTec
(Nakamura *et al.*, 1987)	
Anti-Flavocytochrome b moAb, FITC Labeled (#D162-4)	MoBiTec

B.5.3 Cell lines

Name	Description	Reference(s)
293T	Derived from 293 cells, a continuous human embryonic kidney cell line. Transformed by sheared Type 5 Adenovirus DNA Graham et al 1977.	(DuBridge *et al.*, 1987) ATCC CRL-1573
SC-1	Mouse embryonic fibroblasts. Exhibit a greater sensitivity than other mouse lines to MuMLV.	(Hartley and Rowe, 1975)
PLB-985	Human, diploid, myeloid leukemia cell line. Obtained from the peripheral blood of a patient with refractory myeloblastic leukemia. With the capacity for both granulocytic and monocyte/macrophage maturation in the presence of inducing agents.	(Tucker *et al.*, 1987) DSMZ Cat. Code: ACC 139

X-CGD PLB-985	PLB-985 derivative cell line. Based on disruption by homologous recombination of the X-linked gp91^{phox} gene in XO PLB-985 cells. Widely used to study functionality, reconstitution and structure of the NADPH oxidase.	(Zhen *et al.*, 1993)

B.6 Cell culture methods

B.6.1 Common cell culture

All mammalian cells were maintained at 37ºC in an incubator in 5% CO_2 and 95% air humidity. The adherent 293T cells were used to generate the viral particles and the adherent SC1 cells were used for titer determination of ecotropic pseudotyped particles. For standard culture, these cell lines were grown in DMEM complemented with 10% heat-inactivated fetal bovine serum (FBS), 4 mM L-Glutamine and antibiotic (100 U/ml Penicillin and 100 mg/L Streptomycin) in flasks of varying sizes depending on the requirement of cells. The cells were then allowed to grow until confluence of 80-90% had been reached, whereupon the cells were subsequently split by trypsinization and re-seeded at a lower density. Trypsin treatment of cells was performed by removal of the culture medium from the cells, followed by one wash with Ca^{2+}/ Mg^{2+} free PBS. After removal of PBS 1-3 ml trypsin, for the T25 and T75 respectively, was applied to the cells and the cells incubated at 37ºC until they became detached as observed under a low-powered microscope. Fresh medium was then directly applied and the cells re-plated at desired density in new flasks or Petri dishes. For the retroviral vector production 293T should be used at low passage number (<p20) and kept as frozen stocks in liquid nitrogen. The non adherent growing cells PLB-985 and its derivatives were used for titer determination of GaLV pseudotyped viral particles and for functional assays. They were grown in RPMI complemented with 10% heat inactivated FBS, 4 mM L-Glutamine and antibiotic (100 U/ml Penicillin and 100 mg/L Streptomycin) in flasks of varying sizes depending on the application. The cells were maintained in culture with a density between $1x10^5$ and $1x10^6$ cells/ml with a medium renewal every 3 days.

B.6.2 Thawing and freezing cells

To thaw liquid nitrogen frozen cells a fast management is recommended. The cells were quickly placed at 37ºC until almost all were thawed. Immediately 1 ml of medium was added to the freezing vial and gently transferred to a 15 ml falcon. Further 5 ml of medium were added and carefully mixed. The cells were spin down at 1.200 rpm for 5 min and the supernatant was discarded. This washing step was repeated once again to completely remove the freezing medium. Lastly the cells were re-suspended in medium according to the number of cells and transferred to an appropriate culture flask.

To freeze cells it is recommended that the cells are frozen prior to confluence in order to assure the viability of the cell line. The cells were washed and trypsinized as described above and transferred to a 15 ml falcon and spin down at 1200 rpm for 5 min. The medium was discarded and 1 ml of freezing solution per 10^6 cells was used to re-suspend the cells (90% heat-inactivated FBS, 10% DMSO). The mixture was transferred to a cryogenic vial and placed at -80ºC overnight. Lastly the cells were transferred to liquid nitrogen to long-term conservation.

B.6.3 Assessing cell viability by Trypan Blue exclusion

The viability of cultured cells was determined by trypan blue exclusion. Trypan blue is a vital dye which reactivity is based on the fact that the chromopore is negatively charged and does not interact with the cell unless the membrane is damaged. Therefore, all the cells which exclude the dye are viable (Freshney, 1987).

The cell suspension was diluted with trypan blue solution and set up in a KOVA Glasstic Slide. Viable cells were then counted under light microscope. The concentration of cells per ml is calculated by:

$$\text{Cell density [cells/ml]} = \text{counted cells} \times \text{dilution factor} \times 10^4$$

$$\text{Total cell number} = \text{cell density} \times \text{volume [ml]}$$

B.6.4 Retroviral particle production via calcium phosphate $Ca_3(PO4)_2$ mediated transfection

The Calcium Phosphate transfection is a method for introduction of DNA into mammalian cells based on the formation of a calcium phosphate-DNA precipitate (Graham and van der Eb, 1973; Wigler *et al.*, 1977). The procedure is routinely used to transfect a wide variety of cell types for either transient expression or for the production of stable transformants. The DNA is mixed directly with 0.25 mM $CaCl_2$ in 0.1xTE:dH_2O 2:1. This is then added dropwise to the same end volume of 2xHBS buffer (50 mM HEPES pH 7.05, 280 mM NaCl, 1.5 mM Na_2HPO_4) where a precipitation of calcium phosphate occurs. Finally, the dispersion is given to the cell culture where the calcium phosphate is thought to facilitate the binding of the DNA to the cell surface and is believed that then the DNA enters the cell by endocytosis (Welzel *et al.*, 2004).

In the present study HEK 293T cells were seed, 24 hours prior to transfection, at $5x10^6$ cells per 100 mm plate in DMEM 10% FCS to achieve 70-80% confluence at the time of transfection. At the day of transfection chloroquine, which is a weak base that inhibits fusion of the endosome with the lysosome by buffering the lysosome interior, was added to the medium to a final concentration of 10 µM, 5 min prior to transfection (Walker *et al.*, 1996). Thereafter, 5 µg transfer vector, 7.5 µg pcDNA3MLVg/p (kindly provided by Prof. Dr. M. v. Laer, Frankfurt/GSH) and 2 µg envelope-containing plasmid were

cotransfected using the calcium phosphate precipitation method. The used envelope depends on the nature of the target cells. In the present study GaLV pseudotyped particles were produced to infect human derivative cells, and ecotropic particles for mice cells. The medium was changed after 16 hours to avoid cell toxic effects of the chloroquine treatment. Supernatant containing the viral particles was collected 48-72 hours after transfection, filtered through a 0.22 µm filter and used immediately for transduction or stored at -80ºC until required. Equal transfection efficiencies were controlled by immunostaining the cells with FITC labeled Anti-Flavocytochrome b_{558} monoclonal antibody and by flow cytometric analysis.

B.6.5 Titer determination and transduction of target cells

Titers (transducing units/ml) of the viral supernatants were determined by transducing predefined number of X-CGD PLB-985 or SC-1 target cells with serial dilutions of viral supernatant. Transduction was performed by spinoculation (90 min at 2.500 rpm and 32ºC) assisted by adding 4 mg/ml protamine sulfate (Cornetta and Anderson, 1989). Cells were grown for 3 days before analysis of the percentage of positive cells by flow cytometry with FITC labeled Anti-Flavocytochrome b_{558} monoclonal antibody which recognizes an external epitope of $gp91^{phox}$ (7D5; (Yamauchi *et al.*, 2001)) or isotype control antibody.

Transducing Units /ml = seeded cells x dilution factor x (% positive cells / 100)

B.6.6 Flow cytometry

Also referred to as Fluorescence Activated Cell Sorting (FACS) this technique is used to characterize the phenotype of different cell types by analysis of cell surface membrane protein. In the present study usually 1-2 x 10^5 cells were washed with PBS. The supernatant was poured off and the cells were incubated with a primary antibody or a fluorescent dye bound antibodies for 20 min. Then, one wash step was performed with FACS Buffer (1% FBS, 0.1% NaN_3 in 1x PBS) and if required a secondary antibody added to the cells. After discarding the supernatant of the last wash 200 µl of FACS fix solution (1% Formaldehyde in 1x PBS) were added to fix the cells. Control staining with appropriate isotype-matched control mAbs was included to establish thresholds for positive staining and background linear scaled mean fluorescence intensity (MFI) values. The percentage (%) of positive cells was calculated as % of positive cells stained with specific mAb - % of background staining with corresponding isotype control. ΔMFI was calculated as MFI of cells stained with specific mAb - MFI of cells stained with corresponding isotype control.

B.6.7 Cell differentiation

For granulocytic-like cell differentiation, in the case of PLB-985 and derivatives, logarithmically growing cells at a density of $2x10^5$ cells/ml were exposed to 1.25%

dimethylsulfoxid (DMSO) for 6 days in the presence of only 2.5% FBS. Flow cytometry was performed to ensure the differentiation with labeled cells with anti-CD11b+ antibody.

B.6.8 Magnetic Cell Sorting

The Magnetic cell sorting procedure is based in the magnetic beads which are extremely small, superparamagnetic particles and in columns containing an optimized matrix to generate a strong magnetic field when placed in a permanent magnet.

In the present study $gp91^{phox}$ containing cells were selected with this system by the MACS MicroBeads, the MS columns and the MiniMACS separator. Up to $2x10^8$ cells (containing up to $1x10^7$ positive cells) were resuspended in 400µl PBS and 400µl 7D5 antibody against the cytochrome b558 (Nakamura *et al.*, 1987) and incubated for 20 min at RT. Then the cells were washed with PBS and resuspended in 1ml PBS. Following addition of 30µl RAM-IgG1 FITC Ab an incubation step of 15 min at RT was performed. The cells were washed twice with MACS Buffer (PBS pH 7.2, 0.5% BSA and 2 mM EDTA) and lastly incubated with 50µl Anti-FITC MicroBeads for 15 min at 4°C. One last washing step with MACS buffer was performed prior to apply the cells to the column placed in a MiniMACS™ Separator (magnet). Three washing steps were performed to remove the unlabeled cells before removing the column from the separator. To elute labeled cells 1 ml of MACS buffer was loaded onto the column. To increase the purity of the magnetically labeled fraction it was passed over a second column following the same protocol. The percentage of positive cells was finally assessed by FACS analysis of the eluted fraction.

B.6.9 Cytochrome C assay

A continuous cytochrome c reduction assay is a quantitative method to measure the superoxide production by a determined number of cells. In the present study it was used to quantify the superoxide formation by granulocyte-differentiated PLB-985 cells, mSca-1^+ cells and derivative cell lines (Mayo and Curnutte, 1990). Briefly, $1x10^6$ PLB-985 cells and derivatives, or $2.5x10^6$ mSca-1^+ cells and derivatives were washed in 7.5 mM glucose $HBSS^{++}$. Cells were spin down and re-suspended in pre-warmed 250 µl $HBSS^{++}$ 7.5 mM glucose containing 75 µM cytochrome C and plated in a 96 well plate. The assay was performed at 37 °C using a Spectra MAX 340 reader (Molecular Devices) after cell stimulation with freshly prepared PMA (400 ng/ml). Superoxide production was quantified using an extinction coefficient of 21.1 mM^{-1} cm^{-1} for cytochrome C based on a light path of 0.6 cm. Data were analyzed using the SOFTmax Version 2.02 PRO software to determine Vmax over a 1.8 min interval.

B.6.10 DHR assay

This method describes the functional analysis of the NADPH oxidase and can be used to investigate its reconstitution in $gp91^{phox}$ transduced X-CGD cells. It is also known as Burst-Test and uses dihydrorhodamine 123 (DHR 123) as a substrate for the respiratory burst reaction in stimulated neutrophils. DHR123 is oxidized by intracellular H_2O_2 to rhodamine 123 which is a fluorescent compound detectable by FACS analysis in the first channel. It is really useful since it identifies the carrier phenotype and discerns between other pathologies such as complete myeloperoxidase deficiency (Mauch *et al.*, 2007).

For the PLB-985 cells , mSca-1^+ and both derivatives $1x10^6$ cells of interest were diluted in 1ml with pre-warmed HBSS (with Ca^{2+}, Mg^{2+}, 0.5% BSA and 7.5 mM glucose) in FACS tubes (preparing two samples for each cell type, 1x non-stimulated and 1x stimulated). Then, the cells were incubated at 37°C in the 5% CO_2 incubator for 5 min. 40 µl catalase (1.000 U) were added to both samples and 10 µl of PMA 1mg/ml to the stimulated sample. The cells were then incubated at 37°C in the 5% CO_2 incubator for 5 min. 25 µl of the 1mM DHR were then added to both stimulated and the non-stimulated sample. A last incubation step was performed at 37°C in 5% CO_2 incubator for 15 min. The tubes were then placed on ice to stop the reaction and the samples were measured in flow cytometer within the next 30 min.

For the peripheral blood samples obtained from transplanted mice, the Phagoburst® Kit from ORPEGEN Pharma was used. Briefly 1 ml peripheral blood (preparing two samples, 1x non-stimulated and 1x stimulated) was placed on ice for 10 min. 20 µl of PMA solution (supplied with the kit) were added to the stimulated sample and the mixture was incubated for 10 min at 37ºC. Then, 20 µl of DHR solution (supplied with the kit) were added to both samples and 10 min incubation was again performed at 37ºC. Thereafter, 2 ml of lysis buffer (supplied with the kit) were added to the samples and incubated 10 min at RT. After washing with the supplied wash buffer, 200 µl of DNA staining solution (supplied with the kit) were added to the samples to exclude aggregation artifacts of bacteria or cells helping then to identify the granulocytic and monocytic populations in the FACS analysis which was performed after 10 min incubation on ice.

B.7 Primary cells and animal experiments

B.7.1 Breeding of Animals

All mice used in the experiments were bred in the animal centre of the Georg-Speyer-Haus (Frankfurt, Germany). The health status of the animal centre was monitored based on the guidelines of the Federation of European Laboratory Animal Science Associations (FELASA). They were bred in standard sterile cages (5 mice/cage)

and feed with standard rodent diets and water. For the bone marrow cell preparation, mice of an age between 6-8 weeks were chosen. All experiments were performed according to the German Animal Protection Law.

B.7.2 Preparation of murine Bone Marrow Cells

The mice chosen for the bone marrow cell preparation were sacrificed after narcosis with enfluran. Bone marrow from femurs and tibias of each mouse was isolated by flushing with a 23-gauge needle and 5 ml RPMI supplemented with antibiotics (100 U/ml Penicillin and 100 mg/L Streptomycin). The bone marrow cells were suspended well and centrifuged at 1200 rpm and 4° C for 5 minutes. The cell pellet was resuspended at a concentration of 1 x 10^8 cells/ml in PBS supplemented with 1 mM EDTA and 2% FBS for further Sca-1^+ magnetic cell sorting.

B.7.3 mSca-1^+ selection from murine Bone Barrow preparations

The mSca-1^+ cells are a subpopulation of the bone marrow (BM) identified as hematopoietic stem (Spangrude *et al.*, 1988; Spangrude, 1989).

The mSca-1^+ cells were isolated from freshly prepared bone marrow with the EasySep® Mouse SCA1 Selection Kit as indicated by the manufacturer. Up to 2x10^8 fresh prepared mBM cells were counted with Tuerk solution and suspended at a concentration of 1 x 10^8 cells/ml in buffer containing 1x PBS, 1 mM EDTA and 2% FBS. Murine FcR blocker (supplied with the kit) was added to the cells at a concentration of 10 µl/ml. Then Sca-1 PE labeling reagent was added at a concentration of 15 µl/ml and the sample was incubated at 4° C for 15 min. The cells were washed once with 10-fold excess buffer and resuspended in half of the original volume and further transferred to a 12 x 75 mm polystyrene tube. Thereafter, 100 µl/ml PE-selection cocktail was added to the sample and incubated at 4° C for 15 min. At last, EasySep™ Magnet nanoparticles were added at 50 µl/ml to the sample and the mixture was further incubated at room temperature for 10 min. The total sample volume was brought up to 2.5 ml by adding buffer. Finally the tube was placed into the magnet and set aside for 5 minutes. Then the supernatant fraction was poured off and the magnetically labeled cells remained inside the tube. The tube containing the negative sample was removed from the magnet and 2.5 ml buffer were added to elute the cells. The sample was mixed by gently pipetting up and down 2-3 times and placed into the magnet again. This process was repeated 6 times and at the end the selected cells were suspended in the suitable culture medium for further experiments.

B.7.4 Lineage depeletion

Lineage negative cells are isolated by depletion of cells expressing so-called “lineage” antigens. In the present study the Lineage Cell Depletion Kit (Miltenyi Biotec) was used following manufacturer instructions. BM cells were passed through 30µm nylon mesh to

remove cell clumps. Thereafter cells were centrifuged at 300xg for 10 min and supernatant was pipetted off. Cells were resuspended in 40µl of 0.5% BSA and 2 mM EDTA in PBS per 10^7 cells. 10 µl of Biotin-Antibody Cocktail (CD2, CD3, CD11b, CD14, CD15, CD16, CD19, CD123, and CD235a) per 10^7 cells was added and the mixture was incubated for 10 min at 4ºC. Further 30 µl of of 0.5% BSA and 2mM EDTA in PBS per 10^7 cells were added to the mixture prior to the Anti-Biotin MicroBeads which were added to a concentration of 20 µl per 10^7 cells. Following to a 15 min incubation step at 4ºC, the cells were washed by adding 1-2 ml of buffer per 10^7 cells and centrifugation at 300xg for 10 min. The supernatant was pipetted off and the cells were then resuspended in 500 µl 0.5% BSA and 2mM EDTA in PBS per 10^8 cells prior to magnetic separation with the autoMACS™ separator and the "Deplete" program. The purity of the enriched population was then evaluated by flow cytometry.

B.7.5 Transduction of mSca-1^+ cells

mSca-1^+ cells were pre-stimulated for two days prior to transduction in RPMI1640 complemented with 10% heat-inactivated (FBS), 4mM L-Glutamine, antibiotic (100 U/ml Penicillin and 100 mg/L Streptomycin) and cytokines (50-100 ng/ml mSCF, 50 ng/ml mIL-6 and 10 ng/ml mIL-3). Twenty four hours prior to transduction a 24-well plate (non-tissue culture) was coated with 10.5 µg/cm^2 RetroNectin and incubated over night. At the transduction day RetroNectin solution was replaced by 1 ml of 2% HSA in H_2O in order to block the plate for 30 min at RT. The HSA solution was discarded and the wells were washed with 1 ml HBSS/2.5% (v/v), 1M Hepes and 1 ml 1x PBS. The 1x PBS remained in the wells until the viral supernatant was added. The ecotropic pseudotyped viral supernatant, previously tittered in SC1 cells, was thawed quickly in a 37°C water bath and added into the RetroNectin coated wells with the required MOI (the total volume of the viral supernatant never exceeded 1.5 ml). The virus-loaded plate was centrifuged at 3000 rpm for 30 min at 4° C. Then, the supernatant was discarded and the viral loading process was repeated as many times as needed to reach the desired MOI. Since only about 50% of the infectious particles remain bound to the RetroNectin (Li *et al.*, 2003) the double amount of infecting particles for the desired MOI was preloaded. In the transduction day the cells were diluted to a concentration of $7.5x10^5$ cells/ml and 400 µl of the cell suspension were added into the prepared wells after removing of the last viral supernatant. This process was repeated the next day. Twenty four hours after the last transduction cycle the transduced cells were washed twice with 1x PBS and used for further studies.

B.7.6 Bone Marrow transplantation of genetically modified cells

The recipient mice were lethally irradiated with a total dose of 11 Gy split into two doses of 5.5 Gy in two consecutive days from a Cs γ-ray source at the

Georg-Speyer-Haus (Frankfurt/Main, Germany). The cells for transplantation with the appropriate cell number were washed 3 times with PBS, and then kept on ice until transplantation. 2-4 hours after irradiation, transplantation was performed through injection of the cells into the tail vein of the recipient mice. From that day on and during two weeks, the mice were treated with 1.67 mg/ml Neomycin supplemented H_2O as preventive antibiotic. The analysis of the mice was carried out 6 weeks after transplantation.

B.7.7 *In vitro* differentiation of mSca-1^+ cells

For *in vitro* differentiation of mSca-1^+ cells and derivatives, stimulated cells at a density of $3x10^5$ cells/ml were exposed to 10ng/ml IL-3 and 100ng/ml G-CSF during 9 days. The cell density was maintained constant during this time by adding more media or splitting the cells into two culture flasks. Differentiation was ensured at day 9 with Gr-1 and CD11b immunolabeling. The differentiated cells were then used for functional assays such as cytochrome c and DHR assay which are previously described (see B.6.9 Cytochrome C assay and B.6.10 DHR assay).

B.7.8 Methylcellulose Based CFU-assay

This method was used to determine the potential of hematopoietic progenitor cells in total bone marrow or peripheral blood to form colonies in semi-solid medium since methylcellulose based medium allows cells, derived from the same progenitor cell, to build colonies. 6000 mSca-1^+ were diluted in 300 µl IMDM medium supplemented with antibiotics (1000 U/ml Penicillin and 1000 mg/L Streptomycin), and then mixed with 2.7 ml methylcellulose in a poly tube. After vortexing the samples were set aside 5-10 min until the air bubbles disappeared. Then 1 ml mixtures were dispensed into each of two 35 mm culture dishes using a 3 ml syringe and a 16 gauge blunt-end needle. The dishes were gently rotated to spread the methylcellulose evenly and placed in a 100 mm petri dish with a third 35 mm dish containing 3 to 4 ml of sterile water. This plate was incubated for 10 days at 37° C in the 5% CO_2 incubator. When counting the colonies, the cell populations over 50 cells per colony were calculated as one colony.

B.7.9 NBT assay

After 10 days in culture hematopoietic colonies were counted and assayed for NADPH oxidase activity by the nitroblue tetrazolium (NBT) assay. For this, the cultures were overlaid with 0.2% NBT solution in PBS containing 1 mg/ml PMA and kept at 37ºC, 5% CO_2 for 60 min. The NBT reaction was stopped by adding directly to the cultures 1.5% paraformaldehyde. NBT-positive colonies were detected with an inverted microscope.

B.8 Retroviral vectors - Cloning strategies

The SIN.11.SF.GFP.pre vector kindly provided by Prof. Dr. C.Baum was used to clone in the gp91^{phox} cDNA from the MSCV.gp91 (Dr. M.Grez). The SIN vector was digested with BamHI and then underwent blunt end with Klenow and dephosphorilation with Antarctic Phosphatase to avoid religation of the plasmid. The MSCV.gp91 plasmid was open at 5' end of the gp91^{phox} cDNA with BamHI digestion followed of bunt ending with the Klenow polymerase and then excised with EcoRV digestion. Both insert and plasmid were isolated and ligated originating the intermediate plasmid SIN.11.SF.gp91.pre.

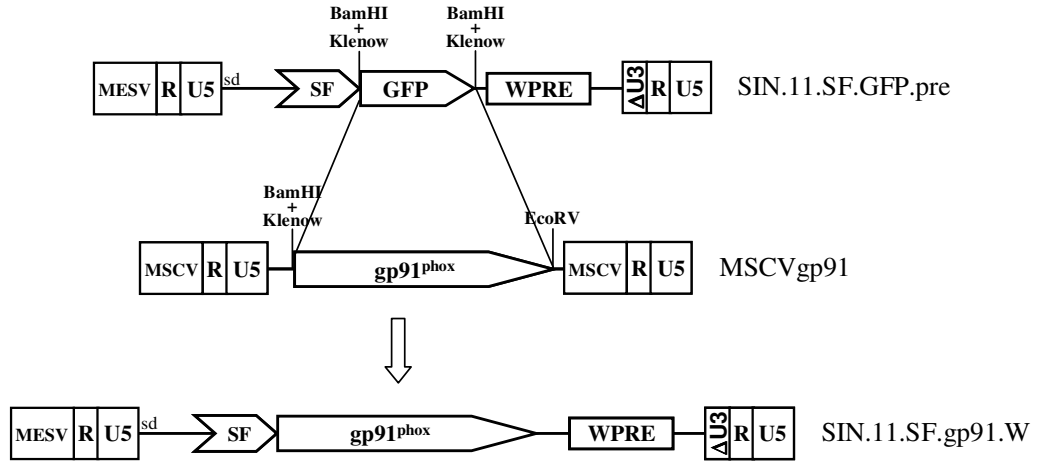

Fig. 9: Cloning strategy of the gp91^{phox} expressing SIN gammaretroviral vectors. The gp91^{phox} cDNA was excised from the MSCVgp91 plasmid and cloned in the SIN.11.SF.GFP.pre backbone substituting for the GFP sequence. Note that the nomenclature has changed; W is used to define the WPRE element instead of pre.

This plasmid was used to exchange the MESV 5'LTR for the RSV 5'LTR from the SRS11.SF.GFP.pre plasmid provided by Prof. Dr. C.Baum (Schambach *et al.*, 2006c). To this end both plasmid were excised with NdeI and SacII. Following isolation and ligation of the fragments, the resulting plasmid was named SRS11.SF.gp91.W-1.

This plasmid underwent destruction of the NdeI cleavage site by NdeI digestion, blunt ending and religation. It was named SRS11.SF.gp91.W-2. Furthermore, a NotI site was introduced upstream of the internal promoter to help with further promoter exchanges. Therefore oligonucleotides were designed so that the fragment was amplified containing the NotI site. The PCR amplification fragment was then cloned into the pCR®2.1-TOPO® plasmid and then by means of a three fragment ligation transferred to the SRS11.SF.gp91.W-2 plasmid. The PCR fragment was excised from the pCR®2.1-TOPO® plasmid with SacII-NheI and the SRS11.SF.gp91.W plasmid was cut once with SacII-DraIII and twice with NheI-DraIII. Following isolation of the fragments and ligation the resulting plasmid was called SRS11.SF.gp91.W.

The SRS11.SF.gp91.W was used to exchange the leader regions always by SacII-NotI digestion. The leader 71 was obtained from the SF71gp91^{phox} (kindly provided by Dr. S. Stein) and the leader 110 from the SR110.SF.GFP.pre (Prof. Dr. C.Baum).

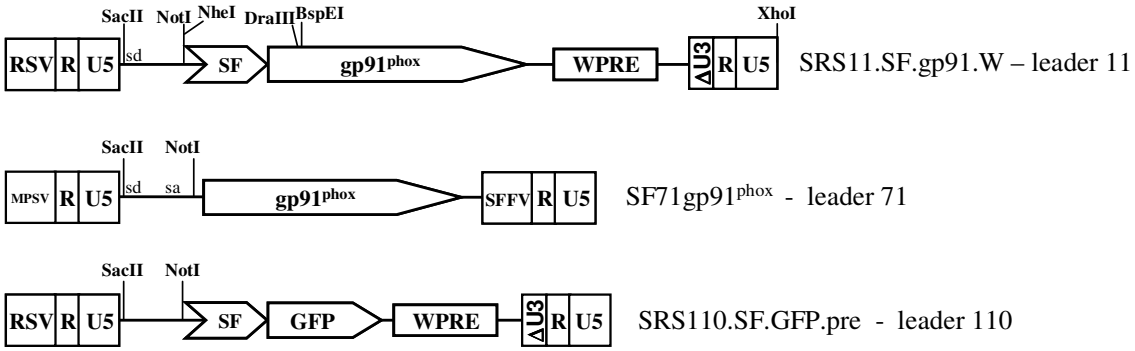

Fig. 10: Schematic representation of the three different leaders in their corresponding initial vectors.

The mutation in the gp91^{phox} sequence was created as elsewhere explained (see B.3.16 Site-Directed Mutagenesis and C.1.2 Site-directed mutagenesis of the gp91phox).

The intronless version of the MRP8 promoter was obtained from the pSLMRP8dN-Intgp91b plasmid (Dr. S.Stein). It was excised in a fragment containing also a part from the gp91^{phox} cDNA with SpeI-BspEI. The SRS11.SF.gp91.W-2 plasmid digested in two pieces with NheI–XhoI and XhoI–BspEI. After isolation of the three fragments a three fragment ligation was performed. The obtained plasmid was named SRS11.M8dNdI.W.

To introduce the MRP8 first intron in the SRS11.M8dNdI.W PCR amplification was performed with the pSL1180-MRP8dNGb plasmid (Dr. S.Stein) as template and modified oligonucleotides (BM-P1 and BM-P2) so that they introduce an NdeI cleavage site at each end of the intron. The PCR fragment was cloned in the pCR®2.1-TOPO® plasmid and then transferred by NdeI digestion to the SRS11.M8dNdI.gp91m.W plasmid also opened with NdeI. After isolation, ligation and analysis of the resulting clones, the correct orientation was ensured by sequencing.

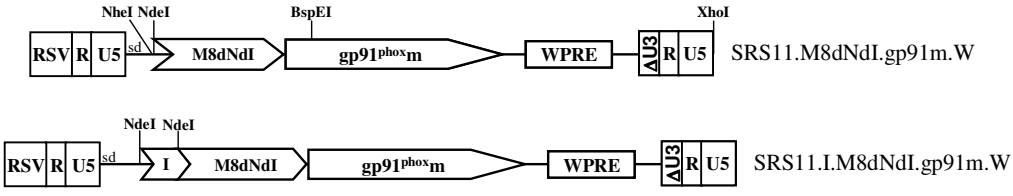

Fig. 11: Schematic representation of the SIN gammaretroviral constructs containing the MRP8 promoter and its enhancer

The c-fes promoter was amplified by PCR cycling from the Topo fes #7 plasmid (cloned by Dr. K.Sadler) with modified oligonucleotides so that a 3'SalI and a 5'NotI cleavage sites were introduced. This fragment was cloned again in a pCR®2.1-TOPO® plasmid

from where was later excised by NotI-SalI digestion. The SRS11.SF.gp91m.W was opened also with NotI-SalI to exchange the promoters. The resulting plasmid was called SRS11.fes.gp91m.W.

To clone the reverse cassette plasmid, the SRS11.fes.gp91m.W was used to amplify a fragment by PCR with oligonucleotides introducing a HindIII at the 5' end of the c-fes promoter and an NdeI at the 3' end of the gp91^{phox}m cDNA. This fragment was cloned into the pCR®2.1-TOPO® plasmid and then isolated. The bgh was cut with NdeI–NotI from a pCR®2.1-TOPO® plasmid in the correct orientation (Dr. S.Stein). Lastly the SRS11.fes.gp91m.W was opened with NotI-HindIII and a three fragment ligation was performed resulting in the SRS11.bgh.gp91m.fes construct.

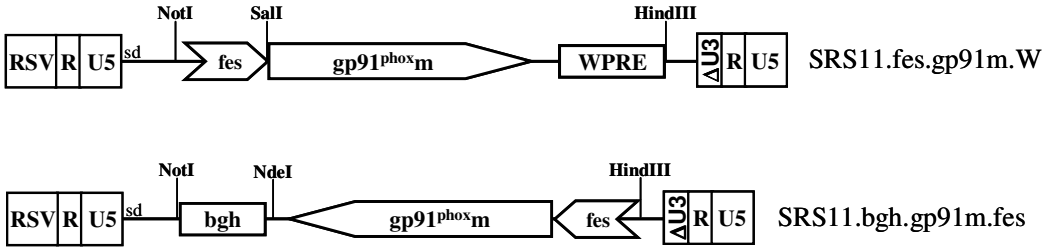

Fig. 12: Schematic representation of SIN gammaretroviral constructs containing the c-fes promoter

To construct the SERS11.gp91m.W the whole 5'LTR containing the SV40 enhancer was cut with NarI-SacII from the SERS11.SF.GFP.pre (kindly provided by Prof. Dr. C.Baum). The SRS11.SF.gp91m.W plasmid was then opened with NarI-SacII. After isolation and ligation the resulting plasmid was analyzed by sequencing.

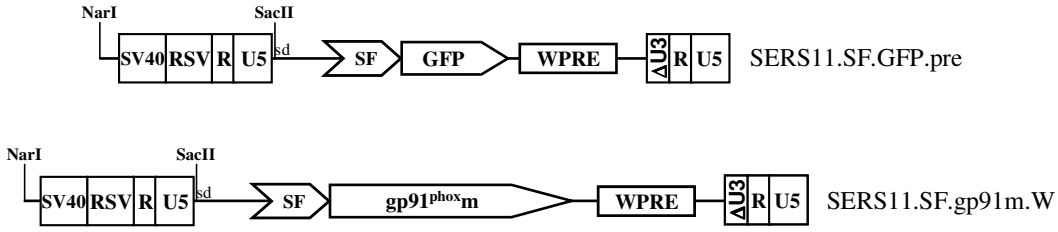

Fig. 13: Schematic representation of SIN gammaretroviral vectors containing the SV40 enhancer.

The SERS11.SF.gp91m.W was digested with SacII-SalI and HindIII-SacII, and both fragments were isolated after gel separation. The gp91^{phox}s was excised by digestion with SalI-HindII from the 0600161pPCRscript SK+gp91^{phox}s plasmid (Dr. M. Grez). A three fragment ligation was set and the obtained plasmid was called SERS11.SF.gp91s. This plasmid did not contain the WPRE element. The modified WPRE (WPREm) was excised with SalI-SspI from the M661 plasmid (kindly provided by Prof. Dr. M. v. Laer) and introduced in the SERS11.SF.gp91s opened with XhoI-SspI. After fragment isolation and ligation the resulting plasmid was named SERS11.SF.gp91s.Wm.

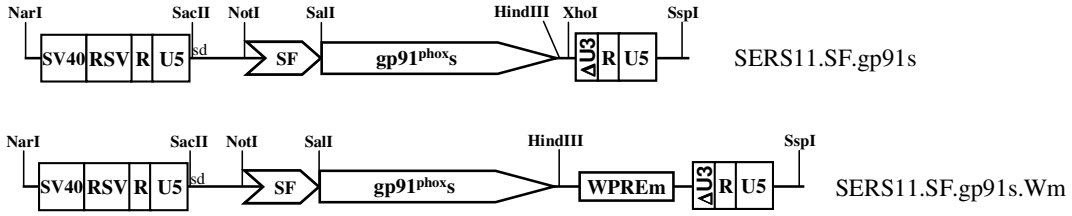

Fig. 14: Schematic representation of the intermediate SERS11.SF.gp91s plasmid and the SERS11.SF.gp91s.Wm vector.

The four promoters (EFs, SP146, c-fes and MRP8) were cloned by NotI-SalI digestion in all the cases in the SERS11.SF.gp91s.Wm also digested with NotI-SalI. The c-fes promoter was obtained from the SRS11.fes.gp91m.W plasmid. The M8dN version of the MRP8 promoter was NotI-SalI excised from the pSL1180-MRP8dNGb (Dr. S. Stein) and ligated with the NotI-SalI opened SERS11.SF.gp91s.Wm. The EFs promoter was obtained from the EF/myc/ER/GFP plasmid (Invitrogen Corporation). It was amplified by PCR with modified oligonucleotides (EF1 for and EF1 rev) and cloned into the pCR®2.1-TOPO® plasmid. Thereafter it was excised from the TOPO plasmid with NotI-SalI digestion and ligated with the SERS11.SF.gp91s.Wm opened with the same enzymes. The Li promoter was obtained from the lenti 3 107-gp91(K02)#3 plasmid kindly provided by Dr. S. Li (San Antonio, USA). It was amplified by PCR with modified oligonucleotides to introduce NotI (Li NotI for) and SalI (Li SalI rev) cleavage sites. The PCR fragment was then cloned into the pCR®2.1-TOPO® plasmid. Thereafter it was excised from the TOPO plasmid with NotI-SalI digestion and ligated with the SERS11.SF.gp91s.Wm opened with the same enzymes (see Fig. 37).

C. RESULTS

C.1 Design of SIN gammaretroviral vectors driving the expression of gp91^{phox}

C.1.1 Construction of wild-type gp91^{phox} expressing vectors

In the present study a series of SIN gammaretroviral vectors driving the expression of gp91^{phox} cDNA was constructed based on the Sin11.SF.eGFP.W vector, kindly provided by Prof. Dr. C. Baum (Schambach *et al.*, 2006c) (see B.8 Retroviral vectors - Cloning strategies). The 5' MPSV promoter region in the LTR of the transfer plasmid was replaced by the promoter of Rous Sarcoma Virus (RSV) since it has been shown to overcome the promoter competition with the Spleen Focus Forming Virus (SFFV) promoter as internal promoter. The RSV promoter enables efficient full-length RNA expression in packaging cells (Yamamoto *et al.*, 1980; Schambach *et al.*, 2006c).

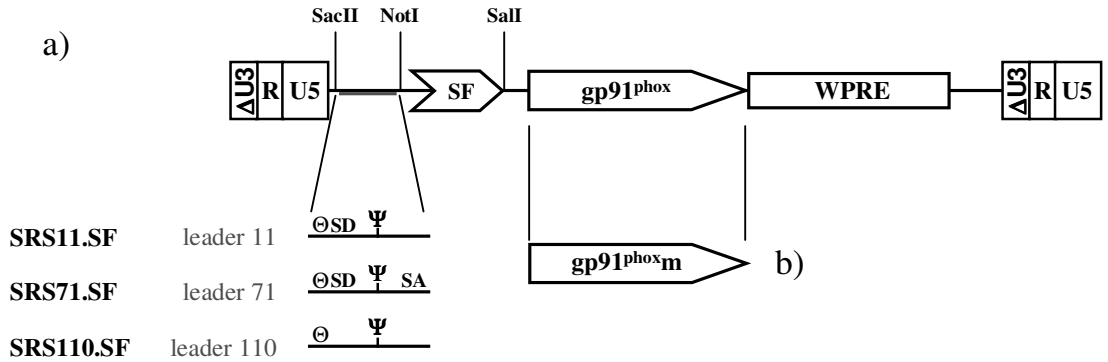

Fig. 15: Schematic design of SIN vectors used in this study. (a) Three different self-inactivating retroviral vectors were cloned differing only in the presence of splicing sites in the leader region. They all contain the enhancer-promoter deleted MESV LTR (ΔU3), the SFFV U3 promoter (SF), the cDNA of gp91^{phox} as transgene and the WPRE to enhance the nuclear export. Within the leader region the primer binding site (Θ), the packaging signal (Ψ), and splice donor (SD) and acceptors (SA) are indicated. The provirus form is depicted. (b) The gp91^{phox} sequence was mutated and cloned into the three different vectors generating a second set of vectors.

Moreover, these vectors contained a 3' LTR from Murine Embryonic Stem cell Virus (MESV) in which enhancer-promoter sequences were deleted. This 3' LTR U3 region was fully deleted leaving only the first 22 bp (upstream of the enhancer) and the last 14 bp (downstream of the TATA box). Such 3' LTR modifications are automatically copied to the 5' LTR in the transduced cells thereby generating enhancer-deleted proviruses also called self-inactivating vectors. Hence, they required an internal promoter to drive the expression of the transgene and thus the U3 promoter-enhancer sequences of SFFV region plus the adjacent R region stem loop (RSL) was cloned directly upstream of the transgene. This vector was used to insert cDNA coding for

gp91^{phox} by replacing the enhanced Green Fluorescent Protein (eGFP) at the position of the retroviral gag gene, and followed by the WPRE as a module to increase titer and transgene expression (Zufferey *et al.*, 1999). In this first vector series, three different gag-deleted leader regions were compared. Leader 11 and 110 were both derived from the MESV. Leader 11 contained only a splice-donor site and the leader 110 was a splicing sites-less leader generated by enzymatic restriction of leader 11 (Fig. 1). Finally, leader 71 contained both splice donor and acceptor sites derived from the Mo-MLV to create a full intron (Hildinger *et al.*, 1999).

C.1.2 Site-directed mutagenesis of the gp91^{phox} cDNA

The presence of cryptic splice sites in the transgene inserted into a retroviral vector is likely to cause aberrant transcripts both in packaging cells and in transduced cells. This was previously shown to cause a decrease in viral titers and transgene expression.

In this study the presence of cryptic splice sites in the gp91^{phox} cDNA was assumed by both sequencing analysis and previous experimental observations (data not shown). In order to further verify the existence of such sequences, a retroviral vector containing a splice donor site upstream of the gp91^{phox} cDNA was transfected into the producer cell line 293T. Total cellular RNA extraction and reverse transcription was performed to obtain cDNA form. Oligonucleotides for PCR amplification were designed for the gp91^{phox} cDNA binding directly upstream of the splice donor site and downstream at the 3' end of the gp91^{phox} cDNA sequence. Following RT-PCR amplification, one band corresponding to the designed fragment (~ 2600 bp) would be expected, if no cryptic splicing sites are present in the region. However, two bands were detected indicating the presence of a cryptic splice acceptor (cSA) in the gp91^{phox} gene, which was functional in the context of packaging cells and might lead to a reduction in the viral titer (Fig. 16a). This band was cloned and sequenced to determine the exact position of the cSA (Fig. 16b). This splice site was found at the 5' end of the gp91^{phox} cDNA exactly 239 bp from the first nucleotide of the gp91^{phox} cDNA (the gp91^{phox} cDNA spans 1713 bp), matching the splice acceptor consensus sequence with 100% homology (Fig. 16c). Whether this splice variant leads to the formation of a truncated protein was not investigated. It is believed, though, that truncated and therefore aberrant gp91^{phox} protein is unstable since it is degraded by the cell (Kaneda *et al.*, 1999).

Since the presence of splice sites might compromise expression of the transgene as well as viral particle production due to the generation of incorrect transcripts the gp91^{phox} cDNA was mutated in order to remove the cSA. The most conserved nucleotides at intron-exon boundaries in eukaryotic pre-mRNAs are the GU and AG at the 5' and 3' ends of the intron. The cSA found in the gp91^{phox} cDNA contained these nucleotides.

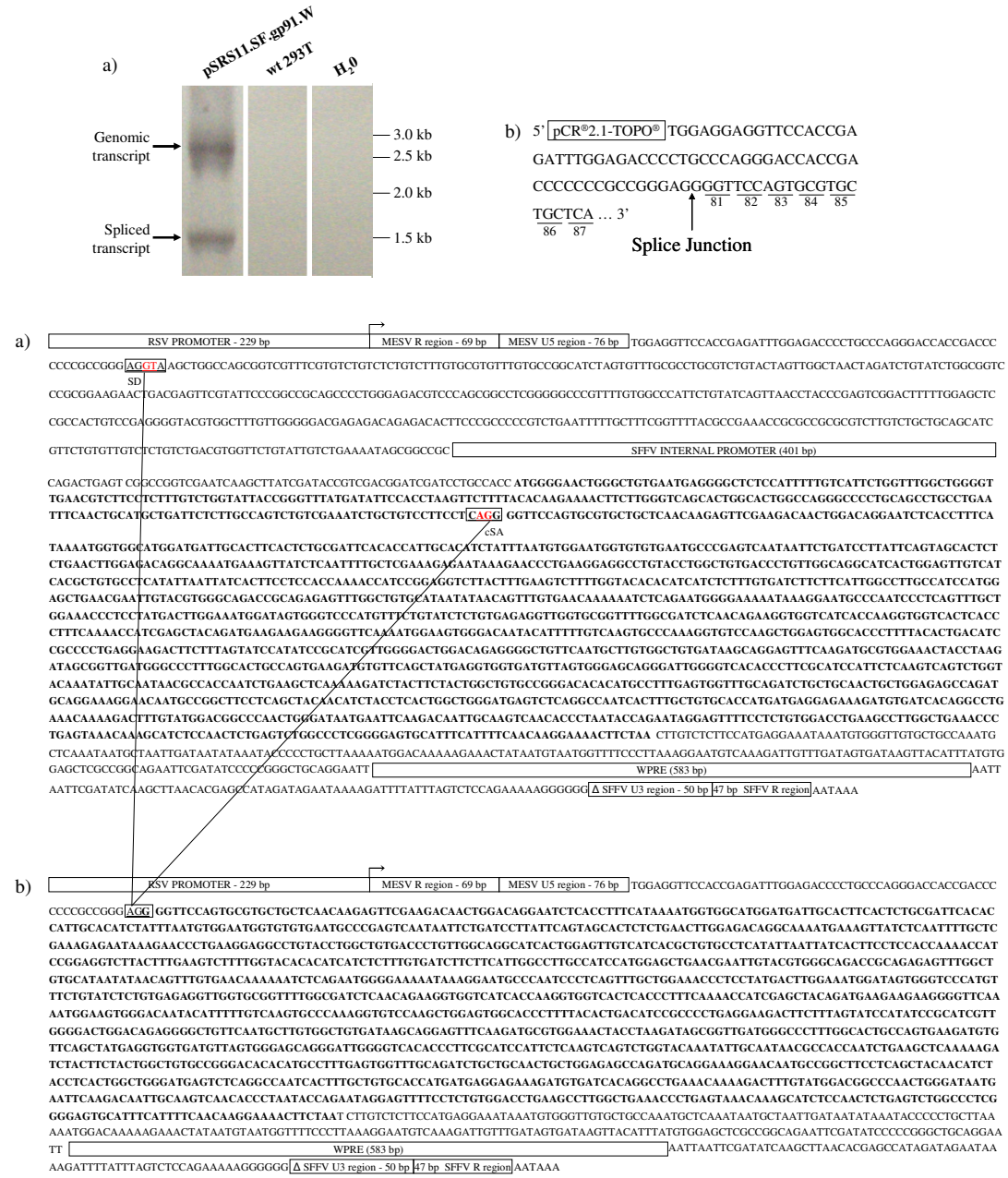

Fig. 16: The cDNA of the gp91^{phox} bears a cryptic splice acceptor (cSA). (a) Products obtained after RT-PCR amplification with primer P1 and R8 of total cDNA from pSRS11.SF.gp91.W transfected cells revealed the presence of the full-length transcript and an additional band due to an alternative splicing event. (b) The obtained band was cloned into pCR2.1-TOPO vector and sequenced. This fragment is shown and the position of the cSA is indicated. Amino acid positions of gp91^{phox} are indicated below the sequence. (c) Sequence of the pSRS11.SF.gp91.W plasmid showing between the promoter and the polyadenylation signal. The transcription start site is marked by an arrow. The gp91^{phox} sequence is presented in bold letters. The consensus sequences in the splice sites are underlined and the 100% conserved sites are indicated in red. (d) The splice variant expressed by the viral construct is shown. The fusion of the SD and cSA sites is boxed.

Therefore, mutation of one of the nucleotides was believed to reduce or even abolish splicing events at that particular site. However, the gp91^{phox} gene appears to be extremely sensitive to mutations, especially to missense and nonsense mutations (60% of all described mutations) (Rezvani *et al.*, 2005). Consequently, it was of crucial

importance to maintain not only the open reading frame but also the encoded amino acid sequence. The only possible mutation of the cSA-site was to introduce a cytosine instead of the invariable adenosine, thereby changing the coding AGG into a CGG codon, which both translate into the same amin oacid, arginine (see Fig. 17).

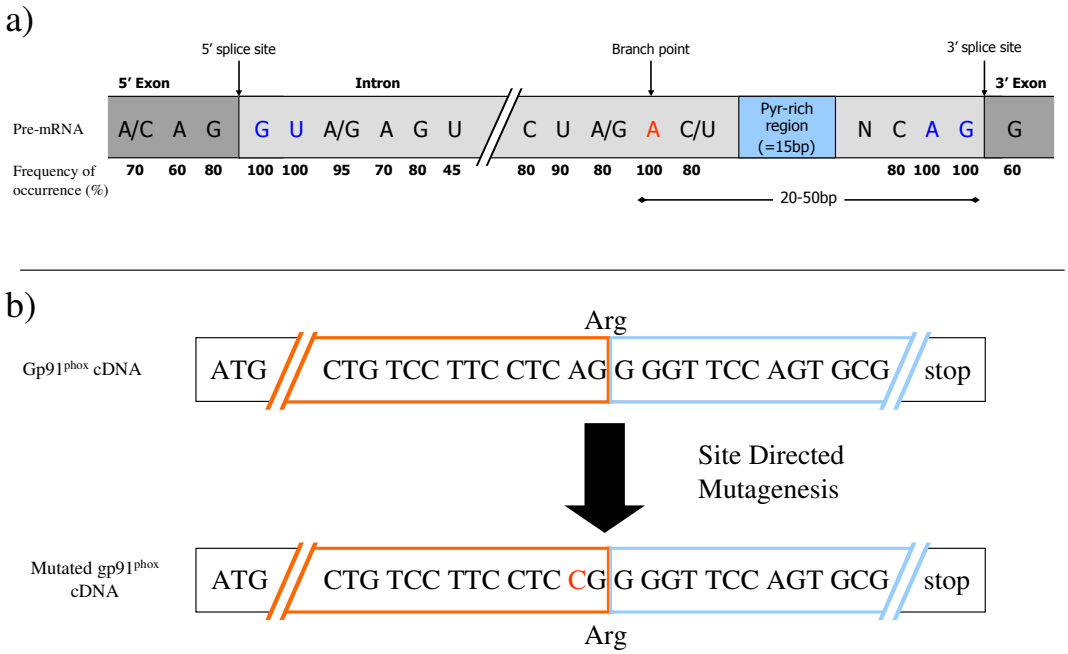

Fig. 17: Consensus sequences around 5' and 3' intron splice sites in vertebrate pre-mRNAs. (a) The frecuency of the bases found at the indicated position is given. (b) Strategy used to mutate the cryptic splice acceptor site (cSA) by site-directed mutagenesis. The adenosine of the consensus AG at the cSA located in an Arg codifying triplet was mutated to cytosine by site directed mutagenesis.

Mutated primers were designed to amplify the whole gp91^{phox} containing plasmid and to introduce the mutation. After verifying the occurrence of the mutation by sequencing the PCR product, the new gp91^{phox} variant was cloned in the three different retroviral vectors obtaining thus a 2 series of 3 constructs (Fig. 15b).

C.1.3 Transduction efficiency of X-CGD PLB-985 cells

One of the most limiting factors for therapeutical applications of retroviral vectors is the viral titer. To investigate this issue, GaLV pseudotyped retroviral particles were generated by calcium phosphate transfection into 293T cells. The number of infecting units per ml of the viral supernatant was assessed by transduction of human X-CGD PLB-985 cells, a myelomonocytic cell line in which the gp91^{phox} gene was knocked out (Zhen *et al.*, 1993). Transduction efficiencies were measured three days post-transduction to avoid pseudotransduction phenomena and false positives. False positive cells express the transgene transiently from non-integrated viral genomes which could lead to overestimation of the transduction efficiency (Haas *et al.*, 2000). The percentage of gp91^{phox} expressing cells was determined by FACS analysis of cells immunostained with a 7D5 moAb, which recognizes an extracellular epitope of the

flavocytochrome b_{558} (Yamauchi *et al.*, 2001). Additionally, genomic DNA of transduced cells was isolated to quantify the number of viral integrants per cell by semi-quantitative PCR amplification. Genomic DNA isolated from a cell clone containing 1 proviral copy per cell (previously determined using LM-PCR by C. Preiss) was used as reference for quantification (Fig. 18).

A high variability between the measurements was observed. Titers quantified by PCR reached from 2.0 to 3.0 $x10^6$ t.u./ml whereas up to 1.2 $x10^6$ t.u./ml were obtained by FACS determination. The lowest titers of $3.3x10^5$ t.u./ml and $7.1x10^5$ t.u./ml were obtained with the SRS110.SF.gp91.W vector by FACS or PCR analysis, respectively. Moreover, differences from up to 3-fold in titer were observed between the semi-quantitative PCR measurements and FACS determinations, which might be explained by the presence of integrated proviruses that do not express the transgene. When comparing the three different leaders present in the constructs, vectors with leader 11 appear to have slightly higher titers than other vectors both in FACS and PCR analysis. Only in one case leader 71 showed better titers than leader 11 using FACS analysis of wild-type $gp91^{phox}$ containing constructs; however, the data had high standard deviation levels. Between wild-type and mutated $gp91^{phox}$ cDNA therefore were no significant differences. However, a 3.4-fold higher PCR-titer was observed for the SRS110.SF.gp91m.W when compared to the SRS110.SF.gp91.W. The FACS measurements also showed differences in the titers reached by both vectors containing the leader 71 but again the levels of standard deviation reached doubts about the significance of this difference.

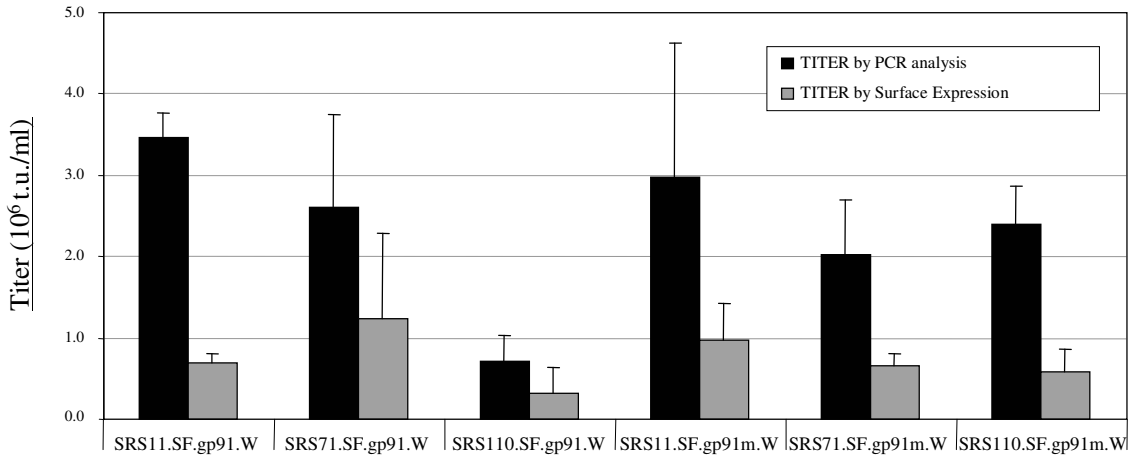

Fig. 18: Determination of vector titers by transduction of X-CGD PLB-985 cells. FACS analysis and semi-quantitative PCR were used to determine the titers of GaLV pseudotyped SIN gammaretroviral particles after transduction of X-CGD PLB-985 cells with serial dilutions of the viral supernatants. The titer is indicated in transducing units (t.u.) observed per ml viral supernatant used for transduction. Bars represent mean values ± standard deviations of at least three independent transfection/transduction procedures.

Overall, these results indicate that between the six constructs the leaders 11 and 71 performed slightly better than the leader 110 containing vectors and that, although high standard deviations were calculated, all these vectors reached titers that are high enough to their use in therapeutic applications.

C.1.4 Magnetic cell sorting of gp91^{phox} positive cells

Together with the capacity of generating high titers, the most important characteristic of a gene transfer vector for the treatment of CGD is the ability to reconstitute the oxidase activity to physiological levels. In order to be able to compare the performance of the six different retroviral vectors, populations of 100% positive cells harboring the same amounts of integrants per cell were required. Consequently, a selection procedure of gp91^{phox} positive cells was set up by which populations of 5 to 15% positive (7D5 positive) cells were enriched to up to 95%. It was desirable to start with populations with 5 to 15% gp91^{phox} expressing cells since the aim was to obtain populations with one integrated viral genome per cell. Previous studies have shown that an exponential increase in integration numbers correlates with a linear increase of gene transfer rates (percentage of positive cells after transduction as measured by FACS analysis of transgene expressing cells), defined as Poisson-like distribution (Kustikova *et al.*, 2003). Therefore, transduced cell populations for each vector were immunostained with antibodies against gp91^{phox} coupled to magnetic beads prior to selection by passing the labeled cells through a magnetic field. After washing and eluting, the gp91^{phox} positive cell enrichment was assessed by FACS analysis.

As shown in Fig. 19 all transduced populations were efficiently sorted by the MACS procedure, reaching about 98% for almost all constructs. Note that the mean fluorescence intensity (ΔMFI) of transduced cells prior to selection was higher in wild-type gp91^{phox}-expressing cells than in cells expressing the mutated gp91^{phox} protein, but reached equivalent levels after sorting.

Additionally, the mean copy number was analyzed by semi-quantitative PCR amplification again using a population with a known copy number as a standard reference. This analysis revealed a uniform 1 copy per cell for all the enriched populations (data not shown).

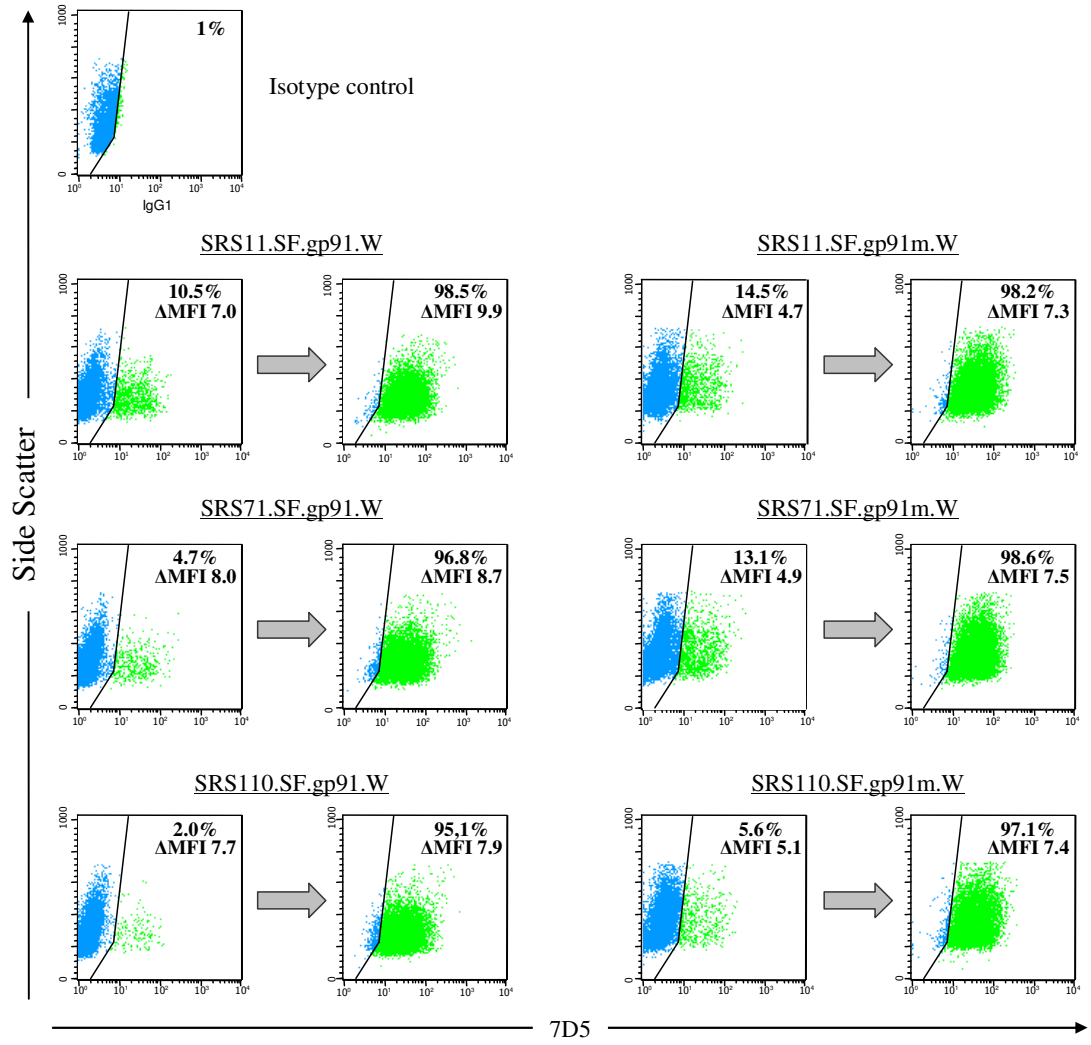

Fig. 19: Magnetic cell sorting allows purification of gp91^{phox} expressing cells by positive selection. X-CGD PLB-985 cells were transduced with the two series of SIN gammaretroviral vectors. They were then labeled with antibodies against gp91^{phox} coupled to magnetic beads prior to selection by passing the labeled cells through a magnetic field. FACS analysis data of gp91^{phox} expressing cells (7D5 positive) before, left panel, and after, right panel, cell sorting are shown**.**

C.1.5 Functional analysis of the gp91^{phox} transduced cells

The NADPH oxidase activity has been shown to be restricted to terminally differentiated granulocytes, monocytes and B lymphocytes. Upon stimulation granulocytes promote assembly and activation of the oxidase enabeling the generation of high amounts of superoxide. PLB-985 cells have the ability to differentiate to granulocyte-like cells, thus providing an excellent model to test the performance of the retrovirally transferred gp91^{phox} to reconstitute the activity of the oxidase. Several protocols are being used to induce differentiation of myeloid cell lines. DMSO, DMF, Vit. D_3 or phorbol myristate acetate (PMA) stimulation are most commonly used (Rovera *et al.*, 1979).

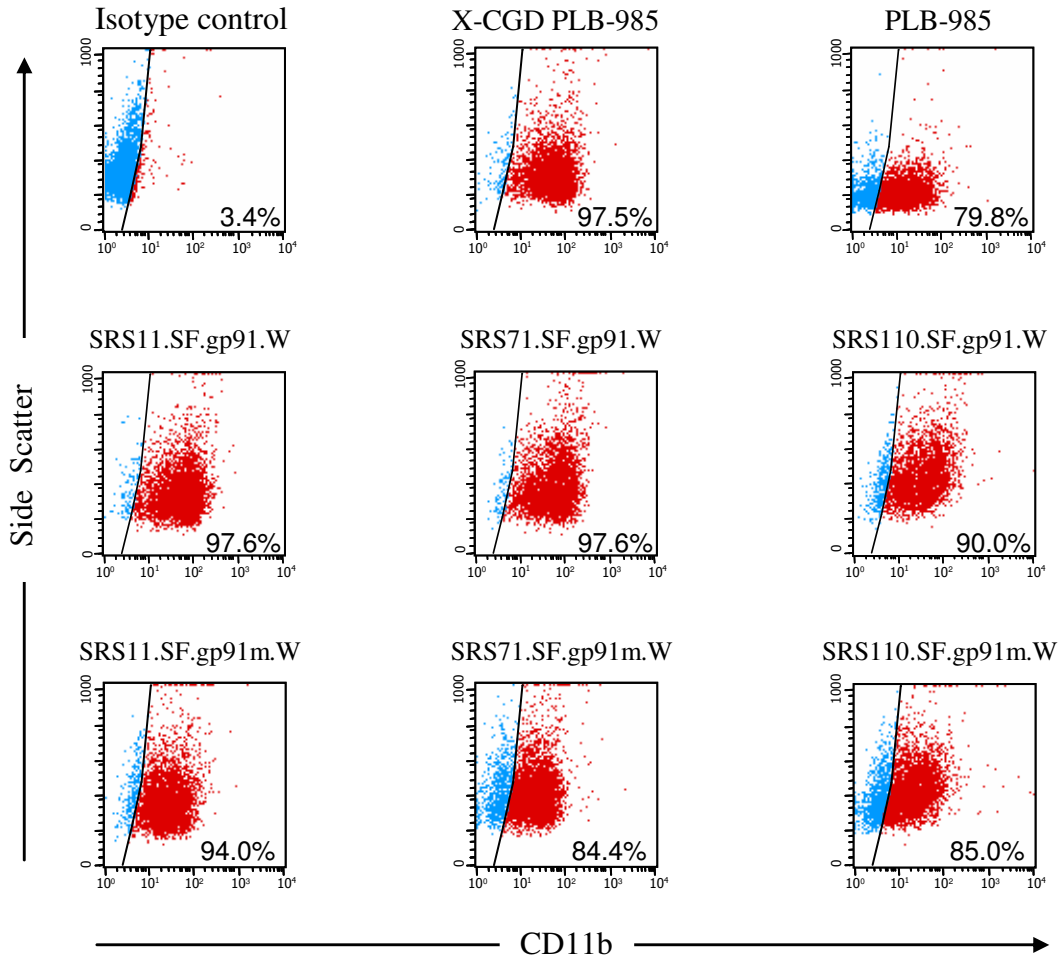

Fig. 20: Granulocyte-like cell differentiation of the sorted cell populations transduced with gp91^{phox}-viral particles. PLB-985 cells and transduced derivatives described in Fig. 19 were incubated with 1.25% DMSO for 6 days. The expression of the CD11b monocyte/macrophage differentiation marker was ensured by FACS analysis.

In the present study incubation with 1.25% DMSO for 6 days was used to stimulate maturation of the MACS-selected cell populations. The CD11b surface marker was used to ensure the differentiation of the transduced cells by flow cytometry. In all the cases, about 80-90% of the cells were positive for CD11b (Fig. 20).

Since it was possible to differentiate the transduced cell populations, it was then possible to investigate the ability of SIN gammaretroviral vectors to reconstitute the NADPH oxidase activity. The cytochrome c assay was used, which is a quantitative method to measure the cellular superoxide anion production. DMSO differentiated populations were stimulated with PMA, a powerful stimulant that triggers O_2^- production. The superoxide production per cell was measured by reduction of ferricytochrome c over time. Differentiated wild-type PLB-985 cells were always used as a reference value.

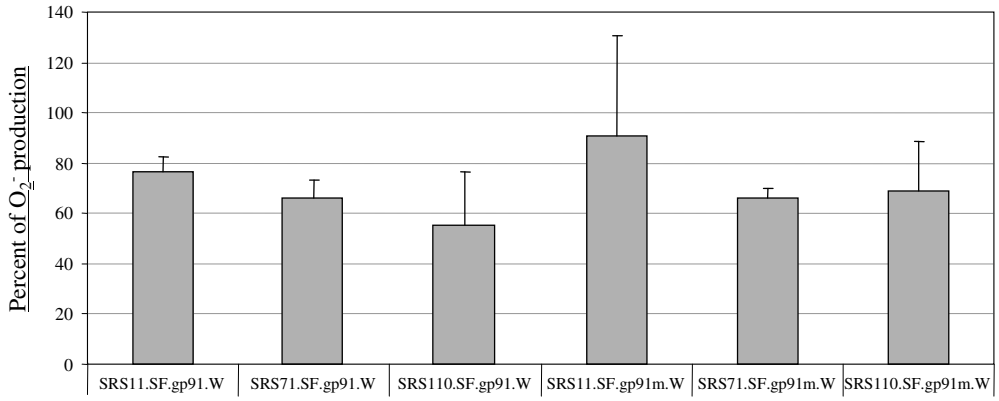

Fig. 21: Percentage of superoxide production in X-CGD PLB-985 cells after SIN gammaretrovirus-mediated gene transfer. Transduced cells were immunomagnetically sorted, expanded, and cultivated for 6 days in the presence of 1.25% DMSO to induce granulocyte-like cell differentiation. The total amount of superoxide production was measured by a continuous cytochrome c assay after PMA stimulation. Data are shown in percent superoxide production relative to the amount of superoxide produced by differentiated wild-type PLB-985 cells. The mean values ± standard deviations of at least three independent experiments are represented.

As shown in Fig. 21 all constructs were able to reconstitute the oxidase activity to high extents reaching in some cases the same levels than wild-type PLB-985 cells. Although the standard deviation is high, the 11 leader-containing vectors SRS11.SF.gp91.W and SRS11.SF.gp91m.W showed the best preformance. By using the SRS110.SF.gp91.W construct only 60% of the wild-type activity could be reached.

The levels of oxidase reconstitution reached by all these vectors might be enough to ensure adequate microbicidal activity, since female X-CGD carriers with as few as 5-10% oxidase-positive neutrophils often display a symptom-less disease (Johnston *et al.*, 1985; Woodman *et al.*, 1995).

C.1.6 Analysis of myeloid-specific promoters for targeted expression of retroviral vectors

Since the activity of the NADPH oxidase is required mainly in phagocytic cells, the restriction of the expression of the retrovirally introduced $gp91^{phox}$ to myeloid cells is of great interest. The SIN vectors represent an excellent model to test cell-specific promoters, since in these vectors the transgene expression in transduced cells is under the control of an internal promoter. Various promoters can be used for this purpose. Since the $gp91^{phox}$ is transferred into deficient cells of CGD patients, the use of the $gp91^{phox}$ promoter itself would be the best option. However, additional studies are required to identify all the required sequences of the $gp91^{phox}$ promoter for proper transgene expression. Currently, different fragments of the $gp91^{phox}$ proximal promoter are being analyzed to elucidate all the regulatory factors affecting the $gp91^{phox}$ expression (Samuelson *et al.*, 2001; Islam *et al.*, 2002).

Therefore, two human myeloid-specific MRP8 and c-fes promoters were chosen as alternative. They were tested in the SRS11.SF.gp91m.W vector configuration, since it showed the best performance regarding titer and reconstitution of the NADPH oxidase activity in the previous experiments.

C.1.6.1 The MRP8 promoter

The MRP8 promoter drives the expression of the myeloid related protein 8, which has been shown to be involved in several cellular processes during transendothelial migration of phagocytes such as, *inter alia*, microtubule reorganization and arachidonic acid transport but also during differentiation of myeloid cells (Kerkhoff *et al.*, 1999; Vogl *et al.*, 2004). Moreover, recent studies have shown that MRP8, in a hetero-dimeric form with MRP14, are also implicated in the activation of the NADPH oxidase complex (Berthier *et al.*, 2003; Paclet *et al.*, 2007). The MRP8 protein is tightly regulated during differentiation of myeloid cells. Its expression level is low in common myeloid progenitors and their granulocyte/monocyte progenitors whereas MRP8 expression can reach up to 45% and 1% of the cytosolic protein content in neutrophils and monocytes, respectively (Edgeworth *et al.*, 1991; Hessian *et al.*, 1993). Thus, due to this characteristic, the MRP8 promoter has been used to drive the expression of different transgenes in several myeloid leukemia transgenic mouse models (Yuan *et al.*, 2001; Jaiswal *et al.*, 2003).

In the present study, a fragment containing 1176 bp, from -1159 to +17, of the MRP8 upstream regulatory sequence was used. It spann 17 bp of the first exon of the gene, but contained a mutated ATG triplet. It was changed to ACT by PCR amplification with oligonucleotides containing the mutation. This was important to avoid translation initiation (Dr. S. Stein, pers. commun.). Since this sequence was able to drive efficiently the expression of eGFP after transduction of X-CGD cells in the context of a lentiviral backbone (Dr. S. Stein; pers. commun.), it was cloned in both the wild-type and mutated gp91^{phox} cDNA-containing vectors and is labeled as M8dNdI (Fig. 22 and Fig. 23a).

```
-1162                                                    TATGCTTATTGACCATTTGTATATCTTCTTCGGAGAAGTGTCTATTTGAGTCTTTTCCCCAA
-1100 TTTTTGATTGGTTTGTTTGTTTTTTGTTGTTGAGTTGTAGGGATTCTTTTATATTCTGGATATTAATCCCTTATCAGATATTTGTTTTACAAATATTTTC
-1000 TTTGTAACAACAGAAACACACCACAGTCTTCAAGGTTGGAAGCCAGTTAATCTGAGTAGCATTTTGTTAGTGGTGGGGAGAGGATTTGTTCCTCCTGAAA
 -900 TCCTGGGGAATTGGCCACCTCCTCTTCTCCTCTTAGGCATGAAGCGCGTCTGGCTTCTCCAAAGAACTCTTCCCCTCCACTACCTCAGAGTTAGCTTCCT
 -800 CTCTTCAGCCAGTGATCCTGGGGTCCCAGACACAATAATTAACCAAGAGAGGGTGAAAGGCTCCCTGCTGTGTTTATGCAATGGCTCAGGCCCTTGTGAA
 -700 GTGCCGAGGGACCCCAAGCAGCCTCCATCTCCCAGGGCATGGTCCATCCCCAGCTTCACAGAACAGGAAAGCTGTGGAGGAGTGTGGGCAGCAGGGTAGG
 -600 AATGGATATAGCCCTTGGCAACAACACATTTCCCCACAAAGCACCCACCCAAAAGAACAACAACGATAGTTTTAGTTTTTAGTAATGAGAACAATAGTTC
 -500 TCATGACTAAAAGCCATCAGCCAGGACACGTGTTCTCAACCCTTTTGCGGTCTTTGGACCCTTTGAAACTCTGACAGAAGCCATGGAGGAATGTTCTCAC
 -400 TGAGTGCATGCACTCAAAATGATGCATTCAACTTCAATTCAGTTTCAGGGATGTATGGCCTGACCACCAATGCAGGGGATTAGCAATCGCAATAGTGGAG
 -300 AGGGCATGGGAGTGGGAATCTGGCTGGATCAAGCAAGTGGATGCCAGCAGCCCAGAAAAAGAGCCCCCCTACCTGCTTTTTCCTTCTGGGCACTATTGCC
 -200 CAGCAAATGCCTTCCTCTTTCCGCTTCTCCTACCTCCCCACCCAAAATTTTCATTCTGCACAGTGATTGCCACATTCACCTGGTTGAGAAACCAGAGACT
          CAAT BOX                                                                              TATA BOX
 -100 GTAGCAACTCTGGCAGGGAGAAGCTGTCTCTGATGGCCTGAAGCTGTGGGCAGCTGGCCAAGCCTAACCGCTATAAAAAGGAGCTGCCTCTCAGCCCTGC
        Exon 1
    1 ★ACGTCTCTTGTCAGCTG
```

Fig. 22: Nucleotide sequence of the MRP8 promoter used in this study. The exon sequence is boxed and conserved promoter elements are overlined. Nucleotides are numbered according to the cap site (position +1).

Following transduction of X-CGD PLB-985 cells with GaLV pseudotyped particles gp91^{phox} expression was almost undetectable with the MRP8 containing-vectors (less than 4% gp91^{phox} positive cells), whereas expected levels were achieved if gp91^{phox} is under the control of the SF promoter (30%). Under the caveat that the obtained levels of positive cells were close to the non-specific binding of the antibody in the assay (background), a slightly higher percentage of gene transfer was seen by the combination of MRP8 and mutated gp91^{phox} (Fig. 23b).

Previous studies have shown that immature human myeloid cell lines (such as HL60, U937 and TPH-1) increase the expression of the MRP8 protein when myeloid differentiation is induced (Lagasse and Clerc, 1988). To investigate whether X-CGD PLB-985 cells equally transduced cells with the SRS11.M8dNdI.gp91.W or the SRS11.M8dNdI.gp91m.W construct also experienced an increase in transgene expression, these cell populations were used to assess for gp91^{phox} expression after granulocyte-like cell differentiation. However, again no gp91^{phox} expression was observed in the transduced populations, neither with the wild-type gp91^{phox} nor with the mutated sequence. The obtained levels of positive cells were similar to the values generated by non-specific binding (background levels) assessed by FACS analysis of differentiated X-CGD PLB-985 cells (Fig. 23c).

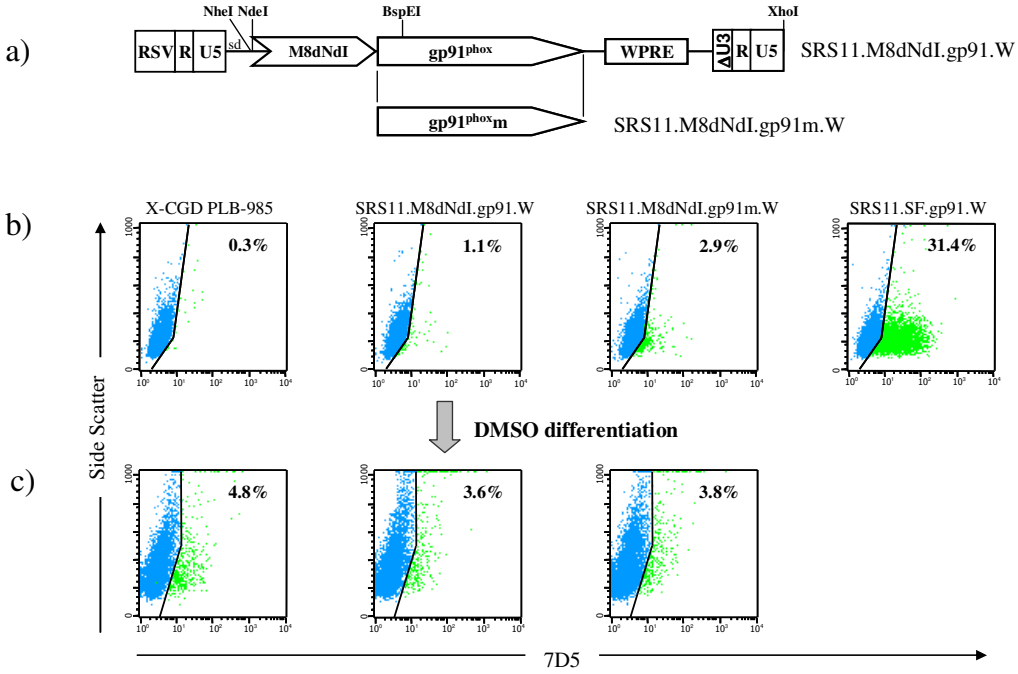

Fig. 23: The MRP8 myeloid-specific promoter driving the expression of gp91^{phox} in a SIN gammaretroviral vector. (a) Schematic presentation of the MRP8 promoter-containing SIN gammaretroviral vector (b) GaLV pseudotyped particles were used to transduce X-CGD PLB-985 cells with serial viral dilutions and FACS analysis was performed to analyze the expression of gp91^{phox}. Cells transduced with a 10-fold dilution of viral supernatant of both MRP8-containing constructs and the SF as control are shown. (c) The increase in transgene expression of transduced cell populations was assessed after DMSO differentiation by FACS analysis.

To analyze whether the absence of transgene expression in transduced cells was due to the lack of integrated proviruses, genomic DNA of transduced cells was prepared and PCR amplification was performed with oligonucleotides binding in the gp91^{phox} sequence (Fig. 24a). Amplification of β-actin was used as a control for DNA quality. A band indicating the presence of the transgene was detected for both transduced populations indicating that the viral particles were indeed produced and able to properly infect the target cells. Therefore, it was presumed that either absent or wrong processing of the transgene could be the cause of the extremely low expression level. To assess this possibility Northern Blot analysis of total RNA from transduced cell populations was performed to investigate the presence or absence of the internal transcript. Although the loaded amount of total RNA was higher than in the positive control sample, gp91^{phox} mRNA was not detectable for any of the MRP8-containing vectors (Fig. 24b).

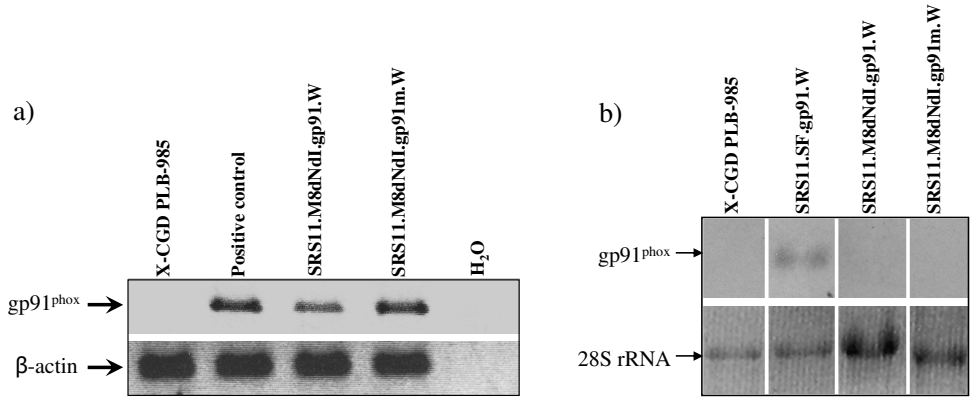

Fig. 24: Molecular analyses of gammaretroviral vectors containing an internal MRP8 promoter. (a) PCR reaction of genomic DNA of transduced X-CGD PLB-985 cells using primers gp-for-01 and gp-rev-02 to amplify the gp91^{phox} gene and primers ACT5' and ACT3' to amplify β-actin as a control was performed to ensure the presence of transgene. (b) Northern blot analysis of 3 µg total RNA from transduced cells. ^{32}P-labelled specific probe against gp91^{phox} sequence was used and the 28S rRNA band is shown as loading control.

The absence of transcription could be related to the lack of enhancer modules present in the genomic configuration of the endogenous MRP8 protein. Previous studies have shown the existence of an enhancer in the first intron of the MRP14 sequence (Melkonyan *et al.*, 1998). This cis-acting element has been shown to increase transcriptional efficiency up to 9.8-fold in Mono Mac 6 cells when cloned to a heterologous promoter. This sequence functions independently of its position and shares a high homology with the first intron of MRP8.

Therefore, to further investigate the effect of the enhancer in the MRP8 driven expression, a 392 bp fragment containing the intron of the MRP8 gene (+575 to +967) was placed upstream of the promoter into the retroviral vectors (Fig. 25).

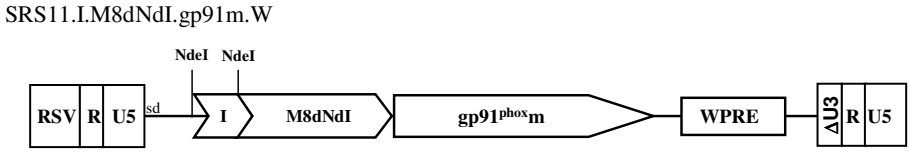

Fig. 25: The first intron of MRP8 as possible cis-acting activator of transgene expression. Schematic presentation of the SIN gammaretroviral vector containing the MRP8 promoter and intron sequences. 392 bp of the first intron (position +575 to +967) of MRP8 gene were cloned upstream of the promoter in the SIN gammaretroviral constructs in direct orientation.

X-CGD PLB-985 cells were transduced and the percentage of gp91^{phox} expressing cells was assessed by flow cytometry of 7D5 antibody stained cells. As shown in Fig. 26a there was again less than 5% gp91^{phox} positive cells three days post-transduction as well as after granulocyte-like cell differentiation. The differentiation of these cells was successful since FACS analysis revealed between 75 and 90% of CD11b positive cells (Fig. 26b).

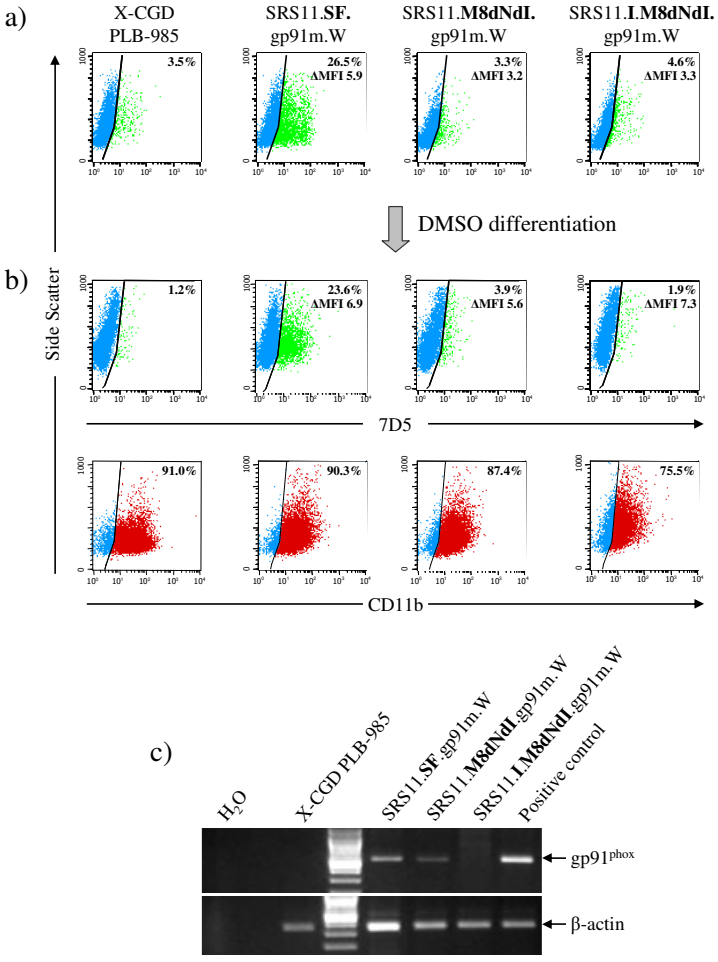

Fig. 26: MRP8 enhancer as possible cis-acting activator of transgene expression. (a) Transduction of X-CGD PLB-985 cells was performed with GaLV pseudotyped particles. FACS analysis assessing the presence of gp91^{phox} positive cells in transduced population with a 10-fold viral dilution is shown. The SF-containing vector is also shown as control. (b) Changes in transgene expression were analyzed following 1.25% DMSO granulocyte-like cell differentiation of transduced cells. Immunostaining with anti-CD11b surface marker to verify successful differentiation is also shown. (c) The presence of integrated proviruses was analyzed by PCR amplification of genomic DNA isolated from transduced cells. PCR amplification of β-actin was used as loading control.

Further investigations were performed in order to assess whether the transduced cells contained detectable numbers of proviral integrations. Therefore gp91^{phox} PCR amplification of genomic DNA of equally transduced cells was performed. The analysis of the obtained band revealed the presence of proviral integrations in cells transduced with the MRP8-containing construct. Proviral integrations were not detectable for the intron-containing construct as shown by the absence of a band in the corresponding PCR lane (Fig. 26c).

C.1.6.2 The c-fes promoter

The c-fes gene encodes a cytoplasmic protein tyrosine-kinase that has been detected in hematopoietic cells, predominantly in immature myeloid progenitors, in differentiated granulocytes and macrophages, and in vascular endothelial cells. Fes expression is also evident in leukemia cell lines, which can be differentiated *in vitro* along the granulocyte and monocyte pathways, but is absent in cell lines resistant to myeloid differentiation (Carlson *et al.*, 2005). The c-fes promoter in combination with untranslated gene sequences have been used in some transgenic mice models to uncover roles for this kinase in hematopoiesis, innate immunity, inflammation and angiogenesis. It has also been shown to be involved in regulation of the tubulin cytoskeleton as a process implicated in proliferation and differentiation (Laurent *et al.*, 2004). Furthermore, c-fes plays a role in signal transduction pathways for several hematopoietic cytokines such as IL-3, IL-4, IL-6, granulocyte-macrophage colony-stimulating factor (GM-CSF) and erythropoietin (Smithgall *et al.*, 1998).

Analysis of upstream regulatory sequences of the endogenous expression of c-fes revealed binding sites for several transcription factors, such as PU.1 and Sp1. (Heydemann *et al.*, 1996). Moreover, it was also shown that the locus control region (LCR), a cis-acting DNA element that enhances expression of the linked gene, present in the c-fes gene is an important element in the regulation of appropriate gene expression. Additionally, a minimal 446 bp promoter cassette was shown to efficiently direct expression of luciferase reporter gene towards myeloid cells (Greer *et al.*, 1990; Heydemann *et al.*, 2000).

```
-446                                                                GAATTCCGTGAGGTGGGGAGGGCTGGGACCAGGGTTCCCTCTTTCTC
-400 TTCTGCGGTGGCCCTGGCCTGGTGCTAGGACTGCGCGCCTCCCCTCAGTACCCGCGGACACCCTGGGCTTCCCTGGGCCCAGCATCTGCCTGGGGCCTCG
          Sp1
-300 CCCTGGGCTCCCCCTCCTGACCCCCACCTTGCGCCCCTTCCCGGTGTTCCCGGGGCGCTGCCGGGCCCTGGGGCCTGCGGGGCGCGGGCGGCTCTTGGCT
-200 GGGCCATTCTTTCCCGGCCCCCTCCTCCCTTCCGTTTCCGTGGCCGTGCGGCCGGCTAGAGGCTGCGGCCCAGCGCGGAGCAGGGGGGCTGGCAGGCGTC
                Sp1       Sp1          Sp1                                          PU.1/Elf-1
-100 GGGGCGGTCGGGCCGGTCCCGCCCGCCCCTTCCCCTCCACAGGCCCGCCCCGGGGCCTGGGCCAACTGAAACCGCGGGAGGAGGAAGCGCGGAATCAGGA
   1 ACTGGCCGGGGTCCGCACCGGGCCTGAGTCGGTCCGAGGCCGTCCCAGGAGCAGCGCCCG
```

Fig. 27: Nucleotide sequence of the c-fes promoter used in this study. Consensus sites for Sp1 and PU.1/Elf-1 are overlined. Nucleotides are numbered according to the cap site (position +1).

In the present study, the c-fes promoter was cloned in the SRS11.SF.gp91m.W construct substituting the SF promoter to test its performance in the X-CGD PLB-985 cell model (Fig. 27).

The gene transfer efficiency was evaluated by FACS analysis of transduced cells three days post-infection. As shown in Fig. 28b the c-fes construct efficiently drove the expression of the gp91^{phox} although to slightly lower levels than the SF-containing construct. About 11.4% of positive cells were detected after transduction with a 10-fold dilution of viral supernatant with the SRS11.fes.gp91m.W vector whereas 26.5% were obtained with the SF construct. Moreover, analysis of the ΔMFI revealed a 2.3-fold lower level of gp91^{phox} expression in the c-fes transduced population compared to the SF transduced cells. Further investigation of these cells following 1.25% DMSO differentiation showed minimal changes in the transgene expression level by the c-fes promoter since the ΔMFI after differentiation was 1.2-fold higher for the cells transduced with the SF-containing construct (i.e. around non-specific binding levels) and 1.5 for the fes-promoter transduced population.

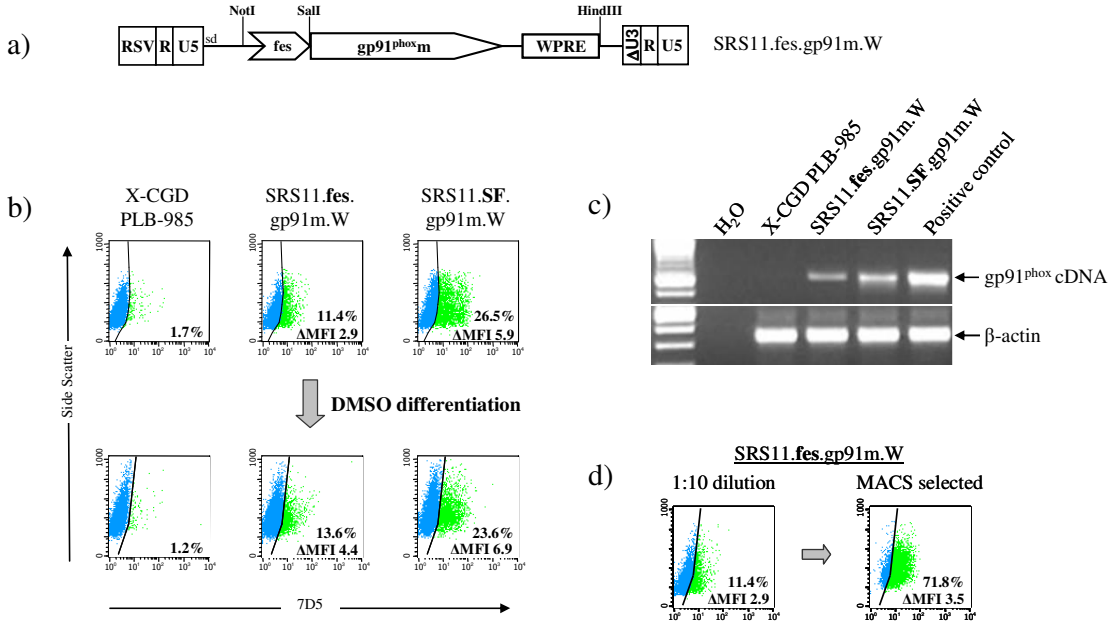

Fig. 28: Testing the c-fes promoter as internal promoter for a SIN vector. (a) The c-fes promoter was cloned into the SRS11.SF.gp91m.W vector replacing the SFFV promoter and the map of the transfer vector is depicted. (b) GaLV pseudotyped viral particles were produced by transient transfection of 293T cells. Transduction of X-CGD PLB-985 cells with a 10-fold dilution of supernatant is shown. The SF-containing vector was used as control. The increase of transgene expression was evaluated by FACS analysis after differentiation with 1.25% DMSO. (c) The presence of proviral integrations was assessed by genomic DNA PCR of transduced cells. β-actin was used as loading control. (d) MACS selection starting with a population of 11.4% gp91^{phox} positive cells was performed and FACS analysis was used to analyze the outcome of the sorting. ΔMFI values are indicated.

Further genomic DNA analysis revealed that the lower percentage of gp91^{phox} positive cells reached by the c-fes construct compared to SF was possibly due to a lower number

of integrants detected by PCR as shown in Fig. 28c. Therefore the lower titer reached by the fes-containing construct, which was half the SF construct titer, could be caused by less integration events.

A population of transduced cells with the c-fes promoter-containing construct was enriched by magnetic cell sorting for further functional analysis. As shown in Fig. 28d, a population transduced with a 10-fold dilution of viral supernatants underwent positive selection and about 72% of $gp91^{phox}$ expressing cells were obtained as assessed by FACS analysis.This sorted population, as well as X-CGD PLB-985 and MACS selected SRS11.SF.gp91m.W, were induced to differentiate by DMSO incubation. CD11b immunostaining was performed to analyze the differentiation degree at day 6, and positive cells were measured by flow cytometry. As shown in Fig. 29a, about 90% of granulocytic cells were detected in each population.

Further investigations of the MACS selected populations after differentiation were performed by protein analysis. In granulocytes, $gp91^{phox}$ normally present in different forms, generating multiple bands with a wide range of molecular mass (76-90 kDa) in Western Blots as shown for the control lysate of granulocytes in Fig. 29b. However, the bands detected in lysates of the studied populations showed a different pattern. In the SF-vector containing cells a band of about 90-100 kDa was detected by the $gp91^{phox}$ antibody (moAB 48). This band is almost invisible in cells transduced with the fes-construct. Additionally, the 65 kDa high-mannose glycoprotein precursor of the $gp91^{phox}$ was clearly detected in both populations by the $gp91^{phox}$ antibody. A decrease in the content of the precursor was observed in both MACS selected populations if lysated between before and after differentiation are compared. This observation correlates with the above mentioned description of this precursor, which is an intermediate form that needs association with $p22^{phox}$ to complete the maturation. The decrease in 65 kDa precursor amounts indicated completion of the maturation process of the flavocytochrome b_{558}, which goes parallel with granulocytic differentiation. Another additional band of about 55 kDa was detected on the blot, which might correspond to the protein core of $gp91^{phox}$ and was described in previous studies (Porter *et al.*, 1993). A strong decrease in the 55 kDa band was observed after differentiation of both populations.

The cytochrome c assay was used as functional study to analyze the reconstitution of superoxide activity in the selected populations. The MACS selected populations containing the c-fes construct did reach only half the O_2^- levels as detected for the cells transduced with the SF construct. Even after 24 min of PMA stimulation the superoxide levels only reached 60% (Fig. 29c). Moreover, the amount of superoxide produced by these populations reached only about 10% related to the wild-type PLB-985 cells, although this population contained 72% positive cells (Fig. 29d).

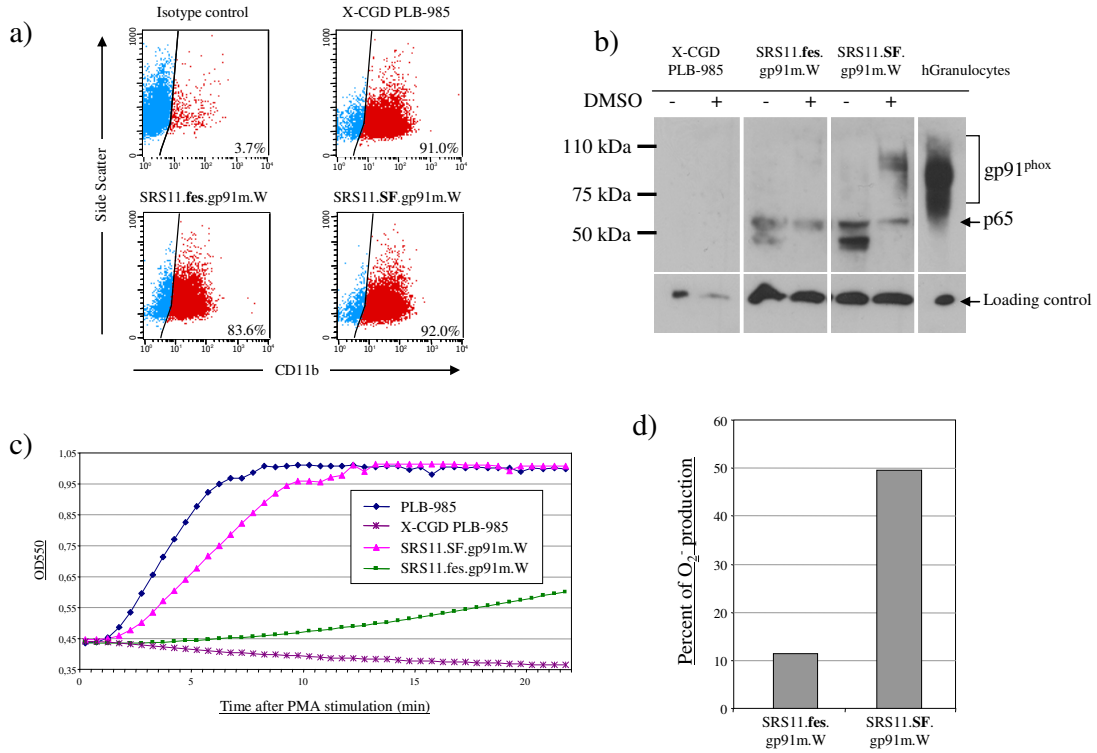

Fig. 29: Reconstitution of the NAPDH oxidase activity by the c-fes promoter-containing vector. (a) Myeloid differentiation of the sorted population assessed by FACS analysis of CD11b positive cells. (b) Protein extracts obtained from sorted cells comparing proliferating cells (- DMSO) and granulocytic-like cells (+ DMSO) were subjected to electrophoresis on a 10% SDS-polyacrylamide gel. Immunoblotting was performed using the moAB48 antibody (1:400) against gp91^{phox}. β-actin was used to ensure equal loading of total protein. (c) Kinetics of superoxide production by DMSO-differentiated MACS-selected cells was elicited by PMA induction. Reduction of ferri cytochrome C to its ferrous form over time was measured. (d) Percentage of superoxide anion production of PMA-stimulated cells expressed in percent relativ to the wild-type PLB-985 cells for which the O_2^- production was set to 100%.

Another variant of the c-fes promoter containing construct was cloned (SRS11.bgh.gp91^{phox}m.fes). This construct contained the expression cassette in the inverse orientation and a polyadenylation signal of the bovine growth hormone downstream of gp91^{phox} (Fig. 30a). Previous studies showed that this expression cassette cloned in a lentiviral backbone, achieved significant restoration of the oxidase activity *in vitro* with myeloid-lineage specific expression (Dr. S. Stein, pers. commun.).

As previously described GaLV pseudotyped retroviral particles were produced in the packaging cell line and were used to transduce X-CGD PLB-985 cells. As shown in Fig. 30b, there were no gp91^{phox} positive cells detectable when measured three days post-transduction although the SF- and fes- containing constructs did reach the expected levels.

To further analyze whether this lack in transgene expression was due to a defect in transgene transcription of integrated viruses, genomic DNA of transduced cells was prepared and investigated for the presence of the gp91^{phox} sequences by PCR amplification. There was no detectable transgene in the population of transduced cells

neither with 1:2 nor 1:50 viral supernatant dilution, which indicated a failure in the viral particle production (Fig. 30c).

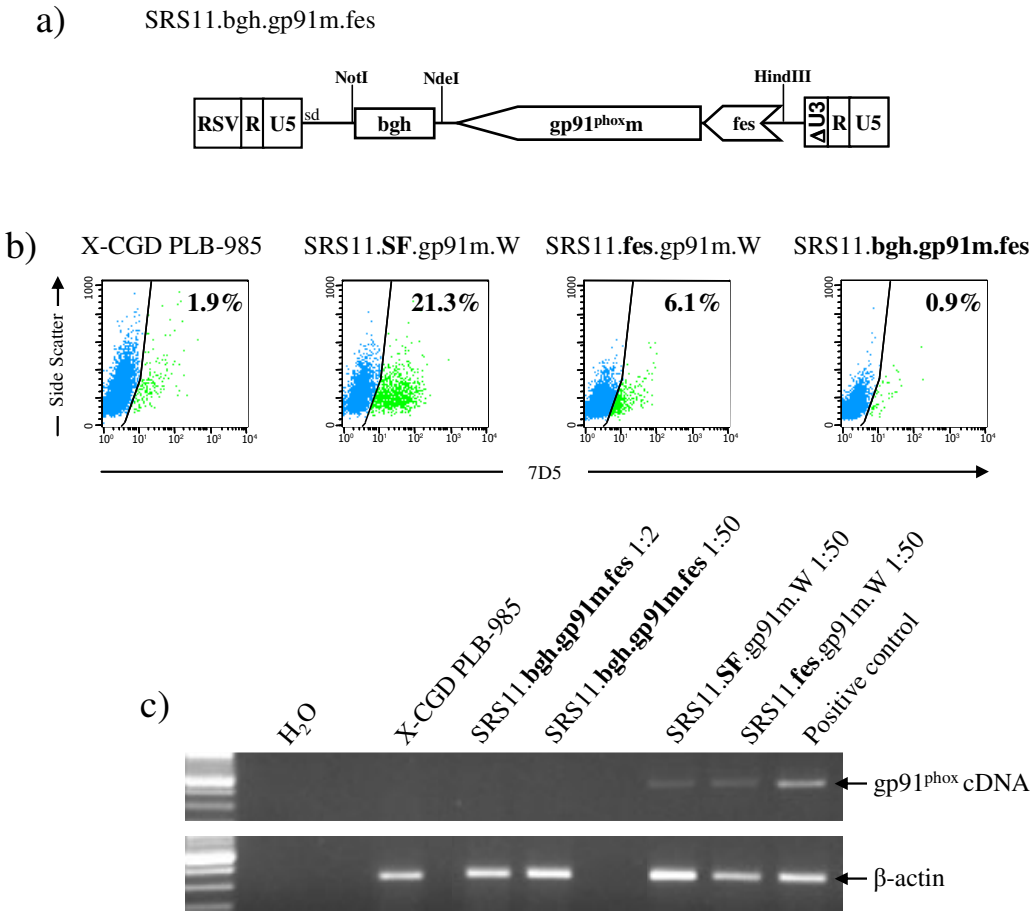

Fig. 30: Performance of a reverse expression cassette. (a) The c-fes promoter followed by the mutated gp91^{phox} and the polyadenylation signal of the bovine growth hormone gene were cloned in a SIN gammaretroviral vector in reverse orientation. The structure of this vector is represented (b) GaLV pseudotyped viral particles and X-CGD PLB-985 transduction were performed as described above. FACS analysis of the cells transduced with the 1:10 viral dilution is shown. (c) PCR amplification from genomic DNA obtained from transduced cells with 1:2 and 1:50 viral supernatant dilutions is shown. β-actin PCR amplification was used to check for equal loaded quantities.

C.2 Codon optimization of gp91^{phox} sequence

C.2.1 Synthetic sequence and SV40 enhancer improve the performance of SIN vectors

Previous attempts to generate a SIN gammaretroviral vector expressing either the wild-type or the mutated gp91^{phox} under the control of a myeloid-specific promoter (MRP8 or c-fes promoters) failed because the titer of the virus produced by transient transfection protocols were very low (<5x10^5 t.u./ml) and because low transgene expression levels. Various modifications including the addition of enhancer elements or reversion of the expression cassette neither improved titer values nor increased the transgene expression level. Therefore, a codon optimization of the gp91^{phox} cDNA was

considered as an alternative. Codon optimization is a strategy that is used to improve heterologous gene expression of genes introduced in foreign genomes. All codons of a protein are adjusted to the optimal codon usage pattern of the targeted organism. This methodology has already been used for widely known reporter proteins like GFP and luciferase (Cubitt *et al.*, 1995; Heim *et al.*, 1995; Yang *et al.*, 1996) and has shown to overcome poor transgene expression in several organisms (Kanekiyo *et al.*, 2005; Patterson *et al.*, 2005).

The company GeneArt (Regensburg, Germany) analyzed the gp91^{phox} wild-type mRNA sequence and improved the codon content by substituting codons with lower frequency of utilization with the preferred ones as represented by the respective tRNA content in the cell. The codon adaptation index (CAI), which indicates the relative number of matches between the given sequence and the codon preference of a determined organism, was optimized from originally 0.77 to 0.99. Additionally, several motifs were found which might interfere with either gene expression or virus production. Internal polyadenylation sites, additional cryptic splice sites and RNA instability motifs as AU-rich elements were then deleted.

The synthetic gp91^{phox} gene was used to replace the eGFP cDNA in the SERS11.SF.GFP.Wm backbone (kindly provided by Prof. Dr. C. Baum) (Schambach *et al.*, 2006c). This backbone contains an additional 233 bp SV40 enhancer (E) placed upstream of the RSV promoter as shown in Fig. 31a. For the SV40 enhancer it is known that it significantly increases gene expression in a wide variety of tissues and species (Schirm *et al.*, 1987). It also enhances the expression of the genomic transcript in packaging cells, thereby overcoming the promoter competition for the transcriptional machinery (Schambach *et al.*, 2006c). Moreover, previous data obtained from WHV-associated hepatocellular carcinomas suggest a relation between sequences overlapping with the PRE and tumorigenesis, especially if encoding a C-terminally truncated version of the WHV X protein. Although a role of the PRE remained suspect, to minimize potentially harmful effects of the PRE, a mutated version, which is devoid of the X protein promoter and any remnant open reading frame (ORF) larger than 25 amino acids by mutating residual ATGs (Wm), was introduced (Schambach *et al.*, 2006a). For comparison, a vector containing the gp91^{phox}m cDNA in combination with the SV40 enhancer was also constructed.

GaLV pseudotyped particles were produced in 293T packaging cells and used to transduced X-CGD PLB-985 cells. Synthetic gp91^{phox}-containing vectors showed a 2.7-fold increase in gene transfer rate by FACS analysis (Fig. 31b) which correlates with a corresponding increase in titer (Fig. 31c). Moreover, the amount of surface protein detected on the transduced cells was markedly higher with the synthetic gp91^{phox}-containing construct as compared to gp91^{phox}m-construct. This was shown by the fact that the ΔMFI value increased from 6.4 to 8.6 (Fig. 31b).

To further investigate the correlation between the amount of genomic RNA and the increase in titer, Northern Blot analysis of total RNA content of 293T packaging cells was performed (Fig. 31d). Transfection was carried out with an ecotropic envelope to avoid re-infection and RNA production from integrated proviruses. Finally, the intensities of the obtained bands in the blots were evaluated by densitometry. Indeed a higher production (1.1-fold) of genomic transcripts derived from the vector containing the synthetic gp91^{phox} sequence was observed, and this correlates with the higher titers. Moreover, an increase in the amount of internal transcripts (starting at the SF promoter) of about 1.4-fold was also detected when the synthetic gp91^{phox} was compared with the mutated gp91^{phox} transcript levels in transfected cells (Fig. 31d).

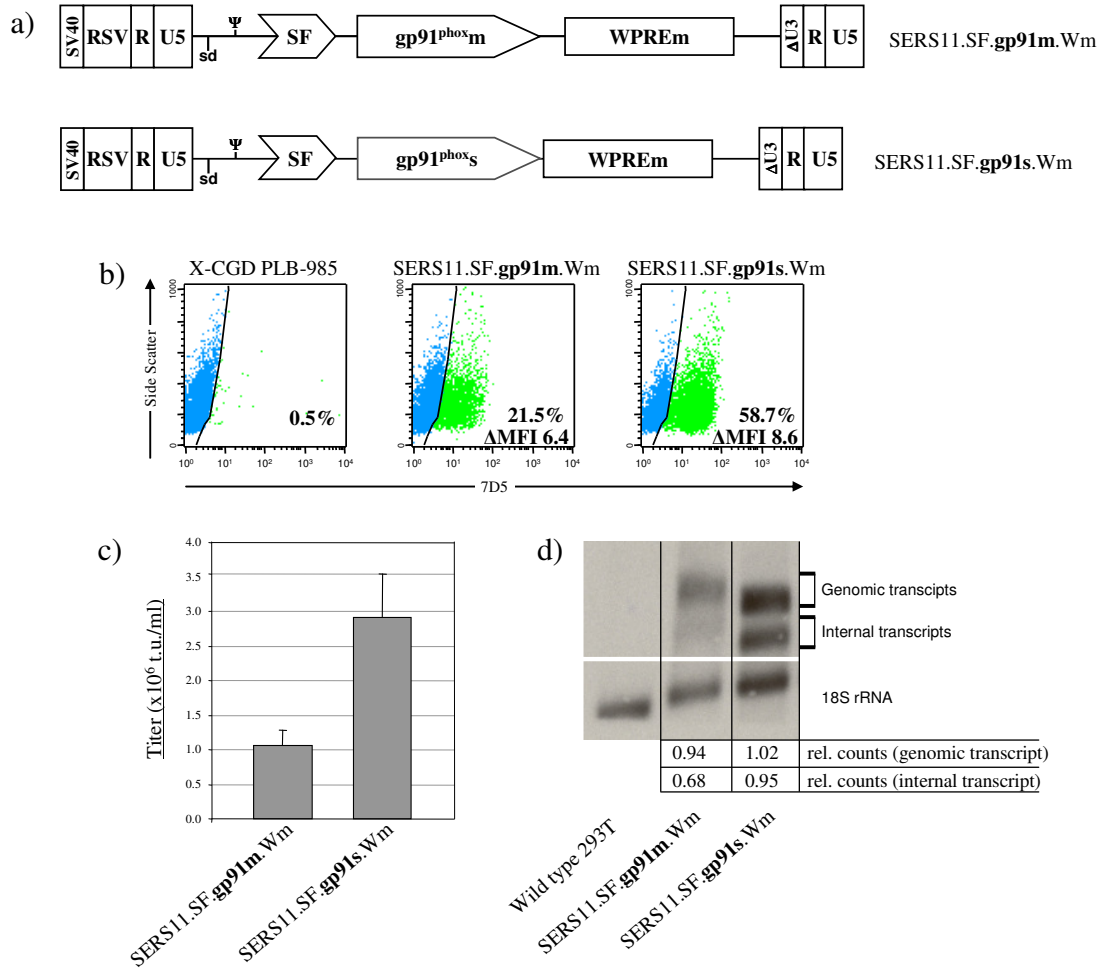

Fig. 31: Codon optimized gp91^{phox} increases vector titers and its gene expression level. (a) Schematic drawing of the SIN vector backbone used to evaluate the mutated or synthetic gp91^{phox} versions. The plasmid form contains a SV40 enhancer upstream of the RSV promoter. (b) Expression of gp91^{phox} in X-CGD PLB-985 cells after transduction with the same viral supernatant dilution (10-fold). FACS data of one representative experiment is shown with the corresponding ΔMFI value. Note the improved separation of the transduced cell population from the non-transduced cells in case of the gp91^{phox}s construct (c) Titers were determined as described above. The mean values ± standard deviations (SD) of at least three independent experiments are shown. (d) Northern blot analysis of 3 µg total RNA of 293T packaging cells. The expected RNA products are named on the right side of the blot. A specific WPREm probe was used to detect the gp91^{phox} transcript and an 18S rRNA probe to assess equal loading of the samples. The relative counts for the genomic and internal transcripts (normalized according to 18S rRNA levels) are given.

In order to compare the functional performance of both vectors, MACS selection of transduced cells was performed prior to vector copy number (VCN) analysis by semi-quantitative PCR amplification. To generate standard curves, genetically modified X-CGD PLB-985 cell populations containing 1 copy of gp91^{phox} transgene per cell (SF71gp#1 and Lenti MM5 transduced cells for the native and synthetic sequence, respectively) were used. Three different amounts (25, 50 and 100 ng) of genomic DNA were included in the PCR reaction amplifying gp91^{phox} and GAPDH, thereby ensuring maximal primer efficiency (Fig. 32).

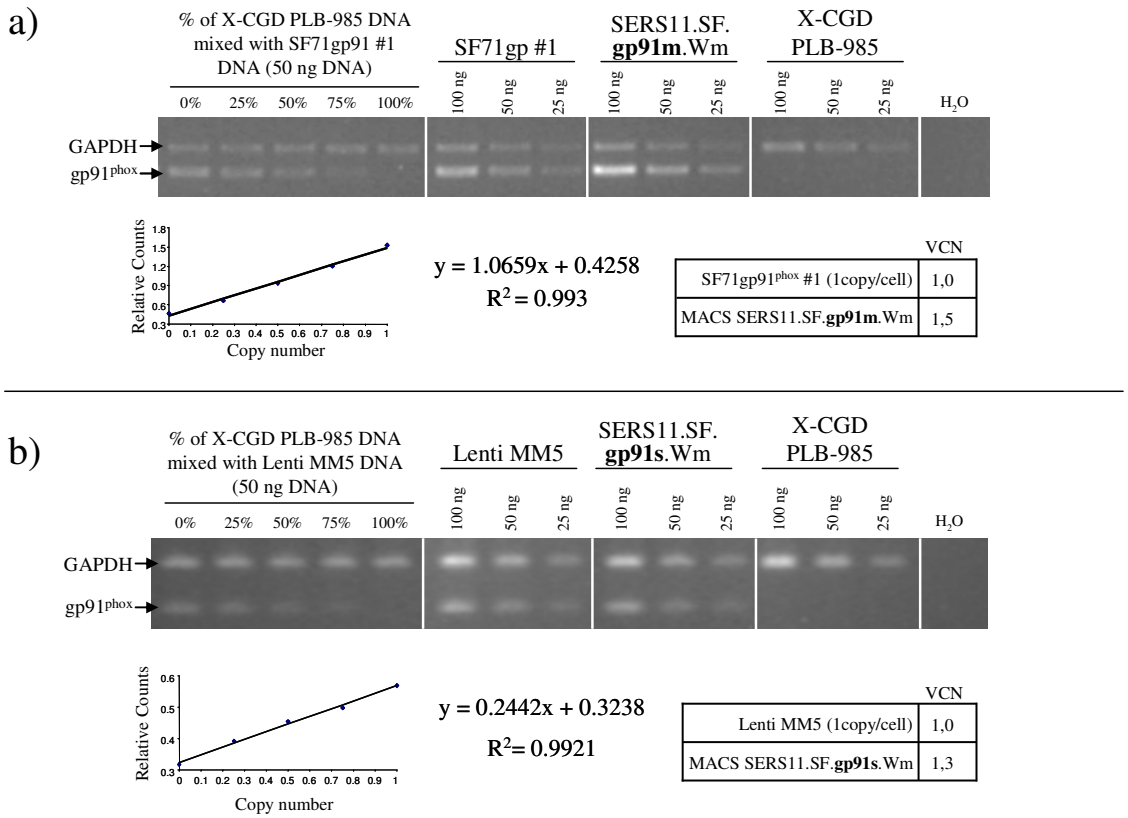

Fig. 32: Determination of the vector copy number (VCN) by semi-quantitative PCR. (a) Oligonucleotides gp91S-2for and gp91S-2rev for synthetic gp91^{phox} and GAPDH/5 and GAPDH/3 for GAPDH (loading control) were used to amplify genomic DNA of the sorted population. Different mixtures of DNA from a known population with one copy of transgene per cell (SF71gp#1) and X-CGD cells were used as standard. Analysis of band intensities of the standards allows the generation of a mathematic correlation which can be used to calculate the vector copy number in the samples. Linear regression and R-square values are shown. (b) Analysis of the VCN of the sorted SERS11.SF.gp91m.Wm transduced population using the Lenti MM5 cell population as standard. Primers gp-for-01 and gp-rev-02 were used in this case. PCR amplification and band intensity analysis was performed as described in (a).

Band intensity quantification and comparison with the standard values revealed similar numbers of integrations for both populations. The mutated gp91^{phox}-containing population had a mean of 1.5 proviral integrations per cell, whereas for the synthetic gp91^{phox} 1.3 copies were detected in the transduced population. FACS analysis of the sorted populations revealed a 2.2-fold increase in the expression level of the transgene with the synthetic sequence (Fig. 33). Additionally no changes were observed in the

transgene expression levels (ΔMFI) after 1.25% DMSO granulocyte-like cell differentiation, as expected for SF driven gene expression.

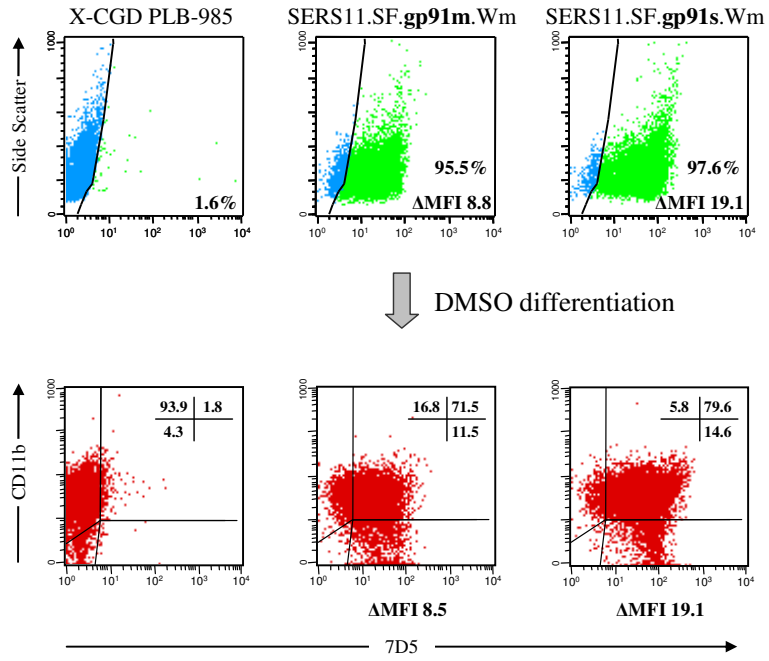

Fig. 33: Surface expression of gp91^{phox} in MACS-selected populations. Sorted populations underwent granulocytic-like cell differentiation by incubating the cells for 6 days with 1.25% DMSO. FACS analyses of gp91^{phox} (=7D5) and CD11b expressing cells are shown. Data of one representative experiment are shown with the corresponding ΔMFI.

C.2.2 Molecular and functional analyses

Northern Blot analysis performed as described above revealed marked differences in the expression level of the gp91^{phox}m and gp91^{phox}s-containing constructs. All cells of the sorted populations expressed the full length transcript initiated at the internal promoter and terminating at the 3'LTR. However, densitometry analysis showed hardly any change in transgene expression after DMSO differentiation for both constructs. Only a slight, non-significant decrease in transcription was observed for both constructs after differentiation. However, when comparing both gp91^{phox} versions, either proliferating or differentiated cells, higher transgene expression was detected for the synthetic gp91^{phox}-containing cells, corresponding to 4.7- and 15-fold increase, respectively (Fig. 34a). Note that the low intensity of the SERS11.SF.gp91m.Wm differentiated sample could be responsible for an underestimation of the values, thereby erroneously magnifying the differences in gp91^{phox} transcript amount between both differentiated populations.

To assess whether these differences correlated also with the protein levels of these cells, western blotting analysis was performed. Unfortunately, due to the differences in the amount of loaded proteins (as detected with β-actin) between undifferentitated and differentiated populations, it was not possible to study the changes in protein amounts

after granulocyte-like cell maturation. Nevertheless, as shown in Fig. 34b, when levels of gp91^{phox} protein obtained with the synthetic sequence were compared with the amount achieved by the mutated gene, a 2-fold increase in the protein content of differentiated cells was detected for the synthetic gp91^{phox} gene and a 5.5-fold increase when compared to differentiated wild-type PLB-985 cells.

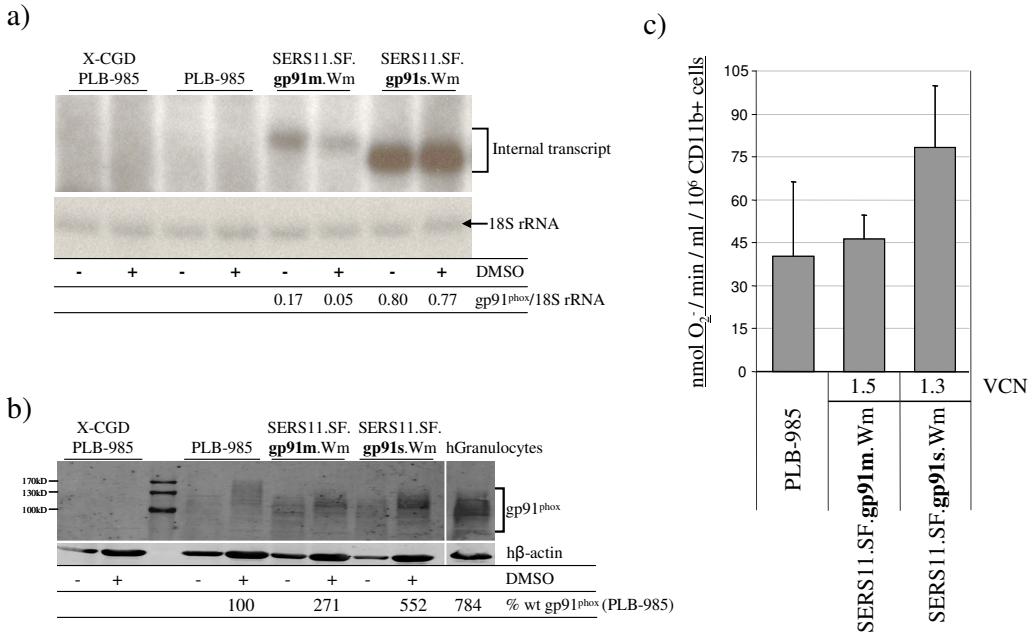

Fig. 34: The synthetic gp91^{phox} cDNA promotes higher expression and higher superoxide production. (a) Northern blot analysis of total RNA from MACS-selected population before (- DMSO) and after (+ DMSO) granulocytic-like cell differentiation. The analysis of the gp91^{phox} band intensity (normalized according to 18S rRNA) is shown. (b) Western blot analysis of 30 µg of total protein from sorted cells before (- DMSO) and after (+ DMSO) differentiation. The samples were loaded onto a 10% SDS-polyacrylamide gel and subjected to electrophoresis. Immunoblotting was performed as previously described, using a monoclonal antibody against gp91^{phox}. Quantification of the gp91^{phox} content (normalized to β-actin) for each sample is shown as percentage values related to the PLB-985 value. (c) DMSO-induced cells were used to analyze the superoxide production in a cytochrome C assay. The nanomols of superoxide produced per one million of cells, per min and per ml were measured after PMA. The means and standard deviations of at least three experiments are shown. The proviral VCN of the corresponding population is also indicated.

The functionality of the synthetic gp91^{phox}-containing construct was also assessed by the cytochrome c assay as previously described. The superoxide production was measured in 1.25% DMSO differentiated cells stimulated with PMA. As shown in Fig. 34c, a 1.7-fold increase in superoxide production was achieved with the synthetic gp91^{phox}-containing cells when compared to the wild-type PLB-985 and mutated gp91^{phox}-containing populations. This 1.7-fold increase in superoxide production correlated with the higher amounts of protein detected in these cells (Fig. 34b). However, no correlation was found when the wild-type cells were compared to the mutated gp91^{phox}-transduced cells since half the levels of protein were observed in PLB-985 cells although reached the same levels of superoxide production.

C.3 Transcriptional targeting with SIN gammaretroviral vectors

Targeting the transgene expression towards granulocytes would be a major improvement for the gene therapy of CGD. To this end several tissue-specific internal promoters were tested to drive the transgene expression.

Based on the SERS11.SF.gp91s.Wm vector as a backbone, the performance of three myeloid-specific promoters was assessed; c-fes, MRP8 and SP146. Beside the SF promoter and the already described c-fes promoter, an alternative version of the MRP8 promoter was used which comprises 1.7 kb of the upstream human MRP8 region, including exon 1 and intron 1 (from –1162 bp to +535 bp). The SP146 promoter is a synthetic promoter constructed by random ligation of several short sequences identified as binding sites for myeloid/macrophage transcription factors (Fig. 35b and c). The functionality of this promoter was previously tested in several cells lines, such as human myeloid/monocytic THP-1 cells and Mono Mac-1 cells, and was tested in an apoE$^{-/-}$ mouse model. This promoter spans 423 bp and is comprised of 14 cis-acting modules (He *et al.*, 2006).

a)
-1162 TATGCTTATTGACCATTTGTATATCTTCTTCGGAGAAGTGTCTATTTGAGTCTTTTCCCCAA
-1100 TTTTTGATTGGTTTGTTTGTTTTTTGTTGTTGAGTTGTAGGGATTCTTTTATATTCTGGATATTAATCCCTTATCAGATATTTGTTTTACAAATATTTTC
-1000 TTTGTAACAACAGAAACACACCACAGTCTTCAAGGTTGGAAGCCAGTTAATCTGAGTAGCATTTTGTTAGTGGTGGGGAGAGGATTTGTTCCTCCTGAAA
-900 TCCTGGGGAATTGGCCACCTCCTCTTCTCCTCTTAGGCATGAAGCGCGTCTGGCTTCTCCAAAGAACTCTTCCCCTCCACTACCTCAGAGTTAGCTTCCT
-800 CTCTTCAGCCAGTGATCCTGGGGTCCCAGACACAATAATTAACCAAGAGAGGGTGAAAGGCTCCCTGCTGTGTTTATGCAATGGCTCAGGCCCTTGTGAA
-700 GTGCCGAGGGACCCCAAGCAGCCTCCATCTCCCAGGGCATGGTCCATCCCCAGCTTCACAGAACAGGAAAGCTGTGGAGGAGTGTGGGCAGCAGGGTAGG
-600 AATGGATATAGCCCTTGGCAACAACACATTTCCCCACAAAGCACCCACCCAAAAGAACAACAACGATAGTTTTAGTTTTTAGTAATGAGAACAATAGTTC
-500 TCATGACTAAAAGCCATCAGCCAGGACACGTGTTCTCAACCCTTTTGCGGTCTTTGGACCCTTTGAAACTCTGACAGAAGCCATGGAGGAATGTTCTCAC
-400 TGAGTGCATGCACTCAAAATGATGCATTCAACTTCAATTCAGTTTCAGGGATGTATGGCCTGACCACCAATGCAGGGGATTAGCAATCGCAATAGTGGAG
-300 AGGGCATGGGAGTGGGAATCTGGCTGGATCAAGCAAGTGGATGCCAGCAGCCCAGAAAAAGAGCCCCCCTACCTGCTTTTTCCTTCTGGGCACTATTGCC
-200 CAGCAAATGCCTTCCTCTTTCCGCTTCTCCTACCTCCCCACCCAAAATTTTCATTCTGCACAGTGATTGCCACATTCACCTGGTTGAGAAACCAGAGACT
CAAT BOX TATA BOX
-100 GTAGCAACTCTGGCAGGGAGAAGCTGTCTCTGATGGCCTGAAGCTGTGGGCAGCTGGCCAAGCCTAACCGCTATAAAAAGGAGCTGCCTCTCAGCCCTGC
Exon 1
1 ATGTCTCTTGTCAGCTGTCTTTCAGAAGACCTGGT AAGTGGGACTGTCTGGGTTGGCCCCGCACTTTGGGCTTCTCTTGGGGAGGGTCAGGGAAGTGGAG

100 CAGCCTTCCTGAGAGAGGAGAGAGAAAGCTCAGGGAGGTCTGGAGCAAAGATACTCCTGGAGGTGGGGAGTGAGGCAGGGATAAGGAAGGAGAGTATCCT
200 CCAGCACCTTCCAGTGGGTAAGGGCACATTGTCTCCTAGGCTGGACTTTTCTTGAGCAGAGGGTGGGGTGGTAAGGAAAGTCTACGGGCCCCGTGTGTGT
300 GCACATGTCTCTGTGTGAATGGACCCTTCCCCTTCCCACACGTGTATCCCTATCATCCCACCCTTCCCACCAGAGCCATAGCCATCTGCTGGTTTGGTTA
400 TTTGGAGAGTGCAGGCCAGGACAAGGCCATCGCTTGGGGCATGAATCCTCTGCGTACTGCCCTGGCCAGATGCAAATTCCCTGCCATGGGATTCCCCAGA
500 AGGTTCTGTTTTTCAGGTGGGGCAAGTTCCGTGGG

b)
-423 GGCCGCCGGTACCGAGCTCTTAC
-400 GCGTGCTAGCGAGGGCGGACAAGCGACTTCCTCTTTCCAGCAGAAAAGGAGAAGTAGGAGCCAAGATTTCCAAACTCTGTGGTTGCCTTGAAGCGACTTC
-300 CTCTTTCCAGAAGCGACTTCCTCTTTCCAGCAGAAAAGGAGAAGTAGGAGCTCCTACTTCTCCTTTTCTGCCAAGATTTCCAAACTCTGTGGTTGCCTTG
-200 CTCCTACTTCTCCTTTTCTGCAGAAAAGGAGAAGTAGGAGCTGGAAAGAGGAAGTCGCTTGAGGGCGGACGCTAGCCCGGGCTCGAGTACCCTCCCTGCC
-100 CCCTGTCCCGACCGCGACAAAAGCGACTTCCTCTTTCCAGTGCATTTAAGGCGCAGCCTGGAAGTGCCAGGGAGCACTGGAGGCCACCCAGTACCGGTTG

c)
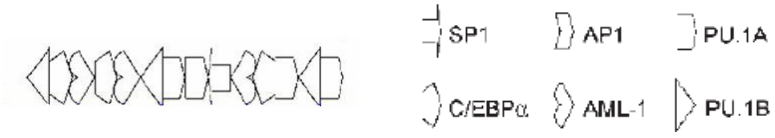

Fig. 35: MRP8 and SP146 promoters. a) Nucleotide sequence of the MRP8 promoter used in the targeted SIN gammaretroviral vector backbone. The exon sequence is boxed and the intron is underlined. Conserved DNA motifs are overlined. Nucleotides are numbered according to the cap site (position +1). (b) Nucleotide sequence of the SP146 promoter cloned in the SIN gammaretroviral vectors. (c) Order and orientation of the randomly ligated SP DNA fragments in the SP146 promoter (modified after He *et* al., 2006).

In addition a eukaryotic constitutive promoter was also tested. The Elongation Factor 1α short (EFs) promoter is a eukaryotic ubiquitous promoter that drives the expression of translation elongation factor 1 alpha (eEF1A) (Negrutskii and El'skaya, 1998). In this study a short intronless version of the promoter (244 bp) was used (Woods *et al.*, 2001; Schambach *et al.*, 2006b). This promoter was chosen since promoters with relatively low activity in hematopoietic stem and progenitor cells are expected to be less likely to upregulate proto-oncogenes in these cell fractions, which might lead to the initiation of leukemia (Dick, 2003). Therefore the EFs promoter might also be an alternative to replace the strong viral SF sequence.

C.3.1 Performance of the targeted SIN vectors in X-CGD PLB-985 cells

Titers (transducing units per ml) of SIN gammaretroviral vectors bearing the SF, EFs, c-fes, SP146 and MRP8 promoters were determined as above by GaLV pseudotyped particles production and following transduction of X-CGD PLB-985 cells with serial dilutions of the viral supernatant. Three days post-transduction the cells were immunolabeled with a FITC coupled antibody against gp91^{phox} and the percentage of positive cells was analyzed by flow cytometry.

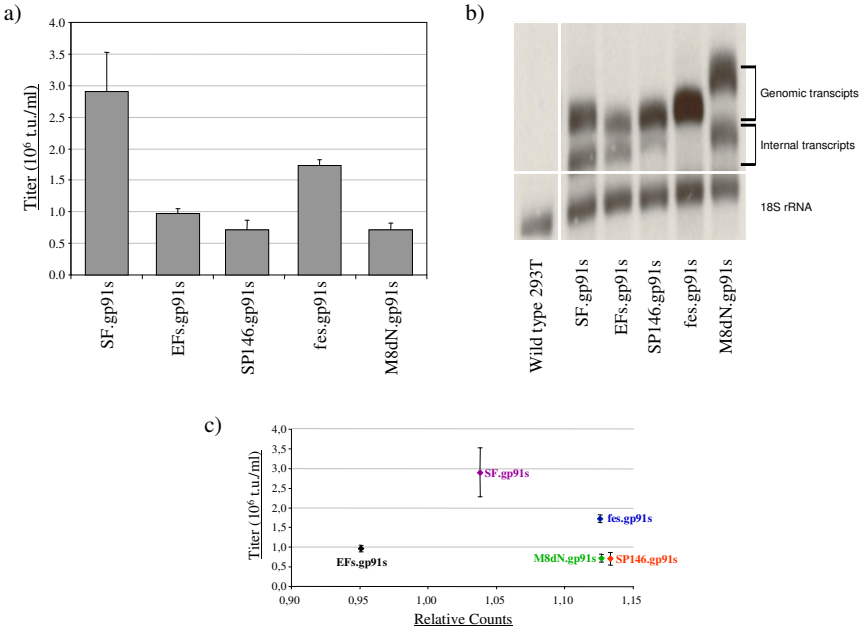

Fig. 36: Evaluation of the performance of several promoters in the SIN vector backbone. (a) Five different promoters driving the expression of synthetic gp91^{phox} were cloned in the SIN vector backbone and analyzed. Titer analysis of the constructs was performed by transduction of X-CGD PLB-985 cells as described previously. Mean and standard deviation of at least three independent transfection/transduction experiments are depicted (b) Northern blot analysis of total RNA of packaging 293T cells. A specific ^{32}P-labeled probe against WPREm was used to detect the gp91^{phox} transcripts. An 18S rRNA probe was used to verify equal loading of the samples. (c) Densitometry analysis. On the x-axis, the signals in relative counts for the genomic viral RNA normalized to 18s rRNA levels obtained in the Northern Blot analysis, plotted against the corresponding titers (y axis) with the standard deviations.

As shown in Fig. 36a, titers range around $1x10^6$ infectious units per ml, with the cellular promoters displaying a ~3-fold reduction in titer when compared to the SF internal promoter. The fes.gp91s construct showed the best performance, with titers up to $1.8x10^6$ t.u./ml, and the lowest titers were obtained with the MRP8 and SP146 promoter-containing constructs.

To further analyze whether this variability was due to differences in viral particle production or transgene expression levels in packaging cells, Northern blot analysis of total RNA from transfected 293T cells was performed. As shown in Fig. 36b the transcripts obtained matched with the expected size for both the genomic and internal transcripts. Interestingly, the internal transcript was not detected in packaging cells transfected with the c-fes promoter-containing vector. In the case of the MRP8 promoter-containing construct the obtained genomic RNA represented the non-spliced sequence, still including the MRP8 intron. Additionally, intensity analysis of the bands revealed a positive correlation between the titer and genomic RNA content for the constitutive promoters, SF and EFs. In contrast the myeloid-specific promoter-containing constructs showed slightly higher genomic RNA contents (normalized to 18S rRNA) but lower titers than those obtained with the constitutive promoter-containing constructs (Fig. 36c). Thus, the lower titers obtained by these vectors cannot be due to the lack in genomic RNA production, but possibly because of problems associated with thepackaging of these molecules or with the lack of transgene expression in the transduced populations.

Further molecular analysis of these constructs included the study of the proper proviral size in transduced cells as assessed by Southern Blot analysis of genomic DNA. Following enzymatic digestion with restriction enzymes (Kpn I and EcoR V) that only cut at both ends of the provirus, the DNA underwent electrophoresis and blotting on a membrane. The band obtained after hybridization with a ^{32}P-labeled WPREm probe should represent the size of the provirus. As shown in Fig. 37a and Fig. 37b, all proviruses were detected in the correct size on the blot except for the SP146 promoter-containing vector. In that particular case an additional unexpected band was observed with a slightly lower size than the proviral one. This indicated the presence of an alternative form of provirus which contained the packaging signal and the LTR sequences required for integration. Whether this proviral form contained and expressed $gp91^{phox}$ was subjected to further investigations (see chapter C.3.2 Functionality of the targeted SIN vectors in sorted populations).

The expression of the $gp91^{phox}$ transgene expression in transduced cells was analyzed by Northern blot analysis of total RNA. Only one transcript is expected for the transduced cells with SIN vectors. It should start at the transcription start site (TSS) in the internal promoter and finish at the polyadenylation signal in the R region of the 5'LTR. The approximate expected size of this transcript for the constructs used in this study is

2535 bp with little variations (+/- 10 bp) due to the position of the TSS in each promoter. As shown by the Fig. 37c only one band was detected which matched the expected size for all constructs. No unexpected forms of internal transcripts were detected thus indicating the proper elimination of transcription from the viral LTR in the transduced cells. The differences in the amounts of transcripts are in this analysis irrelevant because the used cells were from cells transduced with a high MOI with no comparable proviral copy numbers.

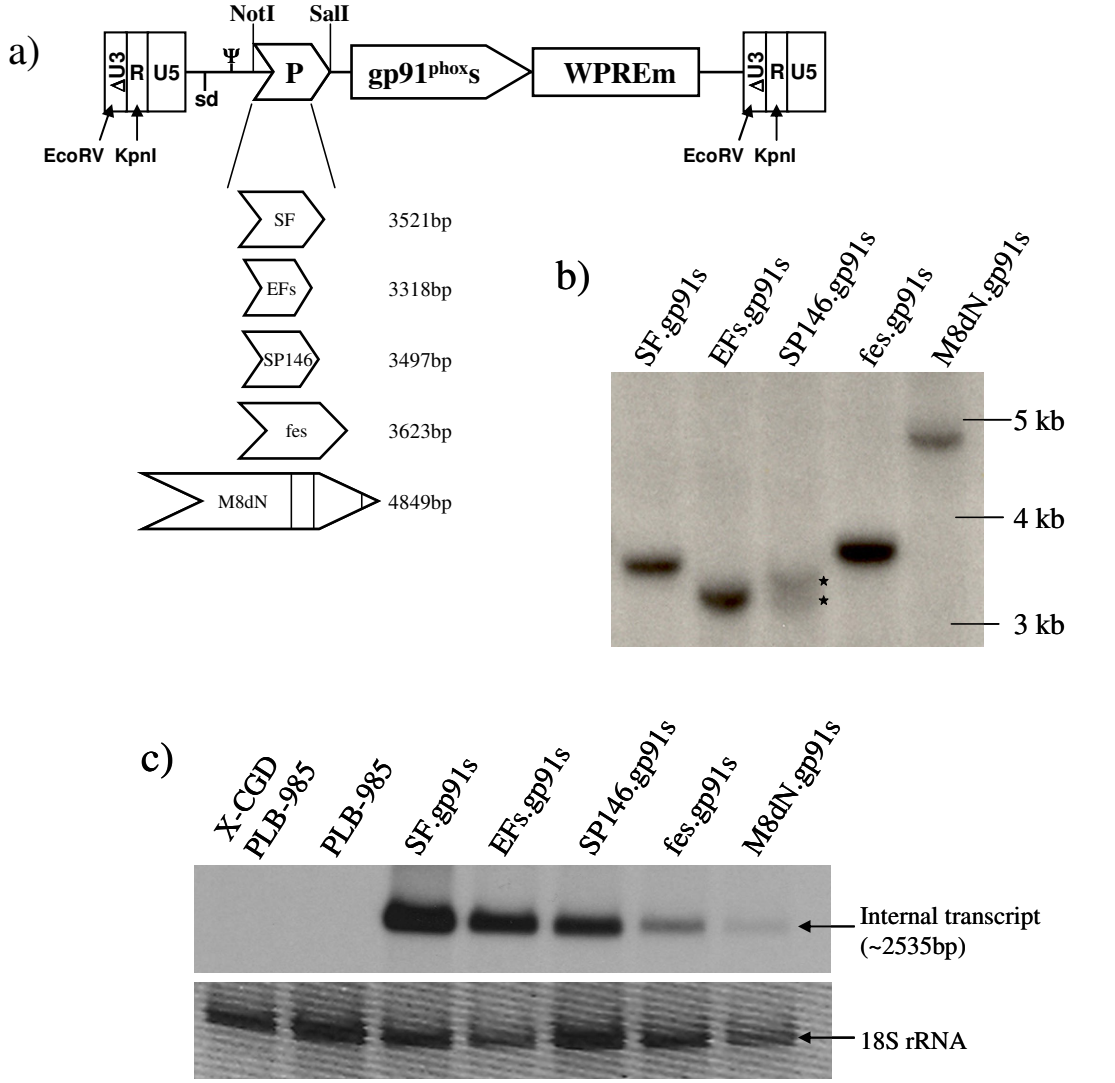

Fig. 37: Molecular analysis of X-CGD PLB-985 transduced cells with five different constructs. (a) Schematic presentation of five constructs differing in the internal promoter. For details see text and B. Materials and methods. (b) Southern blot analysis of transduced cells was performed by digesting genomic DNA with restriction enzymes that cut at both ends of the provirus (KpnI and EcoRV). Cleavage sites are indicated. For detection of the blotted fragments a ^{32}P-labeled WPREm probe was used. (c) Northern blot analysis was performed with total RNA of transduced cells. The same WPREm fragment as above was used to probe the membrane and a ^{32}P-labeled 18S rRNA probe was used to assess for equivalent loading quantities.

C.3.2 Functionality of the targeted SIN vectors in sorted populations

For further molecular and functional analysis, comparable transgene copy numbers were desired and therefore transduced populations of about 10% positive cells underwent positive selection as previously described (Fig. 38).

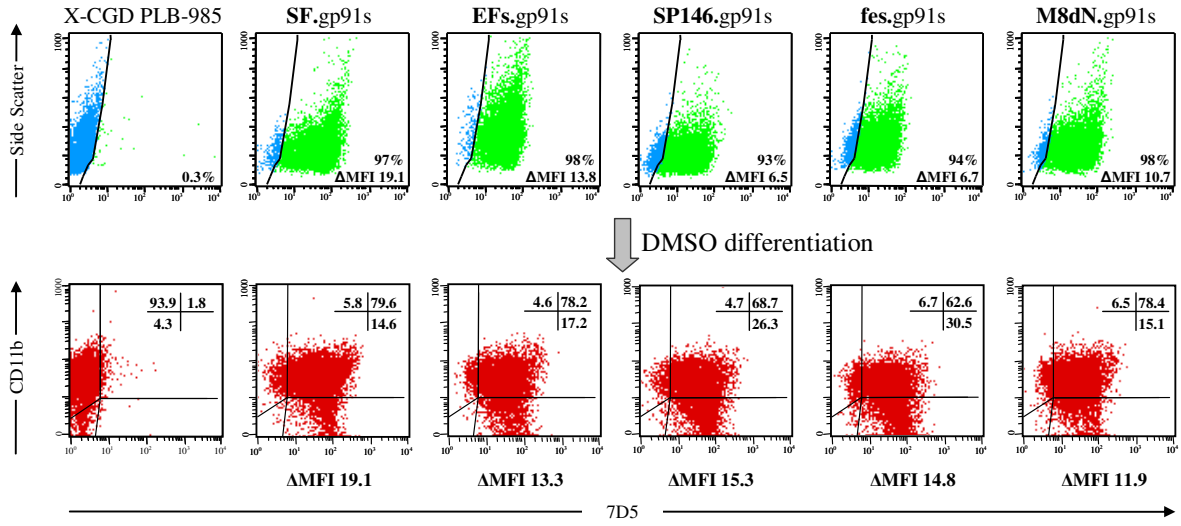

Fig. 38: Myeloid differentiation of the MACS-selected populations. X-CGD cells were transduced with five different constructs, sorted and induced to differentiate by incubation with 1.25% DMSO for six days. Cells were immunostained for CD11b and 7D5. The FACS analysis profile of a representative experiment with the corresponding percentage values for each gate. The ΔMFI is shown below the figures.

Further analysis showed changes in ΔMFI of DMSO differentiated populations. A 2.4-, 2.2- and 1.1-fold increase in expression of gp91^{phox} in the SP146, c-fes and MRP8 promoter-containing cells was observed, respectively. Furthermore, no changes were detected with any of the ubiquitous promoter-containing constructs (Fig. 38).

Vector copy number analysis of these MACS selected cells by semi-quantitative PCR amplification revealed a similar mean of integrants per cell for all populations. The mean values varied between 1.1 copies per cell for the c-fes construct transduced cells and 1.4 for the MRP8 construct-containing cells (Fig. 39a).

Southern blot analysis of sorted cells confirmed the appropriate size of the provirus for all constructs except for the SP146-containing construct (Fig. 39b). The second proviral form of the SP146 vector detected with the WPRE probe was also previously found in non-selected cells (Fig. 37b). Thus, this band should be caused by a rearrangement event or by a mistake that occurred during production of the viral genomes leading to the formation of an alternative form of gp91^{phox}-containing provirus capable to be packaged and inserted.

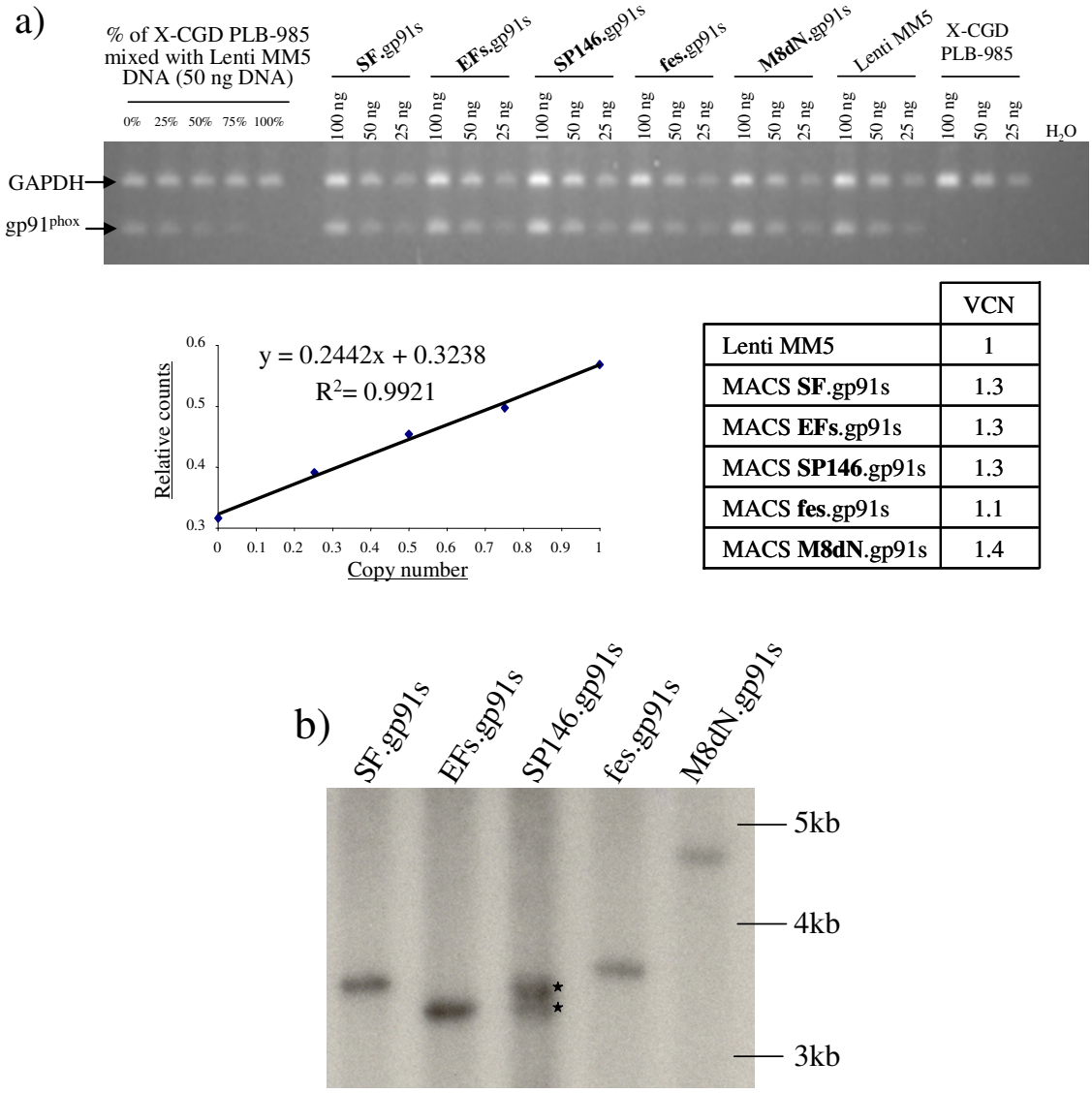

	VCN
Lenti MM5	1
MACS **SF**.gp91s	1.3
MACS **EFs**.gp91s	1.3
MACS **SP146**.gp91s	1.3
MACS **fes**.gp91s	1.1
MACS **M8dN**.gp91s	1.4

Fig. 39: Vector copy number (VCN) and proviral integrity analysis. (a) Semi-quantitative PCR analysis of the proviral copy number in the MACS sorted populations. Genomic DNA was obtained from sorted cells and PCR amplification of a gp91^{phox} fragment (and the corresponding GAPDH loading control) was performed. A standard curve was prepared with serial dilutions of DNA from a genetically modified X-CGD PLB-985 population with 1 copy per cell. With the obtained R square value and linear regression the number of integrated provirus in the samples were calculated. (b) Southern blot analysis of sorted cells. Genomic DNA was isolated and digested with enzymes cutting at both ends of the provirus and blotted onto a nylon membrane as described above. DNA fragments containing proviral DNA fragments were detected after hybridization with a ^{32}P-labeled WPREm specific probe.

To analyze whether the increase in expression of gp91^{phox} after DMSO differentiation could also be detected in RNA and protein levels, Northern and Western blotting of MACS sorted cells was performed. The RNA blot revealed an increase in transcription with all constructs following DMSO differentiation, ranging from 1.3-fold with the SF promoter up to 2.3-fold with the c-fes promoter. The SP146 led to a 2.0-fold increase in internal transcript expression, and showed the highest transcript production, whereas the MRP8 promoter only led to a 1.7-fold increase being the second less active promoter.

The EFs also achieved a 2.0-fold increase although being a ubiquitous promoter (Fig. 40a).

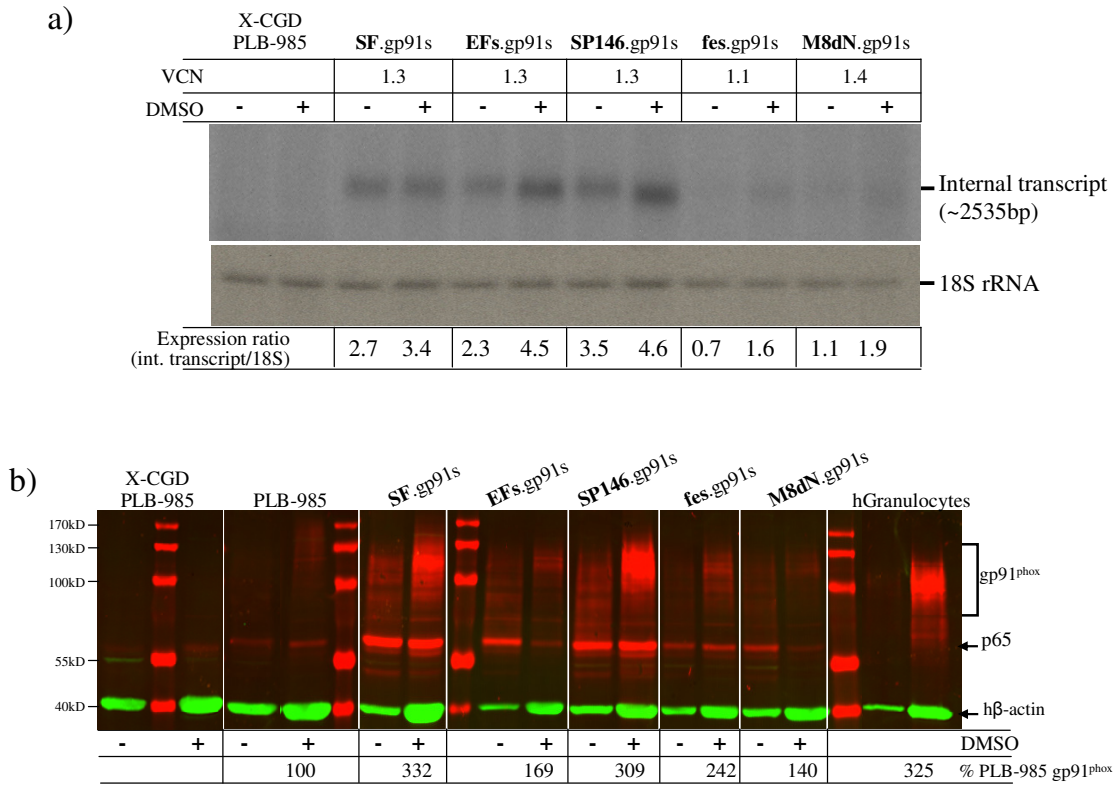

Fig. 40: Transgene expression levels of MACS-selected populations. (a) Northern blot analysis of 7.5 µg total RNA obtained from sorted cells before (- DMSO) and after (+ DMSO) granulocyte-like cell differentiation. ^{32}P-labeled probes against WPREm and 18S rRNA (as loading control) were used and the band intensity analysis is shown. The vector copy number in MACS-selected populations is shown (b) Western blot analysis of MACS-selected cells. Sorted populations were induced to differentiate with 1.25% DMSO and total protein extracts were prepared. 10% SDS-polyacrylamide gel, electrophoresis and Immunoblotting were performed as previously described, using the moAB48 antibody against gp91^{phox}. Quantification of the gp91^{phox} content (normalized to β-actin) for each sample is shown as percentage values related to the PLB-985 value.

When the protein levels were assessed by Western blotting surprising higher amounts of beta actin were seen in the differentiated populations. The extensive difference in the amounts of β-actin before and after granulocyte-like cell differentiation complicated the analisis. Thus, it is unclear whether there was a correlating increase in protein levels. Nevertheless, when comparing the differentiated populations with the wild type PLB-985 cells higher protein levels were detected in all cases. The highest amount was seen with the SF promoter (3.3-fold) followed by the SP146 (3.0-fold) when compared to the wild-type PLB-985 cells. The c-fes and MRP8 led to 2.4- and 1.4-fold higher values of protein which were the lowest values obtained between the myeloid-specific promoters. These results correlate with the mRNA levels detected in Fig. 40a. In the case of the EFs.gp91s construct a 1.7-fold higher amount of gp91^{phox} compared to the levels in wild-type PLB-985 cells was observed, which might indicate that an

overestimation of the RNA values occurred since this is the only value that does not follow the correlation observed between RNA and protein.

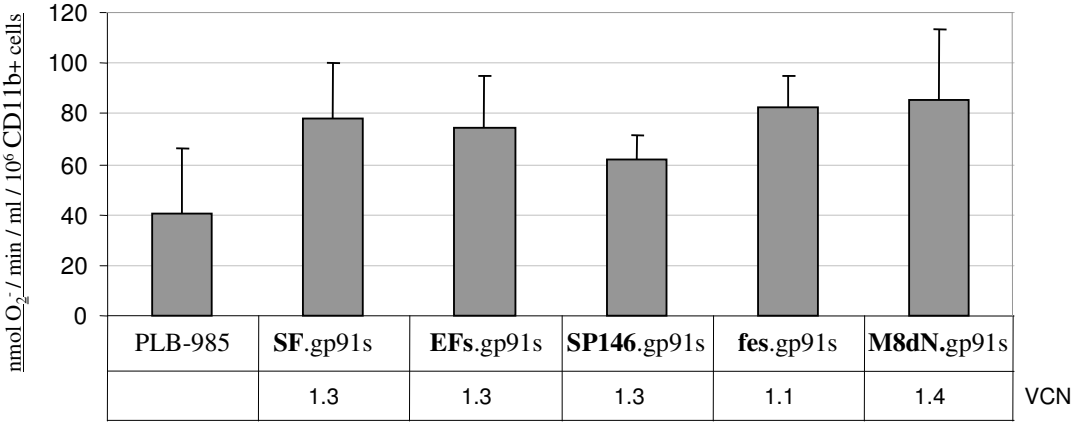

Fig. 41: Reconstitution of respiratory burst activity in PLB-985 cells and derivatives. The amounts of produced superoxide per million of cells, min and ml following PMA stimulation of granulocytic-like cells were measured by the cytochrome c assay. The mean and standard deviation of at least three independent experiments are shown. Additionally, the mean copy numbers of the used populations are indicated.

When reconstitution of the NADPH oxidase was assessed by the cytochrome c assay (Fig. 41) all constructs showed higher levels of superoxide production than those obtained by the wild-type PLB-985 cells. The MRP8 promoter produced the highest rate, more than 2-fold higher than PLB-985 cells. The SP146 promoter showed the lowest value of superoxide production; however, they still were 1.5-fold higher than for the wild-type PLB-985 cells. Furthermore, by relating these results to the mean copy number of the cells, the c-fes containing construct showed the best performance, since it reached the best superoxide production levels per copy of integrated provirus.

Additional functional analysis of differentiated populations included the DHR assay. This assay was first described by (Vowells et al., 1995) and is used to identify the superoxide producing cells as well as the amount of products (by the mean fluorescence intensity) evaluated by flow cytometry. Furthermore, this is the most common test used in the clinic. It is used due to its high reliability, small sample requirement, sensitivity and efficiency (between the available flow cytometric probes) (Jirapongsananuruk *et al.*, 2003); and is specific for H_2O_2 accumulation (Walrand *et al.*, 2003).

As shown in Fig. 42 the granulocyte-like cell differentiated populations were up to 98% Rhodamine positive cells as expected for sorted populations. Furthermore, the SF promoter led to a superoxide production similar to wild-type cells. The rest of the constructs achieved lower levels, with the MRP8 promoter showing the lowest ones. These data did not correlate with the results obtained by the cytochrome c assay where the MRP8 promoter showed the best performance. These differences might be due to the assay itself since the cytochrome c assay measures the generation of extracellular O_2^-

and the DHR is a membrane permeable probe which reacts intracellularly with the superoxide anion (Henderson and Chappell, 1993).

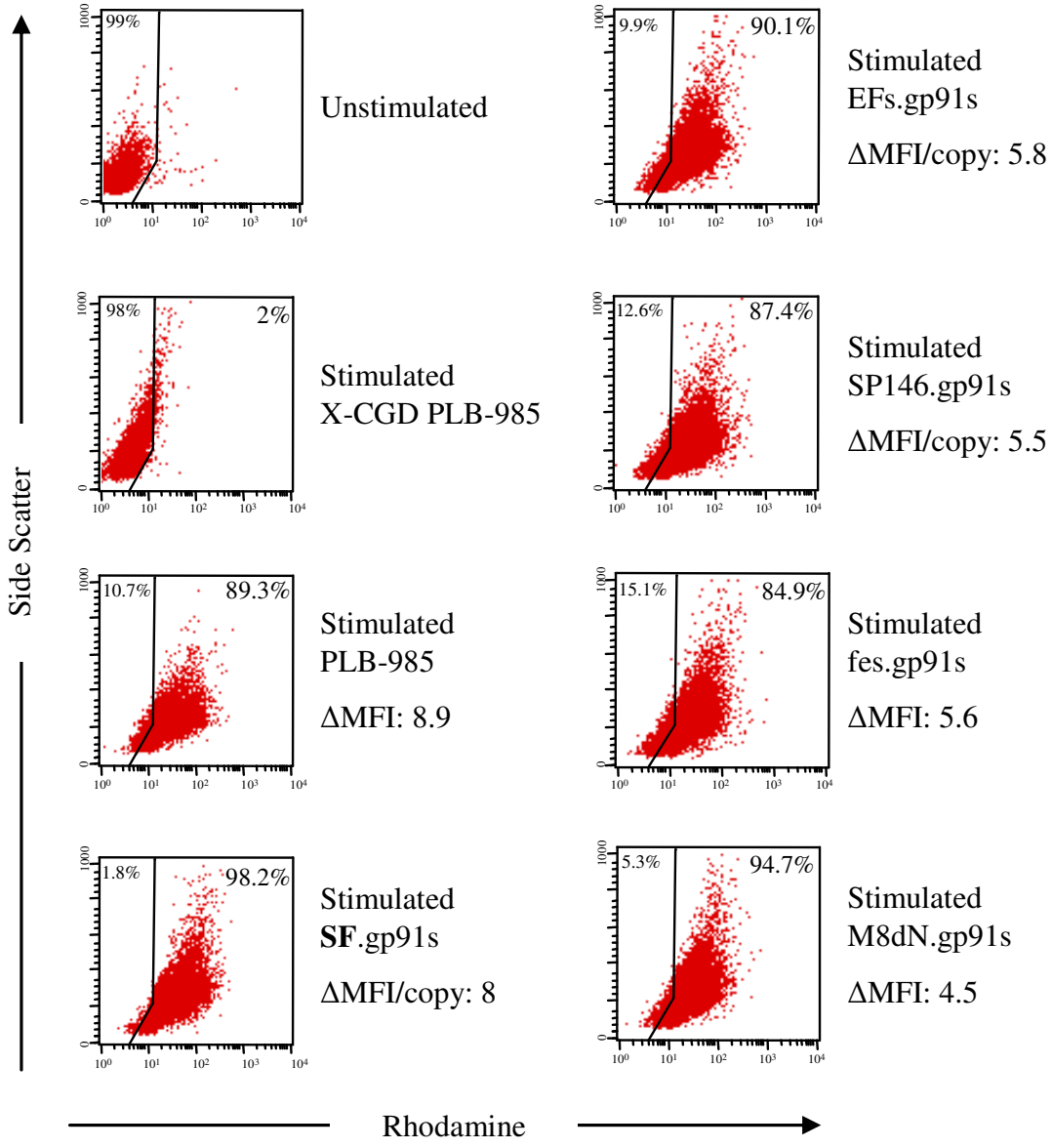

Fig. 42: DHR assay of MACS-selected populations. Dot blots of flow cytometry assays of oxidant production by PMA stimulation in DMSO-induced cells. A representative unstimulated sample and the stimulated measurements for PLB-985 cells and transduced derivatives are shown. The "positive threshold" is set so that at least 95% of stimulated X-CGD PLB-985 cells are to the left of that line. The data shown are of a single experiment.

C.4 Vector testing in primary murine cells

Since the five SIN gammaretroviral vectors were able to generate high titers after transient transfection of 293T packaging cells, to efficiently transduce the X-CGD PLB-985 cell line and to reconstitute the NADPH oxidase activity to a high degree, it was decided to assess the performance of these constructs in primary mouse cells. The stem cell antigen 1 (Sca-1) was used as a marker to select hematopoietic stem/progenitor

cells by FACS and to enrich this population from X-CGD mouse bone marrow (mBM). After positive selection, the percentage of positive cells was about 95% Sca-1$^+$ as assessed by flow cytometry (Fig. 43).

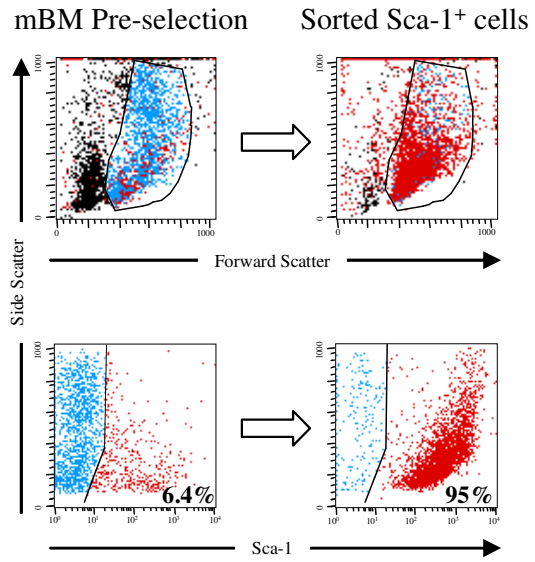

Fig. 43: Selection of Sca-1$^+$ cells. FACS plots of unseparated (left) and Sca-1$^+$ (right) mouse bone marrow (mBM) cells after positive selection.

C.4.1 *Ex vivo* analysis

Ecotropic retroviral supernatants were produced from all different vectors and titers were assessed by SC1 transduction as previously described. Sorted murine X-CGD Sca-1$^+$ cells were stimulated for 48 hours in the presence of mouse Stem Cell Factor (mSCF) (100 ng/ml), mIL-6 (100 ng/ml) and mIL-3 (10 ng/ml). Then the cells were transduced with similar multiplicities of infection (MOI). The transduction was performed on RetroNectin coated plates with preloading of the viral particles and posterior addition of the target cells. Transduction was further enhanced by the use of spinoculation to bring cells and viruses closer together. Two or three rounds of transduction, depending on the desired MOI, were performed over a period of 48 or 72 hours. Three independent analyses (with MOI 5, 5 and 3) were performed and the cells were analyzed 4 days after the last round of infection. The gene transfer rate of each population was assessed by FACS analysis and VCN was determined by semi-quantitative PCR amplification, respectively, as previously described (Fig. 44a). The percentage of gp91^{phox} expressing cells related to the VCN ranged from 45.5% with the SF.gp91s vector to 10% with the M8dN.gp91s. The c-fes promoter drove high expression of the transgene, up to 30%, which is in accordance with previous observations showing high c-fes protein expression levels in mouse and human undifferentiated progenitor cells purified from different sources (Care *et al.*, 1994). The SP146 reached with 39.4% the highest value, and it was similar to the data obtained with the EFs promoter.

Thereafter, the transduced cells were induced to differentiate by incubating the cells with IL-3 (10 ng/ml) and G-CSF (100 ng/ml) for eight days. The differentiation progress was monitored by co-immunostaining of the surface markers Gr-1 and CD11b. Around 80-90% of the cells stained positively in all three experiments (data not shown). If the gp91^{phox} expression level was related to the copy number in differentiated cells slightly higher values for all constructs compared to those of before differentiation were obtained. With the constitutive promoters, a slight increase was also observed except for the SF in one of the assays. The SP146 promoter showed the highest increase although it also exhibited also the highest variability. The lowest inducibility of the gp91^{phox} expression after myeloid-differentiation was shown by the MRP8 promoter. This promoter also showed the lowest levels of transgene expression before and after differentiaion (Fig. 44a).

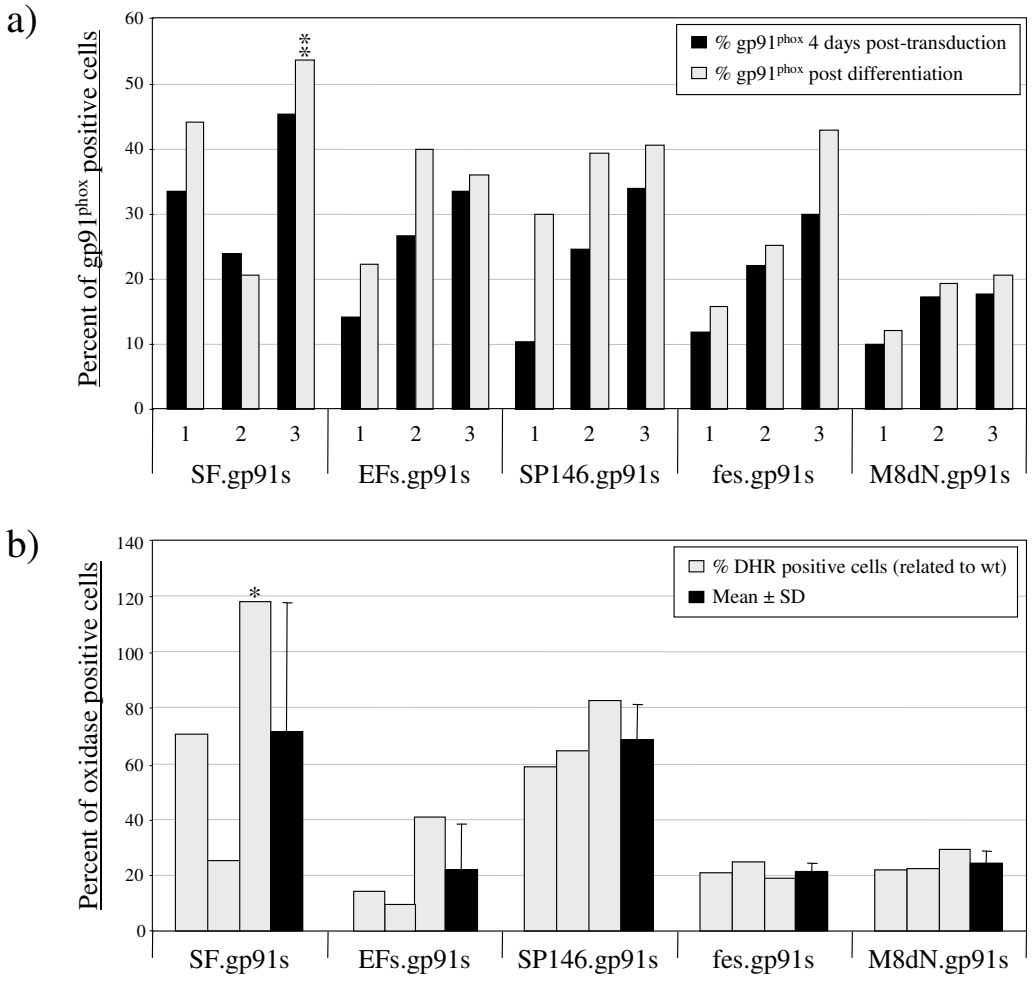

Fig. 44: Performance of the SIN gammaretroviral vectors in sorted murine X-CGD Sca-1$^+$ cells. (a) mSca-1$^+$ cells were selected by magnetic cell sorting and transduced with similar MOIs for all constructs. FACS analysis of gp91^{phox} positive cells was performed prior and after *ex vivo* myeloid differentiation with IL-3 (10 ng/ml) and G-CSF (100 ng/ml). (b) DHR assay of differentiated cells was performed eight days post-differentiation as previously described. Both gp91^{phox} and DHR positive cells are represented normalized to their respective VCN. Results of three independent experiments are shown.

Superoxide production of transduced cells after differentiation was assessed by the DHR assay. The values were normalized to the levels measured for the wild-type cells (Fig. 44b). When this ratio was further normalized to the VCN, the SF.gp91s showed almost 1.2-fold higher DHR positive cells (*) than the wild-type control cells in one of the assays which displayed also the highest level of $gp91^{phox}$ expression (**) after differentiation (Fig. 44a). However, when the mean values for the three experiments were calculated this construct showed also the highest variability in the percentage of DHR positive cells per copy of integrated provirus (71 ± 46%). Although the EFs.gp91s showed more constant levels of DHR reactive cells related to the wild-type and VCN, these were lower than those obtained with the SF promoter (21 ± 16%). The three myeloid-specific promoters showed more constant levels of reactive cells (Fig. 44b). The SP146.gp91s construct was found to be the best myeloid promoter reaching more than 50% of the levels observed in wild-type cells (68 ± 12%), and was followed by the M8dN.gp91s and fes.gp91s which showed only 24 ± 4% and 21% ± 2% of the levels observed in wild-type cells, respectively (Fig. 44b).

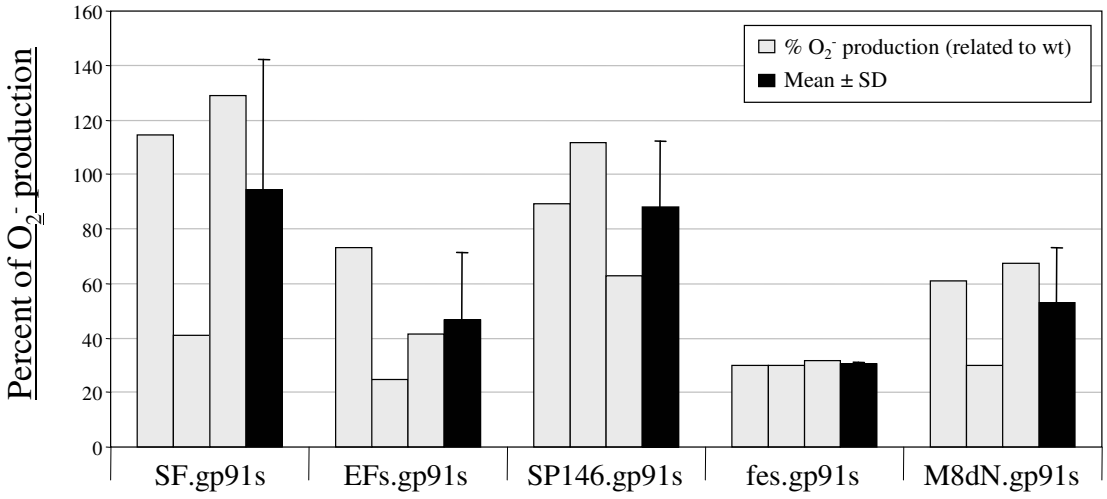

Fig. 45: Cytochrome c assays were performed after nine days of myeloid differentiation. The percentages of superoxide production related to wild-type cells and to the VCN of three independent experiments are depicted.

The measurement of superoxide production by the cytochrome c assay showed the same tendency as the DHR assay (Fig. 45). The SF.gp91s construct led to the highest percentage of superoxide production per copy number relative to the wild-type cells reaching, in two of the three experiments, more than 100% of the wild-type activity. Of the three myeloid-specific promoters the SP146 promoter reached again here the highest values although showing the greater variability between the measurements. Finally, as already observed in the DHR assay, the most constant but lowest results were obtained with the c-fes promoter with about 30% in all the cases (Fig. 45).

The results described above showed that sorted Sca-1^+ murine X-CGD cells were efficiently transduced by these vectors and that reconstitution of the NADPH oxidase

activity was achieved in liquid culture media with these cells. Subsequently, the presence of transduced murine hematopoietic progenitor cells with functional NADPH oxidase in the sorted population was assessed by the methylcellulose based colony forming unit (CFU) assay. Mouse Sca-1$^+$ cells transduced with the five different constructs as well as the control cells were plated in a semi-solid medium containing the appropriate cytokines and were grown for 10 days. After that time, the number of colonies was determined by counting all cell clusters of more than 50 cells.

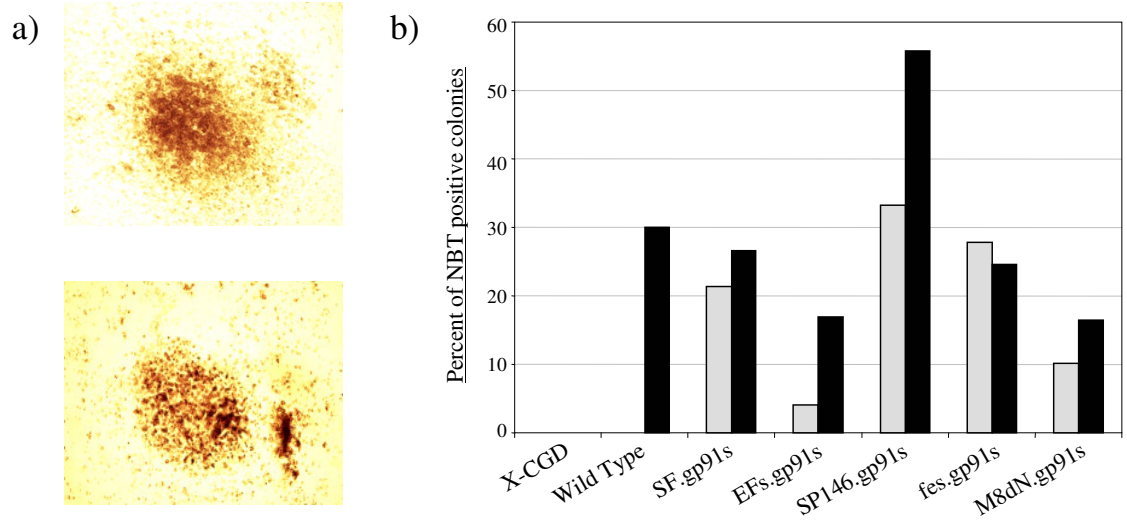

Fig. 46: Restoration of superoxide production (NBT assay) in CFU-GM colonies derived from transduced mSca-1$^+$ cells. (a) An example of NBT negative (upper) and a positive (down) colony. (b) Percentages of NBT$^+$ colonies of two independent experiments related to the corresponding vector copy number are depicted.

The colonies in the methylcellulose plates were assessed for reconstitution of the NADPH oxidase activity by the nitroblue tetrazolium (NBT) test (see B.7.9. NBT assay). Two independent experiments are shown in Fig. 46 where an MOI of 5 was used to transduce the cells with the different viral particles. All constructs were able to transduce progenitor cells, and to reconstitute NADPH oxidase activity after myeloid differentiation although with variable levels. The SP146.gp91s was again the most efficient promoter, since with this promoter the highest percentages of NBT positive (NBT$^+$) CFUs were observed in both assays (33% and 55%). This construct was followed by SF.gp91s and fes.gp91s with similar numbers in both assays, about 25% NBT$^+$ colonies. Finally, with the EFs and MRP8 promoter-containing constructs only low percentages of NBT$^+$ colonies were counted.

C.4.2 Transplantation of genetically modified gp91$^{phox\ -/-}$ mSca-1$^+$ progenitors

To further analyze the performance of these five vectors an X-CGD mouse model (Pollock *et al.*, 1995) was chosen for a transplantation procedure following *ex vivo* transduction of mSca-1$^+$ cells.

Mouse Sca-1$^+$ cells were enriched up to 92% positive cells (see Fig. 43) and stimulated for 48 hours in presence of mSCF (100 ng/ml), mIL-6 (50 ng/ml) and mIL-3 (10 ng/ml). Transduction was preformed as previously described with a final MOI of 3. Twenty-four hours after the last round of infection and prior to transplantation, a small sample of the cells was used to analyze the gene transfer rate by FACS and semi-quantitative PCR amplification. As shown in Fig. 47, the percentage of gp91^{phox} positive cells within the Sca-1$^+$ subpopulation related to the number of integrated viruses reached up to 45.7% with the EFs.gp91s construct. The M8dN.gp91s vector showed the lowest values, as expected for a myeloid-specific promoter. The SF, c-fes and SP146 promoter-containing constructs achieved intermediate levels, with 30-45% gp91^{phox} positive cells.

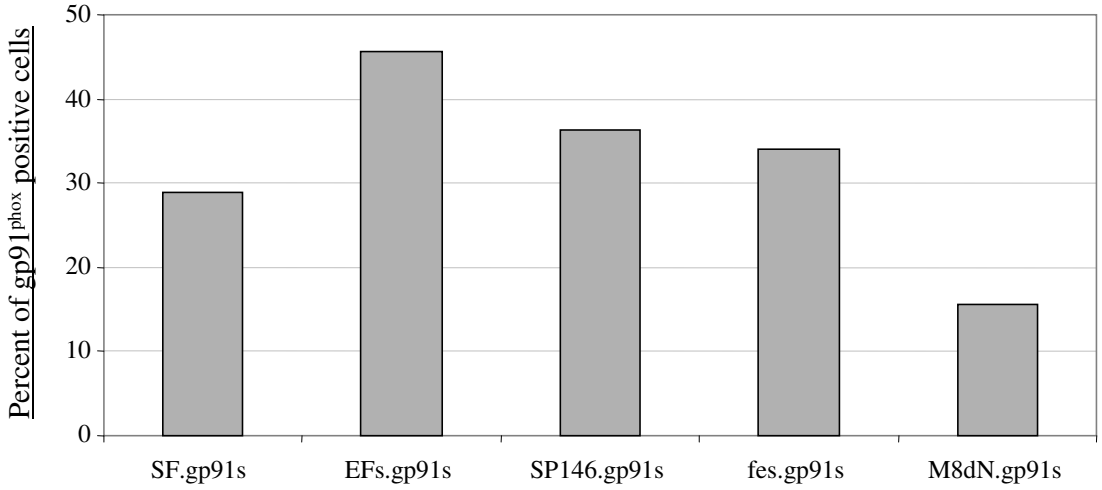

Fig. 47: Transduction efficiency of SIN gammaretroviral vectors in mSca-1$^+$ cells. Sorted cells were transduced as previously described and were analyzed one day post-transduction. FACS analysis of gp91^{phox} positive cells by 7D5 staining related to the respective VCN determined by sq-PCR is shown.

To confirm gene transfer efficiencies, transduced cells were also plated in semi-solid medium and all GM/G colonies arising at day 10 were assayed for generation of superoxide by the NBT assay. When the values of NBT positive (NBT$^+$) colonies were related to the number of integrated provirus, the tendency observed in the percentages of transduced cells prior to transplantation correlated with the functionality of the transduced hematopoietic precursor cells (Fig. 48). In both analyses (Fig. 47 and Fig. 48), the EFs.gp91s construct reached the highest levels of expressing cells (46% gp91^{phox} positive cells and 95% NBT$^+$ colonies). The lowest numbers were obtained for the SF.gp91s, 29% and 44% respectively, and for the M8dN.gp91s (15.5% and 64%). The numbers of NBT$^+$ colonies were about 2-fold higher the number of gp91^{phox} positive Sca-1$^+$ cells after transduction with all the contructs except for the M8dN.gp91s which showed 4-fold higher levels. However, the performance of the M8dN.gp91s construct in the NBT colony assay was not efficienrbest since it showed lower levels of gp91^{phox} positive colonies than the EFs.gp91s vector (1.5-fold). In contrast the data obtained with the SP146 and c-fes constructs were promising.These myeloid-specific constructs gave rose to a high percentage of positive cells as well as a high number of NBT$^+$ colonies.

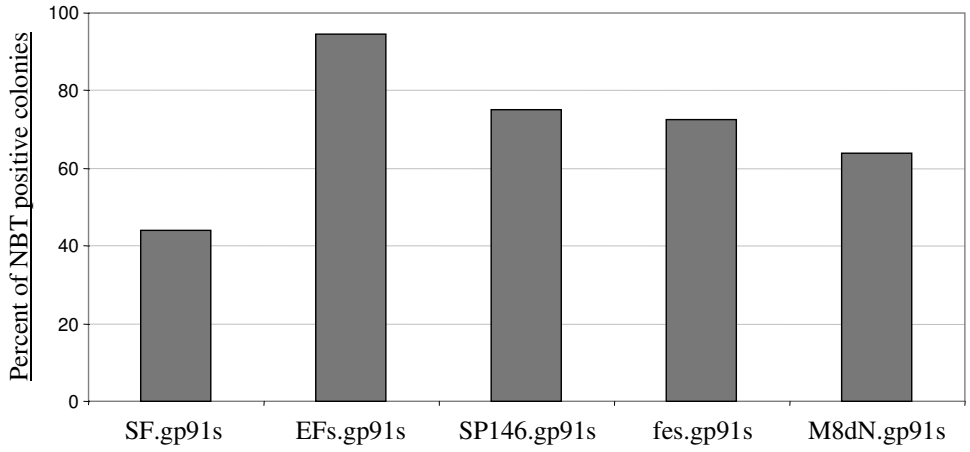

Fig. 48: Analysis of NADPH oxidase activity in reconstituted murine X-CGD Sca-1$^+$ cells. Percentage of colonies scoring positive with NBT. Percentages of positive colonies related to copy number are shown.

To assess the *in vivo* performance of these constructs, four X-CGD mice per construct were lethally irradiated with two doses of 5.5 Gy prior to receive $1x10^6$ transduced cells by intravenously tail injection. Unfortunately, two mice which received the EFs.gp91s transduced cells and one receiving the SP146.gp91s gene modified cells died before being analyzed. Six weeks after transplantation the surviving recipient mice were sacrificed and bone marrow as well as peripheral blood populations were analyzed by flow cytometry to verify multi-lineage reconstitution and functional rescue of the NADPH oxidase activity.

The expression of the gp91^{phox} transgene was assessed by flow cytometry analysis of the different bone marrow lineages from the transplanted mice. Marrow myeloid cells were identified using Gr-1 and CD11b (Mac-1) specific antigens which are mainly expressed at variable levels on monocytes/macrophages, granulocytes and their precursors. The antigen B220 (CD45R) was used to identify B lymphocyte precursor cells, because this marker is almost exclusively expressed on cells of the B lineage in bone marrow. Murine hematopoietic precursor cells were labeled with a Sca-1 antibody as described above. Data were related to the copy number of integrated provirus measured 24 hours post-transduction in the transduced and transplanted cells.

With all the constructs gp91^{phox} positive cells were detected in the mSca-1$^+$ subpopulation with levels ranging between 30% and 84% except for the MRP8 construct, which showed again lower levels of gp91^{phox} positive cells (up to 14%) (Fig. 49).

The percentage of gp91^{phox} expressing cells per integrated provirus within the marrow myeloid subpopulation was similar to those observed for positive gp91^{phox} cells in Sca-1$^+$. The highest difference in gp91^{phox} expression between Sca-1$^+$ and marrow myeloid subpopulation was observed with the SP146 promoter, which showed an increase of 1.15 ± 0.24-fold towards myeloid commitment. The c-fes and MRP8

promoters showed the lowest differences between these populations. The MRP8 construct showed in all mice almost the same percentage of gp91^{phox} positive cells in the Sca-1^{+} and myeloid marrow subpopulations (Fig. 49).

When comparing the gp91^{phox} expression between the HSC precursor and the B lymphoid subpopulation a marked decrease was observed regardless of the type of promoter. This decrease ranged from 1.9-fold with the SP146 promoter to up to 2.4-fold with the MRP8 promoter. Also a 2.3-fold decrease in gp91^{phox} positive cells was observed for the SFFV promoter, which is actually a constitutive regulatory element.

To assess whether there were changes in gp91^{phox} expression after maturation of the myeloid and B lymphoid lineages a sample of peripheral blood cells was analyzed by flow cytometric analysis using the markers previously described. The differences in gp91^{phox} expression between myeloid and B lymphoid circulating cells were lower than those of bone marrow, except for the M8dN.gp91s construct. In the case of the SF.gp91s, the smaller differences between the two peripheral blood lineages were due to an increased percentage of gp91^{phox} in B lymphocytes (from 13-28% to 25-55%) and a decrease of this in granulocytes when compared to the bone marrow percentages (from 43-58% to 24-42%). The two EFs.gp91s mice revealed a decrease in transgene expression in both peripheral blood lineages (myeloid and B lymphoid) but being more pronounced in the commitment towards granulocytes. Moreover, the levels of gp91^{phox} detected in peripheral blood granulocytes and B lymphocytes of the EFs.gp91s mice reached only very low levels, 6-20% and 11-17% respectively. The SP146.gp91s construct showed similar results, although with a smaller difference in the decrease ratios of both subpopulations. With this construct only 7 to 19% of granulocytes and 6 to 14% of B lymphocytes respectively were positive for gp91^{phox} expression, which represented approximately 3- and 2.2-fold lower expression than that of the corresponding marrow subpopulation. In the case of the c-fes construct, there were almost no differences in the transgene expression levels of the myeloid and B-lymphoid lineages in the two compartments. The granulocytes reached 24-36% and 19-33% gp91^{phox} positive cells in bone marrow and peripheral blood respectively, whereas the B lymphocytes reached 12-16% in bone marrow and 9-22% in peripheral blood. The M8dN.gp91s mice showed a high variability in transgene expression in peripheral blood achieving up to 15% in granulocytes and 5% in B lymphocytes. In the rest of the cases, the levels of gp91^{phox} positive B lymphocytes were almost undetectable, with the granulocytes ranging from 2 to 7%.

Reconstitution of the oxidase activity was measured in peripheral blood granulocytes by the DHR assay. Unfortunately; this assay could not be performed with all the samples due to technical problems. When the DHR values were related to the wild-type and the vector copy number, one of the MRP8 blood samples showed a maximum of 2-fold higher levels of oxidase positive cells although previously only 7% of gp91^{phox}

granulocytes were detected (Fig. 49b). In the rest of the MRP8 blood samples 0 to 80% DHR positive cells compared to the wild-type blood samples with up to 15% gp91^{phox} positive peripheral granulocytes. The most constant levels were achieved by the SF.gp91s construct with a 1.1 ± 0.2-fold increase in DHR positive cells when related to the wild-type and 34.9 ± 7.5% of transgene expressing cells. In the case of the EFs.gp91s, only one mouse could be analyzed which reached 64% rhodamine positive cells although only 6.9% gp91^{phox} positive granulocytes were detected. In the two SP146 samples similar oxidase levels as in EFs.gp91s mice were detected, although in this case more than 2-fold higher numbers of gp91^{phox} expressing granulocytes were found. The fes.gp91s construct achieved intermediate DHR levels (around 49 ± 18%), while having almost the same percentage of gp91^{phox} cells as the SF.gp91s mice (Fig. 49b).

a) Bone Marrow

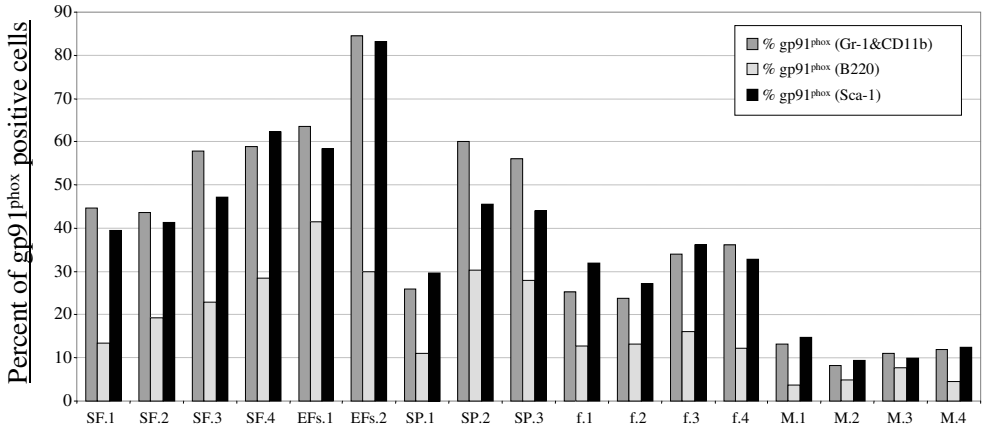

b) Peripheral blood

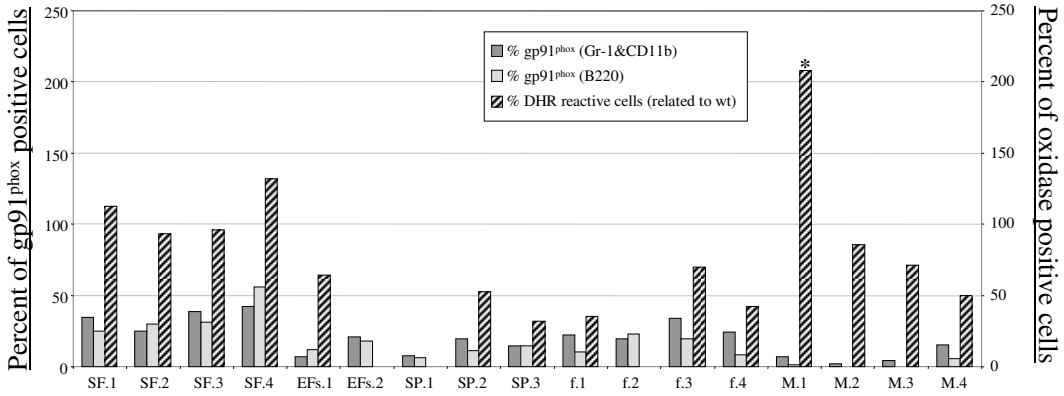

Fig. 49: *In vivo* multilineage reconstitution ability and restoration of the NADPH oxidase activity of transduced mSca-1$^+$ cells. (a) Percentage of gp91^{phox} expressing cells in bone marrow lineages of reconstituted X-CGD mice per VCN. Bone marrow cells from transplanted mice were analyzed for gp91^{phox} expression within the myeloid lineage (Gr-1$^+$ & CD11b$^+$), B lymphoid lineage (B220$^+$) and hematopoietic stem cell subpopulation (Sca-1$^+$). (b) Percentage of gp91^{phox} peripheral blood expressing cells per VCN and DHR reactive cells related to the wild-type sample and the VCN. Peripheral blood cells were immunostained and analyzed for gp91^{phox} positive cells in the myeloid and B lymphoid subpopulations. The percentage of DHR positive cells related to the wild-type sample and the VCN in peripheral blood of the indicated mice is also depicted.

Table 2: Overwiew summarizing the reconstitution of NADPH oxidase activity *in vivo* using SIN viral vectors

Vector	Transduced mSca-1$^+$ cells		Mouse Nr.	Bone Marrow			Peripheral blood		% DHR positive cells	
	% 7D5 positive cells	VCN		% 7D5 positive cells			% 7D5 positive cells			
				in Gr-1$^+$ and CD11b$^+$	in B220$^+$	in Sca-1$^+$	in Gr-1$^+$ and CD11b$^+$	in B220$^+$	12.0	Positive Control
SF.gp91s	25.1	0.87	SF.1	38.8	11.7	34.4	30.0	21.9	11.7	
			SF.2	38.0	16.7	35.9	21.6	25.6	9.7	
			SF.3	50.3	20.0	41.1	33.5	27.3	10.0	
			SF.4	51.2	24.8	54.2	36.6	48.6	13.8	
									27.6	Positive Control
EFs.gp91s	29.7	0.65	EFs.1	41.3	27.0	38.0	4.5	7.6	11.6	
			EFs.2	54.9	19.5	54.1	13.3	11.5	ND	
SP146.gp91s	26.3	0.72	SP.1	18.8	8.0	21.5	5.6	4.5	ND	
			SP.2	43.6	22.0	33.0	14.2	7.9	10.7	
			SP.3	40.6	20.2	31.9	10.3	10.5	6.4	
									34.3	Positive Control
fes.gp91s	35.2	1.03	f.1	26.1	13.1	33.1	22.7	11.1	12.6	
			f.2	24.5	13.7	28.0	20.2	23.4	ND	
			f.3	35.2	16.7	37.4	35.1	19.7	24.9	
			f.4	37.4	12.7	34.0	25.0	8.9	14.9	
									14.0	Positive Control
M8dN.gp91s	15.2	0.98	M.1	13.0	3.6	14.5	7.0	1.3	28.4	
			M.2	8.0	4.8	9.2	1.9	0.0	11.8	
			M.3	10.9	7.5	9.6	4.1	0.0	9.8	
			M.4	11.7	4.4	12.2	15.0	5.1	6.8	

ND: not determined

C.4.3 Transplantation of genetically modified gp91$^{phox\ -/-}$ Lin^{Neg} progenitors

To further investigate the performance of the different gammaretroviral vectors a second *in vivo* experiment was performed. In this case the vectors containing two of the investigated promoters were not included. First, the SF promoter, because it might still elicit transactivation events following proviral integration due to its strength. Second, the SP146 was disclosed since it showed genomic rearrangements phenomenon leading to the formation of aberrant proviral species.

In this second study, mice bone marrow preparations were used to isolate lineage uncommitted cells, which were separated from lineage specific cells up to > 95% (Dr. L. Chen, pers. commun.). The cells were stimulated for 48 hours in growth media containing mSCF (50 ng/ml), mIL-6 (50 ng/ml) and mIL-3 (10 ng/ml). After prestimulation, lineage antigen-negative (Lin^{Neg}) cells were transduced with the three different retroviral vectors at a final MOI of 3 on RetroNectin-coated plates as previously described. After the last round of transduction, cells were maintained in culture under the same cytokine and media conditions for four days. Then the gene transfer efficiencies were assessed by flow cytometry.

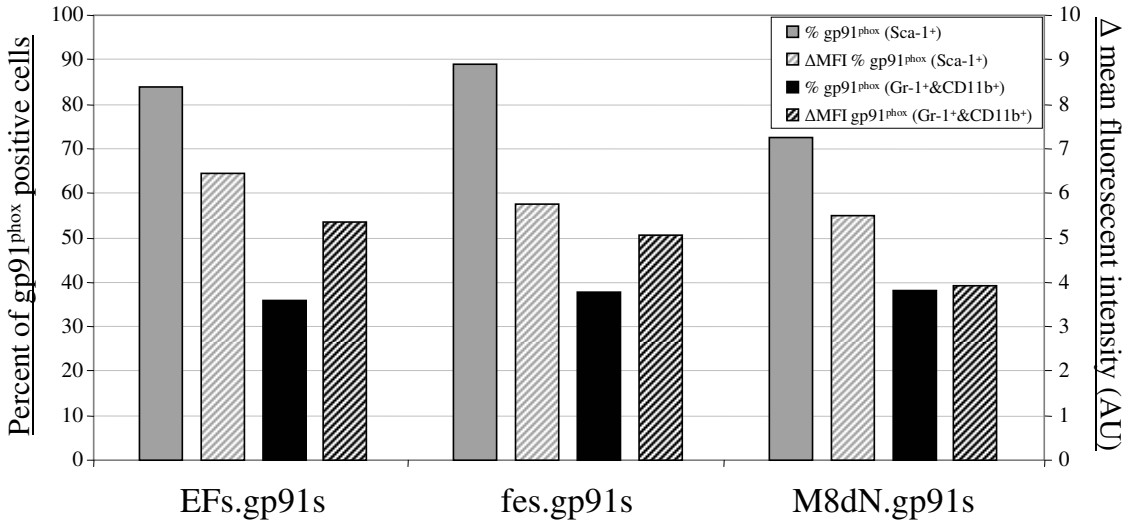

Fig. 50: *Ex vivo* transduction efficiency in mouse bone marrow Lin^{Neg} cells isolated from murine bone marrow. Sorted cells were transduced with the indicated viral constructs and analyzed 4 days post-transduction. Histograms show the distribution of gp91^{phox} positive cell among Sca-1$^+$ and Gr-1$^+$ and CD11b$^+$ subpopulations.

As shown in the Fig. 50, transduction efficiencies of ecotropic virus into murine HSCs, as scored by the percentage of 7D5 positive cells in the Sca-1$^+$ subpopulation, was high for all the constructs (ranging from 72 to 89%). In addition, the percentage of gp91^{phox} positive cells within the myeloid progenitor cell fraction showed almost the same values for all the constructs (ranging from 35.9 to 38.2%). When the MFI was analyzed, the EFs.gp91s vector generated the highest ΔMFI among all the constructs both in the

Sca-1$^+$ (EFs.gp91s, 6.5; fes.gp91s, 5.7; M8dN.gp91s, 5.5) as well as in the myeloid subpopulation (EFs.gp91s, 5.3; fes.gp91s, 5.0; M8dN.gp91s, 3.1).

Groups of eight X-CGD mice per construct were lethally irradiated with two doses of 5.5 Gy prior to transplantation. For this the mice were injected intravenously in the tail vein with around $1.8x10^6$ transduced cells. Unfortunately, two M8dN.gp91s transplanted mice died before being analyzed. Six weeks after transplantation, the recipient mice were sacrificed and the gp91^{phox} expression in bone marrow and peripheral blood lineages, as well as the NADPH oxidase activity reconstitution in peripheral blood granulocytes, was investigated.

Gp91^{phox} expression in marrow myeloid and lymphoid lineages of transplanted mice was analyzed by flow cytometry and the results are summarized in the Fig. 51a. In this study the antibodies used for cell marking were the same as in the previously described experiment. Additionally, T lymphocytes were labeled with a CD3 antibody to analyze transgene expression in these cells as well.

The results show, that mice transplanted with EFs.gp91s and fes.gp91s transduced Lin^{Neg} cells showed extensive mouse-to-mouse variability in gp91^{phox} expression in the different lineajes. When comparing the percentages of gp91^{phox} positive cells within the marrow myeloid subpopulation, the EFs.gp91s mice showed the highest intragroup variability. Levels of gp91^{phox} positive cells ranged from 13.4 to 64.6% (29.9 ± 18.9%). For the c-fes mice the values ranged from 15.3 to 60.5% (35.7 ± 15.2%). The M8dN.gp91s mice showed the lowest levels of gp91^{phox} expression in all marrow lineages. In the myeloid marrow subpopulation M8dN.gp91s values ranged from 4.4 to 22.4% (11.6 ± 6.1%). Interestingly, in six out of eight fes.gp91s mice gp91^{phox} was expressed in at least 30% of the cells, whereas only three of the EFs.gp91s and none of the M8dN.gp91s mice reached this level. The proportion of gp91^{phox} expressing cells within the myeloid subpopulation was in most cases, and notably in all the M8dN.gp91s transplanted mice, higher than those of gp91^{phox} in marrow B cells. As expected, the expression of gp91^{phox} in marrow T lymphocytes was for the M8dN construct almost invariably below that of Gr-1$^+$ and CD11b$^+$ and B220$^+$ populations. In effect was also observed in the EFs mice. In contrast, in three fes.gp91s mice gp91^{phox} expressing T cells reached unexpected higher values than in myeloid cells (f9, f15 and f16) (Fig. 51a).

To assess whether the gp91^{phox} expression levels detected in the bone marrow correlated with that of circulating cells, a sample of peripheral blood from each mice was analyzed by flow cytometry. The percentages of gp91^{phox} positive cells in the blood samples are shown in the Fig. 51b.

When comparing the bone marrow and peripheral blood samples from the EFs.gp91s and fes.gp91s mice, the percentages of gp91^{phox} positive cells within myeloid subpopulations did not reveal any clear tendency. Half of the mice population showed

an increase in gp91^{phox} expression in the cells of the blood samples whereas the other half rather showed a decrease compared to the bone marrow specimen. In contrast, for the M8dN.gp91s mice the percentage of transgene positive cells increased through maturation although the gp91^{phox} level was still low. Only one M8dN.gp91s mice reached the 30% threshold line whereas for the EFs.gp91s and fes.gp91s constructs 5 and 6 out of 8 mice, respectively, reached this threshold.

a) Bone Marrow

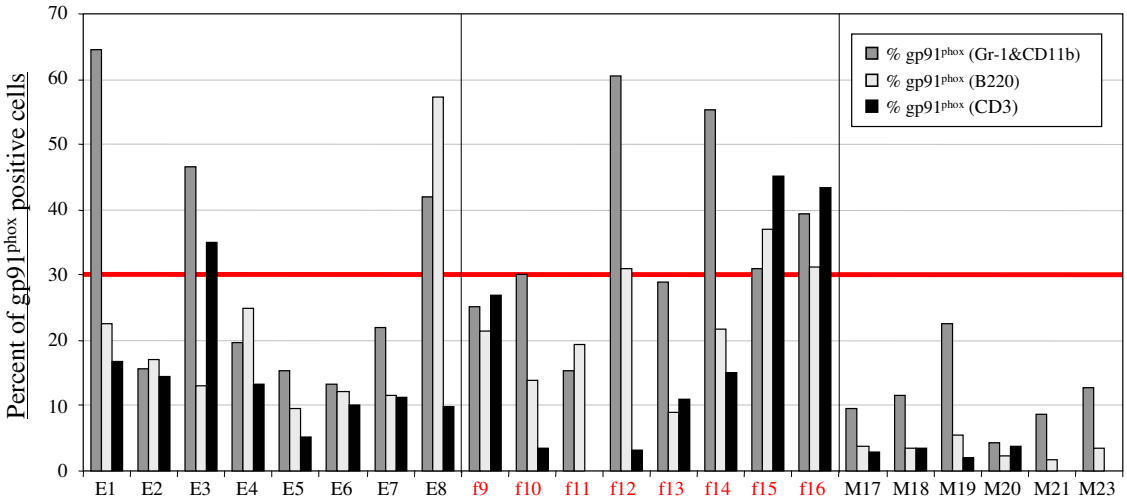

b) Peripheral blood

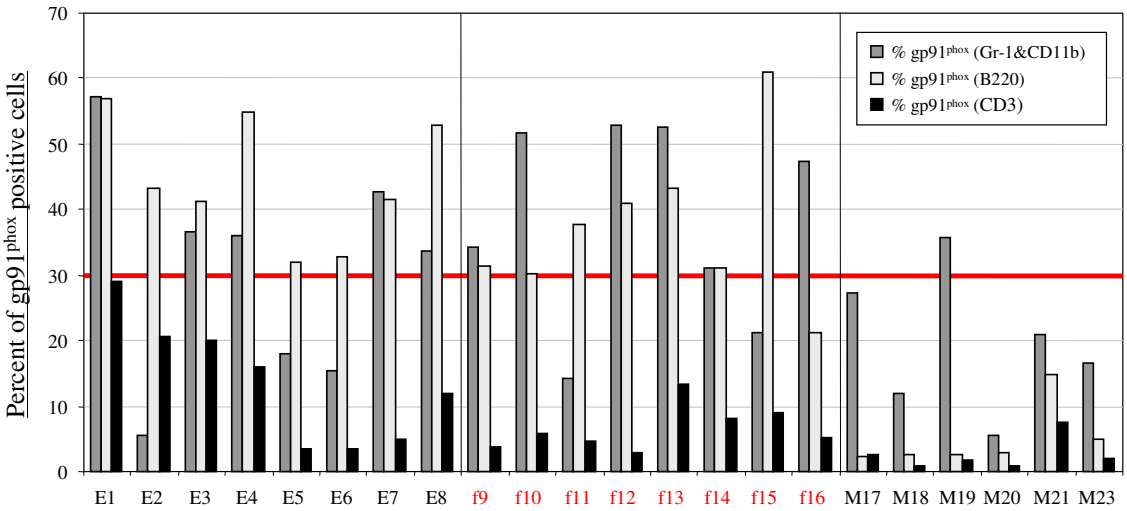

Fig. 51: *In vivo* multilineage reconstitution ability of transduced Lin^{Neg} marrow cells. (a) Percentage of gp91^{phox} expressing cells in bone marrow lineages of irradiated and transplanted X-CGD mice. Bone marrow cells from transplanted mice were analyzed after 6 weeks for gp91^{phox} expression within the different hematopoietic lineages (myeloid-specific markers: Gr-1 and CD11b, B lymphoid marker: B220 and T lymphoid marker: CD3). (b) Percentage of gp91^{phox} expressing cells in peripheral blood populations. Peripheral blood cells were immunostained and analyzed for gp91^{phox} expression in the myeloid and lymphoid lineages as described in (a).

Almost the same pattern in bone marrow and peripheral blood populations was observed for the changes in transgene expression in T cells. Extensive variability was observed in mice transplanted with the EFs.gp91s and fes.gp91s transduced cells, while the M8dN.gp91s did not show significant changes, only one mouse (M21) showed no (0%) $gp91^{phox}$ positive cells in marrow T lymphocytes and reached 7.6% in circulating T cells. It is important to mention that the percentages of $gp91^{phox}$ expressing cells in both T cell sources were generally low, even in the case of the constitutive EFs promoter. In peripheral blood, the fes.gp91s mice showed lower values of transgene expressing T cells than the EFs mices. The lowest values were obtained with the M8dN.gp91s mice, which confirms the myeloid specificity of this promoter.

The differences in $gp91^{phox}$ expression in B cell populations isolated from the bone marrow or the peripheral blood followed clear tendencies. An increase in the expression of $gp91^{phox}$ was detected in all EFs.gp91s and fes.gp91s mice, with only one exception (E8, f16). In contrast, a decrease was observed in most of the M8dN.gp91s mice although to a very low extent (apart from the M21 mouse which showed an 8.2-fold increase in $gp91^{phox}$ expression through maturation). Moreover, without taking the mice which showed a decrease in $gp91^{phox}$ expression (E8, f16) into account, the increase observed with the EFs.gp91s construct was higher and not as variable as the increase in the fes.gp91s mice (2.6 ± 0.8-fold compared to 2.0 ± 1.3-fold, respectively).

To quantify the number of proviral integrations per cell, semiquantitative PCR was performed with the bone marrow and peripheral blood samples of the transplanted mice. However, due to technical problems it was not possible to analyze all mice. The obtained values are depicted in the Fig. 52. There was a high variability in the vector copy number (VCN) observed in all mice, both in bone marrow and peripheral blood samples. Numbers ranged from 0.4 to 1.9 integrated proviruses per bone marrow cell, and from 0.4 to 4 in peripheral blood cells.

The VCN was compared and related to the $gp91^{phox}$ expression in the myeloid subpopulation ($Gr\text{-}1^+$ & $CD11b^+$) of the corresponding bone marrow and peripheral blood mice samples. A clear tendency for a better performance was observed with the fes.gp91s construct (mainly when comparing both myeloid promoters) (Fig. 53a). The fes.gp91s construct showed slightly higher and more constant levels of transgene expression per copy number than the EFs.gp91s in the bone marrow (50.9 ± 4.8% and 44.3 ± 8.8% $gp91^{phox}$ positive cells per integrated vector, respectively). With these promoters almost 4-fold higher levels were obtained than for the M8dN.gp91s construct (13.1 ± 3.6% $gp91^{phox}$ positive cells per integrated vector).

a) Bone Marrow

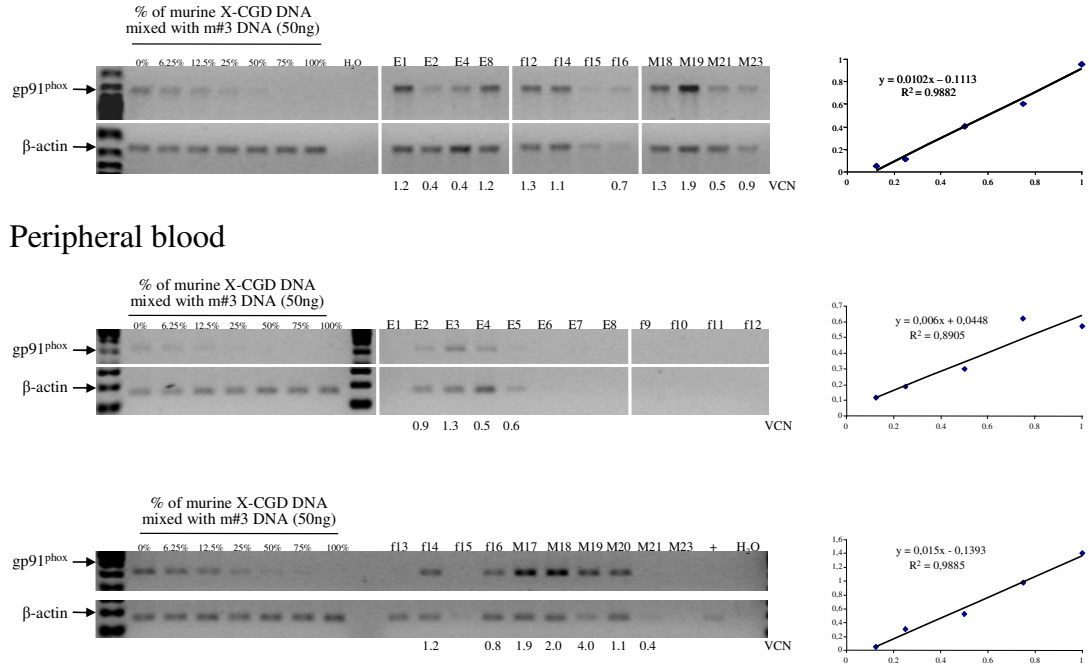

b) Peripheral blood

Fig. 52: VCN analysis of bone marrow and blood samples of the reconstituted X-CGD mice by semi-quantitative PCR. (a) Genomic DNA was obtained from bone marrow samples of recipient mice and PCR amplification of a gp91^{phox} fragment was performed. Amplification of the β-actin was used as loading control. A standard curve was prepared by serial dilution of mouse DNA from a genetically modified population with 1 copy of provirus per cell (m#3), and the linear regression and correlation coefficient R^2 were obtained to calculate the VCN of the samples. (b) DNA from a peripheral blood sample of each mouse was used to VCN determination by PCR amplification. A standard curve was prepared as described for the bone marrow analysis in (a).

The number of integrated proviruses was also assessed in the peripheral blood of transplanted mice (Fig. 53b), but again not all mice could be analyzed due to technical problems (only two fes.gp91s mice could be tested). When the percentage of transgene expressing peripheral granulocytes was related to the VCN, a higher mouse-to-mouse variability than for bone marrow was observed (Fig. 53b). Nevertheless, EFs.gp91s and fes.gp91s constructs showed higher levels of gp91^{phox} expression per integrated provirus, than M8dN.gp91s in almost all the cases (except for the mouse M21, which showed up to 10-fold higher transgene expression per copy number than the other M8dN.gp91s mice). Most of the M8dN.gp91s mice reached markedly low levels, ranging from 5.1 to 14.4% gp91^{phox} positive circulating myeloid cells per integrated proviruses. The EFs.gp91s and fes.gp91s mice displayed a minimum of 20% transgene expressing cells per VCN in the myeloid peripheral blood compartment (except for the E2 mice which due to the low percentage of gp91^{phox} expressing peripheral Gr 1$^+$ and CD11b$^+$ cells (5.6%) only reached 6.3% of expressing cells per integrated provirus).

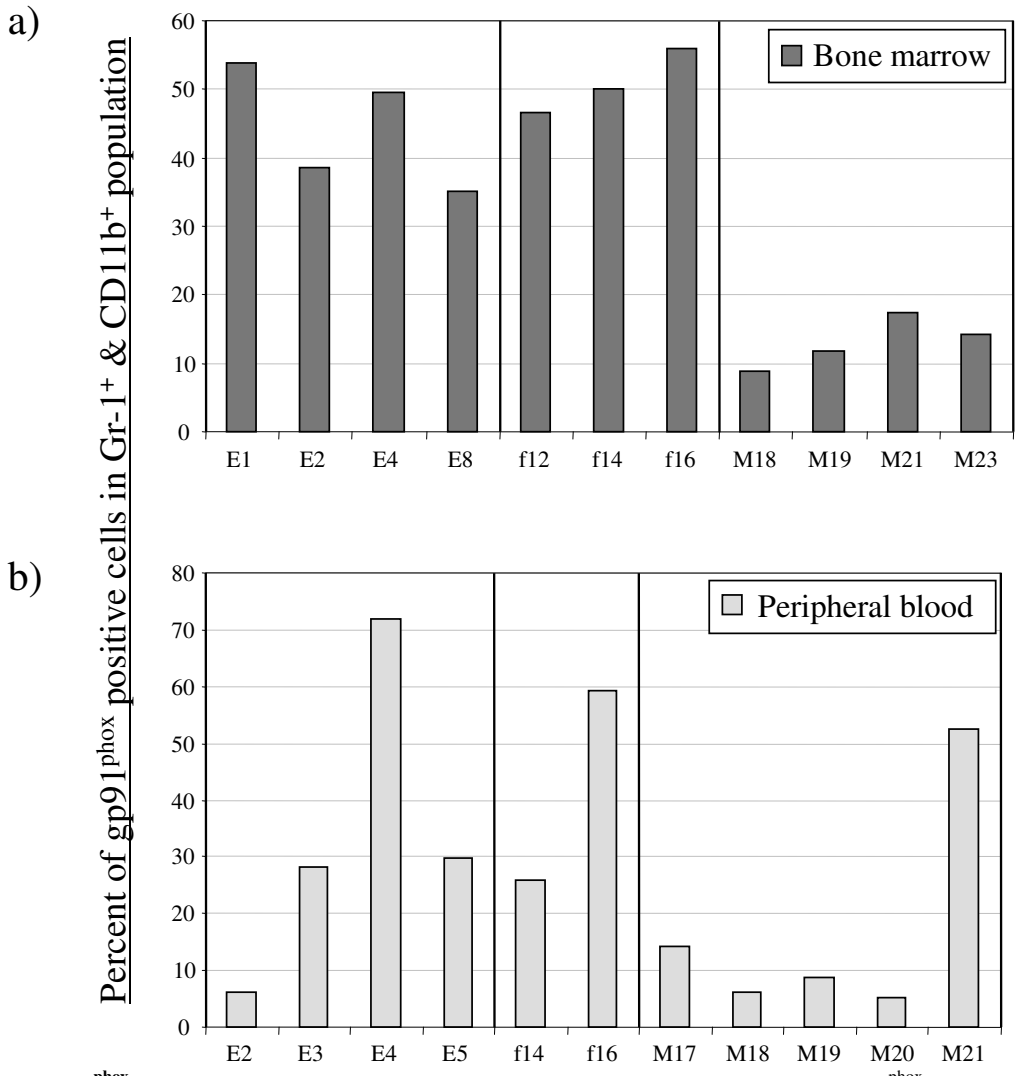

Fig. 53: Gp91^{phox} expression per copy of integrated provirus. The percentage of gp91^{phox} expression in the Gr-1^{+} & CD11b^{+} subpopulation of bone marrow (a) and peripheral blood (b) from recipient X-CGD mice related to the corresponding VCN is represented.

Finally, *in vivo* correction of the enzymatic defect was evaluated in peripheral blood granulocytes by the DHR assay in combination with Gr-1 & CD11b immunostaining and also *in vitro* with clonogenic progenitors using the NBT dye reduction assay.

The percentage of DHR positive cells (normalized according to the wild-type) is represented in histogram shown in Fig. 54. Though a high intragroup variability, the fes.gp91s construct showed the highest proportion of mice going beyond the threshold line of 40% DHR positive cells. Six fes.gp91s mice showed more than 40% DHR positive cells and four out of these six even reached 80% whereas only four mice for EFs and two M8dN.gp91s mice reached 40% of DHR positive cells.

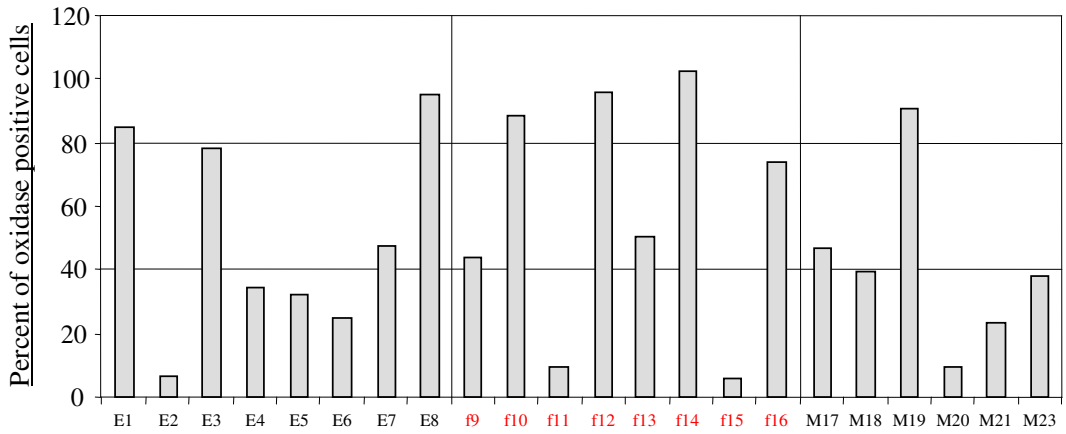

Fig. 54: Reconstitution of the NADPH oxidase activity in irradiated and repopulated X-CGD mice. The percentage of positive cells in the functional DHR analysis of peripheral blood samples from transplanted mice is shown.

When the flow cytometry DHR assay was analyzed in a dot blot form (Fig. 55) an evident shift with the PMA-stimulated wild-type peripheral blood granulocytes could be observed indicating robust oxidase activation upon stimulation. The analysis of the PMA-stimulated granulocytes from transplanted mice resulted in a 3- to 6-fold lower ΔMFI indicating a lower superoxide production in gene modified peripheral granulocytes. Moreover, when comparing the ΔMFI values between the different constructs the M8dN.gp91s seemed to show a slightly better performance (6.9 ± 2.0; 6.6 ± 0.6 and 6.5 ± 1.6 with the M8dN, EFs and c-fes promoters, respectively). However, this promoter was also shown to have more integrated proviruses in circulating granulocytes. Therefore, when the ΔMFI values were related to the number of integrated proviruses the best results were obtained with the EFs.gp91s (9.1 ± 3.3) followed by the fes.gp91s (6.7 ± 0.8) and finally the M8dN.gp91s construct, which also showed the highest mouse-to-mouse variability (5.9 ± 5.0). Of note, although only two fes.gp91s mice could be analyzed for the VCN, this construct showed a markedly lower intragroup variability in the DHR assay (if related to the VCN) than the other groups.

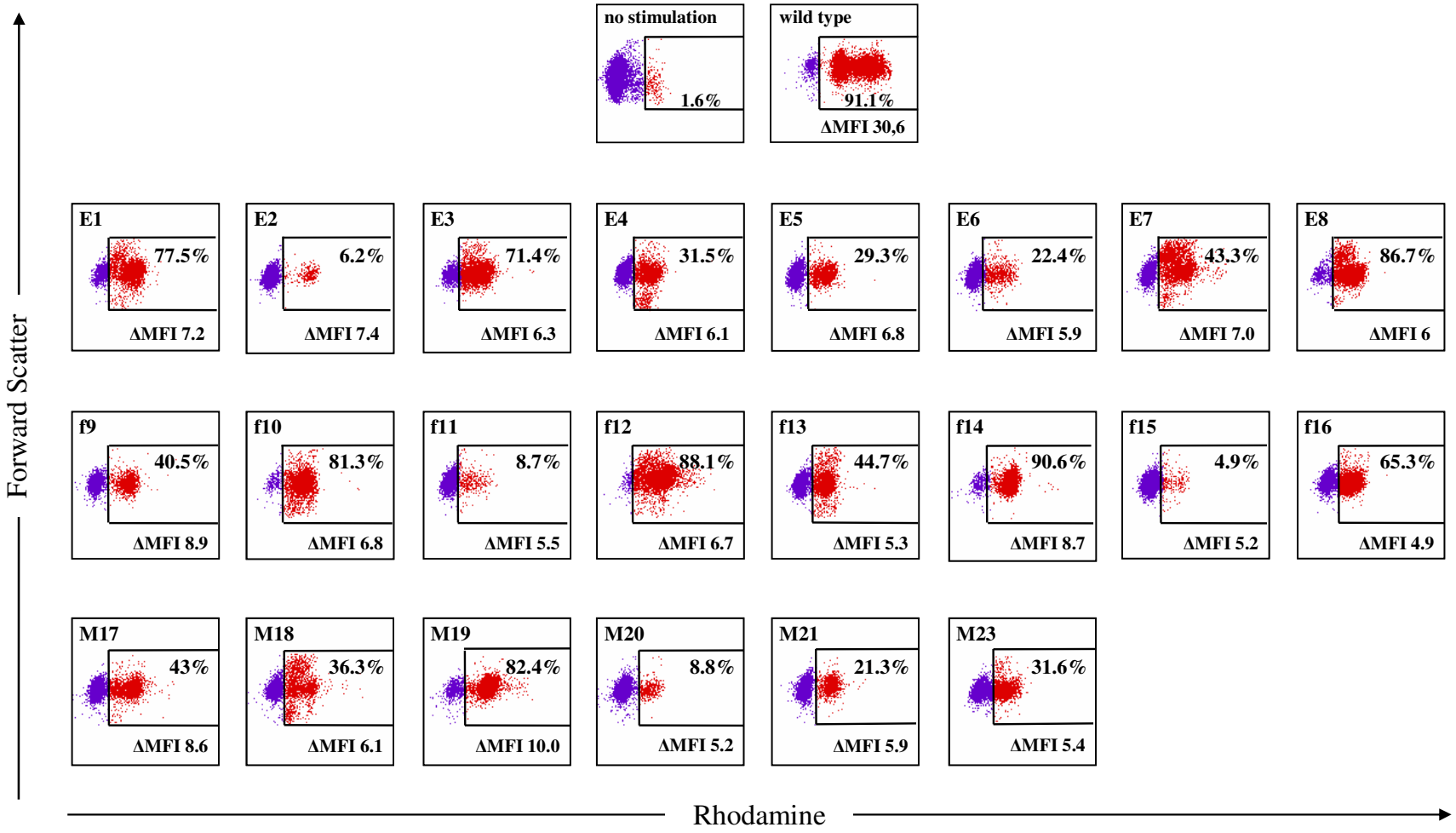

Fig. 55: Correction of oxidase activity in genetically-modified peripheral blood granulocytes of transplanted mice. Dot blot analysis of the flow cytometry DHR assay. Shown are analyses of non-stimulated and stimulated wild-type mouse peripheral granulocytes for comparison, and samples of transplanted mice show the results of stimulated peripheral granulocytes.

In addition to the DHR analysis of the blood cell, myeloid progenitor populations in the bone marrow of transplanted mice and non-transduced control mice were assayed for the ability to reconstitute the NADPH oxidase activity. For this purpose, bone marrow cells from transplanted mice were cultivated in semi-solid collagen-based medium containing mSCF (50 ng/ml), mGM-CSF (10 ng/ml) and mIL-3 (10 ng/ml) to stimulate proliferation and colony formation. After 12 days of incubation, the number of colonies was assessed by counting every cell cluster of more than 50 cells as one colony. The enzymatic correction of the NADPH oxidase was evaluated using the NBT reduction assay (Dr. L. Chen).

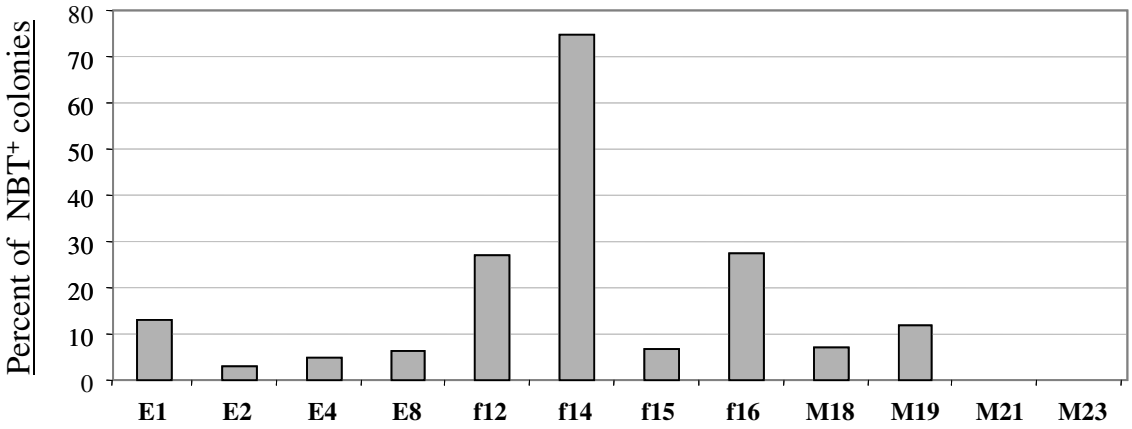

Fig. 56: Analysis of NADPH oxidase activity in clonogenic progenitors of reconstituted X-CGD mice. Percentage of colonies scoring positive with NBT after growth in semi-solid culture medium containing mSCF, mGM-CSF and mIL-3 for 12 days.

As shown in the Fig. 56 a higher percentage of NBT^+ colonies was detected for the clonogenic progenitors of the fes.gp91s transplanted mice than those of the other constructs (about 4.9- and 7.2-fold increase in percentage of NBT^+ colonies when compared to EFs.gp91s and M8dN.gp91s mice, respectively).

D. DISCUSSION

To date, bone marrow transplantation is the most recommended therapy for the CGD, but only if a matched donor is available. However, such ideal match is extremely infrequent and, in addition, several severe side effects may occur after transplantation which might lead to a fatal outcome. Therefore, this treatment possibility should be studied thoroughly before proceeding (Barese *et al.*, 2004).

Gene therapy offers an interesting alternative to BMT, which implies a less invasive treatment and possibly represents a possibly unique curative option for patients with not suitable donor. Gammaretroviral vector were already used in some gene therapy trials for CGD and other immunodeficiencies showing relevant clinical benefit. However, these trials uncovered also mutagenic side effects, which occurred as a direct result of vector integration into the host genome leading to the development of malignant processes (Hacein-Bey-Abina *et al.*, 2003a) or to a selective advantage of affected target cells resulting in a monoclonal repopulation (Deichmann *et al.*, 2007). Therefore there was a need to further improve the safety of these vectors and to this end the self-inactivating gammaretroviral vectors were engineered. Non essential sequences for virus infectivity and integration, which might influence the surrounding gene expression, were deleted in these vectors. Although, these vectors showed low efficiency in virus production, the requirement for an internal promoter was a major advantage. These vectors offer the opportunity to test the performance of tissue-specific promoters driving transgene expression towards the desired cells.

In the present study the suitability and performance of self-inactivating gammaretroviral vectors for the treatment of the CGD was investigated, focusing on improvements of the therapy based on findings obtained with previous clinical studies. The improvements included production of the virus in high titers as well as the selection of an efficient tissue-specific promoter for expression of the transgene.

D.1 Improving retroviral vectors driving gp91^{phox} expression

In the first set of experiments, a series of SIN gammaretroviral vectors was cloned driving the expression of the wild-type gp91^{phox} cDNA under the control of a viral constitutive SFFV promoter. These vectors contained an RSV promoter to drive the expression of the genomic viral transcript in the packaging cells and the WPRE sequence to enhance the export of the intronless RNAs from the nucleus into the cytoplasm. These changes resulted in a substantial increase in the titers of this vectors, which was one major drawback of the former gammaretroviral SIN vectors (Schambach *et al.*, 2006a). Additionally three different leader conformations were design based on the presence or absence of donor and acceptor splicing sites: leader 11 which contains only splice donor site, leader 71 with both splice donor and acceptor, and leader 110

without splicing sites. Previous studies with retroviral vectors have shown that the presence of an intron at the 5'UTR favored the transgene expression in transduced cells likely due to the fact that the mRNA nuclear export process is coupled to the cellular splicing (Kraunus *et al.*, 2004). This idea is supported by studies showing enhanced nuclear export of cellular genes by splicing (Luo and Reed, 1999). Moreover, the presence of the packaging signal in the transcript of the integrated proviral genome was found to reduce transgene expression. This phenomenon might be due to the cellular inhibition of retroviral RNA export or caused by its complex secondary structure (Kraunus *et al.*, 2004). Therefore, the effect of a packaging signal placed within an intron, and upstream of the internal promoter was studied.

In addition to the leader modifications in the first series of vectors, an alternative version of the $gp91^{phox}$ gene, which contains a mutated cryptic splice acceptor (cSA) sequence, was tested. The presence of the cSA within the wild-type $gp91^{phox}$ cDNA was revealed by analyzing the mRNA species produced by pSRS11.SF.gp91.W-transfected 293T cells (Fig. 16), and it was likely to reduce viral titers due to the generation of incorrect transcripts. Therefore, a point mutation was introduced in the consensus sequence of the cSA and its effect on the virus production in combination with the three different leader sequences was studied (Fig. 17). Titer analysis of the six different vectors showed about $1x10^6$ t.u./ml as measured by FACS analysis and about $2.5x10^6$ t.u./ml by PCR amplification (Fig. 18). The differences between FACS and PCR measurements were likely caused by the failure in transgene expression of some integrated vectors, which is dependent on the chromosomal integration site. Between the three different leader sequences no big differences were observed. Also the mutation introduced to avoid aberrant splicing occurring within the $gp91^{phox}$ mRNA did not show significant differences. This indicated that the cSA had no detrimental effect on virus production, probably because the splicing machinery of the producer cells did not efficiently use it. The surprising 3.4-fold increase in titer observed with the mutated versus wild-type $gp91^{phox}$ in combination with leader 110 could not be explained by the avoidance of a splicing event, since this leader has no splice sites able to interact with the cSA of the wild-type $gp91^{phox}$ cDNA. Mostly important, all constructs tested achieved enhanced titers (previously $<5x10^5$ t.u./ml) which is an important requirement for large-scale retroviral vector production and a prerequisite for clinical applications (Schambach and Baum, 2007).

The level of transgene expression within individual cells is an additional critical parameter for functional correction in the gene therapy of the CGD. Previous molecular studies of X-CGD patients showed that low amounts of superoxide production are still related to severe symptoms (Bu-Ghanim *et al.*, 1995; Goebel and Dinauer, 2002). Therefore, studying the efficacy (maximal therapeutic effect with minimal vector copy number) of an improved gene therapy vector is of great interest.

To assess this question, a selection procedure for gp91^{phox} positive cells with a vector copy number of 1 integrant per cell was set up (in order to compare between equally transduced cells). However, the selection process caused changes in the ΔMFI values of the populations transduced with vectors containing the mutated gp91^{phox} sequence. These constructs reached values of about 5 prior to selection and shifted to about 7 after sorting (Fig. 19). These differences might be due to the selection process, but also caused by imprecise measurements prior to sorting. The pre-selected populations contained only a few positive cells, which might not be representative for the whole population. To additionally determine differences in the superoxide production levels between the sorted populations, the cytochrome c assay was performed after granulocyte-like cell differentiation (Fig. 20). This assay is an accurate test, which measures the extracellular O_2^- production of cells upon stimulation, but is also extremely sensitive giving rise to variations between measurements. However, regardless of the high standard deviations, the obtained superoxide levels reached between 60 to 90% of the wild-type PLB-985 cells (Fig. 21), which might be enough to ensure a stable follow-through of the disease. Furthermore, these values are comparable to those obtained in a previous study where X-CGD PLB-985 cells were transduced with a full-length LTR murine stem cell virus-based vector (MSCV vector) expressing the wild-type gp91^{phox} gene. In this case, superoxide production levels of 57 to 119% related to the wild-type PLB-985 cells were detectable in derivative clonal populations (Ding *et al.*, 1996). The cytochrome c assay also revealed that vectors containing the mutated sequence reached slightly higher values of oxidase activity than those harboring the wild-type cDNA. This increase might not be due to the mutation in the cSA of the gp91^{phox} gene itself. In the SIN gammaretroviral vector configuration the splice sites are present in the leader sequence situated upstream of the internal promoter, and thus should not have any influence on the cSA of the transgene. Therefore, the increased values in superoxide production by the mutated sequence might indicate a better performance in transcription or protein processing although the reason is still unknown. In addition, both vectors containing the leader 11 showed the best titers, whereas the highest levels of superoxide production were obtained in combination with the mutated gp91^{phox} cDNA. Therefore, the SRS11.SF.gp91m.W was selected as basal backbone for further modifications such as transcriptional targeting by the use of myeloid-specific promoters.

D.2 Introduction of myeloid cell specificity in retroviral vectors

D.2.1 Evaluation of the MRP8 promoter

The NADPH oxidase is mainly required in phagocytic cells, thus, it would be a desirable and powerful strategy to target the transgene expression towards myeloid cells by the usage of tissue-specific promoter such as the MRP8 and c-fes promoters.

The MRP8 promoter has been widely used to drive the expression of several transgenes, such as bcl-2 or AML-ETO, towards myeloid and neutrophil cells including common myeloid progenitors in transgenic leukemia mouse models (Lagasse and Weissman, 1994; Yuan *et al.*, 2001). Moreover, it has been shown in our group that a fragment of 1176 bp of the MRP8 promoter containing upstream regulatory elements efficiently drives the expression of GFP when cloned in a lentiviral construct (Dr. S. Stein, pers. commun.). Therefore, to test the performance of this sequence, it was cloned into the SRS11.SF.gp91m.W gammaretroviral construct, which previously showed the best results in the cytochrome c assays (Fig. 22). It was shown that viral particles were produced by the packaging cells since $gp91^{phox}$ cDNA could be detected by PCR amplification of genomic DNA of the SRS11.M8dNdI.gp91m.W transduced cells indicating the presence of integrated viral genomes (Fig. 24a). However, when X-CGD PLB-985 cells were transduced with this vector, there was no detectable expression of $gp91^{phox}$ neither prior nor after granulocyte-like cell differentiation (Fig. 23). The absent or inefficient transcription as well as aberrant mRNA products generated by erroneous transcription of the transgene are both possible causes for undetectable levels of $gp91^{phox}$ glycoprotein in the cellular membrane. Therefore, Northern blot analysis was performed to investigate the presence of $gp91^{phox}$ transcripts in the transduced cells. A total lack of $gp91^{phox}$ RNA was shown confirming absent transgene transcription as responsible for the missing expression of the integrated $gp91^{phox}$ cDNA (Fig. 24b). The loss of expression using this vector might be caused by the cloning strategy. In the previous lentiviral construct the expression cassette (MRP8-GFP) was cloned in the inverse orientation, whereas the direct orientation was used for the gammaretroviral construct. Whether changing the orientation of the expression cassette would have led to an enhancement in the transgene expression was not further studied. Instead, a cis-acting regulatory element was introduced to improve the transgene expression (Fig. 25).

Melkonyan and colleagues revealed the existence of a myeloid-specific enhancer in the first intron of the MRP14 gene, which encodes a Ca^{2+}-binding protein of the S-100 family to which the MRP8 protein also belongs to (Rammes *et al.*, 1997). This MRP14 intronic sequence showed enhancing effects (with up to 37-fold increase in transgene expression) and position independent characteristics when cloned, either upstream or downstream of an heterologous promoter, such as the TK promoter (Melkonyan *et al.*, 1998). Furthermore, this is a highly conserved sequence in the human MRP genes, and thus it shares also a high degree of homology with the first intron of the MRP8 gene. Therefore, to assess if this element is able to increase transgene expression, the enhancer sequence located at the first intron of the MRP8 gene was PCR amplified and cloned upstream of the internal MRP8 promoter in the gammaretroviral vectors. However, when virus treated cells were analyzed for transgene expression $gp91^{phox}$ positive cells could not be detected after transduction neither after granulocytic-like cell differentiation (Fig. 26a and b). Moreover, when the presence of integrated proviruses

was investigated in transduced cells gp91^{phox}-containing sequences could not be detected (Fig. 26c). This lack of proviral integrations might be due to absent or defective virus production in the producer cells because of either a transcriptional or a packaging failure, respectively. The large size (~5 kb) of the expression cassette may not be responsible for detrimental packaging of the genomic viral RNA, since it has been previously shown that gammaretroviral vectors are able to package heterologous sequences up to 8 kb in length (O'Connor and Crystal, 2006).

D.2.2 Evaluation of the c-fes promoter

Another myeloid promoter was chosen to test its performance in the context of the gp91^{phox}–containing gammaretroviral vectors, the c-fes promoter. This promoter drives the expression of a non-receptor tyrosine kinase (p92$^{c\text{-}fes}$ protein) involved in several cellular processes including differentiation and proliferation of myeloid cells. Moreover, the c-fes promoter is constantly active during myeloid differentiation, but becomes silenced upon erythroid maturation (Care *et al.*, 1994). The PU.1, a transcription factor required for c-fes promoter activity in myeloid cells, interacts with GATA-1, a zinc finger transcription factor required for erythroid differentiation, thereby blocking erythroid differentiation (Heydemann *et al.*, 1996; Stopka *et al.*, 2005). Previous studies showed that this promoter is influenced by the locus control region (LCR), a cis-acting DNA element that enhances expression of the linked gene, driving a copy number dependent expression. However, they also showed that a 446 bp fragment of the promoter was able to ensure a transgene tissue-specific expression (Heydemann *et al.*, 2000). Therefore, in the present study this short sequence of the c-fes promoter was PCR amplified and placed in the selected viral vector for further testing in X-CGD PLB-985 cells. In contrast to the MRP8 promoter, the c-fes promoter clearly activated detectable gp91^{phox} expression when X-CGD PLB-985 cells were transduced with these viral particles. Nevertheless, the transgene expression of the c-fes promoter showed moderate transcriptional levels since the ΔMFI analysis of SRS11.fes.gp91m.W transduced cells reached only around 50% of gp91^{phox} expression of cells transduced with the SF promoter-containing construct (Fig. 28a). Moreover, titer analysis revealed a reduced virus production possibly caused by transcriptional interference between the c-fes promoter and the RSV promoter located in the plasmid 5'LTR. Titers obtained with the SRS11.SF.gp91m.W construct were twice as high as titers obtained with the c-fes construct. These data correlated with previous studies from Schambach and colleagues also showing that the SF internal enhancer promoter influenced the expression from the RSV 5'LTR (Schambach *et al.*, 2006c). Additional studies on transduced cells, such as genomic detection of integrated provirus, corroborated this observation since lower amounts of integrants were detectable in the SRS11.fes.gp91m.W transduced cells (Fig. 28c). In addition to the low titer only, a slightly increase of the transgene expression was observed after granulocyte-like cell differentiation with the c-fes construct (Fig. 28b). This was also observed in a previous

study showing that the c-fes driven expression did not experience any significant change through differentiation (Haigh *et al.*, 1996). Thus, it can be concluded that in contrast to previous observations, the c-fes is a weak promoter when compared to the SF viral promoter, and that it is not inducible through differentiation. Nevertheless, the transcriptional activity of the c-fes promoter should not be considered as defective. The desired transgene expression should not be necessarily compared to the high levels produced by the SF viral promoter, which might produce an excess of protein compared to the endogenous levels in wild-type cells. Therefore, the functionality of the c-fes promoter-containing construct was further investigated in sorted transduced cell populations containing similar VCN per cell. The purity of the c-fes transduced population reached only 72% of positive cells likely due to the lower amounts of $gp91^{phox}$ expressed by the c-fes promoter, leading to a less efficient labeling and enrichment (Fig. 28d). The NADPH functionality was assessed by the cytochrome c assay in these cell populations after granulocyte-like cell differentiation showing that the c-fes promoter did not reach the wild-type kinetic level even after 25 min of measurement (Fig. 29a and c). In accordance, when comparing the values of superoxide production between both constructs, 5 times lower levels were obtained by the c-fes promoter and only 10% of superoxide production of the wild-type levels were obtained (Fig. 29d). These results were also confirmed by the observation that the $gp91^{phox}$ glycoprotein was almost undetectable in Western blot analysis of the sorted cell population containing the SRS11.fes.gp91m.W construct (Fig. 29b). Overall, these results ruled out this construct for development of an efficient and effective viral vector for X-CGD gene therapy. For this purpose not only the percentage of positive cells, but also the total amounts of superoxide produced by each individual cell has been shown to be crucial for effective treatment of the disease (Johnston *et al.*, 1985).

Previous studies with lentiviral backbones showed an optimal performance (NADPH oxidase reconstitution ability with myeloid-specific expression) of a c-fes construct, in which the expression cassette ($gp91^{phox}$ and bgh polyadenylation signal) was cloned in the inverse orientation (Dr. S. Stein, pers. commun.). Therefore a similar cassette was placed in the SIN gammaretroviral backbone also in the inverse orientation (Fig. 30a). In this gammaretroviral vector the WPRE sequence was deleted since the bgh polyadenylation signal was included in the cassette. The bgh signal is a strong and specialized polyadenylation signal from the bovine growth hormone gene that ensures transcriptional termination. This element was placed downstream of the transgene to avoid possible read-through events from the internal c-fes promoter (Schambach *et al.*, 2007).

Although in the lentiviral context this cassette showed a good performance, the c-fes promoter again failed to induce $gp91^{phox}$ expression in the gammaretroviral backbone (Fig. 30b). No $gp91^{phox}$ positive cells were detected after transduction of target cells and PCR analysis revealed that the provirus didn't integrate in the genome of cells treated

with viral supernatants indicating that no infecting particles were released by the packaging cells (Fig. 30c). The failure to produce infectious particles with this construct might be due to several reasons e.g. the formation of antisense transcripts hybridizing with the sense RNA molecules. This may down regulate gene expression by inhibiting sense mRNA transcription and/or translation (Kumar and Carmichael, 1998). Whether this occurs requires further studies e.g. Northern blot analysis of RNA from transfected cells. Since the c-fes construct (with the expression cassette in the direct orientation) showed a low but detectable transgene expression and a transgene-dependent effect in the efficacy of the vector can not be excluded. Therefore subsequent studies were focused on improving the transgene expression levels by codon optimizing of the gp91^{phox} wild-type sequence.

D.3 Synthetic gp91^{phox}

D.3.1 Improvements of viral titer and transgene expression

Replacement of the viral internal constitutive promoter of the SIN gammaretroviral constructs by myeloid-specific elements caused a reduction in both titer and transgene expression. Further modifications in the leader region, in the gp91^{phox} cDNA itself or in the content of cis-acting elements did not improved the performance of these vectors. Therefore, a complete codon optimization of the native gp91^{phox} cDNA was performed. The codon optimization process requires the knowledge of the codon usage of the target cell. Usage is defined by the relative amounts of the 20 tRNAs available in the cell and the percentage of utilization of each tRNA by the ribosomes. To optimize a sequence, its codon content is evaluated, and each codon for which a better codon is available is exchanged. This technique has multiple applications (e.g. optimize transgene expression, increase genetic stability of vector constructs, reduce homology to wild-type sequences counteracting the risk of homologous recombination events, etc.) and has already shown to increase viral titer and improve transgene expression levels in vectors designed for further gene therapy applications (Radcliffe *et al.*, 2008).

In the present study, the wild-type gp91^{phox} cDNA was optimized (gp91s) for translation in human cells. Additionally, sequences such as internal polyadenylation sites, cryptic splice sites and RNA instability motifs were also detected and eliminated, since they might lead to undesirable and aberrant transcripts thereby exerting a negative influence on viral genome production.

The synthetic gp91^{phox} and the mutated version were then cloned in a new construct based in the SERS11.SF.GFP.W backbone kindly provided by Prof. Dr. C. Baum (Fig. 31a). This construct contained a SV40 enhancer (E) upstream of the LTR plasmid promoter shown to enhance viral particle production of SIN gammaretroviral vectors (Schambach et al., 2006c). Moreover, a X protein promoterless, ORFs deleted WPRE sequence (Wm) was also introduced (Schambach *et al.*, 2006a).

Indeed, when assessing the performance of the synthetic gp91^{phox} sequence cloned into the new SIN gammaretroviral backbone (SERS11.SF.gp91s.Wm vector), a 2.7-fold increase in titer was observed when compared to the SERS11.SF.gp91m.W construct (Fig. 31c). The higher virus production was assumed to be due to an improved translation of this construct in transfected and transduced cells. This hypothesis was first assessed by Northern blot analysis of the viral transcripts in transfected cells which revealed correlating higher amounts of genomic transcripts with the codon optimized vector (Fig. 31d). Moreover, the better transcription of the transgene in transduced cells might have helped also to ensure detection of the integrated proviruses. This phenomenon was assumed to occur since higher amounts of the internal transcript were also observed in SERS11.SF.gp91s.Wm transduced cells with similar VCN (Fig. 34a). The transcriptional enhancement of the synthetic transgene led to a higher protein expression since an increase in ΔMFI, when compared to the mutated gp91^{phox}, was observed in transduced X-CGD PLB-985 cells (1.3-fold) and MACS selected populations (2.2-fold) with similar VCN per cell (Fig. 32). Furthermore, after granulocyte-like cell differentiation of sorted synthetic and mutated gp91^{phox} transduced populations no changes in ΔMFI were detected (Fig. 33), which is consistent with the previously described, constitutive transcriptional activity of the SF promoter (Tumas *et al.*, 1996). Additional analysis revealed that the differences in ΔMFI between undifferentiated and differentiated sorted populations did not correlate with those observed in internal transcript amounts (Fig. 34a). The transcriptional increase was higher than the ΔMFI change thereby showing the beneficial effect of deleting the polyadenylation and RNA instability motifs. However, these differences in transcript and protein amounts have already been shown by previous studies where primary hCD34^{+} cells were transduced with a gp91^{phox}-containing retroviral construct and analyzed after granulocyte-like cell differentiation *in vitro* (Grez *et al.*, 2000). Nevertheless, the analysis of protein amount revealed a correlation with the higher ΔMFI values when comparing both differentiated populations which indicates that the protein amount was directly proportional with its incorporation into the membrane (Fig. 34b). Additionally, there was also an increase in the protein content of transduced cells when compared to the wild-type PLB-985 cells, 2.7- and 5.5-fold increase were achieved by the mutated and synthetic gp91^{phox} sequence respectively.

D.3.2 Enhanced superoxide generation by the synthetic gp91^{phox}

When the restoration of superoxide generation was assessed, the synthetic gp91^{phox}-containing cells showed higher superoxide production (1.7-fold) than the mutated gp91^{phox} transduced cells and even higher levels of O_2^- than those produced by the wild-type cells (Fig. 34c). The functional difference between both transduced populations correlated with that of protein and ΔMFI levels, which indicated that the augmented superoxide production was likely due to the increase in the protein content per cell. However, there was also a 2-fold increase in the protein content of the mutated

gp91^{phox} transduced cells compared to wild-type cells, although here the cytochrome c assay did not show differences in the reconstitution of the NADPH oxidase between these populations. Since the amino acid sequence, and thus the structure of the gp91^{phox} protein, was conserved, regardless of the codon optimization, the 1.7-fold higher superoxide production observed with the synthetic gp91^{phox} sequence cannot be the result of just higher protein content. Therefore, the higher superoxide production observed might be explained by an underlying effect of the codon optimization process, by the sensitivity of the assay, or by non-significant differences.

D.3.3 The EFs promoter

Previous molecular studies in patients as well as gene therapy pre-clinical investigations have shown that the level of NADPH oxidase activity per cell can be an important factor in determining the outcome to certain microorganisms' infection when small numbers of O_2^- neutrophils are present (Dinauer *et al.*, 2001). In the present study it is shown that the use of the synthetic gp91^{phox} sequence in the context of a SIN gammaretroviral vector represents an excellent alternative to those former constructs expressing the mutated or native gp91^{phox} transgene.

Therefore, the SERS11.SF.gp91s.Wm was chosen to investigate the performance of non-viral promoters, since it was postulated that the SF promoter could still cause transactivation of neighboring genes due to its strength (Modlich *et al.*, 2006). One of the tested promoters is the EF-1α promoter, a ubiquitous promoter that efficiently drives the transgene expression in myeloid and lymphoid progeny of engrafting cells (Woods *et al.*, 2001). A short, intron-deleted version of the EF-1α promoter, known as EFs, has already been tested in both gammaretroviral and lentiviral SIN vectors, and it showed a moderate transcriptional activity with acceptable titer (Schambach *et al.*, 2006b).

In the present study, this short EFs sequence was used to analyze the expression of synthetic gp91^{phox} in a SIN gammaretroviral vector. When the EFs promoter was tested in X-CGD PLB-985 cells, a 3-fold lower titer was obtained when compared to the SF promoter (Fig. 36a). This effect might be due to the lower trans-activation potential of the EFs promoter on transcription from the LTR promoter as already seen for the c-fes promoter in the previous constructs of this study. This was confirmed by the fact that the amounts of genomic viral RNA assessed by Northern blot was lower as compared to the transcript amounts achieved by the SF promoter, which indicated a lower transcriptional rate from the LTR promoter (Fig. 36b).

Further investigations showed that the EFs promoter has also less transcriptional strenght than the SF promoter, since the ΔMFI and protein levels in differentiated X-CGD PLB-985 transduced cells showed 1.4- and 2-fold lower values (Fig. 38). Nevertheless, the cytochrome c assay revealed that higher values of superoxide production were reached in the DMSO differentiated transduced cells with the EFs

promoter than the wild-type PLB-985 cells (Fig. 41). When measured in a DHR assay, a slight 1.5-fold lower ΔMFI was observed (Fig. 42). The lack of correlation between the results from these two assays is caused by the fact that these methods measure the external superoxide release or the cytoplasmatic superoxide production, respectively. Furthermore, DHR is oxidized to rhodamine by hydrogen peroxide, whereas cytochrome c is directly reduced by superoxide ions produced by the activation of the NADPH oxidase at the beginning of the reaction (Henderson and Chappell, 1993; Krause *et al.*, 2001). Although these differences were observed, the levels of superoxide production obtained with the EFs.gp91s construct in both assays were high enough to ensure a stable follow-through of the disease. Therefore further investigations using *ex vivo* and *in vivo* models were performed with this promoter.

The EFs promoter-containing vector reached up to 85% $gp91^{phox}$ positive cells within the Sca-1^+ subpopulation when mouse Lin^{Neg} sorted cells were transduced with a final MOI of 3 (Fig. 50). When the gene transfer efficiency was related to the copy number of integrated proviruses, up to 45.7% positive cells were detected following transduction of mouse Sca-1^+ cells using the same final MOI (Fig. 47). It remains to be tested whether the cell source influenced the gene transfer ratio, since the VCN in the Lin^{Neg} cells was not monitored after transduction. However, titers obtained with the SIN constructs were assessed following limiting dilution transduction of murine SC-1 fibroblasts, and although marrow stem cells were subjected to prestimulation, it might be assumed that the transduction of murine Sca-1^+ cells might be less efficient owing to their quiescence, as retroviral transduction requires that the target cells be cycling (Miller *et al.*, 1990). This idea was confirmed by the VCN analysis of the mSca-1^+ transduced cells, in which only 0.65 to 1.03 copies per cell could be monitored although a MOI of 3 was used (Table 2). Additionally, if it is assumed that the VCN per cell is similar for both assays (regardless of the cell source) the fact that the gene transfer efficiency in the mSca-1^+ sorted cells was investigated 24 hours after the last round of transduction might have lead to an underestimation of the gene transfer rate. Further data obtained with the NBT assay in CFUs showing similar ratio of transduction efficiencies for the mSca-1^+ cells and the Lin^{Neg} cells were consistent with the hypothesis that more time is required to achieve full transgene expression levels (Fig. 48).

When the changes in transgene expression were assessed slightly higher percentages, 1.4 ± 0.3-fold, of $gp91^{phox}$ expressing cells were detected after *ex vivo* myeloid differentiaion (Fig. 44a). In Sca-1^+ transplantation analyses the level of $gp91^{phox}$ expressing cells was almost identical in Sca-1^+ and Gr-1^+&$CD11b^+$ bone marrow subpopulations six weeks after transplantation, which decreased when maturation was completed (from 63%-84% in bone marrow to 6%-20% in peripheral blood of two mice) (Fig. 49a and b). Moreover, in Lin^{Neg} transplantation experiments the transgene expression level measured in Sca-1^+ *ex vivo* transduced cells decreased after differentiation into myeloid bone marrow derivatives (Fig. 51a). Then 50% of the mice

experienced an increase and in the other half a decrease was observed after differentiation into myeloid peripheral blood cells (Fig. 51b). It is clear that the engraftment potential of each individual transduced stem cell is different, due to the natural- or retroviral vector-mediated fitness (Baum, 2007a). This might explain the differences in the patterns of transgene expression from engrafted stem cells to myeloid precursors and those from *ex vivo* transduced Sca-1^+ cells to myeloid marrow derivatives.

When the performance of the EFs.gp91s construct was assessed *in vivo* in marrow B lymphoid cells the level of $gp91^{phox}$ positive cells was lower than in granulocytic and stem cell marrow subpopulations in the two mSca-1^+ transplanted mice (Fig. 49a). In contrast mice transplanted with transduced Lin^{Neg} cells showed low and constant levels of $gp91^{phox}$ positive cells (between 10-25%) regardless of the expression in granulocytes (Fig. 51a). Moreover, there was no correlation in the change of expression towards maturation of B lymphocytes, since for the mSca-1^+ experiments a decrease and for the Lin^{Neg} transplantations a increase in percentage of $gp91^{phox}$ expressing cells was detected (Fig. 49b and Fig. 51b).

Although the EF-1alpha promoter has been shown to be expressed in almost all kinds of mammalian cells in a constitutively manner, the results obtained in this study show that short, intron-deleted EFs promoter did not confirm a constant and constitutive transgene expression in the different lineages analyzed (Mizushima and Nagata, 1990).

Despite this discrepancy, the reconstitution of the oxidase activity in pimary mouse transduced cells was assessed. In two of the three experiments the *ex vivo* differentiated cells did not reached 20% DHR positive cells compared to the wild-type cells although 22% and 40% $gp91^{phox}$ positive Gr-1^+ & $CD11b^+$ cells were detected (Fig. 44b and a). Correlation of these data with the results of the mouse Sca-1^+ transplantation experiment could not be assessed, since only one mouse could be analyzed with the DHR assay. In this mouse 50% of the cells were reactive to DHR, related to the wild type control, although only 7% of $gp91^{phox}$ positive peripheral blood granulocytes were detectable (Fig. 49b). The DHR assay performed in the Lin^{Neg} transplantation experiments was combined with Gr-1^+ & $CD11b^+$ immunostaining and in this case four out of eight EFs.gp91s mice reached about 40% DHR positive cells and six out of eight had values above 20% (Fig. 54). The *ex vivo* differentiation conditions or the limited number of assays in comparison to the *in vivo* experiments might explain the fact that higher numbers of DHR reactive cells were detected in the transplantation experiments. Mostly important, the numbers of superoxide producing cells obtained by the *in vivo* studies with the EFs.gp91s construct were similar than those observed in the clinical X-CGD trial conducted by the groups of Dr. M. Grez and Prof. R. A. Seger (over 35% in one patient and ~15% in the second), which led to the eradication of therapy refractory infections (Ott *et al.*, 2006). Moreover, although the ΔMFI values obtained in

the DHR assay of gene-modified granulocytes from Lin^{Neg} transplanted mice were constantly lower than those of wild-type granulocytes (about 5-fold) (Fig. 55), previous studies showed that about 20% of gene-corrected neutrophils (which have commonly lower superoxide production levels than wild-type neutrophils) is the critical threshold required to reduce infectious complications of CGD (Bu-Ghanim *et al.*, 1995; Goebel and Dinauer, 2002).

Overall, the data obtained with the EFs.gp91s construct suggest that this construct might represent a good candidate for gene therapy of CGD.

D.3.4 Targeting of SIN gammaretroviral vectors

D.3.4.1 The SP146 promoter

$Gp91^{phox}$ is primary required in granulocytes and it is still unknown if the ectopic expression of the protein can cause side effects. Therefore, the development of transcriptional targeting vectors was one of the main goals of the present study. In the present study, three different myeloid-specific promoters were tested in combination with the improved SIN vector backbone and the synthetic $gp91^{phox}$ sequence.

The SP146 promoter is a synthetic promoter constructed by random ligation of several short sequences identified as binding sites for myeloid/macrophage transcription factors, such as C/EBPα, AML-1, PU.1A, PU1B, SP1 and AP1 (Fig. 35b and c) (He *et al.*, 2006). The SP146 was selected from a pool of sequences because it showed clear myeloid/macrophage specificity in cell lines as well as *in vivo* mouse studies. This artificial promoter also showed a high efficiency in transgene expression when incorporated upstream of GFP in a lentiviral backbone.

When the SF promoter was replaced by the SP146 in the SERS11.SF.gp91s.Wm construct, a decrease in retroviral particle production was also observed. In contrast to the EFs promoter, this loss in titer was not due to a decrease in the proviral particle production, since the Northern blot analysis of transfected cells revealed even higher amounts of genomic RNA than those obtained by the SF-containing construct (Fig. 36a and b). In order to assess the presence of proviral integrations in transduced cells, Southern Blotting analysis was performed and two fragments corresponding to proviral genomes were detected. One of the bands had the expected size corresponding to the genomic viral RNA (Fig. 37b). The second band was smaller and it was expected to be an integrated provirus without the ability to express $gp91^{phox}$ leading to the reduction in titer. To investigate this hypothesis a Southern blot analysis of the genomic DNA from sorted transduced cells (93% expressing cells) was performed (Fig. 38) and, surprisingly, this band still appeared indicating that it was the genome form of an integrative vector, which may also contain and express the $gp91^{phox}$ gene (Fig. 39c). This suggests that a recombination or rearrangement event occurred most likely during

the viral particle production or during reverse transcription. Moreover, since the promoter was based on the ligation of several motifs, a loop may have formed by the binding of two identical sequences responsible for the loss of a part of the sequence overlooked by the polymerases. This event did not affect the functionality of the promoter since $gp91^{phox}$ expression was detected in transduced cells having also the proper transcript size (Fig. 40a). Nevertheless, this event is an uncontrolled process, which might cause unpredictable side effects. Although having an efficient transgene expression reaching equal or even higher levels than the SF construct, both in RNA and protein from cell lines, this promoter cannot be used for gene therapy vectors.

D.3.4.2 The c-fes promoter

To achieve transcriptional targeting also the c-fes promoter, which has been described above, was used. It was cloned in the SERS11.SF.gp91s.Wm substituting the SF promoter. When tested this myeloid-specific promoter in X-CGD PLB-985 cells it showed encouraging results. It reached the highest titer compared to all the non-viral promoters, and it showed one of the highest amounts of genomic transcript as assessed by Northern blotting analysis of transfected cells (Fig. 36a and b). Moreover, the internal transcript was undetectable in transfected cells which might be due to a high tissue-specific transcription or a weak transcriptional activity of the c-fes promoter, thereby favoring the transcription from the LTR promoter and thus the generation of higher titers. This hypothesis was confirmed by Northern and Western blot analyses of sorted transduced cell populations (Fig. 40a and b). These analyses revealed rather low amounts of internal transcript and protein, respectively. When comparing differentiated sorted populations transduced with the c-fes- and SF-containing constructs 2.1-, 1.4- and 1.3-fold lower levels of RNA, protein and ΔMFI were observed, respectively. All these data followed the same tendency confirming the low transcriptional activity of the c-fes promoter. Nevertheless, cytochrome c assays revealed that the c-fes containing construct drove efficient transgene expression when transduced in X-CGD PLB-985 cells. Superoxide production reached levels that went even beyond those obtained with the SF promoter (Fig. 41). In contrast, the superoxide production levels of each individual cell as indicated by the ΔMFI in the DHR assay showed a 1.6- and 1.4-fold decrease when compared to the PLB-985 and SF transduced cells, respectively (Fig. 42). The cause for the observed differences in superoxide production measured with the two methods have been already mentioned (D.3.3 The EFs promoter).

The c-fes construct reached transduction efficiencies up to 89% when assessed 4 days post transduction within the mSca-1^+ subpopulation of Lin^{Neg} transduced cells and up to 85% as assayed by NBT test in the CFUs derived from mSca-1^+ transduced cells both with a final MOI of 3 (Fig. 50 and Fig. 48). These data correlated with previous studies showing abundant expression of the c-fes protein in undifferentiated progenitors (Care *et al.*, 1994).

When *ex vivo* myeloid differentiation was induced a 1.3 ± 0.1-fold increase in transgene expression was observed whereas in the sorted mSca-1$^+$ *in vivo* assays the situation was inversed (Fig. 44a and Fig. 49). A slight decrease in gp91^{phox} expression was found if stem cells were differentiated towards myeloid precursor and then to granulocytes. Furthermore, the expression pattern of this construct in Lin^{Neg} transplanted mice was the same as for the EFs.gp91s construct. The levels of transgene expression decreased from *ex vivo* transduced cells to myeloid marrow derivatives and then experienced a huge variability in peripheral blood granulocytes of the individual mice. Half the mice showed an increase in transgene expression and the other half a decrease (Fig. 51).

A tissue-specific expression of the c-fes promoter was assessed in the mSca-1$^+$ transplanted mice, a decrease of gp91^{phox} positive cells was detected from bone marrow Sca-1$^+$ cells towards the B lymphoid precursos cells (2.3 ± 0.2-fold) (Fig. 49a). However, this tendency was not followed in the peripheral B lymphocytes. Here 50% of the mice experienced an increase and in the other half a decrease was observed after differentiation into peripheral blood B lymphocytes (Fig. 49b). Additionally, these data were not consistent with those of Lin^{Neg} transplanted mice where an increase in transgene expression towards B lymphocyte differentiation was also observed in seven out of eight mice (Fig. 51). These observations did not correlate with previous studies showing lower or even absent levels of c-fes expression in B-cell lines from the bone marrow (Heydemann *et al.*, 2000). It might be due to the lack of additional genomic sequences that may play a role in the control of the c-fes expression, such as the 2495 bp of Locus Control Region sequence.

Interestingly, the behavior of the c-fes promoter was extremely encouraging when functionally tested in mouse primary cells since it reached the higher levels of superoxide producing cells than the EFs promoter regardless of the assay. In *ex vivo* functional assays, one fifth of the cells were DHR positive while gp91^{phox} expressing granulocyte-like cells ranged from 20 to 42% (Fig. 44a and b). Furthermore, in transplanted mSca-1$^+$ mice up to 70% DHR reactive cells compared to the wild-type mice were detected although only 35% gp91^{phox} positive granulocytes in the peripheral blood (Fig. 49b). In mice transplanted with transduced Lin^{Neg} cells, where the DHR assay was combined with the Gr-1$^+$ & CD11b$^+$ immunostaining, 6 out 8 eight mice reached 40% DHR positive cells although slightly lower ΔMFI values were obtained compared to the EFs.gp91s construct (Fig. 54 and Fig. 55).

All these data indicate that the c-fes-containing construct might be a good choice for the development of an X-CGD gene therapy vector. It showed the highest titer production between all non-viral tested promoters, it reached high enough levels of transgene expression and, when compared to the EFs promoter, it performed slightly better in all funcional assays in mouse primary cells.

D.3.4.3 The MRP8 promoter

A third promoter tested for transgene expression was the MRP8 promoter. In this construct a sequence of about 1700 bp of the upstream regulatory regions of the MRP8 gene (Fig. 35a), including the first exon and intron, were cloned (Lagasse and Clerc, 1988). This version of the MRP8 promoter showed efficient and myeloid-specific transgene expression in previous mouse leukemia models as mentioned above (Lagasse and Weissman, 1994; Yuan *et al.*, 2001).

This promoter showed the lowest titer of all tested vectors although one of the highest levels of genomic RNA was detected in the packaging cells (Fig. 36a and b). This suggests that there was no competition between the internal and LTR promoter in producer cells, but might point out a lack in translation or a packaging problem being responsible for the lower titer. Additionally, the transcript detected in the Northern blot assay corresponded to the unspliced RNA form. This can be explained by the fact that this splicing should be a myeloid-restricted event which cannot occur in the transfected 293T cells, a human embryonic kidney cell line. The cell-specific splicing is a common phenomenon which has shown to help regulating the expression of cellular genes (Black, 2003). In molecular assays the MRP8 promoter showed to be transcriptionally weaker when compared to the SF regulatory sequence, since 1.8-fold less $gp91^{phox}$ transcript amounts were detected in the differentiated population (Fig. 40a). This tendency also corresponded to a 2.4- and 1.6-fold lower level of $gp91^{phox}$ protein and ΔMFI values, respectively (Fig. 40b and Fig. 38). Since the expression levels of the endogenous MRP8 gene have shown to be extremely high in neutrophil and monocyte lineages (representing up to 45% of neutrophil cytosolic proteins (Edgeworth *et al.*, 1991; Hessian *et al.*, 1993)) the results of the present study might indicate that possibly still additional sequences are required to achieve higher transcriptional rates. Nevertheless, this construct showed the highest levels of superoxide production in sorted cells as assessed by the cytochrome c assay, and slightly lower levels, 1.6-fold less, ΔMFI in the DHR assay compared to the SF promoter (Fig. 41 and Fig. 42).

The performance of the MRP8 construct was then addressed in murine primary $Sca\text{-}1^{+}$ cells. A markedly low expression of the transgene (17% $gp91^{phox}$ positive cells per copy of integrated provirus (Fig. 47)) was observed one day post transduction. It also showed the lowest levels of transgene expressing cells when measured within the $Sca\text{-}1^{+}$ subpopulation 4 days post transduction of Lin^{Neg} cells, although reaching up to 72% of positive $gp91^{phox}$ cells (Fig. 50). The functional reconstitution of the NADPH oxidase activity assessed by the NBT assay in CFUs derived from $mSca\text{-}1^{+}$ transduced cells showed up to 63% NBT^{+} colonies representing a 3.7-fold increase (Fig. 48). These higher levels might be explained by the higher specificity of the MRP8 promoter than the previously tested promoters. However, when the $gp91^{phox}$ expression was investigated after *ex vivo* myeloid differentiation an extremely low increase (1.2-fold)

was observed, even lower than the increase obtained by the EFs promoter (Fig. 44a). When analyzed in the *in vivo* context of mSca-1$^+$ transplanted mice, a slight decrease was observed after maturation towards myeloid common precursors, and even lower levels of gp91^{phox} were detected in the granulocytic population of the peripheral blood (Fig. 49). This decrease in expression towards maturation to peripheral granulocytes was not observed in the Lin^{Neg} transplanted mice (Fig. 51). Instead of a decrease, an increase was detected although the rather low levels of gp91^{phox} positive cells were maintained. These observations were not consistent with the previous published data showing that the MRP8 protein reached up to 45% of the cytosolic protein content in neutrophils (Edgeworth *et al.*, 1991; Hessian *et al.*, 1993). As expected, in the lymphoid populations the MRP8 promoter was turned off and consequently the gp91^{phox} protein was undetectable in B and T lymphocytes of the peripheral blood both in mSca-1$^+$ and Lin^{Neg} recipients (Fig. 49 and Fig. 51).

Ex vivo functional assays revealed similar levels of DHR positive cells for the MRP8 promoter than compared to the c-fes construct, but showing slightly lower values of gp91^{phox} expressing cells (Fig. 44b). Moreover, when assessed in peripheral blood granulocytes of mSca-1$^+$ transplanted mice, the MRP8 construct showed surprising high levels of superoxide generating cells, up to 2-fold of the wild-type mice regardless of the lowest percentages of gp91^{phox} positive granulocytes (Fig. 49b). On the contrary, in the Lin^{Neg} transplanted mice only two mice reached values over 40% of DHR reactive cells and the ΔMFI values were highly variable between the mice (from 3- to 6-fold lower than those of wild-type granulocytes) (Fig. 54 and Fig. 55).

With all these results, it can be concluded that despite of the high myeloid specificity of the MRP8 promoter, which might represent a great advantaje for a myeloid cell defect, this construct was less effective in restoring the NADPH oxidase activity than the EFs and c-fes promoters, which is one of the most important aspects for the gene therapy of CGD.

D.4 Conclusions

The EFs and c-fes promoters showed the highest values of superoxide production reconstitution, although on the other hand a constitutive, non tissue-specific transcriptional activity was observed. The c-fes promoter showed the highest values in functional assays but also the expressed in differentiated cell of other lineages than the myeloid. Furthermore, these data were consistent with additional tests performed in repopulating human CD34$^+$ cells transduced with these vectors. In the cytochrome c assay the c-fes promoter almost mimicked the activity observed in wild-type cells, the EFs reached intermediate values whereas the MRP8 promoter showed the lowest superoxide production levels among all (Dr. M. Grez, pers. commun.).

Overall, these data showed that with the novel SIN gammaretroviral vectors constructed in the present study fulfill two crucial points in vector development bringing the clinical application of such vector closer. The constructs are able to generate high titers and to drive efficient transgene expression reaching at least the minimal therapeutic threshold levels of superoxide require to reduce or even avoid the occurrence of recurrent infections.

Between all constructs tested, the c-fes containing construct in combination with the codon optimized $gp91^{phox}$ sequence showed the best performance within the SIN gammaretroviral backbone. It generated the highest titers in combination with a better NADPH oxidase reconstituting ability.

One main goal in the development of SIN gammaretroviral vectors is reducing the genotoxic effect due to random vector integration. An improved gene transfer and expression, and a constant performance are also highly desirable. The present study shows that the SERS11.fes.gp91s.W construct may be considered as an effective gene therapy strategy for the restoration of the NADPH oxidase activity in CGD. It allows the use of a cellular promoter generating adequate physiological levels of the therapeutic protein and reduces the number of vector copies required for a therapeutic benefit.

E. BIBLIOGRAPHY

AHLIN, A., LARFARS, G., ELINDER, G., PALMBLAD, J., and GYLLENHAMMAR, H. (1999). Gamma interferon treatment of patients with chronic granulomatous disease is associated with augmented production of nitric oxide by polymorphonuclear neutrophils. Clin Diagn Lab Immunol **6**, 420-424.

AILLES, L.E., and NALDINI, L. (2002). HIV-1-derived lentiviral vectors. Curr Top Microbiol Immunol **261**, 31-52.

AIUTI, A., SLAVIN, S., AKER, M., FICARA, F., DEOLA, S., MORTELLARO, A., MORECKI, S., ANDOLFI, G., TABUCCHI, A., CARLUCCI, F., MARINELLO, E., CATTANEO, F., VAI, S., SERVIDA, P., MINIERO, R., RONCAROLO, M.G., and BORDIGNON, C. (2002). Correction of ADA-SCID by stem cell gene therapy combined with nonmyeloablative conditioning. Science **296**, 2410-2413.

AKKINA, R.K., WALTON, R.M., CHEN, M.L., LI, Q.X., PLANELLES, V., and CHEN, I.S. (1996). High-efficiency gene transfer into CD34+ cells with a human immunodeficiency virus type 1-based retroviral vector pseudotyped with vesicular stomatitis virus envelope glycoprotein G. J Virol **70**, 2581-2585.

ALBA, R., HEARING, P., BOSCH, A., and CHILLON, M. (2007). Differential amplification of adenovirus vectors by flanking the packaging signal with attB/attP-PhiC31 sequences: Implications for helper-dependent adenovirus production. Virology **doi:10.1016/j.virol.2007.05.014**.

ALMARZA, E., RIO, P., MEZA, N.W., ALDEA, M., AGIRRE, X., GUENECHEA, G., SEGOVIA, J.C., and BUEREN, J.A. (2007). Characteristics of Lentiviral Vectors Harboring the Proximal Promoter of the vav Proto-oncogene: A Weak and Efficient Promoter for Gene Therapy. Mol Ther **15**, 1487-1494.

ASSARI, T. (2006). Chronic Granulomatous Disease; fundamental stages in our understanding of CGD. Medical Immunology **5**, 4.

BARESE, C., and GOEBEL, W.S. (2006). Chronic granulomatous disease in childhood. Current Pediatric Reviews **2**, 63-75.

BARESE, C.N., GOEBEL, W.S., and DINAUER, M.C. (2004). Gene therapy for chronic granulomatous disease. Expert Opin Biol Ther **4**, 1423-1434.

BAUER, T.R., JR., MILLER, A.D., and HICKSTEIN, D.D. (1995). Improved transfer of the leukocyte integrin CD18 subunit into hematopoietic cell lines by using retroviral vectors having a gibbon ape leukemia virus envelope. Blood **86**, 2379-2387.

BAUM, C. (2007a). Insertional mutagenesis in gene therapy and stem cell biology. Curr Opin Hematol **14**, 337-342.

BAUM, C. (2007b). What are the consequences of the fourth case? Mol Ther **15**, 1401-1402.

BAUM, C., VON KALLE, C., STAAL, F.J., LI, Z., FEHSE, B., SCHMIDT, M., WEERKAMP, F., KARLSSON, S., WAGEMAKER, G., and WILLIAMS, D.A. (2004). Chance or necessity? Insertional mutagenesis in gene therapy and its consequences. Mol Ther **9**, 5-13.

BECKER, S., WASSER, S., HAUSES, M., HOSSLE, J.P., OTT, M.G., DINAUER, M.C., GANSER, A., HOELZER, D., SEGER, R., and GREZ, M. (1998). Correction of respiratory burst activity in X-linked chronic granulomatous cells to therapeutically relevant levels after gene transfer into bone marrow CD34+ cells. Hum Gene Ther **9**, 1561-1570.

BERTHIER, S., PACLET, M.H., LEROUGE, S., ROUX, F., VERGNAUD, S., COLEMAN, A.W., and MOREL, F. (2003). Changing the conformation state of cytochrome b558 initiates NADPH oxidase activation: MRP8/MRP14 regulation. J Biol Chem **278**, 25499-25508.

BIBERSTINE-KINKADE, K.J., DELEO, F.R., EPSTEIN, R.I., LEROY, B.A., NAUSEEF, W.M., and DINAUER, M.C. (2001). Heme-ligating histidines in flavocytochrome b(558): identification of specific histidines in gp91(phox). J Biol Chem **276**, 31105-31112.

BIBERSTINE-KINKADE, K.J., YU, L., STULL, N., LEROY, B., BENNETT, S., CROSS, A., and DINAUER, M.C. (2002). Mutagenesis of p22(phox) histidine 94. A histidine in this position is not required for flavocytochrome b558 function. J Biol Chem **277**, 30368-30374.

BLACK, D.L. (2003). Mechanisms of alternative pre-messenger RNA splicing. Annu Rev Biochem **72**, 291-336.

BLAESE, R.M., CULVER, K.W., MILLER, A.D., CARTER, C.S., FLEISHER, T., CLERICI, M., SHEARER, G., CHANG, L., CHIANG, Y., TOLSTOSHEV, P., GREENBLATT, J.J., ROSENBERG, S.A., KLEIN, H., BERGER, M., MULLEN, C.A., RAMSEY, W.J., MUUL, L., MORGAN, R.A., and ANDERSON, W.F. (1995). T lymphocyte-directed gene therapy for ADA- SCID: initial trial results after 4 years. Science **270**, 475-480.

BORREGAARD, N., HEIPLE, J.M., SIMONS, E.R., and CLARK, R.A. (1983). Subcellular localization of the b-cytochrome component of the human neutrophil microbicidal oxidase: translocation during activation. J Cell Biol **97**, 52-61.

BOUARD, D., SANDRIN, V., BOSON, B., NEGRE, D., THOMAS, G., GRANIER, C., and COSSET, F.L. (2007). An acidic cluster of the cytoplasmic tail of the RD114 virus glycoprotein controls assembly of retroviral envelopes. Traffic **8**, 835-847.

BRAY, M., PRASAD, S., DUBAY, J.W., HUNTER, E., JEANG, K.T., REKOSH, D., and HAMMARSKJOLD, M.L. (1994). A small element from the Mason-Pfizer monkey virus genome makes human immunodeficiency virus type 1 expression and replication Rev-independent. Proc Natl Acad Sci U S A **91**, 1256-1260.

BRENNER, S., WHITING-THEOBALD, N.L., LINTON, G.F., HOLMES, K.L., ANDERSON-COHEN, M., KELLY, P.F., VANIN, E.F., PILON, A.M., BODINE, D.M., HORWITZ, M.E., and MALECH, H.L. (2003). Concentrated RD114-pseudotyped MFGS-gp91phox vector achieves high levels of functional correction of the chronic granulomatous disease oxidase defect in NOD/SCID/beta -microglobulin-/- repopulating mobilized human peripheral blood CD34+ cells. Blood **102**, 2789-2797.

BRIDGES, R.A., BERENDES, H., and GOOD, R.A. (1959). A fatal granulomatous disease of childhood; the clinical, pathological, and laboratory features of a new syndrome. AMA Journal of Diseases of Children **97**, 387-408.

BU-GHANIM, H.N., SEGAL, A.W., KEEP, N.H., and CASIMIR, C.M. (1995). Molecular analysis in three cases of X91- variant chronic granulomatous disease. Blood **86**, 3575-3582.

BUNNELL, B.A., MUUL, L.M., DONAHUE, R.E., BLAESE, R.M., and MORGAN, R.A. (1995). High-efficiency retroviral-mediated gene transfer into human and nonhuman primate peripheral blood lymphocytes. Proc Natl Acad Sci U S A **92**, 7739-7743.

CALE, C.M., JONES, A.M., and GOLDBLATT, D. (2000). Follow up of patients with chronic granulomatous disease diagnosed since 1990. Clin Exp Immunol **120**, 351-355.

CALMELS, B., FERGUSON, C., LAUKKANEN, M.O., ADLER, R., FAULHABER, M., KIM, H.J., SELLERS, S., HEMATTI, P., SCHMIDT, M., VON KALLE, C., AKAGI, K., DONAHUE, R.E., and DUNBAR, C.E. (2005). Recurrent retroviral vector integration at the Mds1/Evi1 locus in nonhuman primate hematopoietic cells. Blood **106**, 2530-2533.

CARE, A., MATTIA, G., MONTESORO, E., PAROLINI, I., RUSSO, G., COLOMBO, M.P., and PESCHLE, C. (1994). c-fes expression in ontogenetic development and hematopoietic differentiation. Oncogene **9**, 739-747.

CARLSON, A., BERKOWITZ, J.M., BROWNING, D., SLAMON, D.J., GASSON, J.C., and YATES, K.E. (2005). Expression of c-Fes protein isoforms correlates with differentiation in myeloid leukemias. DNA Cell Biol **24**, 311-316.

CAVAZZANA-CALVO, M., HACEIN-BEY, S., DE SAINT BASILE, G., GROSS, F., YVON, E., NUSBAUM, P., SELZ, F., HUE, C., CERTAIN, S., CASANOVA, J.L., BOUSSO, P., DEIST, F.L., and FISCHER, A. (2000). Gene therapy of human severe combined immunodeficiency (SCID)-X1 disease. Science **288**, 669-672.

CHANG, D.D., and SHARP, P.A. (1989). Regulation by HIV Rev depends upon recognition of splice sites. Cell **59**, 789-795.

CHANOCK, S.J., FAUST, L.R., BARRETT, D., CHRISTENSEN, B., NEWBURGER, P.E., and BABIOR, B.M. (1996). Partial reconstitution of the respiratory burst oxidase in lymphoblastoid B cell lines lacking p67-phox after transfection with an expression vector containing wild-type and mutant p67 -phox cDNAs: Deletions of the carboxy and amino terminal residues of p67-phox are not required for activity. Exp Hematol **24**, 531-536.

CHOI, V.W., MCCARTY, D.M., and SAMULSKI, R.J. (2006). Host cell DNA repair pathways in adeno-associated viral genome processing. J Virol **80**, 10346-10356.

CHRISTODOULOPOULOS, I., and CANNON, P.M. (2001). Sequences in the cytoplasmic tail of the gibbon ape leukemia virus envelope protein that prevent its incorporation into lentivirus vectors. J Virol **75**, 4129-4138.

CHUAH, M.K. (2005). Cutting through the obstacles and resurrecting the promise of gene therapy. IDrugs **8**, 818-821.

COFFIN, J.M. (1992). Retroviral DNA integration. Dev Biol Stand **76**, 141-151.

COFFIN, J.M., HUGHES, S.H., and VARMUS, H.E. (1997). Retroviruses. In C.S.H.L. Press, ed.

CORNETTA, K., and ANDERSON, W.F. (1989). Protamine sulfate as an effective alternative to polybrene in retroviral-mediated gene-transfer: implications for human gene therapy. J Virol Methods **23**, 187-194.

CRONIN, J., ZHANG, X.Y., and REISER, J. (2005). Altering the tropism of lentiviral vectors through pseudotyping. Curr Gene Ther **5**, 387-398.

CROSS, A.R., RAE, J., and CURNUTTE, J.T. (1995). Cytochrome b-245 of the neutrophil superoxide-generating system contains two nonidentical hemes. Potentiometric studies of a mutant form of gp91phox. J Biol Chem **270**, 17075-17077.

CROSS, A.R., and SEGAL, A.W. (2004). The NADPH oxidase of professional phagocytes--prototype of the NOX electron transport chain systems. Biochim Biophys Acta **1657**, 1-22.

CUBITT, A.B., HEIM, R., ADAMS, S.R., BOYD, A.E., GROSS, L.A., and TSIEN, R.Y. (1995). Understanding, improving and using green fluorescent proteins. Trends Biochem Sci **20**, 448-455.

DAI, C., MCANINCH, R.E., and SUTTON, R.E. (2004). Identification of synthetic endothelial cell-specific promoters by use of a high-throughput screen. J Virol **78**, 6209-6221.

DAI, Y., SCHWARZ, E.M., GU, D., ZHANG, W.W., SARVETNICK, N., and VERMA, I.M. (1995). Cellular and humoral immune responses to adenoviral vectors containing factor IX gene: tolerization of factor IX and vector antigens allows for long-term expression. Proc Natl Acad Sci U S A **92**, 1401-1405.

DANG, P.M., JOHNSON, J.L., and BABIOR, B.M. (2000). Binding of nicotinamide adenine dinucleotide phosphate to the tetratricopeptide repeat domains at the N-terminus of p67PHOX, a subunit of the leukocyte nicotinamide adenine dinucleotide phosphate oxidase. Biochemistry **39**, 3069-3075.

DANG, P.M., MOREL, F., GOUGEROT-POCIDALO, M.A., and EL BENNA, J. (2003). Phosphorylation of the NADPH oxidase component p67(PHOX) by ERK2 and P38MAPK: selectivity of phosphorylated sites and existence of an intramolecular regulatory domain in the tetratricopeptide-rich region. Biochemistry **42**, 4520-4526.

DECOURSEY, T.E., and LIGETI, E. (2005). Regulation and termination of NADPH oxidase activity. Cell Mol Life Sci **62**, 2173-2193.

DEICHMANN, A., HACEIN-BEY-ABINA, S., SCHMIDT, M., GARRIGUE, A., BRUGMAN, M.H., HU, J., GLIMM, H., GYAPAY, G., PRUM, B., FRASER, C.C., FISCHER, N., SCHWARZWAELDER, K., SIEGLER, M.L., DE RIDDER, D., PIKE-OVERZET, K., HOWE, S.J., THRASHER, A.J., WAGEMAKER, G., ABEL, U., STAAL, F.J., DELABESSE, E., VILLEVAL, J.L., ARONOW, B., HUE, C., PRINZ, C., WISSLER, M., KLANKE, C., WEISSENBACH, J., ALEXANDER, I., FISCHER, A., VON KALLE, C., and CAVAZZANA-CALVO, M. (2007). Vector integration is nonrandom and clustered and influences the fate of lymphopoiesis in SCID-X1 gene therapy. J Clin Invest **117**, 2225-2232.

DI NUNZIO, F., PIOVANI, B., COSSET, F.L., MAVILIO, F., and STORNAIUOLO, A. (2007). Transduction of Human Hematopoietic Stem Cells by Lentiviral Vectors Pseudotyped with the RD114-TR Chimeric Envelope Glycoprotein. Hum Gene Ther.

DIAZ, R.M., EISEN, T., HART, I.R., and VILE, R.G. (1998). Exchange of viral promoter/enhancer elements with heterologous regulatory sequences generates targeted hybrid long terminal repeat vectors for gene therapy of melanoma. J Virol **72**, 789-795.

DICK, J.E. (2003). Stem cells: Self-renewal writ in blood. Nature **423**, 231-233.

DIEBOLD, B.A., and BOKOCH, G.M. (2001). Molecular basis for Rac2 regulation of phagocyte NADPH oxidase. Nat Immunol **2**, 211-215.

DINAUER, M.C., GIFFORD, M.A., PECH, N., LI, L.L., and EMSHWILLER, P. (2001). Variable correction of host defense following gene transfer and bone marrow transplantation in murine X-linked chronic granulomatous disease. Blood **97**, 3738-3745.

DING, C., KUME, A., BJORGVINSDOTTIR, H., HAWLEY, R.G., PECH, N., and DINAUER, M.C. (1996). High-level reconstitution of respiratory burst activity in a human X-linked chronic granulomatous disease (X-CGD) cell line and correction of murine X-CGD bone marrow cells by retroviral-mediated gene transfer of human gp91phox. Blood **88**, 1834-1840.

DISMUKE, D.J., and AIKEN, C. (2006). Evidence for a functional link between uncoating of the human immunodeficiency virus type 1 core and nuclear import of the viral preintegration complex. J Virol **80**, 3712-3720.

DOUGHERTY, J.P., and TEMIN, H.M. (1987). A promoterless retroviral vector indicates that there are sequences in U3 required for 3' RNA processing. Proc Natl Acad Sci U S A **84**, 1197-1201.

DOUSSIERE, J., BRANDOLIN, G., DERRIEN, V., and VIGNAIS, P.V. (1993). Critical assessment of the presence of an NADPH binding site on neutrophil cytochrome b558 by photoaffinity and immunochemical labeling. Biochemistry **32**, 8880-8887.

DUBRIDGE, R.B., TANG, P., HSIA, H.C., LEONG, P.M., MILLER, J.H., and CALOS, M.P. (1987). Analysis of mutation in human cells by using an Epstein-Barr virus shuttle system. Mol Cell Biol **7**, 379-387.

EDELSTEIN, M.L., ABEDI, M.R., WIXON, J., and EDELSTEIN, R.M. (2004). Gene therapy clinical trials worldwide 1989-2004-an overview. J Gene Med **6**, 597-602.

EDGEWORTH, J., GORMAN, M., BENNETT, R., FREEMONT, P., and HOGG, N. (1991). Identification of p8,14 as a highly abundant heterodimeric calcium binding protein complex of myeloid cells. J Biol Chem **266**, 7706-7713.

EVANS, C.H., GHIVIZZANI, S.C., OLIGINO, T.A., and ROBBINS, P.D. (2001). Future of adenoviruses in the gene therapy of arthritis. Arthritis Res **3**, 142-146.

EVANS, C.H., WHALEN, J.D., EVANS, C.H., GHIVIZZANI, S.C., and ROBBINS, P.D. (1998). Gene therapy in autoimmune diseases. Ann Rheum Dis **57**, 125-127.

EZEKOWITZ, R.A., DINAUER, M.C., JAFFE, H.S., ORKIN, S.H., and NEWBURGER, P.E. (1988). Partial correction of the phagocyte defect in patients with X-linked chronic granulomatous disease by subcutaneous interferon gamma. N Engl J Med **319**, 146-151.

FASSATI, A. (2006). HIV infection of non-dividing cells: a divisive problem. Retrovirology **3**, 74.

FASSATI, A., and GOFF, S.P. (2001). Characterization of intracellular reverse transcription complexes of human immunodeficiency virus type 1. J Virol **75**, 3626-3635.

FERRARI, G., SALVATORI, G., ROSSI, C., COSSU, G., and MAVILIO, F. (1995). A retroviral vector containing a muscle-specific enhancer drives gene expression only in differentiated muscle fibers. Hum Gene Ther **6**, 733-742.

FISCHER, A., HACEIN-BEY, S., LE DEIST, F., SOUDAIS, C., DI SANTO, J.P., DE SAINT BASILE, G., and CAVAZZANA-CALVO, M. (2000). Gene therapy of severe combined immunodeficiencies. Immunol Rev **178**, 13-20.

FONTAYNE, A., DANG, P.M., GOUGEROT-POCIDALO, M.A., and EL-BENNA, J. (2002). Phosphorylation of p47phox sites by PKC alpha, beta II, delta, and zeta: effect on binding to p22phox and on NADPH oxidase activation. Biochemistry **41**, 7743-7750.

FRESHNEY, R. (1987). *Culture of Animal Cells: A Manual of Basic Technique*. (New York).

GINSEL, L.A., ONDERWATER, J.J., FRANSEN, J.A., VERHOEVEN, A.J., and ROOS, D. (1990). Localization of the low-Mr subunit of cytochrome b558 in human blood phagocytes by immunoelectron microscopy. Blood **76**, 2105-2116.

GOEBEL, W.S., and DINAUER, M.C. (2002). Retroviral-mediated gene transfer and nonmyeloablative conditioning: studies in a murine X-linked chronic granulomatous disease model. J Pediatr Hematol Oncol **24**, 787-790.

GOFF, S.P. (2007). Host factors exploited by retroviruses. Nat Rev Microbiol **5**, 253-263.

GRAHAM, F.L., and VAN DER EB, A.J. (1973). A new technique for the assay of infectivity of human adenovirus 5 DNA. Virology **52**, 456-467.

GREER, P., MALTBY, V., ROSSANT, J., BERNSTEIN, A., and PAWSON, T. (1990). Myeloid expression of the human c-fps/fes proto-oncogene in transgenic mice. Mol Cell Biol **10**, 2521-2527.

GREZ, M., BECKER, S., SAULNIER, S., KNOSS, H., OTT, M.G., MAURER, A., DINAUER, M.C., HOELZER, D., SEGER, R., and HOSSLE, J.P. (2000). Gene therapy of chronic granulomatous disease. Bone Marrow Transplant **25 Suppl 2**, S99-104.

GRUTER, P., TABERNERO, C., VON KOBBE, C., SCHMITT, C., SAAVEDRA, C., BACHI, A., WILM, M., FELBER, B.K., and IZAURRALDE, E. (1998). TAP, the human homolog of Mex67p, mediates CTE-dependent RNA export from the nucleus. Mol Cell **1**, 649-659.

GUENECHEA, G., GAN, O.I., INAMITSU, T., DORRELL, C., PEREIRA, D.S., KELLY, M., NALDINI, L., and DICK, J.E. (2000). Transduction of human CD34+ CD38- bone marrow and cord blood-derived SCID-repopulating cells with third-generation lentiviral vectors. Mol Ther **1**, 566-573.

HAAS, D.L., CASE, S.S., CROOKS, G.M., and KOHN, D.B. (2000). Critical factors influencing stable transduction of human CD34(+) cells with HIV-1-derived lentiviral vectors. Mol Ther **2**, 71-80.

HACEIN-BEY-ABINA, S., VON KALLE, C., SCHMIDT, M., LE DEIST, F., WULFFRAAT, N., MCINTYRE, E., RADFORD, I., VILLEVAL, J.L., FRASER, C.C., CAVAZZANA-CALVO, M., and FISCHER, A. (2003a). A serious adverse event after successful gene therapy for X-linked severe combined immunodeficiency. N Engl J Med **348**, 255-256.

HACEIN-BEY-ABINA, S., VON KALLE, C., SCHMIDT, M., MCCORMACK, M.P., WULFFRAAT, N., LEBOULCH, P., LIM, A., OSBORNE, C.S., PAWLIUK, R., MORILLON, E., SORENSEN, R., FORSTER, A., FRASER, P., COHEN, J.I., DE SAINT BASILE, G., ALEXANDER, I., WINTERGERST, U., FREBOURG, T., AURIAS, A., STOPPA-LYONNET, D., ROMANA, S., RADFORD-WEISS, I., GROSS, F., VALENSI, F., DELABESSE, E., MACINTYRE, E., SIGAUX, F., SOULIER, J., LEIVA, L.E., WISSLER, M., PRINZ, C., RABBITTS, T.H., LE DEIST, F., FISCHER, A., and CAVAZZANA-CALVO, M. (2003b). LMO2-associated clonal T cell proliferation in two patients after gene therapy for SCID-X1. Science **302**, 415-419.

HADDAD, E., LANDAIS, P., FRIEDRICH, W., GERRITSEN, B., CAVAZZANA-CALVO, M., MORGAN, G., BERTRAND, Y., FASTH, A., PORTA, F., CANT, A., ESPANOL, T., MULLER, S., VEYS, P., VOSSEN, J., and FISCHER, A. (1998). Long-term immune reconstitution and outcome after HLA-nonidentical T-cell-depleted bone marrow transplantation for severe combined immunodeficiency: a European retrospective study of 116 patients. Blood **91**, 3646-3653.

HAIGH, J., MCVEIGH, J., and GREER, P. (1996). The fps/fes tyrosine kinase is expressed in myeloid, vascular endothelial, epithelial, and neuronal cells and is localized in the trans-golgi network. Cell Growth Differ **7**, 931-944.

HAMMOND, S.M., CRABLE, S.C., and ANDERSON, K.P. (2005). Negative regulatory elements are present in the human LMO2 oncogene and may contribute to its expression in leukemia. Leuk Res **29**, 89-97.

HANENBERG, H., XIAO, X.L., DILLOO, D., HASHINO, K., KATO, I., and WILLIAMS, D.A. (1996). Colocalization of retrovirus and target cells on specific fibronectin fragments increases genetic transduction of mammalian cells. Nat Med **2**, 876-882.

HARTLEY, J.W., and ROWE, W.P. (1975). Clonal cells lines from a feral mouse embryo which lack host-range restrictions for murine leukemia viruses. Virology **65**, 128-134.

HAWLEY, R.G., COVARRUBIAS, L., HAWLEY, T., and MINTZ, B. (1987). Handicapped retroviral vectors efficiently transduce foreign genes into hematopoietic stem cells. Proc Natl Acad Sci U S A **84**, 2406-2410.

HE, W., QIANG, M., MA, W., VALENTE, A.J., QUINONES, M.P., WANG, W., REDDICK, R.L., XIAO, Q., AHUJA, S.S., CLARK, R.A., FREEMAN, G.L., and LI, S. (2006). Development of a synthetic promoter for macrophage gene therapy. Hum Gene Ther **17**, 949-959.

HEARPS, A.C., and JANS, D.A. (2006). HIV-1 integrase is capable of targeting DNA to the nucleus via an importin alpha/beta-dependent mechanism. Biochem J **398**, 475-484.

HEIM, R., CUBITT, A.B., and TSIEN, R.Y. (1995). Improved green fluorescence. Nature **373**, 663-664.

HENDERSON, L.M., and CHAPPELL, J.B. (1993). Dihydrorhodamine 123: a fluorescent probe for superoxide generation? Eur J Biochem **217**, 973-980.

HENEINE, W., SWITZER, W.M., SANDSTROM, P., BROWN, J., VEDAPURI, S., SCHABLE, C.A., KHAN, A.S., LERCHE, N.W., SCHWEIZER, M., NEUMANN-HAEFELIN, D., CHAPMAN, L.E., and FOLKS, T.M. (1998). Identification of a human population infected with simian foamy viruses. Nat Med **4**, 403-407.

HESSIAN, P.A., EDGEWORTH, J., and HOGG, N. (1993). MRP-8 and MRP-14, two abundant Ca(2+)-binding proteins of neutrophils and monocytes. J Leukoc Biol **53**, 197-204.

HEYDEMANN, A., JUANG, G., HENNESSY, K., PARMACEK, M.S., and SIMON, M.C. (1996). The myeloid-cell-specific c-fes promoter is regulated by Sp1, PU.1, and a novel transcription factor. Mol Cell Biol **16**, 1676-1686.

HEYDEMANN, A., WARMING, S., CLENDENIN, C., SIGRIST, K., HJORTH, J.P., and SIMON, M.C. (2000). A minimal c-fes cassette directs myeloid-specific expression in transgenic mice. Blood **96**, 3040-3048.

HEYWORTH, P.G., CROSS, A.R., and CURNUTTE, J.T. (2003). Chronic granulomatous disease. Curr Opin Immunol **15**, 578-584.

HILDINGER, M., ABEL, K.L., OSTERTAG, W., and BAUM, C. (1999). Design of 5' untranslated sequences in retroviral vectors developed for medical use. J Virol **73**, 4083-4089.

HO, C.M., VOWELS, M.R., LOCKWOOD, L., and ZIEGLER, J.B. (1996). Successful bone marrow transplantation in a child with X-linked chronic granulomatous disease. Bone Marrow Transplant **18**, 213-215.

HOBBS, J.R., MONTEIL, M., MCCLUSKEY, D.R., JURGES, E., and EL TUMI, M. (1992). Chronic granulomatous disease 100% corrected by displacement bone marrow transplantation from a volunteer unrelated donor. Eur J Pediatr **151**, 806-810.

HOFFMAN, G.R., and CERIONE, R.A. (2001). Rac inserts its way into the immune response. Nat Immunol **2**, 194-196.

HOGGE, D.E., and HUMPHRIES, R.K. (1987). Gene transfer to primary normal and malignant human hemopoietic progenitors using recombinant retroviruses. Blood **69**, 611-617.

HOLMES, B., QUIE, P.G., WINDHORST, D.B., and GOOD, R.A. (1966). Fatal granulomatous disease of childhood. An inborn abnormality of phagocytic function. Lancet **1**, 1225-1228.

HUANG, Y., and CARMICHAEL, G.G. (1996). A suboptimal 5' splice site is a cis-acting determinant of nuclear export of polyomavirus late mRNAs. Mol Cell Biol **16**, 6046-6054.

ISHIBASHI, F., MIZUKAMI, T., KANEGASAKI, S., MOTODA, L., KAKINUMA, R., ENDO, F., and NUNOI, H. (2001). Improved superoxide-generating ability by interferon gamma due to splicing pattern change of transcripts in neutrophils from patients with a splice site mutation in CYBB gene. Blood **98**, 436-441.

ISLAM, M.R., FAN, C., FUJII, Y., HAO, L.J., SUZUKI, S., KUMATORI, A., YANG, D., RUSVAI, E., SUZUKI, N., KIKUCHI, H., and NAKAMURA, M. (2002). PU.1 is dominant and HAF-1 supplementary for activation of the gp91(phox) promoter in human monocytic PLB-985 cells. J Biochem (Tokyo) **131**, 533-540.

ITO, T., MATSUI, Y., AGO, T., OTA, K., and SUMIMOTO, H. (2001). Novel modular domain PB1 recognizes PC motif to mediate functional protein-protein interactions. Embo J **20**, 3938-3946.

JAGER, U., ZHAO, Y., and PORTER, C.D. (1999). Endothelial cell-specific transcriptional targeting from a hybrid long terminal repeat retrovirus vector containing human prepro-endothelin-1 promoter sequences. J Virol **73**, 9702-9709.

JAISWAL, S., TRAVER, D., MIYAMOTO, T., AKASHI, K., LAGASSE, E., and WEISSMAN, I.L. (2003). Expression of BCR/ABL and BCL-2 in myeloid progenitors leads to myeloid leukemias. Proc Natl Acad Sci U S A **100**, 10002-10007.

JANEWAY, C.A., CRAIG, I., DAVIDSON, M., DOWNEY, W., GITLIN, D., and SULLIVAN, J.C. (1954). Hypergammaglobulinemia associated with severe, recurrent and chronic non-specific infection. AMA Journal of Diseases of Children **88**, 388-392.

JIRAPONGSANANURUK, O., MALECH, H.L., KUHNS, D.B., NIEMELA, J.E., BROWN, M.R., ANDERSON-COHEN, M., and FLEISHER, T.A. (2003). Diagnostic paradigm for evaluation of male patients with chronic granulomatous disease, based on the dihydrorhodamine 123 assay. J Allergy Clin Immunol **111**, 374-379.

JOHNSTON, R.B., 3RD, HARBECK, R.J., and JOHNSTON, R.B., JR. (1985). Recurrent severe infections in a girl with apparently variable expression of mosaicism for chronic granulomatous disease. J Pediatr **106**, 50-55.

KAMANI, N., AUGUST, C.S., CAMPBELL, D.E., HASSAN, N.F., and DOUGLAS, S.D. (1988). Marrow transplantation in chronic granulomatous disease: an update, with 6-year follow-up. J Pediatr **113**, 697-700.

KANAI, F., LIU, H., FIELD, S.J., AKBARY, H., MATSUO, T., BROWN, G.E., CANTLEY, L.C., and YAFFE, M.B. (2001). The PX domains of p47phox and p40phox bind to lipid products of PI(3)K. Nat Cell Biol **3**, 675-678.

KANEDA, M., SAKURABA, H., OHTAKE, A., NISHIDA, A., KIRYU, C., and KAKINUMA, K. (1999). Missense mutations in the gp91-phox gene encoding cytochrome b558 in patients with cytochrome b positive and negative X-linked chronic granulomatous disease. Blood **93**, 2098-2104.

KANEKIYO, M., MATSUO, K., HAMATAKE, M., HAMANO, T., OHSU, T., MATSUMOTO, S., YAMADA, T., YAMAZAKI, S., HASEGAWA, A., YAMAMOTO, N., and HONDA, M. (2005). Mycobacterial codon optimization enhances antigen expression and virus-specific immune responses in recombinant Mycobacterium bovis bacille Calmette-Guerin expressing human immunodeficiency virus type 1 Gag. J Virol **79**, 8716-8723.

KATEN, L.J., JANUSZESKI, M.M., ANDERSON, W.F., HASENKRUG, K.J., and EVANS, L.H. (2001). Infectious entry by amphotropic as well as ecotropic murine leukemia viruses occurs through an endocytic pathway. J Virol **75**, 5018-5026.

KELLY, P.F., CARRINGTON, J., NATHWANI, A., and VANIN, E.F. (2001). RD114-pseudotyped oncoretroviral vectors. Biological and physical properties. Ann N Y Acad Sci **938**, 262-276; discussion 276-267.

KERKHOFF, C., KLEMPT, M., KAEVER, V., and SORG, C. (1999). The two calcium-binding proteins, S100A8 and S100A9, are involved in the metabolism of arachidonic acid in human neutrophils. J Biol Chem **274**, 32672-32679.

KIEM, H.P., ANDREWS, R.G., MORRIS, J., PETERSON, L., HEYWARD, S., ALLEN, J.M., RASKO, J.E., POTTER, J., and MILLER, A.D. (1998). Improved gene transfer into baboon marrow repopulating cells using recombinant human fibronectin fragment CH-296 in combination with interleukin-6, stem cell factor, FLT-3 ligand, and megakaryocyte growth and development factor. Blood **92**, 1878-1886.

KIM, H., LEE, H., and YUN, Y. (1998). X-gene product of hepatitis B virus induces apoptosis in liver cells. J Biol Chem **273**, 381-385.

KINGSMAN, S.M., MITROPHANOUS, K., and OLSEN, J.C. (2005). Potential oncogene activity of the woodchuck hepatitis post-transcriptional regulatory element (WPRE). Gene Ther **12**, 3-4.

KNAUS, U.G., MORRIS, S., DONG, H.J., CHERNOFF, J., and BOKOCH, G.M. (1995). Regulation of human leukocyte p21-activated kinases through G protein--coupled receptors. Science **269**, 221-223.

KOLOKOLTSOV, A.A., WEAVER, S.C., and DAVEY, R.A. (2005). Efficient functional pseudotyping of oncoretroviral and lentiviral vectors by Venezuelan equine encephalitis virus envelope proteins. J Virol **79**, 756-763.

KRAUNUS, J., SCHAUMANN, D.H., MEYER, J., MODLICH, U., FEHSE, B., BRANDENBURG, G., VON LAER, D., KLUMP, H., SCHAMBACH, A., BOHNE, J., and BAUM, C. (2004). Self-inactivating retroviral vectors with improved RNA processing. Gene Ther **11**, 1568-1578.

KRAUSE, R., PATRUTA, S., DAXBOCK, F., FLADERER, P., and WENISCH, C. (2001). The effect of fosfomycin on neutrophil function. J Antimicrob Chemother **47**, 141-146.

KUHLCKE, K., FEHSE, B., SCHILZ, A., LOGES, S., LINDEMANN, C., AYUK, F., LEHMANN, F., STUTE, N., FAUSER, A.A., ZANDER, A.R., and ECKERT, H.G. (2002). Highly efficient retroviral gene transfer based on centrifugation-mediated vector preloading of tissue culture vessels. Mol Ther **5**, 473-478.

KUMAR, M., and CARMICHAEL, G.G. (1998). Antisense RNA: function and fate of duplex RNA in cells of higher eukaryotes. Microbiol Mol Biol Rev **62**, 1415-1434.

KURIBAYASHI, F., NUNOI, H., WAKAMATSU, K., TSUNAWAKI, S., SATO, K., ITO, T., and SUMIMOTO, H. (2002). The adaptor protein p40(phox) as a positive regulator of the superoxide-producing phagocyte oxidase. Embo J **21**, 6312-6320.

KUSTIKOVA, O., FEHSE, B., MODLICH, U., YANG, M., DULLMANN, J., KAMINO, K., VON NEUHOFF, N., SCHLEGELBERGER, B., LI, Z., and BAUM, C. (2005). Clonal dominance of hematopoietic stem cells triggered by retroviral gene marking. Science **308**, 1171-1174.

KUSTIKOVA, O.S., WAHLERS, A., KUHLCKE, K., STAHLE, B., ZANDER, A.R., BAUM, C., and FEHSE, B. (2003). Dose finding with retroviral vectors: correlation of retroviral vector copy numbers in single cells with gene transfer efficiency in a cell population. Blood **102**, 3934-3937.

LAGASSE, E., and CLERC, R.G. (1988). Cloning and expression of two human genes encoding calcium-binding proteins that are regulated during myeloid differentiation. Mol Cell Biol **8**, 2402-2410.

LAGASSE, E., and WEISSMAN, I.L. (1994). bcl-2 inhibits apoptosis of neutrophils but not their engulfment by macrophages. J Exp Med **179**, 1047-1052.

LANDING, B.H., and SHIRKEY, H.S. (1957). A syndrome of recurrent infection and infiltration of viscera by pigmented lipid histiocytes. Pediatrics **20**, 431-438.

LAUFS, S., GENTNER, B., NAGY, K.Z., JAUCH, A., BENNER, A., NAUNDORF, S., KUEHLCKE, K., SCHIEDLMEIER, B., HO, A.D., ZELLER, W.J., and FRUEHAUF, S. (2003). Retroviral vector integration occurs in preferred genomic targets of human bone marrow-repopulating cells. Blood **101**, 2191-2198.

LAURENT, C.E., DELFINO, F.J., CHENG, H.Y., and SMITHGALL, T.E. (2004). The human c-Fes tyrosine kinase binds tubulin and microtubules through separate domains and promotes microtubule assembly. Mol Cell Biol **24**, 9351-9358.

LECHARDEUR, D., and LUKACS, G.L. (2002). Intracellular barriers to non-viral gene transfer. Curr Gene Ther **2**, 183-194.

LEGRAIN, P., and ROSBASH, M. (1989). Some cis- and trans-acting mutants for splicing target pre-mRNA to the cytoplasm. Cell **57**, 573-583.

LETO, T.L., ADAMS, A.G., and DE MENDEZ, I. (1994). Assembly of the phagocyte NADPH oxidase: binding of Src homology 3 domains to proline-rich targets. Proc Natl Acad Sci U S A **91**, 10650-10654.

LEWINSKI, M.K., YAMASHITA, M., EMERMAN, M., CIUFFI, A., MARSHALL, H., CRAWFORD, G., COLLINS, F., SHINN, P., LEIPZIG, J., HANNENHALLI, S., BERRY, C.C., ECKER, J.R., and BUSHMAN, F.D. (2006). Retroviral DNA integration: viral and cellular determinants of target-site selection. PLoS Pathog **2**, e60.

LI, Z., DULLMANN, J., SCHIEDLMEIER, B., SCHMIDT, M., VON KALLE, C., MEYER, J., FORSTER, M., STOCKING, C., WAHLERS, A., FRANK, O., OSTERTAG, W., KUHLCKE, K., ECKERT, H.G., FEHSE, B., and BAUM, C. (2002). Murine leukemia induced by retroviral gene marking. Science **296**, 497.

LI, Z., SCHWIEGER, M., LANGE, C., KRAUNUS, J., SUN, H., VAN DEN AKKER, E., MODLICH, U., SERINSOZ, E., WILL, E., VON LAER, D., STOCKING, C., FEHSE, B., SCHIEDLMEIER, B., and BAUM, C. (2003). Predictable and efficient retroviral gene transfer into murine bone marrow repopulating cells using a defined vector dose. Exp Hematol **31**, 1206-1214.

LIGHT, D.R., WALSH, C., O'CALLAGHAN, A.M., GOETZL, E.J., and TAUBER, A.I. (1981). Characteristics of the cofactor requirements for the superoxide-generating NADPH oxidase of human polymorphonuclear leukocytes. Biochemistry **20**, 1468-1476.

LUO, M.J., and REED, R. (1999). Splicing is required for rapid and efficient mRNA export in metazoans. Proc Natl Acad Sci U S A **96**, 14937-14942.

MALECH, H.L. (2000). Use of serum-free medium with fibronectin fragment enhanced transduction in a system of gas permeable plastic containers to achieve high levels of retrovirus transduction at clinical scale. Stem Cells **18**, 155-156.

MALECH, H.L., CHOI, U., and BRENNER, S. (2004). Progress toward effective gene therapy for chronic granulomatous disease. Jpn J Infect Dis **57**, S27-28.

MALECH, H.L., and HICKSTEIN, D.D. (2007). Genetics, biology and clinical management of myeloid cell primary immune deficiencies: chronic granulomatous disease and leukocyte adhesion deficiency. Curr Opin Hematol **14**, 29-36.

MALECH, H.L., MAPLES, P.B., WHITING-THEOBALD, N., LINTON, G.F., SEKHSARIA, S., VOWELLS, S.J., LI, F., MILLER, J.A., DECARLO, E., HOLLAND, S.M., LEITMAN, S.F., CARTER, C.S., BUTZ, R.E., READ, E.J., FLEISHER, T.A., SCHNEIDERMAN, R.D., VAN EPPS, D.E., SPRATT, S.K., MAACK, C.A., ROKOVICH, J.A., COHEN, L.K., and GALLIN, J.I. (1997). Prolonged production of NADPH oxidase-corrected granulocytes after gene therapy of chronic granulomatous disease. Proc Natl Acad Sci U S A **94**, 12133-12138.

MARDINEY, M., 3RD, JACKSON, S.H., SPRATT, S.K., LI, F., HOLLAND, S.M., and MALECH, H.L. (1997). Enhanced host defense after gene transfer in the murine p47phox-deficient model of chronic granulomatous disease. Blood **89**, 2268-2275.

MARKOWITZ, D., GOFF, S., and BANK, A. (1988). A safe packaging line for gene transfer: separating viral genes on two different plasmids. J Virol **62**, 1120-1124.

MARTYN, K.D., KIM, M.J., QUINN, M.T., DINAUER, M.C., and KNAUS, U.G. (2005). p21-activated kinase (Pak) regulates NADPH oxidase activation in human neutrophils. Blood **106**, 3962-3969.

MAUCH, L., LUN, A., O'GORMAN, M.R., HARRIS, J.S., SCHULZE, I., ZYCHLINSKY, A., FUCHS, T., OELSCHLAGEL, U., BRENNER, S., KUTTER, D., ROSEN-WOLFF, A., and ROESLER, J. (2007). Chronic granulomatous disease (CGD) and complete myeloperoxidase deficiency both yield strongly reduced dihydrorhodamine 123 test signals but can be easily discerned in routine testing for CGD. Clin Chem **53**, 890-896.

MAURICE, M., VERHOEYEN, E., SALMON, P., TRONO, D., RUSSELL, S.J., and COSSET, F.L. (2002). Efficient gene transfer into human primary blood lymphocytes by surface-engineered lentiviral vectors that display a T cell-activating polypeptide. Blood **99**, 2342-2350.

MAYO, L.A., and CURNUTTE, J.T. (1990). Kinetic microplate assay for superoxide production by neutrophils and other phagocytic cells. Methods Enzymol **186**, 567-575.

MCCARTY, D.M., YOUNG, S.M., JR., and SAMULSKI, R.J. (2004). Integration of adeno-associated virus (AAV) and recombinant AAV vectors. Annu Rev Genet **38**, 819-845.

MCCORMACK, M.P., FORSTER, A., DRYNAN, L., PANNELL, R., and RABBITTS, T.H. (2003). The LMO2 T-cell oncogene is activated via chromosomal translocations or retroviral insertion during gene therapy but has no mandatory role in normal T-cell development. Mol Cell Biol **23**, 9003-9013.

MELKONYAN, H., HOFMANN, H.A., NACKEN, W., SORG, C., and KLEMPT, M. (1998). The gene encoding the myeloid-related protein 14 (MRP14), a calcium-binding protein expressed in granulocytes and monocytes, contains a potent enhancer element in the first intron. J Biol Chem **273**, 27026-27032.

MILLER, A.D., and BUTTIMORE, C. (1986). Redesign of retrovirus packaging cell lines to avoid recombination leading to helper virus production. Mol Cell Biol **6**, 2895-2902.

MILLER, A.D., PALMER, T.D., and HOCK, R.A. (1986a). Transfer of genes into human somatic cells using retrovirus vectors. Cold Spring Harb Symp Quant Biol **51 Pt 2**, 1013-1019.

MILLER, A.D., TRAUBER, D.R., and BUTTIMORE, C. (1986b). Factors involved in production of helper virus-free retrovirus vectors. Somat Cell Mol Genet **12**, 175-183.

MILLER, D.G., ADAM, M.A., and MILLER, A.D. (1990). Gene transfer by retrovirus vectors occurs only in cells that are actively replicating at the time of infection. Mol Cell Biol **10**, 4239-4242.

MILLER, D.G., PETEK, L.M., and RUSSELL, D.W. (2004). Adeno-associated virus vectors integrate at chromosome breakage sites. Nat Genet **36**, 767-773.

MILLS, E.L., RHOLL, K.S., and QUIE, P.G. (1980). X-linked inheritance in females with chronic granulomatous disease. J Clin Invest **66**, 332-340.

MIURA, Y., WAKE, H., and KATO, T. (1999). TBE, or not TBE; that is the question. Nagoya Medical Journal **43**, 1-6.

MODLICH, U., BOHNE, J., SCHMIDT, M., VON KALLE, C., KNOSS, S., SCHAMBACH, A., and BAUM, C. (2006). Cell-culture assays reveal the importance of retroviral vector design for insertional genotoxicity. Blood **108**, 2545-2553.

MODLICH, U., KUSTIKOVA, O.S., SCHMIDT, M., RUDOLPH, C., MEYER, J., LI, Z., KAMINO, K., VON NEUHOFF, N., SCHLEGELBERGER, B., KUEHLCKE, K., BUNTING, K.D., SCHMIDT, S., DEICHMANN, A., VON KALLE, C., FEHSE, B., and BAUM, C. (2005). Leukemias following retroviral transfer of multidrug resistance 1 (MDR1) are driven by combinatorial insertional mutagenesis. Blood **105**, 4235-4246.

MOORE, K.A., SCARPA, M., KOOYER, S., UTTER, A., CASKEY, C.T., and BELMONT, J.W. (1991). Evaluation of lymphoid-specific enhancer addition or substitution in a basic retrovirus vector. Hum Gene Ther **2**, 307-315.

MORITZ, T., DUTT, P., XIAO, X., CARSTANJEN, D., VIK, T., HANENBERG, H., and WILLIAMS, D.A. (1996). Fibronectin improves transduction of reconstituting hematopoietic stem cells by retroviral vectors: evidence of direct viral binding to chymotryptic carboxy-terminal fragments. Blood **88**, 855-862.

MOTHES, W., BOERGER, A.L., NARAYAN, S., CUNNINGHAM, J.M., and YOUNG, J.A. (2000). Retroviral entry mediated by receptor priming and low pH triggering of an envelope glycoprotein. Cell **103**, 679-689.

MULLIGAN, R.C. (1993). The basic science of gene therapy. Science **260**, 926-932.

NAKAMURA, M., MURAKAMI, M., KOGA, T., TANAKA, Y., and MINAKAMI, S. (1987). Monoclonal antibody 7D5 raised to cytochrome b558 of human neutrophils: immunocytochemical detection of the antigen in peripheral phagocytes of normal subjects, patients with chronic granulomatous disease, and their carrier mothers. Blood **69**, 1404-1408.

NAKAMURA, R., SUMIMOTO, H., MIZUKI, K., HATA, K., AGO, T., KITAJIMA, S., TAKESHIGE, K., SAKAKI, Y., and ITO, T. (1998). The PC motif: a novel and evolutionarily conserved sequence involved in interaction between p40phox and p67phox, SH3 domain-containing cytosolic factors of the phagocyte NADPH oxidase. Eur J Biochem **251**, 583-589.

NAUSEEF, W.M. (2004). Assembly of the phagocyte NADPH oxidase. Histochem Cell Biol **122**, 277-291.

NEGRUTSKII, B.S., and EL'SKAYA, A.V. (1998). Eukaryotic translation elongation factor 1 alpha: structure, expression, functions, and possible role in aminoacyl-tRNA channeling. Prog Nucleic Acid Res Mol Biol **60**, 47-78.

NG, P., PARKS, R.J., CUMMINGS, D.T., EVELEGH, C.M., SANKAR, U., and GRAHAM, F.L. (1999). A high-efficiency Cre/loxP-based system for construction of adenoviral vectors. Hum Gene Ther **10**, 2667-2672.

O'CONNOR, T.P., and CRYSTAL, R.G. (2006). Genetic medicines: treatment strategies for hereditary disorders. Nat Rev Genet **7**, 261-276.

OTSU, M., ANDERSON, S.M., BODINE, D.M., PUCK, J.M., O'SHEA, J.J., and CANDOTTI, F. (2000). Lymphoid development and function in X-linked severe combined immunodeficiency mice after stem cell gene therapy. Mol Ther **1**, 145-153.

OTT, M.G., MERGET-MILLITZER, H., OTTMANN, O.G., MARTIN, H., BRUGGENOLTE, N., BIALEK, H., SEGER, R., HOSSLE, J.P., HOELZER, D., and GREZ, M. (2002). Mobilization and transduction of CD34(+) peripheral blood stem cells in patients with X-linked chronic granulomatous disease. J Hematother Stem Cell Res **11**, 683-694.

OTT, M.G., SCHMIDT, M., SCHWARZWAELDER, K., STEIN, S., SILER, U., KOEHL, U., GLIMM, H., KUHLCKE, K., SCHILZ, A., KUNKEL, H., NAUNDORF, S., BRINKMANN, A., DEICHMANN, A., FISCHER, M., BALL, C., PILZ, I., DUNBAR, C., DU, Y., JENKINS, N.A., COPELAND, N.G., LUTHI, U., HASSAN, M., THRASHER, A.J., HOELZER, D., VON KALLE, C., SEGER, R., and GREZ, M. (2006). Correction of X-linked chronic granulomatous disease by gene therapy, augmented by insertional activation of MDS1-EVI1, PRDM16 or SETBP1. Nat Med **12**, 401-409.

PACLET, M.H., BERTHIER, S., KUHN, L., GARIN, J., and MOREL, F. (2007). Regulation of phagocyte NADPH oxidase activity: identification of two cytochrome b558 activation states. Faseb J **21**, 1244-1255.

PARKOS, C.A., ALLEN, R.A., COCHRANE, C.G., and JESAITIS, A.J. (1987). Purified cytochrome b from human granulocyte plasma membrane is comprised of two polypeptides with relative molecular weights of 91,000 and 22,000. J Clin Invest **80**, 732-742.

PARKOS, C.A., DINAUER, M.C., JESAITIS, A.J., ORKIN, S.H., and CURNUTTE, J.T. (1989). Absence of both the 91kD and 22kD subunits of human neutrophil cytochrome b in two genetic forms of chronic granulomatous disease. Blood **73**, 1416-1420.

PATTERSON, S.S., DIONISI, H.M., GUPTA, R.K., and SAYLER, G.S. (2005). Codon optimization of bacterial luciferase (lux) for expression in mammalian cells. J Ind Microbiol Biotechnol **32**, 115-123.

PFEIFER, A., and VERMA, I.M. (2001). Gene therapy: promises and problems. Annu Rev Genomics Hum Genet **2**, 177-211.

PIKE-OVERZET, K., DE RIDDER, D., WEERKAMP, F., BAERT, M.R., VERSTEGEN, M.M., BRUGMAN, M.H., HOWE, S.J., REINDERS, M.J., THRASHER, A.J., WAGEMAKER, G., VAN DONGEN, J.J., and STAAL, F.J. (2007). Ectopic retroviral expression of LMO2, but not IL2Rgamma, blocks human T-cell development from CD34+ cells: implications for leukemogenesis in gene therapy. Leukemia **21**, 754-763.

POLLOCK, J.D., WILLIAMS, D.A., GIFFORD, M.A., LI, L.L., DU, X., FISHERMAN, J., ORKIN, S.H., DOERSCHUK, C.M., and DINAUER, M.C. (1995). Mouse model of X-linked chronic granulomatous disease, an inherited defect in phagocyte superoxide production. Nat Genet **9**, 202-209.

POPA, I., HARRIS, M.E., DONELLO, J.E., and HOPE, T.J. (2002). CRM1-dependent function of a cis-acting RNA export element. Mol Cell Biol **22**, 2057-2067.

PORTER, C.D., PARKAR, M.H., LEVINSKY, R.J., COLLINS, M.K., and KINNON, C. (1993). X-linked chronic granulomatous disease: correction of NADPH oxidase defect by retrovirus-mediated expression of gp91-phox. Blood **82**, 2196-2202.

PORTER, C.D., PARKAR, M.H., VERHOEVEN, A.J., LEVINSKY, R.J., COLLINS, M.K., and KINNON, C. (1994). p22-phox-deficient chronic granulomatous disease: reconstitution by retrovirus-mediated expression and identification of a biosynthetic intermediate of gp91-phox. Blood **84**, 2767-2775.

POZZAN, T., LEW, D.P., WOLLHEIM, C.B., and TSIEN, R.Y. (1983). Is cytosolic ionized calcium regulating neutrophil activation? Science **221**, 1413-1415.

PRICE, M.O., ATKINSON, S.J., KNAUS, U.G., and DINAUER, M.C. (2002). Rac activation induces NADPH oxidase activity in transgenic COSphox cells, and the level of superoxide production is exchange factor-dependent. J Biol Chem **277**, 19220-19228.

PUIG, T., KADAR, E., LIMON, A., CANCELAS, J.A., EIXARCH, H., LUQUIN, L., GARCIA, M., and BARQUINERO, J. (2002). Myeloablation enhances engraftment of transduced murine hematopoietic cells, but does not influence long-term expression of the transgene. Gene Ther **9**, 1472-1479.

QUINN, M.T., and GAUSS, K.A. (2004). Structure and regulation of the neutrophil respiratory burst oxidase: comparison with nonphagocyte oxidases. J Leukoc Biol **76**, 760-781.

RADCLIFFE, P.A., SION, C.J., WILKES, F.J., CUSTARD, E.J., BEARD, G.L., KINGSMAN, S.M., and MITROPHANOUS, K.A. (2008). Analysis of factor VIII mediated suppression of lentiviral vector titres. Gene Ther **15**, 289-297.

RAMMES, A., ROTH, J., GOEBELER, M., KLEMPT, M., HARTMANN, M., and SORG, C. (1997). Myeloid-related protein (MRP) 8 and MRP14, calcium-binding proteins of the S100 family, are secreted by activated monocytes via a novel, tubulin-dependent pathway. J Biol Chem **272**, 9496-9502.

RAPER, S.E., CHIRMULE, N., LEE, F.S., WIVEL, N.A., BAGG, A., GAO, G.P., WILSON, J.M., and BATSHAW, M.L. (2003). Fatal systemic inflammatory response syndrome in a ornithine transcarbamylase deficient patient following adenoviral gene transfer. Mol Genet Metab **80**, 148-158.

REEVES, E.P., LU, H., JACOBS, H.L., MESSINA, C.G., BOLSOVER, S., GABELLA, G., POTMA, E.O., WARLEY, A., ROES, J., and SEGAL, A.W. (2002). Killing activity of neutrophils is mediated through activation of proteases by K+ flux. Nature **416**, 291-297.

REZVANI, Z., MOHAMMADZADEH, I., POURPAK, Z., MOIN, M., and TEIMOURIAN, S. (2005). CYBB Gene Mutation Detection in an Iranian Patient with Chronic Granulomatous Disease. Iran J Allergy Asthma Immunol **4**, 103-106.

RINCKEL, L.A., FARIS, S.L., HITT, N.D., and KLEINBERG, M.E. (1999). Rac1 disrupts p67phox/p40phox binding: a novel role for Rac in NADPH oxidase activation. Biochem Biophys Res Commun **263**, 118-122.

ROBBINS, P.D., and GHIVIZZANI, S.C. (1998). Viral vectors for gene therapy. Pharmacol Ther **80**, 35-47.

ROBERTS, A.W., KIM, C., ZHEN, L., LOWE, J.B., KAPUR, R., PETRYNIAK, B., SPAETTI, A., POLLOCK, J.D., BORNEO, J.B., BRADFORD, G.B., ATKINSON, S.J., DINAUER, M.C., and WILLIAMS, D.A. (1999). Deficiency of the hematopoietic cell-specific Rho family GTPase Rac2 is characterized by abnormalities in neutrophil function and host defense. Immunity **10**, 183-196.

ROE, T., REYNOLDS, T.C., YU, G., and BROWN, P.O. (1993). Integration of murine leukemia virus DNA depends on mitosis. Embo J **12**, 2099-2108.

ROSENBERG, S.A., AEBERSOLD, P., CORNETTA, K., KASID, A., MORGAN, R.A., MOEN, R., KARSON, E.M., LOTZE, M.T., YANG, J.C., TOPALIAN, S.L., and ET AL. (1990). Gene transfer into humans--immunotherapy of patients with advanced melanoma, using tumor-infiltrating lymphocytes modified by retroviral gene transduction. N Engl J Med **323**, 570-578.

ROSH, J.R., TANG, H.B., MAYER, L., GROISMAN, G., ABRAHAM, S.K., and PRINCE, A. (1995). Treatment of intractable gastrointestinal manifestations of chronic granulomatous disease with cyclosporine. J Pediatr **126**, 143-145.

ROTH, J., BURWINKEL, F., VAN DEN BOS, C., GOEBELER, M., VOLLMER, E., and SORG, C. (1993). MRP8 and MRP14, S-100-like proteins associated with myeloid differentiation, are translocated to plasma membrane and intermediate filaments in a calcium-dependent manner. Blood **82**, 1875-1883.

ROTROSEN, D., KLEINBERG, M.E., NUNOI, H., LETO, T., GALLIN, J.I., and MALECH, H.L. (1990). Evidence for a functional cytoplasmic domain of phagocyte oxidase cytochrome b558. J Biol Chem **265**, 8745-8750.

ROTROSEN, D., YEUNG, C.L., LETO, T.L., MALECH, H.L., and KWONG, C.H. (1992). Cytochrome b558: the flavin-binding component of the phagocyte NADPH oxidase. Science **256**, 1459-1462.

ROVERA, G., SANTOLI, D., and DAMSKY, C. (1979). Human promyelocytic leukemia cells in culture differentiate into macrophage-like cells when treated with a phorbol diester. Proc Natl Acad Sci U S A **76**, 2779-2783.

SAMUELSON, D.J., POWELL, M.B., LLURIA-PREVATT, M., and ROMAGNOLO, D.F. (2001). Transcriptional activation of the gp91phox NADPH oxidase subunit by TPA in HL-60 cells. J Leukoc Biol **69**, 161-168.

SANDRIN, V., BOSON, B., SALMON, P., GAY, W., NEGRE, D., LE GRAND, R., TRONO, D., and COSSET, F.L. (2002). Lentiviral vectors pseudotyped with a modified RD114 envelope glycoprotein show increased stability in sera and augmented transduction of primary lymphocytes and CD34+ cells derived from human and nonhuman primates. Blood **100**, 823-832.

SANDRIN, V., and COSSET, F.L. (2006). Intracellular versus cell surface assembly of retroviral pseudotypes is determined by the cellular localization of the viral glycoprotein, its capacity to interact with Gag, and the expression of the Nef protein. J Biol Chem **281**, 528-542.

SANDRIN, V., MURIAUX, D., DARLIX, J.L., and COSSET, F.L. (2004). Intracellular trafficking of Gag and Env proteins and their interactions modulate pseudotyping of retroviruses. J Virol **78**, 7153-7164.

SCHAMBACH, A., and BAUM, C. (2007). Vector design for expression of O6-methylguanine-DNA methyltransferase in hematopoietic cells. DNA Repair (Amst) **6**, 1187-1196.

SCHAMBACH, A., BOHNE, J., BAUM, C., HERMANN, F.G., EGERER, L., VON LAER, D., and GIROGLOU, T. (2006a). Woodchuck hepatitis virus post-transcriptional regulatory element deleted from X protein and promoter sequences enhances retroviral vector titer and expression. Gene Ther **13**, 641-645.

SCHAMBACH, A., BOHNE, J., CHANDRA, S., WILL, E., MARGISON, G.P., WILLIAMS, D.A., and BAUM, C. (2006b). Equal potency of gammaretroviral and lentiviral SIN vectors for expression of O6-methylguanine-DNA methyltransferase in hematopoietic cells. Mol Ther **13**, 391-400.

SCHAMBACH, A., GALLA, M., MAETZIG, T., LOEW, R., and BAUM, C. (2007). Improving transcriptional termination of self-inactivating gamma-retroviral and lentiviral vectors. Mol Ther **15**, 1167-1173.

SCHAMBACH, A., MUELLER, D., GALLA, M., VERSTEGEN, M.M., WAGEMAKER, G., LOEW, R., BAUM, C., and BOHNE, J. (2006c). Overcoming promoter competition in packaging cells improves production of self-inactivating retroviral vectors. Gene Ther **13**, 1524-1533.

SCHAMBACH, A., WODRICH, H., HILDINGER, M., BOHNE, J., KRAUSSLICH, H.G., and BAUM, C. (2000). Context dependence of different modules for posttranscriptional enhancement of gene expression from retroviral vectors. Mol Ther **2**, 435-445.

SCHIEDNER, G., MORRAL, N., PARKS, R.J., WU, Y., KOOPMANS, S.C., LANGSTON, C., GRAHAM, F.L., BEAUDET, A.L., and KOCHANEK, S. (1998). Genomic DNA transfer with a high-capacity adenovirus vector results in improved in vivo gene expression and decreased toxicity. Nat Genet **18**, 180-183.

SCHIRM, S., JIRICNY, J., and SCHAFFNER, W. (1987). The SV40 enhancer can be dissected into multiple segments, each with a different cell type specificity. Genes Dev **1**, 65-74.

SCHMIDT, M., ZICKLER, P., HOFFMANN, G., HAAS, S., WISSLER, M., MUESSIG, A., TISDALE, J.F., KURAMOTO, K., ANDREWS, R.G., WU, T., KIEM, H.P., DUNBAR, C.E., and VON KALLE, C. (2002). Polyclonal long-term repopulating stem cell clones in a primate model. Blood **100**, 2737-2743.

SCHNEPP, B.C., JENSEN, R.L., CHEN, C.L., JOHNSON, P.R., and CLARK, K.R. (2005). Characterization of adeno-associated virus genomes isolated from human tissues. J Virol **79**, 14793-14803.

SEGER, R.A., GUNGOR, T., BELOHRADSKY, B.H., BLANCHE, S., BORDIGONI, P., DI BARTOLOMEO, P., FLOOD, T., LANDAIS, P., MULLER, S., OZSAHIN, H., PASSWELL, J.H., PORTA, F., SLAVIN, S., WULFFRAAT, N., ZINTL, F., NAGLER, A., CANT, A., and FISCHER, A. (2002). Treatment of chronic granulomatous disease with myeloablative conditioning and an unmodified hemopoietic allograft: a survey of the European experience, 1985-2000. Blood **100**, 4344-4350.

SELKIRK, S.M. (2004). Gene therapy in clinical medicine. Postgrad Med J **80**, 560-570.

SETH, P. (2005). Vector-mediated cancer gene therapy: an overview. Cancer Biol Ther **4**, 512-517.

SHEPPARD, F.R., KELHER, M.R., MOORE, E.E., MCLAUGHLIN, N.J., BANERJEE, A., and SILLIMAN, C.C. (2005). Structural organization of the neutrophil NADPH oxidase: phosphorylation and translocation during priming and activation. J Leukoc Biol **78**, 1025-1042.

SMITHGALL, T.E., ROGERS, J.A., PETERS, K.L., LI, J., BRIGGS, S.D., LIONBERGER, J.M., CHENG, H., SHIBATA, A., SCHOLTZ, B., SCHREINER, S., and DUNHAM, N. (1998). The c-Fes family of protein-tyrosine kinases. Crit Rev Oncog **9**, 43-62.

SOMEYA, A., NAGAOKA, I., and YAMASHITA, T. (1993). Purification of the 260 kDa cytosolic complex involved in the superoxide production of guinea pig neutrophils. FEBS Lett **330**, 215-218.

SOUDAIS, C., SHIHO, T., SHARARA, L.I., GUY-GRAND, D., TANIGUCHI, T., FISCHER, A., and DI SANTO, J.P. (2000). Stable and functional lymphoid reconstitution of common cytokine receptor gamma chain deficient mice by retroviral-mediated gene transfer. Blood **95**, 3071-3077.

SPANGRUDE, G.J. (1989). Enrichment of murine haemopoietic stem cells: diverging roads. Immunol Today **10**, 344-350.

SPANGRUDE, G.J., HEIMFELD, S., and WEISSMAN, I.L. (1988). Purification and characterization of mouse hematopoietic stem cells. Science **241**, 58-62.

STEIN, S., SILER, U., OTT, M.G., SEGER, R., and GREZ, M. (2006). Gene therapy for chronic granulomatous disease. Curr Opin Mol Ther **8**, 415-422.

STOPKA, T., AMANATULLAH, D.F., PAPETTI, M., and SKOULTCHI, A.I. (2005). PU.1 inhibits the erythroid program by binding to GATA-1 on DNA and creating a repressive chromatin structure. Embo J **24**, 3712-3723.

SUMIMOTO, H., SAKAMOTO, N., NOZAKI, M., SAKAKI, Y., TAKESHIGE, K., and MINAKAMI, S. (1992). Cytochrome b558, a component of the phagocyte NADPH oxidase, is a flavoprotein. Biochem Biophys Res Commun **186**, 1368-1375.

TAYLOR, R.M., BURRITT, J.B., BANIULIS, D., FOUBERT, T.R., LORD, C.I., DINAUER, M.C., PARKOS, C.A., and JESAITIS, A.J. (2004). Site-specific inhibitors of NADPH oxidase activity and structural probes of flavocytochrome b: characterization of six monoclonal antibodies to the p22phox subunit. J Immunol **173**, 7349-7357.

TERRADILLOS, O., BILLET, O., RENARD, C.A., LEVY, R., MOLINA, T., BRIAND, P., and BUENDIA, M.A. (1997). The hepatitis B virus X gene potentiates c-myc-induced liver oncogenesis in transgenic mice. Oncogene **14**, 395-404.

THRASHER, A.J., GASPAR, H.B., BAUM, C., MODLICH, U., SCHAMBACH, A., CANDOTTI, F., OTSU, M., SORRENTINO, B., SCOBIE, L., CAMERON, E., BLYTH, K., NEIL, J., ABINA, S.H., CAVAZZANA-CALVO, M., and FISCHER, A. (2006). Gene therapy: X-SCID transgene leukaemogenicity. Nature **443**, E5-6; discussion E6-7.

TOWBIN, H., STAEHELIN, T., and GORDON, J. (1979). Electrophoretic transfer of proteins from polyacrylamide gels to nitrocellulose sheets: procedure and some applications. Proc Natl Acad Sci U S A **76**, 4350-4354.

TUCKER, K.A., LILLY, M.B., HECK, L., JR., and RADO, T.A. (1987). Characterization of a new human diploid myeloid leukemia cell line (PLB-985) with granulocytic and monocytic differentiating capacity. Blood **70**, 372-378.

TUMAS, D.B., SPANGRUDE, G.J., BROOKS, D.M., WILLIAMS, C.D., and CHESEBRO, B. (1996). High-frequency cell surface expression of a foreign protein in murine hematopoietic stem cells using a new retroviral vector. Blood **87**, 509-517.

UCHIDA, N., SUTTON, R.E., FRIERA, A.M., HE, D., REITSMA, M.J., CHANG, W.C., VERES, G., SCOLLAY, R., and WEISSMAN, I.L. (1998). HIV, but not murine leukemia virus, vectors mediate high efficiency gene transfer into freshly isolated G0/G1 human hematopoietic stem cells. Proc Natl Acad Sci U S A **95**, 11939-11944.

UCKERT, W., BECKER, C., GLADOW, M., KLEIN, D., KAMMERTOENS, T., PEDERSEN, L., and BLANKENSTEIN, T. (2000). Efficient gene transfer into primary human CD8+ T lymphocytes by MuLV-10A1 retrovirus pseudotype. Hum Gene Ther **11**, 1005-1014.

VERGNAUD, S., PACLET, M.H., EL BENNA, J., POCIDALO, M.A., and MOREL, F. (2000). Complementation of NADPH oxidase in p67-phox-deficient CGD patients p67-phox/p40-phox interaction. Eur J Biochem **267**, 1059-1067.

VERHOEVEN, A.J., BOLSCHER, B.G., MEERHOF, L.J., VAN ZWIETEN, R., KEIJER, J., WEENING, R.S., and ROOS, D. (1989). Characterization of two monoclonal antibodies against cytochrome b558 of human neutrophils. Blood **73**, 1686-1694.

VERHOEYEN, E., WIZNEROWICZ, M., OLIVIER, D., IZAC, B., TRONO, D., DUBART-KUPPERSCHMITT, A., and COSSET, F.L. (2005). Novel lentiviral vectors displaying "early-acting cytokines" selectively promote survival and transduction of NOD/SCID repopulating human hematopoietic stem cells. Blood **106**, 3386-3395.

VOGL, T., LUDWIG, S., GOEBELER, M., STREY, A., THOREY, I.S., REICHELT, R., FOELL, D., GERKE, V., MANITZ, M.P., NACKEN, W., WERNER, S., SORG, C., and ROTH, J. (2004). MRP8 and MRP14 control microtubule reorganization during transendothelial migration of phagocytes. Blood **104**, 4260-4268.

VON SCHWEDLER, U., KORNBLUTH, R.S., and TRONO, D. (1994). The nuclear localization signal of the matrix protein of human immunodeficiency virus type 1 allows the establishment of infection in macrophages and quiescent T lymphocytes. Proc Natl Acad Sci U S A **91**, 6992-6996.

VOWELLS, S.J., SEKHSARIA, S., MALECH, H.L., SHALIT, M., and FLEISHER, T.A. (1995). Flow cytometric analysis of the granulocyte respiratory burst: a comparison study of fluorescent probes. J Immunol Methods **178**, 89-97.

WALKER, S., SOFIA, M.J., KAKARLA, R., KOGAN, N.A., WIERICHS, L., LONGLEY, C.B., BRUKER, K., AXELROD, H.R., MIDHA, S., BABU, S., and KAHNE, D. (1996). Cationic facial amphiphiles: a promising class of transfection agents. Proc Natl Acad Sci U S A **93**, 1585-1590.

WALRAND, S., VALEIX, S., RODRIGUEZ, C., LIGOT, P., CHASSAGNE, J., and VASSON, M.P. (2003). Flow cytometry study of polymorphonuclear neutrophil oxidative burst: a comparison of three fluorescent probes. Clin Chim Acta **331**, 103-110.

WEENING, R.S., LEITZ, G.J., and SEGER, R.A. (1995). Recombinant human interferon-gamma in patients with chronic granulomatous disease--European follow up study. Eur J Pediatr **154**, 295-298.

WELZEL, T., RADTKE, I., MEYER-ZAIKA, W., HEUMANN, R., and EPPLE, M. (2004). Transfection of cells with custom-made calcium phosphate nanoparticles coated with DNA. J Mat Chem **14**, 2213-2217.

WIGLER, M., SILVERSTEIN, S., LEE, L.S., PELLICER, A., CHENG, Y., and AXEL, R. (1977). Transfer of purified herpes virus thymidine kinase gene to cultured mouse cells. Cell **11**, 223-232.

WILLIAMS, D.A., TAO, W., YANG, F., KIM, C., GU, Y., MANSFIELD, P., LEVINE, J.E., PETRYNIAK, B., DERROW, C.W., HARRIS, C., JIA, B., ZHENG, Y., AMBRUSO, D.R., LOWE, J.B., ATKINSON, S.J., DINAUER, M.C., and BOXER, L. (2000). Dominant negative mutation of the hematopoietic-specific Rho GTPase, Rac2, is associated with a human phagocyte immunodeficiency. Blood **96**, 1646-1654.

WINKELSTEIN, J.A., MARINO, M.C., JOHNSTON, R.B., JR., BOYLE, J., CURNUTTE, J., GALLIN, J.I., MALECH, H.L., HOLLAND, S.M., OCHS, H., QUIE, P., BUCKLEY, R.H., FOSTER, C.B., CHANOCK, S.J., and DICKLER, H. (2000). Chronic granulomatous disease. Report on a national registry of 368 patients. Medicine (Baltimore) **79**, 155-169.

WITLOX, M.A., LAMFERS, M.L., WUISMAN, P.I., CURIEL, D.T., and SIEGAL, G.P. (2007). Evolving gene therapy approaches for osteosarcoma using viral vectors: review. Bone **40**, 797-812.

WOOD, K.J., and FRY, J. (1999). Gene therapy: potential applications in clinical transplantation. Expert Rev Mol Med **1999**, 1-20.

WOODMAN, R., TEOH, D., JOHNSTON, F., RAE, J., SIM, V., URTON, T., WRIGHT, B., and CURNUTTE, J. (1995). X-linked carriers of gp91phox chronic granulomatous disease (CGD): Clinical

and potential therapeutic implications of extreme unbalanced X chromosome inactivation. Blood **86**, (abstr, suppl).

WOODS, N.B., MIKKOLA, H., NILSSON, E., OLSSON, K., TRONO, D., and KARLSSON, S. (2001). Lentiviral-mediated gene transfer into haematopoietic stem cells. J Intern Med **249**, 339-343.

YAMAMOTO, T., DE CROMBRUGGHE, B., and PASTAN, I. (1980). Identification of a functional promoter in the long terminal repeat of Rous sarcoma virus. Cell **22**, 787-797.

YAMAUCHI, A., YU, L., POTGENS, A.J., KURIBAYASHI, F., NUNOI, H., KANEGASAKI, S., ROOS, D., MALECH, H.L., DINAUER, M.C., and NAKAMURA, M. (2001). Location of the epitope for 7D5, a monoclonal antibody raised against human flavocytochrome b558, to the extracellular peptide portion of primate gp91phox. Microbiol Immunol **45**, 249-257.

YANG, T.T., CHENG, L., and KAIN, S.R. (1996). Optimized codon usage and chromophore mutations provide enhanced sensitivity with the green fluorescent protein. Nucleic Acids Res **24**, 4592-4593.

YU, L., QUINN, M.T., CROSS, A.R., and DINAUER, M.C. (1998). Gp91(phox) is the heme binding subunit of the superoxide-generating NADPH oxidase. Proc Natl Acad Sci U S A **95**, 7993-7998.

YU, L., ZHEN, L., and DINAUER, M.C. (1997). Biosynthesis of the phagocyte NADPH oxidase cytochrome b558. Role of heme incorporation and heterodimer formation in maturation and stability of gp91phox and p22phox subunits. J Biol Chem **272**, 27288-27294.

YU, S.F., VON RUDEN, T., KANTOFF, P.W., GARBER, C., SEIBERG, M., RUTHER, U., ANDERSON, W.F., WAGNER, E.F., and GILBOA, E. (1986). Self-inactivating retroviral vectors designed for transfer of whole genes into mammalian cells. Proc Natl Acad Sci U S A **83**, 3194-3198.

YUAN, Y., ZHOU, L., MIYAMOTO, T., IWASAKI, H., HARAKAWA, N., HETHERINGTON, C.J., BUREL, S.A., LAGASSE, E., WEISSMAN, I.L., AKASHI, K., and ZHANG, D.E. (2001). AML1-ETO expression is directly involved in the development of acute myeloid leukemia in the presence of additional mutations. Proc Natl Acad Sci U S A **98**, 10398-10403.

ZHEN, L., KING, A.A., XIAO, Y., CHANOCK, S.J., ORKIN, S.H., and DINAUER, M.C. (1993). Gene targeting of X chromosome-linked chronic granulomatous disease locus in a human myeloid leukemia cell line and rescue by expression of recombinant gp91phox. Proc Natl Acad Sci U S A **90**, 9832-9836.

ZHU, Y., MARCHAL, C.C., CASBON, A.J., STULL, N., VON LOHNEYSEN, K., KNAUS, U.G., JESAITIS, A.J., MCCORMICK, S., NAUSEEF, W.M., and DINAUER, M.C. (2006). Deletion mutagenesis of p22phox subunit of flavocytochrome b558: identification of regions critical for gp91phox maturation and NADPH oxidase activity. J Biol Chem **281**, 30336-30346.

ZUFFEREY, R., DONELLO, J.E., TRONO, D., and HOPE, T.J. (1999). Woodchuck hepatitis virus posttranscriptional regulatory element enhances expression of transgenes delivered by retroviral vectors. J Virol **73**, 2886-2892.

F. SUMMARY

Chronic granulomatous disease (CGD) is a rare inherited primary immunodeficiency characterized by defective intracellular oxidative killing of ingested invading microbes by PMN and monocytes. It is caused by mutations in one of the four genes coding for the essential subunits of the NADPH oxidase ($gp91^{phox}$, $p47^{phox}$, $p67^{phox}$ and $p22^{phox}$). Approximately 75% of the CGD cases are due to mutations in the $gp91^{phox}$ gene.

If regular care and conventional therapy fail, the recommended therapy is allogeneic bone marrow transplantation (BMT), but only if a matched donor is available. A therapeutic option for patients lacking suitable donors is the genetic modification of autologous hematopoietic stem cells. The gene therapy offers an interesting alternative to BMT since it implies a less invasive treatment and represents a possibly unique curative option for patients with no suitable donor.

Gammaretroviral vectors were already used in some gene therapy trials for CGD and other immunodeficiencies showing relevant clinical benefit. However, these trials uncovered an unexpected mutagenic side effect. If the retrovial integration ocurrs near to, or into proto-oncogenes this might lead to clonal dominance or even malignant transformation (Hacein-Bey-Abina *et al.*, 2003a; Ott *et al.*, 2006). Therefore, there was a need to further improve the safety of these vectors and to this end the self-inactivating gammaretroviral vectors were engineered. Non essential sequences for virus infectivity and integration, which might influence the surrounding gene expression, were deleted in these vectors.

In the first set of experiments, a series of SIN gamma retroviral vectors was cloned driving the expression of the wild-type $gp91^{phox}$ cDNA under the control of a viral constitutive SFFV promoter. However initial studies with these vectors failed because the titers of the virus produced by transient transfection protocols were extremely low ($<5x10^5$ TU/ml). Therefore, a codon optimization of the $gp91^{phox}$ cDNA was considered as an alternative.

The codon optimized synthetic $gp91^{phox}$ gene was used to construct a SIN gammaretroviral vector, again under the control of the SFFV promoter (Schambach et al., 2006c). With this vector an increase in titer was observed compared to the native $gp91^{phox}$ sequence, which was due to the improved transcription in 293T transfected cells. The enhancement of the synthetic $gp91^{phox}$ transcription led to a higher internal transcript production and protein expression. An enhanced superoxide production in transduced myelomonocytic X-CGD PLB-985 populations was also detected. All these data indicate that the synthetic $gp91^{phox}$ might represent an excellent alternative to those former constructs expressing the native $gp91^{phox}$ transgene.

Since it was postulated that the SFFV promoter could still cause transactivation of neighboring genes due to its strength (Modlich *et al.*, 2006), three different non-viral promoters were tested, one constitutive (the EFs promoter) and two myeloid-specific promoters (the c-fes and MRP8 promoter).

The three SIN gammaretroviral vectors were able to generate high titers after transient transfection of 293T packaging cells, to efficiently transduce the X-CGD PLB-985 cell line and to reconstitute the NADPH oxidase activity to a high degree. In mouse transplantation experiments, the EFs promoter showed a high variable transgene expression in the different lineages analyzed, and the c-fes promoter showed also a ubiquitinous expression. In contrast, the MRP8 promoter showed a high myeloid specificity since $gp91^{phox}$ expression in $mSca\text{-}1^{+}$ cells and lymphoid B cells from transplanted mice was extremly low and even absent. However, the lowest levels of transgene expression were observed in the myeloid populations both in bone marrow and peripheral blood with this vector.

When the oxidase reconstitution ability of these promoters was tested, the numbers of superoxide producing cells obtained were similar than those observed in the clinical X-CGD trial conducted by the groups of Dr. M. Grez and Prof. R. A. Seger (over 35% in one patient and ~15% in the second), which led to the eradication of therapy refractory infections (Ott *et al.*, 2006). Between the three constructs, the MRP8 promoter was less effective in restoring the NADPH oxidase activity than the EFs and c-fes promoters. The c-fes promoter reached the highest levels of DHR reactive cells in the highest number of mice.

Overall, these data showed that between all constructs tested, the c-fes containing construct in combination with the codon optimized $gp91^{phox}$ sequence showed the best performance within the SIN gammaretroviral backbone. It generated the highest titers in combination with a better NADPH oxidase reconstituting ability.

One main goal in the development of SIN gammaretroviral vectors is reducing the genotoxic effect due to random vector integration. An improved gene transfer and expression, and a constant performance are also highly desirable. The present study shows that the c-fes SIN vector in combination with the synthetic $gp91^{phox}$ may be considered as an effective gene therapy strategy for the restoration of the NADPH oxidase activity in CGD. It allows the use of a cellular promoter generating adequate physiological levels of the therapeutic protein and reduces the number of vector copies required for a therapeutic effect.

G. ZUSAMMENFASSUNG

Bei der Septischen Granulomatose (*engl.*: CGD *chronic granulomatous disease*) handelt es sich um eine seltene, vererbbare primäre Immunschwäche, welche sich durch einen Defekt im oxidativen Abtöten intrazellulär aufgenommener Mikroben durch Phagozyten auszeichnet. In Folge dessen erleiden Patienten mit CGD immer wieder schwerste Infektionen durch Bakterien und Pilze.

Ursache für die Septische Granulomatose ist eine Mutation in einem der vier Gene ($gp91^{phox}$, $p47^{phox}$, $p67^{phox}$ und $p22^{phox}$), die für die essentiellen Untereinheiten der NADPH Oxidase kodieren. In zirka 75% aller CGD-Fälle treten die Mutationen im $gp91^{phox}$ Gen auf. Weil dieses Gen auf dem X-Chromosom liegt (Xp21.1 Locus), handelt es sich somit um eine X-chromosomal gekoppelte Vererbung. In den übrigen Fällen der CGD erfolgt die Vererbung autosomal-rezessiv. Bei dieser Form der Krankheit sind Frauen und Männer gleichermaßen betroffen.

Führen Standardbehandlungen und konventionelle Therapien zu keinem Erfolg, verbleibt als einziger Therapieansatz eine allogene Knochenmarktransplantation. Diese kann jedoch nur durchgeführt werden, wenn ein passender Spender vorhanden ist. Die begrenzte Verfügbarkeit adäquater Spender, die methodisch bedingte Toxizität der Transplantationsprozedur sowie posttransplantationale Komplikationen, wie beispielsweise die Transplantat-Wirt Krankheit (*engl.* graft versus host disease), erschweren eine breite Anwendung der allogenen Knochenmarktransplantation zur Behandlung von CGD.

Ein alternativer therapeutischer Ansatz ist die genetische Modifikation der eigenen (=autologen) hämatopoetischen Stammzellen. Zwei der wichtigsten Vorteile einer Gentherapie im Vergleich zur allogenen Knochenmarktransplantation sind die geringere Belastung für die Patienten sowie die Möglichkeit der Therapie von Patienten ohne passenden Spender.

In einigen gentherapeutischen Studien zur CGD und anderen Immundefizienzkrankheiten konnten Gammaretrovirale Vektoren einen deutlichen klinischen Nutzen für die Patienten aufzeigen. Die Studien zeigten jedoch teils erhebliche Nebenwirkungen, wie die Entwicklung maligner Zellpopulationen oder einen selektiven Wachstumsvorteil der genkorrigierten Zellen, der zu einer oligo- oder gar monoklonalen Expansion der Zellen führte. Diese Phänomene entstehen in Folge der Integration des Vektors in das Wirtsgenom, welche jedoch ein unumgänglicher Schritt im Replikationszyklus der Retroviren darstellt. Aus diesem Grund bestand der Bedarf die Sicherheit dieser Vektoren weiter zu verbessern, was in der Weiterentwicklung der sog. Selbst-Inaktivierenden Gammaretroviren (SIN Retrovektoren) resultierte. Bei diesen Genvektoren sind Promotor/Enhancer-Bereiche im 3´LTR des Vektors deletiert,

wodurch der Einfluss auf die Genexpression in der Nachbarschaft der Integrationsstelle minimiert werden soll. Wenngleich diese Vektoren häufig eine geringere Effizienz in der Virusproduktion zeigen, stellt die Verwendung eines internen Promotors einen entscheidenden Vorteil dar. So ermöglichen es diese Vektoren z. B. die Expression eines Transgens unter die Kontrolle geeigneter, gewebespezifischer Promotoren in unterschiedlichen Zellen zu stellen.

Die vorliegende Studie begann mit der Klonierung SIN Gammaretroviraler Vektoren. Die ersten getesteten Vektoren exprimieren die gp91^{phox} Wildtyp cDNA, wobei der konstitutive SFFV LTR als interner Promotor fungiert. Anfängliche Studien mit diesen Vektoren scheiterten, da der Virustiter nach transienter Transfektion zu niedrig war (<5x10^5 TU/ml). Da der Spleißvorgang im Zellkern mit dem Kernexportmechanismus der endogenen mRNA gekoppelt ist, wurde vermutet, dass das Einbringen eines Introns in das virale Genom eine Steigerung des mRNA Exports zur Folge hätte. Der Einbau eines Spleißakzeptors und einer Spleißdonorstelle in die Leader Sequenz des Vektors brachte jedoch keine Erhöhung des Titers. Genauso wenig zeigte die gerichtete Mutation (site-directed mutagenesis) eines kryptischen Spleißakzeptors (cSA) in der gp91^{phox} Sequenz (gp91m) einen Effekt auf den Virustiter. Als Alternative kam daher eine vollständige Codonoptimierung der gp91^{phox} cDNA in Betracht. Die Strategie der Codonoptimierung wird benutzt, um die heterologe Genexpression von Genen, die in fremde Genome eingeführt werden, zu verbessern. Alle Codons einer proteinkodierenden DNA werden dabei auf den bevorzugten Codongebrauch im Zielorganismus abgestimmt. Diese Methode wurde bereits für Reporterproteine wie GFP und Luziferase angewandt. In verschiedenen Organismen konnte gezeigt werden, dass eine vorher niedrige Genexpression durch diese Methode erhöht werden kann.

Die Firma GeneArt (Regensburg, Deutschland) analysierte und verbesserte die Sequenz der gp91^{phox} mRNA des Wildtypes. Dabei wurde die Sequenz zunächst so modifiziert, dass wenig verwendete Codons durch häufiger benutzte ersetzt wurden. Der Codon Adaption Index (CAI) ist ein relatives Maß dafür wie nahe - verglichen mit einer Reihe von Referenzgenen - der Codongebrauch eines Genes am Optimum liegt. Der CAI konnte beim gp91^{phox} von 0,77 auf 0,99 optimiert werden. Zusätzlich wurden einige Motive identifiziert, die entweder die Genexpression oder die Virusproduktion beeinträchtigen könnten. Aufgrund dessen wurden interne Polyadenylierungsstellen, zusätzliche kryptische Spleißstellen und RNA instabilisierende Motive, wie z. B. AU-reiche Elemente, gegen weniger kritische Sequenzen ausgetauscht. Wichtig ist dabei anzumerken, dass die Aminosäuresequenz des Gp91^{phox} Proteins bei all diesen Modifikationen nicht verändert wurde.

Die so veränderte synthetische gp91^{phox} cDNA (gp91s) wurde im Folgenden für den SIN Gammaretroviralen Vektor SERS11.SF.gp91s.Wm verwendet. Dieses Plasmid beinhaltet den internen SFFV Promotor und die gleiche Promotor/Enhancer Anordnung

im 5´LTR wie die vorherigen Vektoren. Zusätzlich wurde ein 233bp langer SV40 Enhancer (E) dem RSV Promotor vorgeschaltet. Es ist bekannt, dass der SV40 Enhancer die Genexpression in einer Vielzahl von Organismen und Geweben signifikant steigert. In der Verpackungszelllinie wird dadurch die Expression durch den im 5´LTR befindlichen RSV Promotor zu Gunsten der verpackbaren genomischen Virus mRNA gesteigert. (Schambach et al., 2006c). Des Weiteren wurde im WPRE Element der X-Promotor deletiert und die offenen Leserahmen mutiert (Schambach *et al.*, 2006a).

Tatsächlich war nach transienter Transfektion von 293T-Zellen mit dem SERS11.SF.gp91s.Wm-Vektor der Titer im Vergleich zu Transfektionen mit dem SERS11.SF.gp91m.W-Konstrukt 2,7 fach erhört. Mit Hilfe einer Northern Blot-Analyse konnte gezeigt werden, dass der erhöhte Titer die Folge einer gesteigerten Transkription dieses Konstrukts in den transfizierten 293T-Zellen ist. In transduzierten myelomonozytischen X-CGD PLB-985 Zellen zeigen Northern- bzw. Western Blot-Analysen von Zellen mit gleicher Anzahl integrierter Vektorkopien, dass die verstärkte Transkription des synthetischen $gp91^{phox}$ zu erhöhter Transkriptproduktion und zu gesteigerter Proteinexpression führt. In Übereinstimmung mit der beschriebenen konstitutiven, transkriptionellen Aktivität des SFFV-Promotors wurde keine Veränderung der Expressionsstärke (ΔMFI) nach Differenzierung der Zellpopulationen in Granulozyten-ähnliche Zellen beobachtet. Die Analyse der Proteinmengen in diesen Zellen zeigte eine Korrelation mit den höheren ΔMFI-Werten des synthetischen $gp91^{phox}$ im Vergleich zum gp91m. Dies deutet darauf hin, dass eine erhöhte intrazelluläre $Gp91^{phox}$-Proteinmenge auch zu einer vermehrten Bildung des Flavocytochrom b_{558} Komplexes an der Membran der differenzierten Zellen führt. Zudem war die Proteinmenge in sortierten transduzierten Zellen deutlich höher als in der parentalen PLB-985 Zelllinie. Es wurde eine 2,7 bzw. eine 5,5fache Steigerung mit der gp91m Sequenz bzw. der synthetischen Sequenz gp91s erreicht.

Die Fähigkeit des Vektors die Superoxid-Erzeugung wieder herzustellen wurde durch einen Test der Cytochom C-Reduktion bestimmt, welcher eine quantitative Methode zur Messung der zellulären Superoxid Anionenproduktion bei einer definierten Anzahl von Zellen darstellt. Hierzu wurden DMSO differenzierte Populationen mit PMA, einem starken Stimulans zur O_2^--Produktion, inkubiert. Anschließend wurde die Superoxidproduktion pro Zelle durch die Reduktion des Cytochrome C in Abhängigkeit der Zeit gemessen. Als Referenz wurden differenzierte Wildtyp PLB-985-Zellen verwendet. Die Messung ergab eine 1,7fach höhere Superoxidproduktion in sortierten Zellpopulationen mit SERS11.SF.gp91s.Wm im Vergleich zu sortierten Zellpopulationen mit Vektoren zur Expression von gp91m. Der funktionale Unterschied zwischen beiden transduzierten Populationen korreliert mit den Protein- und ΔMFI-Werten, daher ist die vermehrte Superoxid-Produktion auf eine Steigerung des Proteins pro Zelle zurückzuführen. Die Mengen der O_2^--Produktion in den

SERS11.SF.gp91s.Wm transduzierten Zellen waren sogar höher als in Wildtyp PLB-985-Zellen.

Vorrausgehende molekulare Untersuchungen sowie Klinische Phase I Gentherapie Studien zeigen, dass die Menge der NADPH-Oxidase Aktivität pro Zelle ein ganz wichtiger Faktor für die Wirksamkeit der Infektionsabwehr bestimmter Mikroorganismen ist, insbesondere wenn nur wenige der O_2^- produzierenden neutrophilen Granulozyten vorhanden sind. Die vorliegende Arbeit zeigt, dass die synthetische gp91^{phox} cDNA eine ausgezeichnete Alternative zu den bisher verwendeten gp91^{phox} Transgensequenzen darstellt.

Da der SFFV-Promotor wegen seiner Stärke auch als interner Promotor die Transaktivierung von Nachbargenen verursachen kann, wurde im zweiten Teil der vorliegenden Arbeit der SERS11.SF.gp91s.Wm Vektor ausgewählt um die Effizienz schwächerer, nicht-viraler Promotoren zu untersuchen (Modlich *et al.*, 2006). Es wurden drei verschiedene zelluläre Promotoren getestet: ein konstitutiv exprimierender (der EFs Promotor) und zwei myeloid-spezifische Promotoren (c-fes bzw. MRP8), Letztere sollten die spezifische Expression der korrekten gp91^{phox} cDNA in Phagozyten erlauben, deren defekte NADPH Oxidase die Hauptursache der Symptome der Septischen Granulomatose ist.

Der ubiquitäre EFs Promotor ist eine kurze Intron-deletierte Version des EF-1α Promotors, welcher eine effiziente Expression des Transgens in myeloiden oder lymphoiden Zellen erlaubt. Dieser EFs Promotor ist schon in Gammaretroviralen- und Lentiviralen- SIN-Vektoren getestet worden, und zeigte eine mittelstarke Transkriptionsaktivierung mit moderaten Titern.

C-fes gehört zu der Familie der sog. Nicht-Rezeptortyrosinkinasen und ist für mehrere zelluläre Prozesse, darunter Differenzierung und Proliferation, von großer Bedeutung. Während der myeloischen Differenzierung ist der c-fes Promotor konstitutiv aktiv, wird jedoch während der Reifung der Erythrozyten inaktiviert. Zusätzlich besitzt dieser Promotor eine eigene Kontrollregion (LCR; *engl.: locus control region*), welche die Expression der Fes-Kinase beeinflusst. Frühere Studien zeigten, dass ein 446 bp langes Fragment des c-fes Promotors ausreicht, um eine gewebespezifische Transgenexpression sicherzustellen.

Der MRP8 Promotor steuert die Expression des Myeloid Restricted Protein 8. Es wurde gezeigt, dass MRP8 nicht nur an mehreren zellulären Prozessen während der transendothelialen Migration von Phagozyten, sondern auch an der myeloischen Differenzierung beteiligt ist. Ist die MRP8 Protein-Expression in myeloischen Vorläufern noch äußerst gering, so steigt diese bis auf 45% des zytosolischen Gesamtproteingehalts in Neutrophilen.

Um die Titer der neuen Vektoren zu ermitteln, wurden X-CGD PLB-985 Zellen mit transient produziertem Virusüberstand transduziert und analysiert. Die Titer der Vektoren mit den zellulären Promotoren lagen in der Größenordnung von $1x10^6$ TU/ml. Dies entspricht einer drei fachen Reduzierung im Vergleich zum internen SFFV Promotor. Das c-fes Konstrukt zeigte mit bis zu $1.8x10^6$ TU/ml die höchsten Titer, während das MRP8-Konstrukt die niedrigsten Titer produzierte. In transduzierten und sortierten X-CGD PLB-985 Zellen zeigten alle Promotoren im Cytochrome C Test eine sehr hohe Produktion von Superoxide, welche höher als die der Wildtyp PLB-985 Zellen war. Da die beschriebenen drei gammaretroviralen Vektoren ausreichend hohe Titer produzierten, in der Lage sind X-CGD PLB-985 Zellen effizient zu transduzieren und die NADPH-Oxidase Aktivität *in vitro* in hohem Maße wiederherstellen, wurde im nächsten Schritt die Effizienz dieser Vektoren in primären, murinen Zellen untersucht.

Hierbei zeigte der EFs-Promotor in Transplantationsexperimenten im X-CGD Mausmodell eine recht hohe Variabilität der Transgenexpression in verschiedenen Zellreihen, wohingegen der c-fes Promotor eine mehr oder weniger ubiquitäre $gp91^{phox}$ Expression bewirkte. Dieses Ergebnis korreliert nicht mit den Daten aus früheren Studien transgener Mäuse, die außerhalb des myeloischen Zellkompartments bestenfalls eine niedrige Expression des c-fes Promotors in B-Zellen aus dem Knochenmark zeigten. Die konstitutive Expression des c-fes Promotors könnte damit erklärt werden, dass im verwendeten Vektor einige zusätzliche genomische Sequenzen, wie z.B. die LCR, abwesend waren, die gegebenenfalls die Expression des c-fes Promotors weiter feinregulieren können. Der MRP8 Promotor dagegen zeigt eine hohe myeloische Spezifität, da die $gp91^{phox}$-Expression in Sca-1^+ Zellen und lymphoiden B-Zellen der transplantierten Mäusen sehr niedrig bzw. abwesend war. Allerdings besitzt dieser Promotor im Vergleich zu den beiden anderen die niedrigste Expressionsstärke des Transgenes in myeloischen Zellpopulationen des Knochenmarks so wie im peripheren Blut der Tiere.

Die Fähigkeit der verschiedenen Vektoren die Oxidase-Aktivität im peripheren Blut von transplantierten Mäusen wiederherzustellen wurde mittels des DHR-Assays verglichen. Dabei ist die Anzahl der Superoxid-produzierenden Zellen vergleichbar mit den anfänglichen Werten in der klinischen X-CGD Studie, welche in Frankfurt durchgeführt wurde (über 35% in Patient 1 und etwa 15% in Patient 2). Dieser Prozentsatz war ausreichend um Infektionen in den Patienten zu eliminieren, die vorher nicht mehr auf konventionelle Therapien ansprachen (Ott et al., 2006). Unter den drei Konstrukten hatte der MRP8 Promotor im Vergleich zum EFs und c-fes Promotor die niedrigste Effizienz, was die Wiederherstellung der NADPH-Oxidase-Aktivität betrifft. Der c-fes Promotor dagegen erzielte die höchste Anzahl an DHR-reaktiven Zellen.

Parallel in der Arbeitsgruppe Grez durchgeführte Experimente mit humanen X-CGD $CD34^+$ Zellen bestätigen diese Daten. Im Cytochrom C Test, welcher nach *ex vivo*

Differenzierung in Granulozyten durchgeführt wurde, zeigte der c-fes Promotor eine ähnlich starke Aktivität wie differenzierte Zellen aus einem Normalspender. Das EFs Konstrukt erreichte durchschnittliche Werte. Der MRP8 Promotor hingegen zeigte auch hier die niedrigste Superoxid-Produktion (Dr. M. Grez, pers. Mitteilung).

Insgesamt zeigen diese Daten, dass die in der vorliegenden Arbeit neu konstruierten SIN gammaretroviralen Vektoren zwei wichtige Punkte in der Entwicklung von Vektoren erfüllen, um eine Weiterführung der klinischen Studie für X-CGD zu ermöglichen:

- Zum einen erzeugen die Vektoren hohe Titer und zeigen eine effiziente Transgenexpression.
- Darüber hinaus wird die Produktionsmenge an Superoxid erreicht, die therapeutisch notwendig ist, um eine Infektionen wirksam zu bekämpfen.

Innerhalb des SIN gammaretroviralen Hintergrundes zeigte von allen getesteten Konstrukten der c-fes Vektor in Kombination mit der synthetischen $gp91^{phox}$ Sequenz das beste Ergebnis. Dieser erzeugte die höchsten Titer und führte zur Wiederherstellung der NADPH-Oxidase Aktivität in einem Ausmaß, das im Bereich der Normalaktivität lag.

Ein Ziel bei der Entwicklung von SIN retroviralen Vektoren ist, die Wahrscheinlichkeit der Entstehung unerwünschter Nebenwirkungen zu reduzieren, die aufgrund der Vektor-Integration entstehen. Grundvoraussetzungen hierfür bleiben aber ein verbesserter Gen-Tranfer und eine optimale, stabile Gen-Expression der SIN Vektoren. Die vorliegende Arbeit zeigt, dass das SERS11.fes.gp91s.Wm Konstrukt als effizienter neuer Gentherapievektor zur Wiederherstellung der NADPH-Oxidase-Aktivität bei X-CGD Patienten angesehen werden kann. Dieser Vektor erlaubt die Verwendung eines zellulären Promotors, welcher physiologisch angemessene Proteinmengen erzeugt und so die für einen therapeutischen Effekt benötige Menge an Vektorkopien reduziert.

H. APENDIX

H.1 ACKNOWLEDGEMENTS

AGRADECIMIENTOS

I wish to thank Prof. Dr. Starzinski-Powitz and Prof. Dr. Groner for giving me the opportunity to pursue this work.

In particular I wish to thank my supervisor Dr. Manuel Grez for his direction, advice and discussion of my doctoral dissertation.

I have to single out the former members and current members of the Grez's Lab. Their scientific (and by times not so cientific) input was decisive in putting forward this work.

A mis amig@s, por sus consejos, incluso en aquellos momentos en que no entendían del todo de que hablaba.

Y por último, pero más importante, a mi familia, por su apoyo, por su inagotable ayuda, por sus continuos ánimos y por darme todo lo que he necesitado (y aun más) para concluir este trabajo.

H.2 CURRICULUM VITAE

Bibiana Moreno Carranza
Heinrich-Seliger-Str. 34
60528 Frankfurt am Main
00-49-17624202437
bi.moreno@med.uni-frankfurt.com

Personal Information:

Name:	Bibiana Moreno Carranza
Birthday:	November 6th, 1980
Place of birth:	Barcelona
Marital status:	Single
Nationality:	Spanish

Education and Working Experience:

09/1986 – 06/1994 Elementary School
Mireia C.E. - Montgat, Spain

09/1994 – 07/1998 High School
Mireia C.E. – Montgat, Spain

10/1998 – 09/2004 Degree in Biology, Universitat de Barcelona – Barcelona, Spain

- Erasmus scholarship (10/2003 – 02/2004)
  Institut für Mickrobiologie und Genetik
  Darmstadt University of Technology, Germany
- Intership in Virology (04/2004 – 09/2004)
  Georg-Speyer-Haus – Institute for Medical Research
  Frankfurt am Main, Germany

Publications, abstracts and poster presentations:

11/2005: 13th Annual Congress of the European Society of Gene Therapy
"Development of gamma SIN retroviral vectors for gene therapy of X-linked Chronic Granulomatous Disease"
Moreno-Carranza B, Macias-Pardo A, Kunkel H, Schambach A, Baum C, Stein S, Ott MG and Grez M

07/2006 13th Annual Congress of the DG-GT and 4th Annual Workshop "Viral Vectors and Gene Therapy" of the GfV
"Enhancer-deleted gammaretroviral vectors for the correction of chronic granulomatous disease"
Arnold E, Stein S, Moreno-Carranza B, Schambach A, Baum C and Grez M

11/2006: 14th Annual Congress of the European Society of Gene Therapy
"Evaluation of self inactivating gamma retroviral vectors for gene therapy of X-linked Chronic Granulomatous Disease"
Moreno-Carranza B, Rudolf E, Barese C, Kunkel H, Schambach A, Baum C, Stein S and Grez M

7/2007 14th Annual Meeting of the DG-GT and 5th Annual Workshop "Viral Vectors and Gene Therapy" of the GfV
"SIN Gammaretroviral Vectors for the Gene Therapy of X-linked Chronic Granulomatous Disease"
Moreno-Carranza B, Rudolf E, Chen-Wichmann L, Kunkel H, Schambach A, Baum C, Stein S and Grez M

09/2007 4th Conference on Stem Cell Gene Therapy
"SIN Gammaretroviral Vectors for the Gene Therapy of X-linked Chronic Granulomatous Disease"
Chen-Wichmann L, Stein S, Rudolf E, Moreno-Carranza B, Kunkel H, Schambach A, Baum C and Grez M

10//2007 15th Annual Congress of the European Society of Gene Therapy
"SIN Gammaretroviral Vectors for the Gene Therapy of X-linked Chronic Granulomatous Disease"
Stein S, Chen-Wichmann L, Rudolf E, Moreno-Carranza B, Kunkel H, Schambach A, Baum C and Grez M

11/2007 2nd Annual Meeting of the DFG-Schwerpunktprogramms 1230 - Mechanisms of Gene Vector Entry and Persistence
"Vector-Chromatin Interaction: Molecular basis of retroviral integration clusters"
Grauvogel C, Moreno-Carranza B and Grez M

2008 "Transgene optimization significantly improves vector titers and reconstitution of superoxide production in gp91^{phox}-deficient cells by SIN gammaretroviral and lentiviral vectors"
Moreno-Carranza B, Gentsch M, Stein S, Schambach A, Rudolf E, Ryser M F, Baum C, Brenner S and Grez M
Manuscript in preparation

Frankfurt am Main, den …… ……..……...
(Bibiana Moreno Carranza)

Eidesstattliche Erklärung

Hiermit erkäre ich, dass ich die vorliegende Dissertation selbstsändig und ohne unerlaubte Hilfe angefertigt habe und mich keener anderen Hilfsmittel als der angegebenen bedient habe. Entlehnungen aus anderen Schriften sind als solche kenntlich gemacht.

Frankfurt am Main, den …… ……..……...

(Bibiana Moreno Carranza)

SERS11.SF.gp91s.W proviral sequence

AATGAAAGACCCCACCGCTAGCGATATCGAATTCACAACCCCTCACTCGGGCGCCAGTCCTC
CGATTGACTGAGTCGCCCGGGTACCCGTATTCCCAATAAAGCCTCTTGCTGTTTGCATCCGAA
TCGTGGACTCGCTGATCCTTGGGAGGGTCTCCTCAGATTGATTGACTGCCCACCTCGGGGGT
CTTTCATTTGGAGGTTCCACCGAGATTTGGAGACCCCTGCCCAGGGACCACCGACCCCCCCG
CCGGGAGGTAAGCTGGCCAGCGGTCGTTTCGTGTCTGTCTCTGTCTTTGTGCGTGTTTGTGCC
GGCATCTAGTGTTTGCGCCTGCGTCTGTACTAGTTGGCTAACTAGATCTGTATCTGGCGGTCC
CGCGGAAGAACTGACGAGTTCGTATTCCCGGCCGCAGCCCCTGGGAGACGTCCCAGCGGCCT
CGGGGGCCCGTTTTGTGGCCCATTCTGTATCAGTTAACCTACCCGAGTCGGACTTTTTGGAGC
TCCGCCACTGTCCGAGGGGTACGTGGCTTTGTTGGGGGACGAGAGACAGAGACACTTCCCGC
CCCCGTCTGAATTTTTGCTTTCGGTTTTACGCCGAAACCGCGCCGCGCGTCTTGTCTGCTGCA
GCATCGTTCTGTGTTGTCTCTGTCTGACGTGGTTCTGTATTGTCTGAAAATAGCGGCCGCAGC
TAGCTGCAGTAACGCCATTTTGCAAGGCATGGAAAAATACCAAACCAAGAATAGAGAAGTTC
AGATCAAGGGCGGGTACATGAAAATAGCTAACGTTGGGCCAAACAGGATATCTGCGGTGAG
CAGTTTCGGCCCCGGCCCGGGGCCAAGAACAGATGGTCACCGCAGTTTCGGCCCCGGCCCGA
GGCCAAGAACAGATGGTCCCCAGATATGGCCCAACCCTCAGCAGTTTCTTAAGACCCATCAG
ATGTTTCCAGGCTCCCCCAAGGACCTGAAATGACCCTGCGCCTTATTTGAATTAACCAATCAG
CCTGCTTCTCGCTTCTGTTCGCGCGCTTCTGCTTCCCGAGCTCTATAAAAGAGCTCACAACCC
CTCACTCGGCGCGCCAGTCCTCCGACAGACTGAGTCGGCCGGTCGAATCAAGCTTATCGATA
CCGTCGACCGATCCTGCCACCATGGGCAACTGGGCCGTGAACGAGGGCCTGAGCATCTTCGT
GATCCTGGTGTGGCTGGGCCTGAACGTGTTCCTGTTCGTGTGGTACTACCGGGTGTACGACA
TCCCCCCCCAAGTTCTTCTACACCCGGAAGCTGCTGGGCAGCGCCCTGGCCCTGGCCAGAGCC
CCTGCCGCCTGCCTGAACTTCAACTGCATGCTGATCCTGCTGCCCGTGTGCCGGAACCTGCTG
TCCTTCCTGCGGGGCAGCAGCGCCTGCTGCAGCACCAGAGTGCGGCGGCAGCTGGACCGGAA
CCTGACCTTCCACAAGATGGTGGCCTGGATGATCGCCCTGCACAGCGCCATCCACACCATCG
CCCACCTGTTCAACGTGGAGTGGTGCGTGAACGCCCGGGTGAACAACAGCGACCCCTACAGC
GTGGCCCTGAGCGAGCTGGGCGACCGGCAGAACGAGAGCTACCTGAACTTCGCCCGGAAGC
GGATCAAGAACCCCGAGGGCGGCCTGTACCTGGCCGTGACCCTGCTGGCCGGCATCACCGGC
GTGGTGATCACCCTGTGCCTGATCCTGATCATCACCAGCAGCACCAAGACCATCCGGCGGAG
CTACTTCGAGGTGTTCTGGTACACCCACCACCTGTTCGTGATCTTTTTCATCGGCCTGGCCAT
CCACGGCGCCGAGCGGATCGTGAGGGGCCAGACCGCCGAGAGCCTGGCCGTGCACAACATC
ACCGTGTGCGAGCAGAAAATCAGCGAGTGGGGCAAGATCAAAGAGTGCCCCATCCCCCAGT
TCGCCGGCAACCCCCCCCATGACCTGGAAGTGGATCGTGGGCCCCATGTTCCTGTACCTGTGC
GAGCGGCTGGTGCGGTTCTGGCGGAGCCAGCAGAAAGTGGTGATTACCAAGGTGGTGACCC
ACCCCTTCAAGACCATCGAGCTGCAGATGAAGAAAAAGGGCTTCAAGATGGAAGTGGGCCA
GTACATCTTTGTGAAGTGCCCCAAGGTGTCCAAGCTGGAATGGCACCCCTTCACCCTGACCA
GCGCCCCTGAAGAGGACTTCTTCAGCATCCACATCAGAATCGTGGGCGACTGGACCGAGGGC
CTGTTCAATGCCTGCGGCTGCGACAAGCAGGAATTCCAGGACGCCTGGAAGCTGCCCAAGAT
CGCCGTGGACGGCCCCTTTGGCACCGCCAGCGAGGACGTGTTCAGCTACGAGGTGGTGATGC
TGGTCGGAGCCGGCATCGGCGTGACCCCCTTCGCCAGCATCCTGAAGAGCGTGTGGTACAAG
TACTGCAACAACGCCACCAACCTGAAGCTGAAGAAGATCTACTTCTACTGGCTGTGCCGGGA
CACCCACGCCTTCGAGTGGTTCGCCGATCTGCTGCAGCTGCTGGAAAGCCAGATGCAGGAAC
GGAACAACGCCGGCTTCCTGAGCTACAACATCTACCTGACCGGCTGGGACGAGAGCCAGGCC
AACCACTTCGCCGTGCACCACGACGAGGAAAAGGACGTGATCACCGGCCTGAAGCAGAAAA
CCCTGTACGGCAGGCCCAACTGGGACAACGAGTTTAAGACCATCGCCAGCCAGCACCCCAAC
ACCCGGATCGGCGTGTTTCTGTGCGGCCCTGAGGCCCTGGCCGAGACACTGAGCAAGCAGAG
CATCAGCAACAGCGAGAGCGGCCCCAGGGGCGTGCACTTCATCTTCAACAAAGAAAACTTCT
GATGACTCGACGAATTCGAGCATCTTACCGCCATTTATTCCCATATTTGTTCTGTTTTTCTTGA

TTTGGGTATACATTTAAATGTTAATAAAACAAAATGGTGGGGCAATCATTTACATTTTTAGG
GATATGTAATTACTAGTTCAGGTGTATTGCCACAAGACAAACATGTTAAGAAACTTTCCCGTT
ATTTACGCTCTGTTCCTGTTAATCAACCTCTGGATTACAAAATTTGTGAAAGATTGACTGATA
TTCTTAACTATGTTGCTCCTTTTACGCTGTGTGGATATGCTGCTTTATAGCCTCTGTATCTAGC
TATTGCTTCCCGTACGGCTTTCGTTTTCTCCTCCTTGTATAAATCCTGGTTGCTGTCTCTTTTA
GAGGAGTTGTGGCCCGTTGTCCGTCAACGTGGCGTGGTGTGCTCTGTGTTTGCTGACGCAAC
CCCCACTGGCTGGGGCATTGCCACCACCTGTCAACTCCTTTCTGGGACTTTCGCTTTCCCCCT
CCCGATCGCCACGGCAGAACTCATCGCCGCCTGCCTTGCCCGCTGCTGGACAGGGGCTAGGT
TGCTGGGCACTGATAATTCCGTGGTGTTGTCGAATTCGAAGCTTAACACGAGCCATAGATAG
AATAAAAGATTTTATTTAGTCTCCAGAAAAAGGGGGGAATGAAAGACCCCACCGCTAGCGAT
ATCGAATTCACAACCCCTCACTCGGGCGCCAGTCCTCCGATTGACTGAGTCGCCCGGGTACC
CGTATTCCCAATAAAGCCTCTTGCTGTTTGCATCCGAATCGTGGACTCGCTGATCCTTGGGAG
GGTCTCCTCAGATTGATTGACTGCCCACCTCGGGGGTCTTTCATTTGGAGGTTCCACCGAGAT
5' delta U3 SFFV region – 1...50
5' R MESV region – 51...119
5' U5 MESV region – 120...195
SFFV promoter – 686...1086
gp91^{phox}s – 1145...2857
mWPRE – 2872...3454
3' delta U3 SFFV region – 3522...3571
3' R MESV region – 3572...3640
5' U5 MESV region – 3641...3716

SERS11.EFs.gp91s.W proviral sequence

AATGAAAGACCCCACCGCTAGCGATATCGAATTCACAACCCCTCACTCGGGCGCCAGTCCTC
CGATTGACTGAGTCGCCCGGGTACCCGTATTCCCAATAAAGCCTCTTGCTGTTTGCATCCGAA
TCGTGGACTCGCTGATCCTTGGGAGGGTCTCCTCAGATTGATTGACTGCCCACCTCGGGGGT
CTTTCATTTGGAGGTTCCACCGAGATTTGGAGACCCCTGCCCAGGGACCACCGACCCCCCCG
CCGGGAGGTAAGCTGGCCAGCGGTCGTTTCGTGTCTGTCTCTGTCTTTGTGCGTGTTTGTGCC
GGCATCTAGTGTTTGCGCCTGCGTCTGTACTAGTTGGCTAACTAGATCTGTATCTGGCGGTCC
CGCGGAAGAACTGACGAGTTCGTATTCCCGGCCGCAGCCCCTGGGAGACGTCCCAGCGGCCT
CGGGGGCCCGTTTTGTGGCCCATTCTGTATCAGTTAACCTACCCGAGTCGGACTTTTTGGAGC
TCCGCCACTGTCCGAGGGGTACGTGGCTTTGTTGGGGGACGAGAGACAGAGACACTTCCCGC
CCCCGTCTGAATTTTTGCTTTCGGTTTTACGCCGAAACCGCGCCGCGCGTCTTGTCTGCTGCA
GCATCGTTCTGTGTTGTCTCTGTCTGACGTGGTTCTGTATTGTCTGAAAATAGCGGCCGCTTC
GTGAGGCTCCGGTGCCCGTCAGTGGGCAGAGCGCACATCGCCCACAGTCCCCGAGAAGTTGG
GGGGAGGGGTCGGCAATTGAACCGGTGCCTAGAGAAGGTGGCGCGGGGTAAACTGGGAAAG
TGATGTCGTGTACTGGCTCCGCCTTTTTCCCGAGGGTGGGGGAGAACCGTATATAAGTGCAG
TAGTCGCCGTGAACGTTCTTTTTCGCAACGGGTTTGCCGCCAGAACACAGTCGACCGATCCT
GCCACCATGGGCAACTGGGCCGTGAACGAGGGCCTGAGCATCTTCGTGATCCTGGTGTGGCT
GGGCCTGAACGTGTTCCTGTTCGTGTGGTACTACCGGGTGTACGACATCCCCCCCAAGTTCTT
CTACACCCGGAAGCTGCTGGGCAGCGCCCTGGCCCTGGCCAGAGCCCCTGCCGCCTGCCTGA
ACTTCAACTGCATGCTGATCCTGCTGCCCGTGTGCCGGAACCTGCTGTCCTTCCTGCGGGGCA
GCAGCGCCTGCTGCAGCACCAGAGTGCGGCGGCAGCTGGACCGGAACCTGACCTTCCACAAG
ATGGTGGCCTGGATGATCGCCCTGCACAGCGCCATCCACACCATCGCCCACCTGTTCAACGT
GGAGTGGTGCGTGAACGCCCGGGTGAACAACAGCGACCCCTACAGCGTGGCCCTGAGCGAG
CTGGGCGACCGGCAGAACGAGAGCTACCTGAACTTCGCCCGGAAGCGGATCAAGAACCCCG

AGGGCGGCCTGTACCTGGCCGTGACCCTGCTGGCCGGCATCACCGGCGTGGTGATCACCCTG
TGCCTGATCCTGATCATCACCAGCAGCACCAAGACCATCCGGCGGAGCTACTTCGAGGTGTT
CTGGTACACCCACCACCTGTTCGTGATCTTTTTCATCGGCCTGGCCATCCACGGCGCCGAGCG
GATCGTGAGGGGCCAGACCGCCGAGAGCCTGGCCGTGCACAACATCACCGTGTGCGAGCAG
AAAATCAGCGAGTGGGGCAAGATCAAAGAGTGCCCCATCCCCCAGTTCGCCGGCAACCCCCC
CATGACCTGGAAGTGGATCGTGGGCCCCATGTTCCTGTACCTGTGCGAGCGGCTGGTGCGGT
TCTGGCGGAGCCAGCAGAAAGTGGTGATTACCAAGGTGGTGACCCACCCCTTCAAGACCATC
GAGCTGCAGATGAAGAAAAAGGGCTTCAAGATGGAAGTGGGCCAGTACATCTTTGTGAAGT
GCCCCAAGGTGTCCAAGCTGGAATGGCACCCCTTCACCCTGACCAGCGCCCCTGAAGAGGAC
TTCTTCAGCATCCACATCAGAATCGTGGGCGACTGGACCGAGGGCCTGTTCAATGCCTGCGG
CTGCGACAAGCAGGAATTCCAGGACGCCTGGAAGCTGCCCAAGATCGCCGTGGACGGCCCCT
TTGGCACCGCCAGCGAGGACGTGTTCAGCTACGAGGTGGTGATGCTGGTCGGAGCCGGCATC
GGCGTGACCCCCTTCGCCAGCATCCTGAAGAGCGTGTGGTACAAGTACTGCAACAACGCCAC
CAACCTGAAGCTGAAGAAGATCTACTTCTACTGGCTGTGCCGGGACACCCACGCCTTCGAGT
GGTTCGCCGATCTGCTGCAGCTGCTGGAAAGCCAGATGCAGGAACGGAACAACGCCGGCTTC
CTGAGCTACAACATCTACCTGACCGGCTGGGACGAGAGCCAGGCCAACCACTTCGCCGTGCA
CCACGACGAGGAAAAGGACGTGATCACCGGCCTGAAGCAGAAAACCCTGTACGGCAGGCCC
AACTGGGACAACGAGTTTAAGACCATCGCCAGCCAGCACCCCAACACCCGGATCGGCGTGTT
TCTGTGCGGCCCTGAGGCCCTGGCCGAGACACTGAGCAAGCAGAGCATCAGCAACAGCGAG
AGCGGCCCCAGGGGCGTGCACTTCATCTTCAACAAAGAAAACTTCTGATGACTCGACGAATT
CGAGCATCTTACCGCCATTTATTCCCATATTTGTTCTGTTTTTCTTGATTTGGGTATACATTTA
AATGTTAATAAAACAAAATGGTGGGGCAATCATTTACATTTTTAGGGATATGTAATTACTAG
TTCAGGTGTATTGCCACAAGACAAACATGTTAAGAAACTTTCCCGTTATTTACGCTCTGTTCC
TGTTAATCAACCTCTGGATTACAAAATTTGTGAAAGATTGACTGATATTCTTAACTATGTTGC
TCCTTTTACGCTGTGTGGATATGCTGCTTTATAGCCTCTGTATCTAGCTATTGCTTCCCGTACG
GCTTTCGTTTTCTCCTCCTTGTATAAATCCTGGTTGCTGTCTCTTTTAGAGGAGTTGTGGCCCG
TTGTCCGTCAACGTGGCGTGGTGTGCTCTGTGTTTGCTGACGCAACCCCCACTGGCTGGGGC
ATTGCCACCACCTGTCAACTCCTTTCTGGGACTTTCGCTTTCCCCCTCCCGATCGCCACGGCA
GAACTCATCGCCGCCTGCCTTGCCCGCTGCTGGACAGGGGCTAGGTTGCTGGGCACTGATAA
TTCCGTGGTGTTGTCGAATTCGAAGCTTAACACGAGCCATAGATAGAATAAAAGATTTTATT
TAGTCTCCAGAAAAAGGGGGGAATGAAAGACCCCACCGCTAGCGATATCGAATTCACAACCC
CTCACTCGGGCGCCAGTCCTCCGATTGACTGAGTCGCCCGGGTACCCGTATTCCCAATAAAG
CCTCTTGCTGTTTGCATCCGAATCGTGGACTCGCTGATCCTTGGGAGGGTCTCCTCAGATTGA
TTGACTGCCCACCTCGGGGGTCTTTCATTTGGAGGTTCCACCGAGAT

5' delta U3 SFFV region – 1...50

5' R MESV region – 51...119

5' U5 MESV region – 120...195

EFs promoter – 680...923

gp91^{phox}s – 942...2654

mWPRE – 2669...3251

3' delta U3 SFFV region – 3319...3368

3' R MESV region – 3369...3437

5' U5 MESV region – 3438...3513

SERS11.SP146.gp91s.W proviral sequence

AATGAAAGACCCCACCGCTAGCGATATCGAATTCACAACCCCTCACTCGGGCGCCAGTCCTC
CGATTGACTGAGTCGCCCGGGTACCCGTATTCCCAATAAAGCCTCTTGCTGTTTGCATCCGAA
TCGTGGACTCGCTGATCCTTGGGAGGGTCTCCTCAGATTGATTGACTGCCCACCTCGGGGGT
CTTTCATTTGGAGGTTCCACCGAGATTTGGAGACCCCTGCCCAGGGACCACCGACCCCCCCG
CCGGGAGGTAAGCTGGCCAGCGGTCGTTTCGTGTCTGTCTCTGTCTTTGTGCGTGTTTGTGCC
GGCATCTAGTGTTTGCGCCTGCGTCTGTACTAGTTGGCTAACTAGATCTGTATCTGGCGGTCC
CGCGGAAGAACTGACGAGTTCGTATTCCCGGCCGCAGCCCCTGGGAGACGTCCCAGCGGCCT
CGGGGGCCCGTTTTGTGGCCCATTCTGTATCAGTTAACCTACCCGAGTCGGACTTTTTGGAGC
TCCGCCACTGTCCGAGGGGTACGTGGCTTTGTTGGGGGACGAGAGACAGAGACACTTCCCGC
CCCCGTCTGAATTTTTGCTTTCGGTTTTACGCCGAAACCGCGCCGCGCGTCTTGTCTGCTGCA
GCATCGTTCTGTGTTGTCTCTGTCTGACGTGgTTCTGTATTGTCTGAAAATAGCGGCCGCCGG
TACCGAGCTCTTACGCGTGCTAGCGAGGGCGGACAAGCGACTTCCTCTTTCCAGCAGAAAAG
GAGAAGTAGGAGCCAAGATTTCCAAACTCTGTGGTTGCCTTGAAGCGACTTCCTCTTTCCAG
AAGCGACTTCCTCTTTCCAGCAGAAAAGGAGAAGTAGGAGCTCCTACTTCTCCTTTTCTGCCA
AGATTTCCAAACTCTGTGGTTGCCTTGCTCCTACTTCTCCTTTTCTGCAGAAAAGGAGAAGTA
GGAGCTGGAAAGAGGAAGTCGCTTGAGGGCGGACGCTAGCCCGGGCTCGAGTACCCTCCCT
GCCCCCTGTCCCGACCGCGACAAAAGCGACTTCCTCTTTCCAGTGCATTTAAGGCGCAGCCTG
GAAGTGCCAGGGAGCACTGGAGGCCACCCAGTACCGGTTGTCGACCGATCCTGCCACCATGG
GCAACTGGGCCGTGAACGAGGGCCTGAGCATCTTCGTGATCCTGGTGTGGCTGGGCCTGAAC
GTGTTCCTGTTCGTGTGGTACTACCGGGTGTACGACATCCCCCCCAAGTTCTTCTACACCCGG
AAGCTGCTGGGCAGCGCCCTGGCCCTGGCCAGAGCCCCTGCCGCCTGCCTGAACTTCAACTG
CATGCTGATCCTGCTGCCCGTGTGCCGGAACCTGCTGTCCTTCCTGCGGGGCAGCAGCGCCT
GCTGCAGCACCAGAGTGCGGCGGCAGCTGGACCGGAACCTGACCTTCCACAAGATGGTGGCC
TGGATGATCGCCCTGCACAGCGCCATCCACACCATCGCCCACCTGTTCAACGTGGAGTGGTG
CGTGAACGCCCGGGTGAACAACAGCGACCCCTACAGCGTGGCCCTGAGCGAGCTGGGCGAC
CGGCAGAACGAGAGCTACCTGAACTTCGCCCGGAAGCGGATCAAGAACCCCGAGGGCGGCC
TGTACCTGGCCGTGACCCTGCTGGCCGGCATCACCGGCGTGGTGATCACCCTGTGCCTGATC
CTGATCATCACCAGCAGCACCAAGACCATCCGGCGGAGCTACTTCGAGGTGTTCTGGTACAC
CCACCACCTGTTCGTGATCTTTTTCATCGGCCTGGCCATCCACGGCGCCGAGCGGATCGTGAG
GGGCCAGACCGCCGAGAGCCTGGCCGTGCACAACATCACCGTGTGCGAGCAGAAAATCAGC
GAGTGGGGCAAGATCAAAGAGTGCCCCATCCCCCAGTTCGCCGGCAACCCCCCCATGACCTG
GAAGTGGATCGTGGGCCCCATGTTCCTGTACCTGTGCGAGCGGCTGGTGCGGTTCTGGCGGA
GCCAGCAGAAAGTGGTGATTACCAAGGTGGTGACCCACCCCTTCAAGACCATCGAGCTGCAG
ATGAAGAAAAAGGGCTTCAAGATGGAAGTGGGCCAGTACATCTTTGTGAAGTGCCCCAAGG
TGTCCAAGCTGGAATGGCACCCCTTCACCCTGACCAGCGCCCCTGAAGAGGACTTCTTCAGC
ATCCACATCAGAATCGTGGGCGACTGGACCGAGGGCCTGTTCAATGCCTGCGGCTGCGACAA
GCAGGAATTCCAGGACGCCTGGAAGCTGCCCAAGATCGCCGTGGACGGCCCCTTTGGCACCG
CCAGCGAGGACGTGTTCAGCTACGAGGTGGTGATGCTGGTCGGAGCCGGCATCGGCGTGACC
CCCTTCGCCAGCATCCTGAAGAGCGTGTGGTACAAGTACTGCAACAACGCCACCAACCTGAA
GCTGAAGAAGATCTACTTCTACTGGCTGTGCCGGGACACCCACGCCTTCGAGTGGTTCGCCG
ATCTGCTGCAGCTGCTGGAAAGCCAGATGCAGGAACGGAACAACGCCGGCTTCCTGAGCTAC
AACATCTACCTGACCGGCTGGGACGAGAGCCAGGCCAACCACTTCGCCGTGCACCACGACGA
GGAAAAGGACGTGATCACCGGCCTGAAGCAGAAAACCCTGTACGGCAGGCCCAACTGGGAC
AACGAGTTTAAGACCATCGCCAGCCAGCACCCCAACACCCGGATCGGCGTGTTTCTGTGCGG
CCCTGAGGCCCTGGCCGAGACACTGAGCAAGCAGAGCATCAGCAACAGCGAGAGCGGCCCC
AGGGGCGTGCACTTCATCTTCAACAAAGAAAACTTCTGATGACTCGACGAATTCGAGCATCT
TACCGCCATTTATTCCCATATTTGTTCTGTTTTTCTTGATTTGGGTATACATTTAAATGTTAAT

AAAACAAAATGGTGGGGCAATCATTTACATTTTTAGGGATATGTAATTACTAGTTCAGGTGT
ATTGCCACAAGACAAACATGTTAAGAAACTTTCCCGTTATTTACGCTCTGTTCCTGTTAATCA
ACCTCTGGATTACAAAATTTGTGAAAGATTGACTGATATTCTTAACTATGTTGCTCCTTTTAC
GCTGTGTGGATATGCTGCTTTATAGCCTCTGTATCTAGCTATTGCTTCCCGTACGGCTTTCGT
TTTCTCCTCCTTGTATAAATCCTGGTTGCTGTCTCTTTTAGAGGAGTTGTGGCCCGTTGTCCGT
CAACGTGGCGTGGTGTGCTCTGTGTTTGCTGACGCAACCCCCACTGGCTGGGGCATTGCCAC
CACCTGTCAACTCCTTTCTGGGACTTTCGCTTTCCCCCTCCCGATCGCCACGGCAGAACTCAT
CGCCGCCTGCCTTGCCCGCTGCTGGACAGGGGCTAGGTTGCTGGGCACTGATAATTCCGTGG
TGTTGTCGAATTCGAAGCTTAACACGAGCCATAGATAGAATAAAAGATTTTATTTAGTCTCC
AGAAAAAGGGGGGAATGAAAGACCCCACCGCTAGCGATATCGAATTCACAACCCCTCACTCG
GGCGCCAGTCCTCCGATTGACTGAGTCGCCCGGGTACCCGTATTCCCAATAAAGCCTCTTGCT
GTTTGCATCCGAATCGTGGACTCGCTGATCCTTGGGAGGGTCTCCTCAGATTGATTGACTGCC
CACCTCGGGGGTCTTTCATTTGGAGGTTCCACCGAGAT

5' delta U3 SFFV region – 1...50
5' R MESV region – 51...119
5' U5 MESV region – 120...195
SP146 promoter – 680...1102
gp91^{phox}s – 1121...2833
mWPRE – 2848...3430
3' delta U3 SFFV region – 3498...3547
3' R MESV region – 3548...3616
5' U5 MESV region – 3617...3692

SERS11.fes.gp91s.W proviral sequence

AATGAAAGACCCCACCGCTAGCGATATCGAATTCACAACCCCTCACTCGGGCGCCAGTCCTC
CGATTGACTGAGTCGCCCGGGTACCCGTATTCCCAATAAAGCCTCTTGCTGTTTGCATCCGAA
TCGTGGACTCGCTGATCCTTGGGAGGGTCTCCTCAGATTGATTGACTGCCCACCTCGGGGGT
CTTTCATTTGGAGGTTCCACCGAGATTTGGAGACCCCTGCCCAGGGACCACCGACCCCCCCG
CCGGGAGGTAAGCTGGCCAGCGGTCGTTTCGTGTCTGTCTCTGTCTTTGTGCGTGTTTGTGCC
GGCATCTAGTGTTTGCGCCTGCGTCTGTACTAGTTGGCTAACTAGATCTGTATCTGGCGGTCC
CGCGGAAGAACTGACGAGTTCGTATTCCCGGCCGCAGCCCCTGGGAGACGTCCCAGCGGCCT
CGGGGGCCCGTTTTGTGGCCCATTCTGTATCAGTTAACCTACCCGAGTCGGACTTTTTGGAGC
TCCGCCACTGTCCGAGGGGTACGTGGCTTTGTTGGGGGACGAGAGACAGAGACACTTCCCGC
CCCCGTCTGAATTTTTGCTTTCGGTTTTACGCCGAAACCGCGCCGCGCGTCTTGTCTGCTGCA
GCATCGTTCTGTGTTGTCTCTGTCTGACGTGGTTCTGTATTGTCTGAAAATAGCGGCCGCCAG
TGTGATGGATATCTGCAGAATTCGCCCTTGAATTCCGTGAGGTGGGGAGGGCTGGGACCAGG
GTTCCCTCTTTCTCTTCTGCGGTGGCCCTGGCCTGGTGCTAGGACTGCGCGCCTCCCCTCAGT
ACCCGCGGACACCCTGGGCTTCCCTGGGCCCAGCATCTGCCTGGGGCCTCGCCCTGGGCTCC
CCCTCCTGACCCCCACCTTGCGCCCCTTCCCGGTGTTCCCGGGGCGCTGCCGGGCCCTGGGGC
CTGCGGGGCGCGGGCGGCTCTTGGCTGGGCCATTCTTTCCCGGCCCCCTCCTCCCTTCCGTTT
CCGTGGCCGTGCGGCCGGCTAGAGGCTGCGGCCCAGCGCGGAGCAGGGGGGCTGGCAGGCG
TCGGGGCGGTCGGGCCGGTCCCGCCCGCCCCTTCCCCTCCACAGGCCCGCCCCGGGGCCTGG
GCCAACTGAAACCGCGGGAGGAGGAAGCGCGGAATCAGGAACTGGCCGGGGTCCGCACCGG
GCCTGAGTCGGTCCGAGGCCGTCCCAGGAGCAGCGCCCGAAGGTCGACCGATCCTGCCACCA
TGGGCAACTGGGCCGTGAACGAGGGCCTGAGCATCTTCGTGATCCTGGTGTGGCTGGGCCTG
AACGTGTTCCTGTTCGTGTGGTACTACCGGGTGTACGACATCCCCCCCAAGTTCTTCTACACC
CGGAAGCTGCTGGGCAGCGCCCTGGCCCTGGCCAGAGCCCCTGCCGCCTGCCTGAACTTCAA
CTGCATGCTGATCCTGCTGCCCGTGTGCCGGAACCTGCTGTCCTTCCTGCGGGGCAGCAGCG

CCTGCTGCAGCACCAGAGTGCGGCGGCAGCTGGACCGGAACCTGACCTTCCACAAGATGGTG
GCCTGGATGATCGCCCTGCACAGCGCCATCCACACCATCGCCCACCTGTTCAACGTGGAGTG
GTGCGTGAACGCCCGGGTGAACAACAGCGACCCCTACAGCGTGGCCCTGAGCGAGCTGGGC
GACCGGCAGAACGAGAGCTACCTGAACTTCGCCCGGAAGCGGATCAAGAACCCCGAGGGCG
GCCTGTACCTGGCCGTGACCCTGCTGGCCGGCATCACCGGCGTGGTGATCACCCTGTGCCTG
ATCCTGATCATCACCAGCAGCACCAAGACCATCCGGCGGAGCTACTTCGAGGTGTTCTGGTA
CACCCACCACCTGTTCGTGATCTTTTTCATCGGCCTGGCCATCCACGGCGCCGAGCGGATCGT
GAGGGGCCAGACCGCCGAGAGCCTGGCCGTGCACAACATCACCGTGTGCGAGCAGAAAATC
AGCGAGTGGGGCAAGATCAAAGAGTGCCCCATCCCCCAGTTCGCCGGCAACCCCCCCCATGAC
CTGGAAGTGGATCGTGGGCCCCATGTTCCTGTACCTGTGCGAGCGGCTGGTGCGGTTCTGGC
GGAGCCAGCAGAAAGTGGTGATTACCAAGGTGGTGACCCACCCCTTCAAGACCATCGAGCTG
CAGATGAAGAAAAAGGGCTTCAAGATGGAAGTGGGCCAGTACATCTTTGTGAAGTGCCCCA
AGGTGTCCAAGCTGGAATGGCACCCCTTCACCCTGACCAGCGCCCCTGAAGAGGACTTCTTC
AGCATCCACATCAGAATCGTGGGCGACTGGACCGAGGGCCTGTTCAATGCCTGCGGCTGCGA
CAAGCAGGAATTCCAGGACGCCTGGAAGCTGCCCAAGATCGCCGTGGACGGCCCCTTTGGCA
CCGCCAGCGAGGACGTGTTCAGCTACGAGGTGGTGATGCTGGTCGGAGCCGGCATCGGCGTG
ACCCCCTTCGCCAGCATCCTGAAGAGCGTGTGGTACAAGTACTGCAACAACGCCACCAACCT
GAAGCTGAAGAAGATCTACTTCTACTGGCTGTGCCGGGACACCCACGCCTTCGAGTGGTTCG
CCGATCTGCTGCAGCTGCTGGAAAGCCAGATGCAGGAACGGAACAACGCCGGCTTCCTGAGC
TACAACATCTACCTGACCGGCTGGGACGAGAGCCAGGCCAACCACTTCGCCGTGCACCACGA
CGAGGAAAAGGACGTGATCACCGGCCTGAAGCAGAAAACCCTGTACGGCAGGCCCAACTGG
GACAACGAGTTTAAGACCATCGCCAGCCAGCACCCCAACACCCGGATCGGCGTGTTTCTGTG
CGGCCCTGAGGCCCTGGCCGAGACACTGAGCAAGCAGAGCATCAGCAACAGCGAGAGCGGC
CCCAGGGGCGTGCACTTCATCTTCAACAAAGAAAACTTCTGATGACTCGACGAATTCGAGCA
TCTTACCGCCATTTATTCCCATATTTGTTCTGTTTTTCTTGATTTGGGTATACATTTAAATGTT
AATAAAACAAAATGGTGGGGCAATCATTTACATTTTTAGGGATATGTAATTACTAGTTCAGG
TGTATTGCCACAAGACAAACATGTTAAGAAACTTTCCCGTTATTTACGCTCTGTTCCTGTTAA
TCAACCTCTGGATTACAAAATTTGTGAAAGATTGACTGATATTCTTAACTATGTTGCTCCTTT
TACGCTGTGTGGATATGCTGCTTTATAGCCTCTGTATCTAGCTATTGCTTCCCGTACGGCTTT
CGTTTTCTCCTCCTTGTATAAATCCTGGTTGCTGTCTCTTTTAGAGGAGTTGTGGCCCGTTGTC
CGTCAACGTGGCGTGGTGTGCTCTGTGTTTGCTGACGCAACCCCCACTGGCTGGGGCATTGC
CACCACCTGTCAACTCCTTTCTGGGACTTTCGCTTTCCCCCTCCCGATCGCCACGGCAGAACT
CATCGCCGCCTGCCTTGCCCGCTGCTGGACAGGGGCTAGGTTGCTGGGCACTGATAATTCCG
TGGTGTTGTCGAATTCGAAGCTTAACACGAGCCATAGATAGAATAAAAGATTTTATTTAGTC
TCCAGAAAAAGGGGGGAATGAAAGACCCCACCGCTAGCGATATCGAATTCACAACCCCTCAC
TCGGGCGCCAGTCCTCCGATTGACTGAGTCGCCCGGGTACCCGTATTCCCAATAAAGCCTCTT
GCTGTTTGCATCCGAATCGTGGACTCGCTGATCCTTGGGAGGGTCTCCTCAGATTGATTGACT
GCCCACCTCGGGGGTCTTTCATTTGGAGGTTCCACCGAGAT

5' delta U3 SFFV region – 1...50

5' R MESV region – 51...119

5' U5 MESV region – 120...195

c-fes promoter – 718...1224

gp91^{phox}s – 1247...2959

mWPRE – 2974...3556

3' delta U3 SFFV region – 3624...3673

3' R MESV region – 3674...3742

5' U5 MESV region – 3743...3818

SERS11.M8dN.gp91s.W proviral sequence

AATGAAAGACCCCACCGCTAGCGATATCGAATTCACAACCCCTCACTCGGGCGCCAGTCCTC
CGATTGACTGAGTCGCCCGGGTACCCGTATTCCCAATAAAGCCTCTTGCTGTTTGCATCCGAA
TCGTGGACTCGCTGATCCTTGGGAGGGTCTCCTCAGATTGATTGACTGCCCACCTCGGGGGT
CTTTCATTTGGAGGTTCCACCGAGATTTGGAGACCCCTGCCCAGGGACCACCGACCCCCCCG
CCGGGAGGTAAGCTGGCCAGCGGTCGTTTCGTGTCTGTCTCTGTCTTTGTGCGTGTTTGTGCC
GGCATCTAGTGTTTGCGCCTGCGTCTGTACTAGTTGGCTAACTAGATCTGTATCTGGCGGTCC
CGCGGAAGAACTGACGAGTTCGTATTCCCGGCCGCAGCCCCTGGGAGACGTCCCAGCGGCCT
CGGGGGCCCGTTTTGTGGCCCATTCTGTATCAGTTAACCTACCCGAGTCGGACTTTTTGGAGC
TCCGCCACTGTCCGAGGGGTACGTGGCTTTGTTGGGGGACGAGAGACAGAGACACTTCCCGC
CCCCGTCTGAATTTTTGCTTTCGGTTTTACGCCGAAACCGCGCCGCGCGTCTTGTCTGCTGCA
GCATCGTTCTGTGTTGTCTCTGTCTGACGTGGTTCTGTATTGTCTGAAAATAGCGGCCGCCAT
ATGCTTATTGACCATTTGTATATCTTCTTCGGAGAAGTGTCTATTTGAGTCTTTTCCCCAATTT
TTGATTGGTTTGTTTGTTTTTTGTTGTTGAGTTGTAGGGATTCTTTTATATTCTGGATATTAAT
CCCTTATCAGATATTTGTTTTACAAATATTTTCTTTGTAACAACAGAAACACACCACAGTCTT
CAAGGTTGGAAGCCAGTTAATCTGAGTAGCATTTTGTTAGTGGTGGGGAGAGGATTTGTTCC
TCCTGAAATCCTGGGGAATTGGCCACCTCCTCTTCTCCTCTTAGGCATGAAGCGCGTCTGGCT
TCTCCAAAGAACTCTTCCCCTCCACTACCTCAGAGTTAGCTTCCTCTCTTCAGCCAGTGATCC
TGGGGTCCCAGACACAATAATTAACCAAGAGAGGGTGAAAGGCTCCCTGCTGTGTTTATGCA
ATGGCTCAGGCCCTTGTGAAGTGCCGAGGGACCCCAAGCAGCCTCCATCTCCCAGGGCATGG
TCCATCCCCAGCTTCACAGAACAGGAAAGCTGTGGAGGAGTGTGGGCAGCAGGGTAGGAAT
GGATATAGCCCTTGGCAACAACACATTTCCCCACAAAGCACCCACCCAAAAGAACAACAACG
ATAGTTTTAGTTTTTAGTAATGAGAACAATAGTTCTCATGACTAAAAGCCATCAGCCAGGAC
ACGTGTTCTCAACCCTTTTGCGGTCTTTGGACCCTTTGAAACTCTGACAGAAGCCATGGAGGA
ATGTTCTCACTGAGTGCATGCACTCAAAATGATGCATTCAACTTCAATTCAGTTTCAGGGATG
TATGGCCTGACCACCAATGCAGGGGATTAGCAATCGCAATAGTGGAGAGGGCATGGGAGTG
GGAATCTGGCTGGATCAAGCAAGTGGATGCCAGCAGCCCAGAAAAAGAGCCCCCCTACCTGC
TTTTTCCTTCTGGGCACTATTGCCCAGCAAATGCCTTCCTCTTTCCGCTTCTCCTACCTCCCCA
CCCAAAATTTTCATTCTGCACAGTGATTGCCACATTCACCTGGTTGAGAAACCAGAGACTGT
AGCAACTCTGGCAGGGAGAAGCTGTCTCTGATGGCCTGAAGCTGTGGGCAGCTGGCCAAGCC
TAACCGCTATAAAAAGGAGCTGCCTCTCAGCCCTGCATGTCTCTTGTCAGCTGTCTTTCAGAA
GACCTGGTAAGTGGGACTGTCTGGGTTGGCCCCGCACTTTGGGCTTCTCTTGGGGAGGGTCA
GGGAAGTGGAGCAGCCTTCCTGAGAGAGGAGAGAGAAAGCTCAGGGAGGTCTGGAGCAAAG
ATACTCCTGGAGGTGGGGAGTGAGGCAGGGATAAGGAAGGAGAGTATCCTCCAGCACCTTC
CAGTGGGTAAGGGCACATTGTCTCCTAGGCTGGACTTTTCTTGAGCAGAGGGTGGGGTGGTA
AGGAAAGTCTACGGGCCCCGTGTGTGTGCACATGTCTCTGTGTGAATGGACCCTTCCCCTTCC
CACACGTGTATCCCTATCATCCCACCCTTCCCACCAGAGCCATAGCCATCTGCTGGTTTGGTT
ATTTGGAGAGTGCAGGCCAGGACAAGGCCATCGCTTGGGGCATGAATCCTCTGCGTACTGCC
CTGGCCAGATGCAAATTCCCTGCCATGGGATTCCCCAGAAGGTTCTGTTTTTCAGGTGGGGC
AAGTTCCGTGGGATCATAGATCTGTCATGATGATCATTGCAATTGGATCCATATATAGGGCC
CGGGTTATAATTACCTCAGGTCGACCGATCCTGCCACCATGGGCAACTGGGCCGTGAACGAG
GGCCTGAGCATCTTCGTGATCCTGGTGTGGCTGGGCCTGAACGTGTTCCTGTTCGTGTGGTAC
TACCGGGTGTACGACATCCCCCCCAAGTTCTTCTACACCCGGAAGCTGCTGGGCAGCGCCCT
GGCCCTGGCCAGAGCCCCTGCCGCCTGCCTGAACTTCAACTGCATGCTGATCCTGCTGCCCGT
GTGCCGGAACCTGCTGTCCTTCCTGCGGGGCAGCAGCGCCTGCTGCAGCACCAGAGTGCGGC
GGCAGCTGGACCGGAACCTGACCTTCCACAAGATGGTGGCCTGGATGATCGCCCTGCACAGC
GCCATCCACACCATCGCCCACCTGTTCAACGTGGAGTGGTGCGTGAACGCCCGGGTGAACAA
CAGCGACCCCTACAGCGTGGCCCTGAGCGAGCTGGGCGACCGGCAGAACGAGAGCTACCTG

AACTTCGCCCGGAAGCGGATCAAGAACCCCGAGGGCGGCCTGTACCTGGCCGTGACCCTGCT
GGCCGGCATCACCGGCGTGGTGATCACCCTGTGCCTGATCCTGATCATCACCAGCAGCACCA
AGACCATCCGGCGGAGCTACTTCGAGGTGTTCTGGTACACCCACCACCTGTTCGTGATCTTTT
TCATCGGCCTGGCCATCCACGGCGCCGAGCGGATCGTGAGGGGCCAGACCGCCGAGAGCCTG
GCCGTGCACAACATCACCGTGTGCGAGCAGAAAATCAGCGAGTGGGGCAAGATCAAAGAGT
GCCCCATCCCCCAGTTCGCCGGCAACCCCCCCATGACCTGGAAGTGGATCGTGGGCCCCATG
TTCCTGTACCTGTGCGAGCGGCTGGTGCGGTTCTGGCGGAGCCAGCAGAAAGTGGTGATTAC
CAAGGTGGTGACCCACCCCTTCAAGACCATCGAGCTGCAGATGAAGAAAAAGGGCTTCAAG
ATGGAAGTGGGCCAGTACATCTTTGTGAAGTGCCCCAAGGTGTCCAAGCTGGAATGGCACCC
CTTCACCCTGACCAGCGCCCCTGAAGAGGACTTCTTCAGCATCCACATCAGAATCGTGGGCG
ACTGGACCGAGGGCCTGTTCAATGCCTGCGGCTGCGACAAGCAGGAATTCCAGGACGCCTGG
AAGCTGCCCAAGATCGCCGTGGACGGCCCCTTTGGCACCGCCAGCGAGGACGTGTTCAGCTA
CGAGGTGGTGATGCTGGTCGGAGCCGGCATCGGCGTGACCCCCTTCGCCAGCATCCTGAAGA
GCGTGTGGTACAAGTACTGCAACAACGCCACCAACCTGAAGCTGAAGAAGATCTACTTCTAC
TGGCTGTGCCGGGACACCCACGCCTTCGAGTGGTTCGCCGATCTGCTGCAGCTGCTGGAAAG
CCAGATGCAGGAACGGAACAACGCCGGCTTCCTGAGCTACAACATCTACCTGACCGGCTGGG
ACGAGAGCCAGGCCAACCACTTCGCCGTGCACCACGACGAGGAAAAGGACGTGATCACCGG
CCTGAAGCAGAAAACCCTGTACGGCAGGCCCAACTGGGACAACGAGTTTAAGACCATCGCCA
GCCAGCACCCCAACACCCGGATCGGCGTGTTTCTGTGCGGCCCTGAGGCCCTGGCCGAGACA
CTGAGCAAGCAGAGCATCAGCAACAGCGAGAGCGGCCCCAGGGGCGTGCACTTCATCTTCAA
CAAAGAAAACTTCTGATGACTCGACGAATTCGAGCATCTTACCGCCATTTATTCCCATATTTG
TTCTGTTTTTCTTGATTTGGGTATACATTTAAATGTTAATAAAACAAAATGGTGGGGCAATCA
TTTACATTTTTAGGGATATGTAATTACTAGTTCAGGTGTATTGCCACAAGACAAACATGTTAA
GAAACTTTCCCGTTATTTACGCTCTGTTCCTGTTAATCAACCTCTGGATTACAAAATTTGTGA
AAGATTGACTGATATTCTTAACTATGTTGCTCCTTTTACGCTGTGTGGATATGCTGCTTTATA
GCCTCTGTATCTAGCTATTGCTTCCCGTACGGCTTTCGTTTTCTCCTCCTTGTATAAATCCTGG
TTGCTGTCTCTTTTAGAGGAGTTGTGGCCCGTTGTCCGTCAACGTGGCGTGGTGTGCTCTGTG
TTTGCTGACGCAACCCCCACTGGCTGGGGCATTGCCACCACCTGTCAACTCCTTTCTGGGACT
TTCGCTTTCCCCCTCCCGATCGCCACGGCAGAACTCATCGCCGCCTGCCTTGCCCGCTGCTGG
ACAGGGGCTAGGTTGCTGGGCACTGATAATTCCGTGGTGTTGTCGAATTCGAAGCTTAACAC
GAGCCATAGATAGAATAAAAGATTTTATTTAGTCTCCAGAAAAAGGGGGGAATGAAAGACC
CCACCGCTAGCGATATCGAATTCACAACCCCTCACTCGGGCGCCAGTCCTCCGATTGACTGA
GTCGCCCGGGTACCCGTATTCCCAATAAAGCCTCTTGCTGTTTGCATCCGAATCGTGGACTCG
CTGATCCTTGGGAGGGTCTCCTCAGATTGATTGACTGCCCACCTCGGGGGTCTTTCATTTGGA
GGTTCCACCGAGAT

5' delta U3 SFFV region – 1...50

5' R MESV region – 51...119

5' U5 MESV region – 120...195

M8dN promoter – 688...2390

MRP8 exon 1 – 1850…1882

MRP8 intron 1 – 1883…2365

MRP8 exon 2 – 2366…2390

gp91^{phox}s – 2473...4185

mWPRE – 4200...4782

3' delta U3 SFFV region – 4850...4899

3' R MESV region – 4900...4968

5' U5 MESV region – 4969...5044